



NGA.SIG.0026.08\_1.0\_ACCXDQA  
2019-11-18

## **NGA STANDARDIZATION DOCUMENT**

### **Accuracy and Predicted Accuracy in the NSG: External Data and its Quality Assessment**

#### **Technical Guidance Document (TGD) 2f**

**(2019-11-18)**

**Version 1.0**

## Forward

This handbook is approved for use by all Departments and Agencies of the Department of Defense.

Comments, suggestions, or questions on this document should be addressed to the GWG World Geodetic System (WGS) and Geomatics (WGSG) Focus Group, ATTN: Chair, WGS/Geomatics Standards Focus Group, [ncgis-mail.nga.mil](mailto:ncgis-mail.nga.mil) or to the National Geospatial-Intelligence Agency Office of Geomatics (SFN), Mail Stop L-41, 3838 Vogel Road, Arnold, MO 63010 or emailed to [GandG@nga.mil](mailto:GandG@nga.mil).

## Summary of Changes and Modifications

Revision	Date	Status	Description

## Contents

Forward .....	iii
Summary of Changes and Modifications .....	iii
1 Scope.....	1
2 Applicable Documents .....	2
2.1 Government specifications, standards, and handbooks.....	3
3 Definitions.....	4
3.1 Key Terms Used in the Document.....	4
3.1.1 Accuracy .....	4
3.1.2 Accuracy Assessment Model.....	5
3.1.3 Commodities .....	5
3.1.4 Crowd-sourcing .....	5
3.1.5 Data/product realization.....	5
3.1.6 Empirical Quality Model.....	5
3.1.7 Error .....	5
3.1.8 External Data.....	6
3.1.9 Ground Truth .....	6
3.1.10 Metadata.....	6
3.1.11 Mixed Gaussian Random Field (MGRF).....	6
3.1.12 National System for Geospatial Intelligence (NSG) .....	6
3.1.13 Outsourced Data .....	6
3.1.14 Predicted Accuracy.....	6
3.1.15 Predicted Accuracy Model .....	7
3.1.16 Predictive Statistics .....	7
3.1.17 Quality Assurance .....	7
3.1.18 Quality Assessment.....	7
3.1.19 Sample Statistics .....	7
3.1.20 Sensor Model .....	7
3.1.21 Scalar Accuracy Metrics .....	8
3.1.22 Quality Assessment Summary.....	8
3.2 Other Relevant Terms .....	8
3.3 Abbreviations and Acronyms .....	9
4 Introduction to External Data and its Quality Assessment in the NSG.....	10
4.1 Outsourcing.....	10
4.2 Quality Assessment.....	11

4.3	Intended Audience and Detailed Guide to the Document .....	13
4.3.1	Intended Audience .....	13
4.3.2	Overall Guide .....	14
4.3.3	Practical Guide .....	15
4.3.4	Top-level terminology and what the document does not address.....	17
5	Methodology and Algorithms for External Data and its Quality Assessment .....	18
5.1	Quality Assessment Overview.....	18
5.1.1	Examples of External Data .....	20
5.1.1.1	Small-Sat Imagery .....	20
5.1.1.2	3d Point Clouds .....	22
5.1.1.3	Crowd-sourcing Digital Maps .....	23
5.2	Quality Assessment Management Function .....	24
5.2.1	Quality Assessment Summary file/report.....	26
5.2.1.1	Predicted Accuracy Summary Metrics .....	28
5.2.1.2	Data/product reliability metric .....	29
5.2.2	Quality Assessment may take a long time to complete for some data/products .....	30
5.2.3	An Exception – Some Commodities data require minimal Quality Assessment.....	30
5.2.3.1	Examples and why they are preferred.....	31
5.2.3.2	Common characteristic .....	32
5.2.4	Encouraging Explicit Accuracy Specifications.....	32
5.2.4.1	Any Advertised Accuracy should be verified.....	33
5.2.4.2	Specifications for exploitation tools .....	33
5.2.5	Functional Flow of the Quality Assessment Management Function .....	33
5.3	Quality Assessment Analysis Function.....	35
5.3.1	Accuracy assessment and predicted accuracy models and interrelationships.....	38
5.3.1.1	Relationships to the data/product’s sensor model and corresponding terminology.....	39
5.3.1.2	The importance of the predicted accuracy model.....	41
5.3.2	Accuracy assessment and predicted accuracy model definitions and content .....	44
5.3.2.1	Geolocation Product Predicted Accuracy Model .....	47
5.3.2.2	Geolocation Product Accuracy Assessment Model .....	51
5.3.2.3	Geolocation Data Predicted Accuracy Model: Sensor-space.....	51
5.3.2.4	Geolocation Data Predicted Accuracy Model: Measurement-space.....	53
5.3.2.5	Geolocation Data Accuracy Assessment Model .....	58
5.3.3	Companion Components .....	59

5.3.3.1	Adjustment.....	59
5.3.3.2	Full Motion Video.....	67
5.3.3.3	Mixed Gaussian Random Field .....	69
5.3.4	Guide to detailed examples of accuracy assessment and predicted accuracy models .....	78
5.3.5	Analysis techniques for the population of models .....	80
5.3.5.1	Ground truth and various alternatives .....	80
5.3.5.2	Sample error statistics .....	81
5.3.5.3	Real-world example of accuracy assessment: initial processing and a common issue ..	85
5.3.6	The Empirical Quality Model for Crowd-sourcing data/products.....	90
5.3.6.1	Model contents/definition.....	92
5.3.6.2	Analysis techniques for population of models for Crowd-sourcing.....	93
5.3.7	The data/product is needed now, but accuracy assessments are not available .....	93
5.4	Summary .....	96
5.4.1	Key Recommendations .....	96
5.4.2	Recommended future applied research .....	98
6	Notes.....	100
6.1	Intended Use.....	100
7	References .....	100
	Appendix A: Additional Terms and Definitions .....	101
	Appendix B: Geolocation Product Accuracy Models – the basics.....	112
B.1	Population of the accuracy assessment model .....	115
B.1.1	Absolute accuracy.....	116
B.1.2	Relative accuracy .....	118
B.1.3	Outputs .....	123
B.2	Population of the predicted accuracy model.....	124
B.2.1	Absolute accuracy.....	125
B.2.2	Relative accuracy .....	126
B.2.3	Outputs .....	130
B.3	Applications.....	131
B.4	Performance assessment of the populated models .....	132
B.4.1	Descriptions of the performance assessment experiments .....	132
B.4.2	Performance results .....	137
B.4.3	Additional sensitivity and robustness experiments.....	140
B.4.4	Summary .....	144

B.5 Extension of results.....	145
B.5.1 All components of 3d geolocation error.....	145
B.5.2 Support of MGRF representation of predicted accuracy .....	146
B.5.3 Recommended applied research.....	147
Appendix C: Geolocation Data Accuracy Models – the basics.....	147
C.1 Population of the accuracy assessment model .....	150
C.2 Population of the predicted accuracy model.....	150
C.3 Optional processing .....	151
C.3.1 Generalization of spdcf.....	151
C.3.2 Sensor-mensuration error and predicted accuracy.....	153
C.3.3 Temporal correlation .....	154
C.4 Applications.....	154
Appendix D: Adjustment of Geolocation Data.....	156
D.1 Background information.....	157
D.2 The correction grid, its solution, and subsequent adjustment of the image .....	158
D.2.1 Detailed definitions and their related processing.....	159
D.2.2 WLS solution.....	165
D.2.3 Correction of an arbitrary measurement or location in the image.....	167
D.2.4 Summary: Why a correction grid?.....	167
D.3 Correction grid performance and comparison to an affine-transformation based correction.....	169
D.3.1 Simulation results.....	170
D.3.1.1 Definitions and a priori values.....	170
D.3.1.2 Specific results .....	171
D.3.1.3 Distance constant specifies relatively high spatial correlation .....	172
D.3.1.4 Distance constant specifies lower spatial correlation.....	175
D.3.2 Sensitivities of the baseline “cor grid” solution method.....	179
D.3.3 Summary and conclusions.....	181
Appendix E: MGRF representation and adjustment of Geolocation Products .....	195
E.1 Preliminaries: Statistics corresponding to random variables and random vectors .....	198
E.2 Mixed Gaussian Random Field (MGRF): Descriptive content and <i>a priori</i> statistics.....	202
E.2.1 Geolocation errors represented by random fields .....	205
E.2.2 Statistics corresponding to geolocations and their errors contained in partitions .....	210
E.2.3 Statistics corresponding to arbitrary geolocations and their errors in the MGRF.....	213
E.2.4 Optional generalizations .....	221

E.2.5 Computation of scalar accuracy metrics and their importance .....	223
E.2.6 Summary of relevant MGRF statistical terminology/symbology .....	228
E.3 Adjustability of the MGRF (product) .....	230
E.3.1 Adjustment of a product .....	230
E.3.1.1 Solution/algorithm overview .....	231
E.3.1.2 Alternate solution approach: optimal and recommended .....	235
E.3.1.3 Correction of the product .....	236
E.3.2 Generalization to the fusion of products .....	237
E.3.2.1 Relevant modifications: bilinear interpolation assumed .....	237
E.3.2.2 Relevant modifications: expanded adjustment vector assumed .....	239
E.3.2.3 Relevant modifications for the correction of products .....	240
E.3.2.4 Ancillary and detailed comments/recommendations .....	240
E.3.2.5 Fusion example .....	242
E.4 Concept of Operations using MGRF with examples .....	247
E.4.1 Examples of MGRF-based realizations of errors associated with instances of the product ...	248
E.4.2 Overview of Concept of Operations .....	252
E.4.2.1 Alternate Concepts of Operations .....	255
E.4.2.2 Relationships of the MGRF with accuracy assessments and GPM .....	255
E.5 Recommended MGRF content-format associated with a geolocation product .....	257
E.5.1 Metadata example .....	259
E.6 Summary .....	263
Appendix F: Pseudo-code for the generation of MGRF derived statistics .....	264
F.1 Printed output example .....	267
F.2 Pseudo-code .....	272
Appendix G: Melted Roof-top Edges, Crop/forest Anomalies, and General Production anomalies .....	291
G.1 Melted Roof-Top Edges .....	291
G.2 Crop/Forest Anomalies .....	292
G.3 General Production Anomalies .....	293
Appendix H: Alternate methods for the generation of ground truth .....	293

# 1 Scope

This Technical Guidance Document (TGD) 2f is a specific topic document on External Data and its Quality Assessment, and one of a series of information and guidance documents regarding Accuracy and Predicted Accuracy in the National System for Geospatial Intelligence (NSG). As the title suggests, it focuses on methods, practices and applications for assessing the quality of External Data in the NSG within the context of a larger scope of work which includes a more generalized overview and additional topic specific technical guidance. Documents in this series are listed below:

TGD 1	Accuracy and Predicted Accuracy in the NSG:	Overview and Methodologies
TGD 1-G	Accuracy and Predicted Accuracy in the NSG:	Glossary of Terms
TGD 2a	Accuracy and Predicted Accuracy in the NSG:	Predictive Statistics
TGD 2b	Accuracy and Predicted Accuracy in the NSG:	Sample Statistics
TGD 2c	Accuracy and Predicted Accuracy in the NSG:	Specification and Validation
TGD 2d	Accuracy and Predicted Accuracy in the NSG:	Estimators and their Quality Control
TGD 2e	Accuracy and Predicted Accuracy in the NSG:	Monte-Carlo Simulation
TGD 2f	Accuracy and Predicted Accuracy in the NSG:	External Data and its Quality Assessment

All documents in the series, “Accuracy and Predicted Accuracy in the NSG”, are intended to provide technical guidance to inform the development of geospatial data accuracy characterization for NSG GEOINT collectors, producers and consumers -- accuracy characterization as required to describe the trustworthiness of geolocations for defense and intelligence use and to support practices that acquire, generate, process, exploit, and provide geolocation data and information based on geolocation data. Today, both the sources and desired uses for geospatial data are quickly expanding. Throughout the NSG, trusted conveyance of geospatial accuracy is broadly required for a variety of traditional and evolving missions including those supported by manual, man-in-the-loop, and automated processes. This guidance is the foundation layer for a collection of common techniques, methods, and algorithms ensuring that geospatial data within the NSG can be clearly requested, delivered and evaluated as fit for desired purpose whether by decision makers, intelligence analysts, or as input to further processing techniques.

TGD 2f contains references to and is referenced by other Technical Guidance Documents. The documents in this series, TGD 1, TGD 2a - TGD 2e, also have cross-references among themselves. All Technical Guidance Documents also reference external public as well as “NGA approved for public release” documents for further insight/details. While each individual document contains definitions for important relevant terms, TGD 1-G compiles all important terms and respective definitions of use particular to this series of documents to ensure continuity and provide ease of reference.

The TGD 2 documents, including this document focused on External Data and its Quality Assessment, are also considered somewhat top-level in that they are not directed at specific systems. They do provide general guidance, technical insight, and recommended algorithms. The relationship of the Technical Guidance Documents with specific GEOINT Standards documents and specific Program Requirements documents is presented in Figure 1-1, where arrows refer to references. That is, in general, specific product requirement documents reference specific GEOINT standards documents which reference specific technical guidance documents.

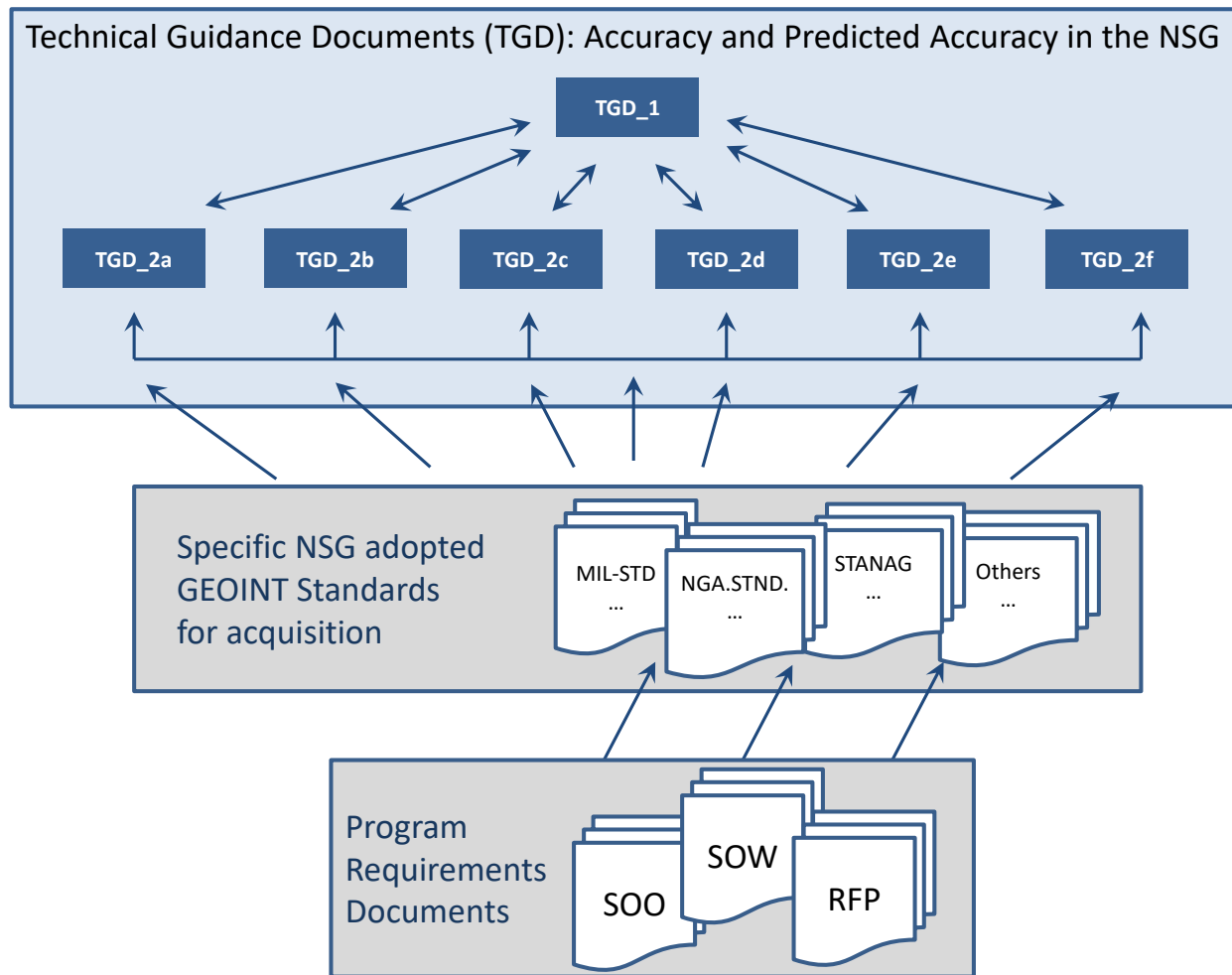


**Figure 1-1:** The relationships between the Technical Guidance Documents, GEOINT Standards Documents, and Program Requirement Documents

Accuracy and Predicted Accuracy in the NSG: External Data and its Quality Assessment, Technical Guidance Document (TGD) 2f is for guidance only and cannot be cited as a requirement.

## 2 Applicable Documents

The documents listed below are not necessarily all of the documents referenced herein, but are those needed to understand the information provided by this information and guidance document.

## **2.1 Government specifications, standards, and handbooks**

NGA.SIG.0026.01\_1.0\_ACCOVER, Accuracy and Predicted Accuracy in the NSG: Overview and Methodologies, Technical Guidance Document (TGD) 1

NGA.SIG.0026.02\_1.0\_ACCGLOS, Accuracy and Predicted Accuracy in the NSG: Glossary of Terms, Technical Guidance Document (TGD) 1-G

NGA.SIG.0026.03\_1.0\_ACCPRED, Accuracy and Predicted Accuracy in the NSG: Predictive Statistics, Technical Guidance Document (TGD) 2a

NGA.SIG.0026.04\_1.0\_ACCSAMP, Accuracy and Predicted Accuracy in the NSG: Sample Statistics, Technical Guidance Document (TGD) 2b

NGA.SIG.0026.05\_1.0\_ACCSPEC, Accuracy and Predicted Accuracy in the NSG: Specification and Validation, Technical Guidance Document (TGD) 2c

NGA.SIG.0026.06\_1.0\_ACCESQC, Accuracy and Predicted Accuracy in the NSG: Estimators and their Quality Control (TGD) 2d

NGA.SIG.0026.07\_1.0\_ACCMTCO, Accuracy and Predicted Accuracy in the NSG: Monte-Carlo Simulation, Technical Guidance Document (TGD) 2e

### 3 Definitions

There are a number of authoritative guides as well as existing standards within the NSG and Department of Defense for definitions of the identified key terms used in this technical guidance document. In many cases, the existing definitions provided by these sources are either too general or, in some cases, too narrow or dated by intended purposes contemporary to the document's development and publication. The definitions provided in this document have been expanded and refined to explicitly address details relevant to the current and desired future use of accuracy in the NSG. To acknowledge the basis and/or lineage of certain terms in Section 3.1, we reference the following sources considered as either foundational or contributory:

- [a] Anderson, James M. and Mikhail, E., *Surveying: Theory and Practice*, 7<sup>th</sup> Edition, WCB/McGraw-Hill, 1998.
- [b] DMA-TR-8400.1, DMA Technical Report: Error Theory as Applied to Mapping, Charting, and Geodesy.
- [c] Defense Mapping Agency, *Glossary of Mapping, Charting, and Geodetic Terms*, 4<sup>th</sup> Edition, Defense Mapping Agency Hydrographic/Topographic Center, 1981.
- [d] ISO TC/211 211n2047, Text for ISO 19111 Geographic Information - Spatial referencing by coordinates, as sent to the ISO Central Secretariat for issuing as FDIS, July 17, 2006.
- [e] Joint Publication (JP) 1-02, Department of Defense Dictionary of Military and Associated Terms, November 8, 2010 as amended through January 15, 2016.
- [f] MIL-HDBK-850, *Military Handbook: Glossary of Mapping, Charting, and Geodetic Terms*, January 21, 1994.
- [g] MIL-STD-2401, Department of Defense Standard Practice; Department of Defense World Geodetic System (WGS), January 11, 1994
- [h] MIL-STD-600001, Department of Defense Standard Practice; Mapping, Charting and Geodesy Accuracy, February 26, 1990.
- [i] *National System for Geospatial Intelligence* [Brochure] Public Release Case #15-489.
- [j] NGA.STND.0046\_1.0, *The Generic Point-cloud Model (GPM): Implementation and Exploitation*, Version 1.0, October 03, 2015.
- [k] Oxford Dictionaries ([www.oxforddictionaries.com/us/](http://www.oxforddictionaries.com/us/)) copyright © 2016 by Oxford University Press.
- [l] Soler, Tomas and Hothem, L., "Coordinate Systems Used in Geodesy: Basic Definitions and Concepts", *Journal of Surveying Engineering*, Vol. 114, No. 2, May 1988.

### 3.1 Key Terms Used in the Document

#### 3.1.1 Accuracy

The range of values for the error in an object's metric value with respect to an accepted reference value expressed as a probability. See Appendix A for a more detailed and augmented definition. [f]

### **3.1.2 Accuracy Assessment Model**

A collection of sample statistics that, when populated, characterize the geolocation accuracy or sensor measurement accuracy of a specific data/product or a collection of data/products that correspond to the same type, such as an image/metadata or a geolocation product from a specific provider, date-range, etc.

There are two categories of Accuracy Assessment Models: (1) Geolocation Product and (2) Geolocation Data. The former corresponds to geolocation products per se, such as 3d Point Clouds, and the latter corresponds to geolocation data that can be used to generate geolocation products, such as an image and its metadata. A populated Accuracy Assessment model is typically used for the population of a Predicted Accuracy Model.

### **3.1.3 Commodities**

In the context of this document, data/products that can be obtained, typically through purchase, from a public source.

### **3.1.4 Crowd-sourcing**

The process of obtaining data, in particular geospatial data, via individual contributions from a large group of people such as an online community, typically on a volunteered basis.

### **3.1.5 Data/product realization**

A realization or instance of a data/product that corresponds to a specific and specified type of data/product that is geolocation-related, and is sometimes simply referred to as a data/product. The type of data/product typically corresponds to External Data relative to the NSG, and its Quality Assessment is of particular interest. The combination of both “data” and “product” in the term “data/product” corresponds to either a geolocation product, such as a 3d Point Cloud, or to data, such as an image and its metadata, from which geolocations may be computed.

- An example of a relevant type of data/product are 3d Point Clouds from a specified provider, generated within a specified date-range, and using a specified underlying data/generation technique, such as LIDAR.
- A data/product realization can be further subcategorized as arbitrary or specific, the latter corresponding to a specific data/product that was already generated and available.

### **3.1.6 Empirical Quality Model**

A combination of accuracy assessment and predicted accuracy for a Crowd-sourced geolocation-related data/product.

### **3.1.7 Error**

The difference between the observed or estimated value and its ideal or true value. See Appendix A for a more detailed and augmented definition. [f]

### **3.1.8 External Data**

In the context of this document, External Data is geospatial data that is obtained by purchase or openly available public sources. Outsourced data, Commodities data, and crowd-sourced data are examples of External Data.

### **3.1.9 Ground Truth**

The reference or (assumed) true value of a geolocation of a measured quantity (e.g. associated with an absolute geolocation, or a relative mensuration).

### **3.1.10 Metadata**

Higher level or ancillary data describing a collection of data, e.g., the sensor support data corresponding to an image, which specifies corresponding sensor position, attitude, interior orientation parameters, etc.

### **3.1.11 Mixed Gaussian Random Field (MGRF)**

An MGRF is the core component of a predicted accuracy model for Commodities-based geolocation products, such as 3d Point Clouds. It provides for the predicted accuracy for each geolocation in the product in a rigorous yet practical manner requiring a relatively small amount of corresponding metadata or its equivalent. It also allows for variation of predicted accuracy across various portions of the product.

An MGRF consists of a collection or “mixture” of specified Gaussian distributed random fields, their defining predictive statistics, a subcategorization or mapping of the random fields to different partitions across the product, and the approximate *a priori* probability of the partitions that sum to 1. Partitions are defined by textual description. MGRF content allows for the rigorous computation of the predicted accuracy for a geolocation either known to correspond to a particular partition or to an unknown or arbitrary partition.

### **3.1.12 National System for Geospatial Intelligence (NSG)**

The operating framework supported by producers, consumers or influencers of geospatial intelligence (GEOINT). Spanning defense, intelligence, civil, commercial, academic and international sectors, the NSG contributes to the overall advancement of the GEOINT function within the strategic priorities identified by the Functional Manager for Geospatial Intelligence in the role established by Executive Order 12333. The framework facilitates community strategy, policy, governance, standards and requirements to ensure responsive, integrated national security capabilities. [i]

### **3.1.13 Outsourced Data**

Data obtained through purchase (contract) which may be contingent on specified collection or production criteria.

### **3.1.14 Predicted Accuracy**

The range of values for the error in a specific object’s metric value expressed as a probability derived from an underlying and accompanying detailed statistical error model. See Appendix A for a more detailed and augmented definition.

### 3.1.15 Predicted Accuracy Model

A collection of predictive statistics that characterize the geolocation accuracy or related sensor measurement accuracy in an arbitrary data/product of a specified type. When a populated Predicted Accuracy Model is assigned to a specific data/product, it becomes its predicted accuracy.

There are two categories of Predicted Accuracy Models: (1) Geolocation Product and (2) Geolocation Data, the latter subcategorized by sensor-space and measurement-space. A Predicted Accuracy Model is typically populated based on a corresponding populated accuracy assessment model.

### 3.1.16 Predictive Statistics

Statistics corresponding to the mathematical modeling of assumed *a priori* error characteristics contained in a statistical error model.

### 3.1.17 Quality Assurance

The maintenance of a desired level of quality in a service or product, especially by means of attention to every stage of the process of delivery or production. [k]

### 3.1.18 Quality Assessment

Processes and procedures intended to verify the reliability of provided data and processes, typically performed independent of collection or production. For example, if ground truth is available, then comparison of actual (sample) errors to predicted errors (statistical values via rigorous error propagation) is a key part of this process.

### 3.1.19 Sample Statistics

Statistics corresponding to the analysis of a collection of physical observations, a sample of the population, as compared to an assumed true or an *a priori* value.

### 3.1.20 Sensor Model

A sensor model for a data/product provides the ground-to-data/product relationship or correspondence. For example, if the data/product is an image, it provides the ground-to-image correspondence: given a 3d ground location input, it outputs the corresponding image location or coordinate. This correspondence is a mathematical function, such as a ground-to-image polynomial which is also invertible, i.e., given an image location and an assumed elevation, it provides the corresponding horizontal ground location assuming representation of geolocations in a Local Tangent Plane Coordinate System.

The above sensor model is a “basic sensor model”. When adjustable parameters are included that represent errors in the sensor model due to underlying data/product metadata (e.g. sensor pose) as well as the *a priori* predicted accuracy corresponding to those errors, the sensor model is termed a “complete sensor model”. When its adjustable parameters explicitly correspond to physical parameters associated with the sensor and its metadata, the sensor model is termed a “complete physical” sensor model.

A complete sensor model is typically and simply termed a sensor model. If a sensor model is not complete, it is termed a basic sensor model.

A Community Sensor Model (CSM) is a particular API for a sensor model and its associated functionality.

### 3.1.21 Scalar Accuracy Metrics

Convenient one-number summaries of geolocation accuracy and geolocation predicted accuracy expressed as a probability: (1) Linear Error (LE) corresponds to 90% probable vertical error, (2) Circular Error (CE) correspond to 90% probable horizontal radial error, and (3) Spherical Error (SE) corresponds to 90% spherical radial error. See Appendix A for a more detailed and augmented definition. [b], [f], [h]

### 3.1.22 Quality Assessment Summary

A file/report summarizing the Quality Assessment results for a specific type of geolocation-related data/product.

## 3.2 Other Relevant Terms

Appendix A contains definitions of the following additional terms relevant to the content of this document:

- *A priori*
- *A posteriori*
- Absolute Horizontal Accuracy
- Absolute Vertical Accuracy
- Accuracy (augmented definition)
- Bias Error
- CE-LE Error Cylinder
- Circular Error (CE)
- Confidence Ellipsoid
- Confidence Interval
- Correlated Error
- Correlated Values
- Covariance
- Cross-covariance Matrix
- Degree of freedom
- Deterministic Error
- Elevation
- Error (augmented definition)
- Fusion
- Linear Error (LE)
- Local Tangent Plane Coordinate System
- Mean-Value
- Monte-Carlo Simulation
- Multi-Image Geopositioning (MIG)
- Multi-State Vector Error Covariance Matrix
- Predicted Accuracy (Augmented definition)
- Principal Matrix Square Root
- Probability density function
- Probability distribution
- Probability distribution function (cdf)
- Radial Error
- Random Error
- Radom variable
- Random Error Vector
- Random Field
- Random Variable
- Random Vector
- Realization
- Relative Horizontal Accuracy
- Relative Vertical Accuracy
- Scalar Accuracy Metrics (augmented definition)
- Spatial Correlation
- Spherical Error (SE)
- Standard Deviation
- State Vector
- State Vector Error
- Statistical Error Model
- Stochastic Process

- Strictly positive definite correlation function (spdcf)
- Temporal Correlation
- Uncorrelated Error
- Variance

### 3.3 Abbreviations and Acronyms

Abbreviation/Acronym	Definition
1d	One dimension
2d	Two dimensions
3d	Three dimensions
AOI	Area of Interest
API	Application Program Interface
cdf	cumulative (probability) distribution function
CE	Circular error
DEM	Digital Elevation Model
dof	Degrees of freedom
DSM	Digital Surface Model
EO	Electro-optical
FMV	Full Motion Video
GEOINT	Geospatial Intelligence
GPM	Generic Point-Cloud Model
LIDAR	Light Detection and Ranging
LOS	Line-of-sight
MIG	Multi-Image geopositioning
NSG	National System for Geospatial Intelligence
pdf	probability density function
QA	Quality assurance
QC	Quality control
RPC	Rational Polynomial Coefficient sensor model
RSM	Replacement Sensor Model
s/w	Software or “code”
TGD	Technical Guidance Document
WLS	Weighted Least Squares

## 4 Introduction to External Data and its Quality Assessment in the NSG

This document presents an overview and detailed recommendations for External Data and its Quality Assessment in the NSG, and is part of the Technical Guidance Document (TGD) series, *Accuracy and Predicted Accuracy in the NSG*. It references other documents in this series where appropriate.

The NSG is becoming increasingly more reliant on External Data: ranging from “semi-external” outsourcing of tasks, to Commodities and Crowd-sourcing data. For the latter two, assessing accuracy and quality (reliability) is and will continue to be challenging, as detailed metadata and pedigree may be nil or unreliable, particularly so for Crowd-sourcing data. Outsourced data is usually generated against an NSG-supplied specification of performance requirements. The challenge is to continuously ensure, as best as possible, that the product requirements are being met without formal and expensive (re)testing.

Figure 4-1 is a graphical depiction of the overall process of accuracy and Quality Assessment of External Data in the NSG. This overall process is addressed in this document, but is limited to “geolocation” data/products and corresponding quality and geolocation accuracy.

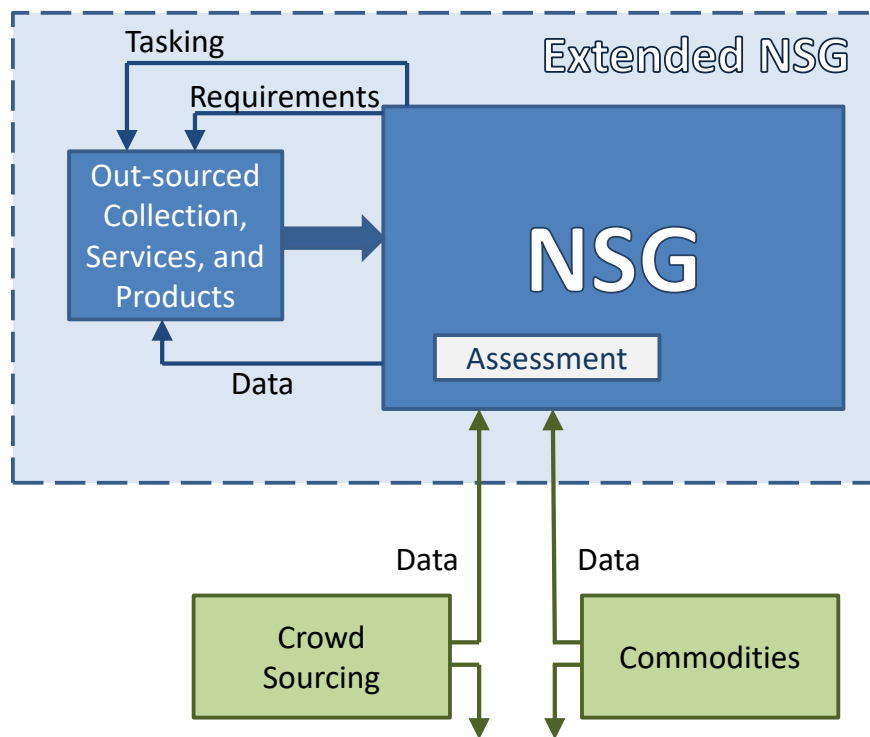


**Figure 4-1: Functional flow of External Data into the NSG**

### 4.1 Outsourcing

For outsourcing, some Quality Assurance (QA), as opposed to simply Quality Assessment, of the outsourced product is typically built-in to the requirements for the particular outsourcing contract. However, the “tasking” module within the NSG would like more confidence regarding the Quality

Assurance (QA) and corresponding Quality Control (QC) for each specific product delivered without the expense and delay of detailed testing on a per product-delivery basis. A recommended approach is to include in the requirements that the data for internal QC checks be delivered by the contractor along with the nominal product, so as to ensure that these checks were indeed performed by the contractor (or at least the required internal metrics were generated). In addition, the NSG tasking module can review these results with appropriate feedback to the contractor, if necessary.

Of course, the specific QA/QC internal metrics vary with the type of outsourced product. As an example, for an outsourced image registration task involving a large number of overlapping images (aka “triangulation” or “bundle adjustment”), internal metrics could include detailed shear statistics (not just a one or two number summary per stereo model), detailed y-parallax statistics, number and distribution of tie points used, and various (WLS batch) estimator internal performance metrics, such as the measurement residual Chi-Square value, values of the various parameter corrections normalized by their *a priori* error covariance, internal measurement editing results, etc. These types of metrics can ensure that the solution is at least internally consistent. See TGD 2d (Estimators and their Quality Control) and its “easy-to-read” summary [5] for additional details.

Both the generation of requirements for contractor-generated QC metrics and the operational review of corresponding populated metrics by the tasking module is recommended to be performed on a per-NSG organization basis, i.e., implemented by each organization that performs outsourcing. Further details are not in the charter of this document, and correspondingly, Outsourcing is not discussed further in this document.

## 4.2 Quality Assessment

The Quality Assessment of externally generated data, such as Commodities and Crowd-sourcing data, is more difficult, as the NSG has virtually no control of the data generation and its internal QA processes, if any. In addition, the range of data is virtually unlimited, and includes: (1) Small-Sat imagery, (2) 3d Point Clouds, and (3) Crowd-sourcing Digital Maps, for example. A recommended top-level approach to NSG Quality Assessment is presented in Figure 4.2-1:

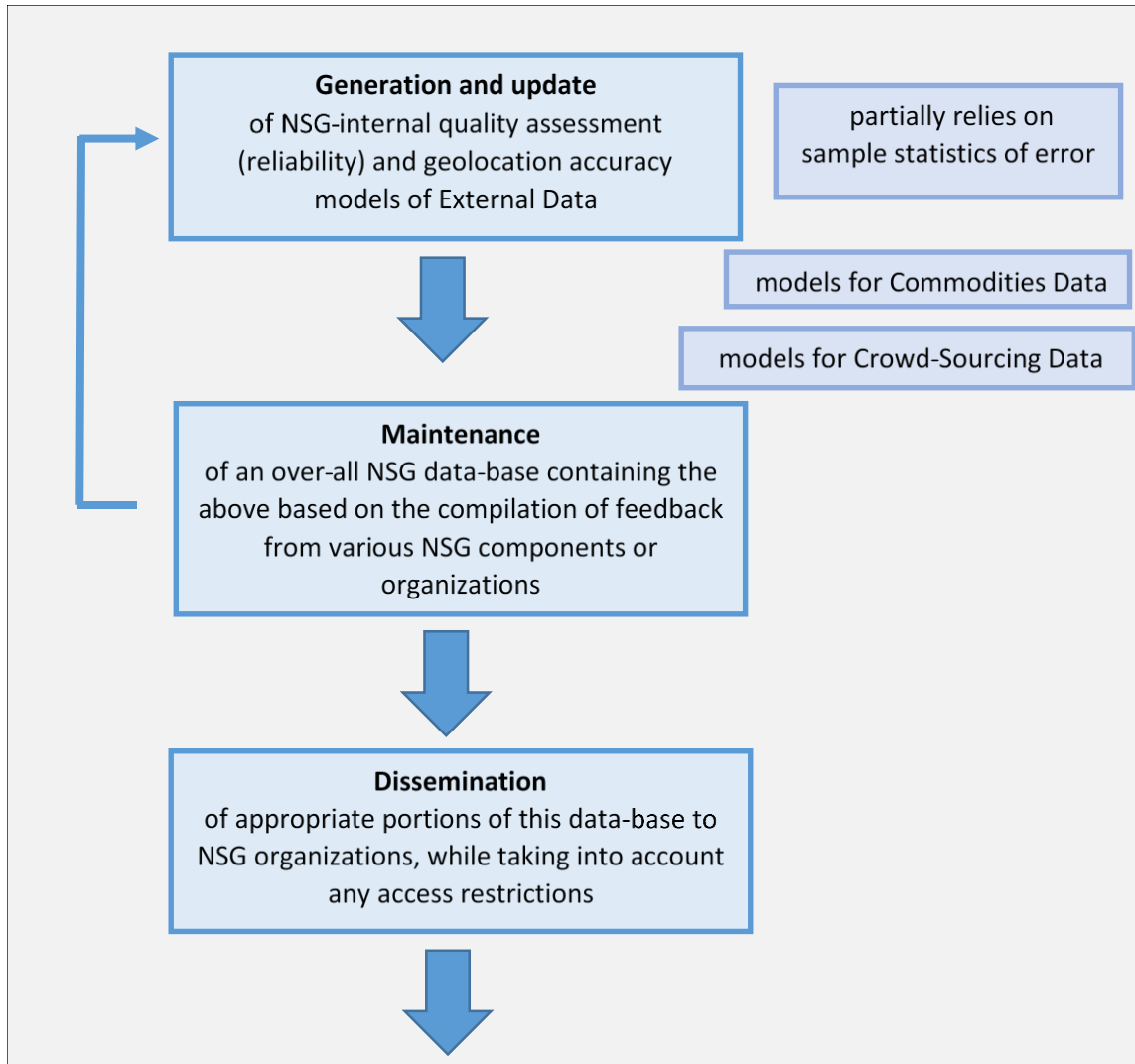


**Figure 4.2-1:** Recommended top-level approach to NSG Quality Assessment of External Data

The above reflects population of a different set of models depending on whether the External Data corresponds to Commodities data or to Crowd-sourcing data. This is due to the latter's extreme lack of pedigree, wide variations in quality over specific data/products, and propensity for data/products to be both incomplete and contain blunders. Therefore, details regarding quality in general are of more concern for Crowd-sourcing data/products than are relatively high-fidelity assessments and predictions regarding geolocation accuracy per se; hence, population of empirical quality models are performed for Crowd-sourcing data instead of population of accuracy assessment and predicted accuracy models performed for Commodities data.

As detailed later in this document and relevant to Commodities data, populated accuracy assessment models are based on sample statistics of geolocation error from specific data/products. The samples of geolocation error are based on comparisons of the data/product to overlapping ground truth.

Populated predicted accuracy models contain predictive statistics of error applicable to arbitrary data/products from a specified type or class of data/product. They are typically initialized and subsequently “tuned” using populated accuracy assessment models corresponding to the same specified type or class of data/product. For example, EO-generated 3d Point Clouds from vendor “abc”, in date-range “123”, etc.

The sample statistics contained in a populated empirical quality model for Crowd-sourcing data may include sample/predictive statistics of geolocation error (typically of lesser fidelity due to the non-availability of accurate ground truth), but also include sample statistics concerning completeness of data, blunders, etc. The sample statistics are typically based on comparisons of overlapping data/products (e.g., digital maps) between multiple collectors, such as OpenStreetMap, Wikimapia, Google MyMaps, etc. A populated empirical quality model corresponds to a specified type or class of Crowd-sourcing data.

The general task of Quality Assessment and accuracy prediction of External Data used by the NSG requires additional applied research. However, what we currently “know”, related issues, and what we recommend are detailed in Section 5 of this document. As these recommendations are implemented and more experience and knowledge gained throughout the NSG, these recommendations will be modified accordingly. A guide to Section 5 of the document is presented in Section 4.3 below.

### **4.3 Intended Audience and Detailed Guide to the Document**

This section of the document presents various guides and related information regarding the remainder of the document:

#### **4.3.1 Intended Audience**

The topics addressed in the remainder of this document include the following and their intended audience:

1. The management of Quality Assessment in the NSG by a central organization and/or individual organizations in the NSG
  - a. Intended audience includes:
    - i. Managers, technical managers, and/or operational managers
    - ii. Developers of corresponding top-level functionality (s/w engineers)
2. The assessment of the accuracy of a specific type or class of geolocation product (e.g., 3d Point Cloud) or geolocation data (e.g. image) and the population of a corresponding predicted accuracy model
  - a. Intended audience: individual or small groups of scientists, analysts, and/or developers
3. The optimal use of the geolocation data/product based on a populated predicted accuracy model
  - a. Intended audience: the previous audience plus “down-stream” users/applications

The above addresses External Data – Commodities as well as Crowd-sourcing. The above topics and the development of corresponding capabilities are intended to “flow-down” in numerical order, i.e., from 1 to 3. However, if need be, topics 2 and 3 can be carried out independent of topic 1 but on a necessarily smaller scale.

#### 4.3.2 Overall Guide

Table 4.3.2-1 presents an overall guide to this document. In particular, Section 5 which addresses Quality Assessment, and more specifically, the reliability and geolocation accuracy of geolocation data and products. Section 6 and Section 7 are also included, which contain notes and references, respectively.

**Table 4.3.2-1:** Overall guide to sections

Section	abbreviated title	Comments
Section 4	Overview of External Data and its Quality Assessment	assumed already read
Section 5:	Methodology and Algorithms	overall title to the following:
Section 5.1	Quality Assessment Overview	presents an overview of Quality Assessment
Section 5.2	Quality Assessment Management	describes the Quality Assessment Management function
Section 5.3	Quality Assessment Analysis	describes the Quality Assessment Analysis function details models for population: Accuracy Assessment, Predicted Accuracy, and Empirical Quality; describes population of models and applications
Section 5.4	Summary	key "takeaways" recommended applied research
Section 6	Notes	
Section 7	References	

As a reminder, and as stated previously at the end of Section 4.1, Outsourcing is not discussed further in this document consistent with the document's charter. Only details of Quality Assessment are applicable and discussed further per the above guide to the document.

In addition, a number of appendices are also available containing supporting details and summarized in Table 4.3.2-2:

**Table 4.3.2-2:** Overall guide to appendices

Appendix	abbreviated title	Comments
A	Additional terms and definitions	Subset of glossary
B	Geolocation Product Accuracy Models - the basics	Details the population of accuracy assessment and predicted accuracy models and their use for Geolocation Products (e.g., 3d Point Clouds)
C	Geolocation Data Accuracy Models - the basics	Details the population of accuracy assessment and predicted accuracy models and their use for Geolocation Data (e.g., images and their metadata)
D	Adjustment of Geolocation Data	Details the adjustment of geolocation data (an image and its metadata) for improved accuracy based on a populated predicted accuracy model and control information (e.g. ground control points)
E	MGRF representation and adjustment of Geolocation Products	Details a Mixed Gaussian Random Field (MGRF) as an optional but recommended core component of a predicted accuracy model for Geolocation Products (e.g., 3d Point Clouds); also details adjustment of Geolocation Products for improved accuracy
F	Pseudo-code for MGRF	Pseudo-code for the computation of MGRF predictive statistics and corresponding metadata
G	MGRF partitions	Descriptions of MGRF "anomalous" partitions; e.g., "melted roof-top edges"
H	Ground truth alternate generation	Alternate methods for the generation of ground truth

### 4.3.3 Practical Guide

The following presents practical guides to this document per the readers' assumed general interests:

#### Managers, Technical Managers, and Operational Managers:

Table 4.3.3-1 presents an outline of all of the sections in this document recommended to managers or those less interested in technical details (subsections appended with \* are recommended as optional):

**Table 4.3.3-1:** Practical Guide for Operations and Technical Managers (\* optional)

<b>Recommended Section</b>	<b>abbreviated title</b>	<b>Recommended Subsections</b>	<b>abbreviated titles</b>
<b>Section 4</b>	<b>Overview of External Data and its Quality Assessment</b>	all of its subsections; assumed already read	...
<b>Section 5.1</b>	<b>Quality Assessment Overview</b>	all of its subsections	...
<b>Section 5.2</b>	<b>Quality Assessment Management</b>	all of its subsections	...
<b>Section 5.3</b>	<b>Quality Assessment Analysis</b>	following subsections: 5.3.1	Accuracy and Pred Accuracy Models and Interrelationships for Commodities Data
		5.3.1.1	relationship to sensor model
		5.3.1.2	importance of pred acc model
		5.3.5*	Analysis Techniques
		5.3.5.1*	ground truth
		5.3.5.2*	sample error statistics
		5.3.5.3*	real-world example
		5.3.6	Emperical Quality Model for Crowd-Sourcing Data
<b>Section 5.4</b>	<b>Summary</b>	subsections: 5.4.1 5.4.2	Key "takeways" Recommended Applied Research

**Scientists, Analysts, Developers and others interested in technical details:**

For those readers interested in technical and development details, the entire main body of the document is recommended and those Appendices (or their subsections) as referenced therein and per the reader's specific interests (see Tables 4.3.2-1 and 4.3.2-2). Those interested in technical and development details may include "down-stream" users of geospatial data/products and the developers of corresponding applications.

#### 4.3.4 Top-level terminology and what the document does not address

Finally, as reflected in the above guides, the charter of this document is the Quality Assessment of geospatial information, and primarily geolocation information. For example, and in reference to “geolocation” information versus the more general term “geospatial” information:

- “geolocation” information:
  - The geolocations (points) and their accuracy and predicted accuracy in a 3d Point Cloud correspond to “geolocation” information in a geolocation product.
  - The image locations (line,sample) and their accuracy and predicted accuracy in an image correspond to “geolocation” information in geolocation data.
    - This data can be subsequently used for the generation of geolocations per se and for the corresponding propagation of predicted accuracy to ground-space.
      - Corresponding image locations are considered measurements into this generation process and their errors are considered measurement errors.
    - Image location errors primarily correspond to the effects of image metadata errors, such as errors in underlying sensor pose, etc.
- “geospatial” information:
  - Various geolocations associated with features as represented by a digital map provided by Crowd-sourcing, bounds on their accuracy and predicted accuracy, and the percent of missing features together correspond to “geospatial” information in a geolocation data/product.
- As in practice, the terms “geospatial” and “geolocation” are used somewhat interchangeably throughout the document.

The term “geolocation product” corresponds to a product per se, such as a 3d Point Cloud. The term “geolocation data” corresponds to data that is related to geolocations, such as an image and its metadata. The image includes a set of image locations.

The term “geolocation data/product” is used to represent either geolocation data or geolocation products, and is also frequently termed “data/products” throughout this document, or more specifically, “data” or “products”, as is warranted – the descriptor “geolocation” is implied. Thus, an image is data, a 3d Point Cloud is a product, and when either is applicable, a data/product. A digital map provided by Crowd-sourcing is termed a data/product as it is considered somewhat of a hybrid between data and product.

The charter of this document does not include:

- Accuracy and predicted accuracy for a general feature considered as a whole, i.e., as a collection of nodes (geolocations), edges, etc. considered together as one entity.
  - Corresponding errors include a combination of geolocation errors corresponding to the various nodes (points), interpolation errors for arbitrary geolocation along the edges between nodes, etc.

- Summary accuracy and predicted accuracy metrics for a feature and its possible attributes are defined and populated based on the underlying core principles and techniques presented in this document, including the spatial correlation of errors.
  - Accuracy and predicted accuracy metrics in reference to errors in:
    - computed feature attributes such as centroids, areas, and volumes
    - an arbitrary point's location along a building's horizontal base or polygon
  - Future applied research is recommended for their development per Section 5.4.2
- Quality Assessment of predictive analytics
  - A corresponding future technical document is recommended

## 5 Methodology and Algorithms for External Data and its Quality Assessment

### 5.1 Quality Assessment Overview

It is recommended that Quality Assessment be “managed” by one government organization in the NSG with inputs/outputs to other organizations in the NSG. It is not the charter of this document to recommend a specific organization, but the organization should have consistent funding in support of this task. If no such organization accepts this task, each NSG organization should have its own “management” function for assessment. However, this is not ideal or efficient, and the sharing of information between organizations will be more ad hoc and possibly lead to incomplete and/or inconsistent assessments.

Quality Assessment compiles information on the quality of various geospatial data and products, categorized by type of data/product, including generating organization/vendor or provider. It is recommended that the assessment consist of four types of information: (1) top-level Quality Assessment summary, (2) accuracy assessment, (3) predicted accuracy, and (4) detailed empirical quality. The top-level Quality Assessment summary is primarily qualitative as opposed to quantitative, and consists of a textual overview of the data or product and its general quality or reliability. The accuracy assessment and predicted accuracy are applicable to Commodities data and its corresponding geolocation accuracy. Detailed empirical quality is applicable to Crowd-sourcing data and its corresponding coverage, completeness, blunders, as well as low-fidelity estimates or bounds on its geolocation accuracy.

Figure 5.1-1 presents a summary of the correspondence between the types of External Data to the corresponding types of information used to represent their quality. In general, the overall amount of collective information “grows” as Quality Assessment is continuously performed in the NSG.

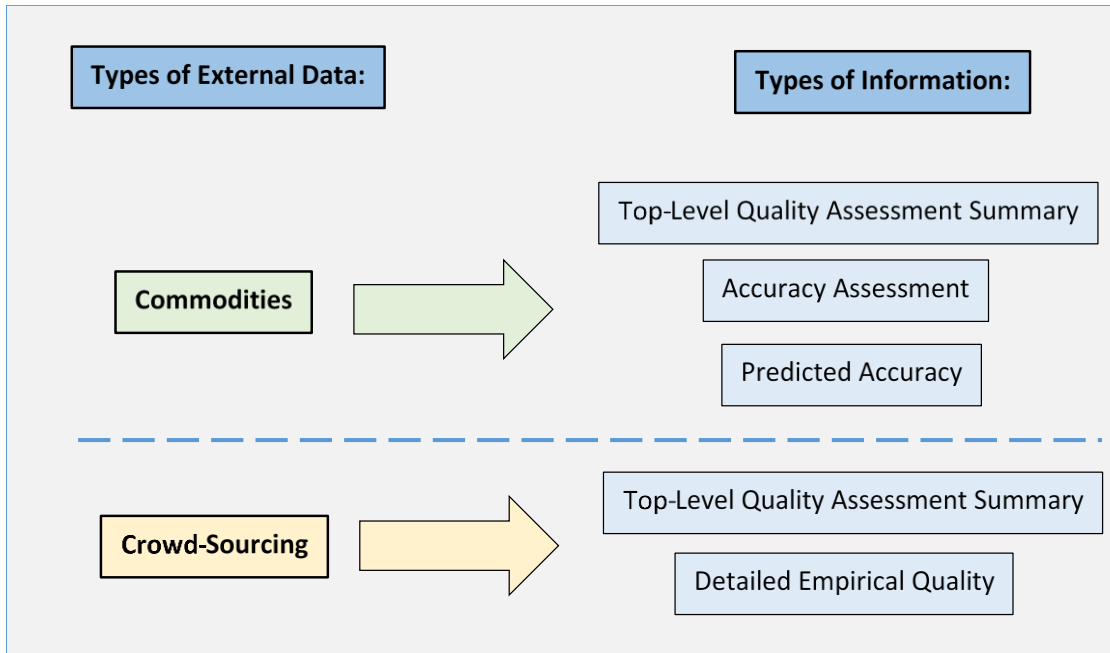


**Figure 5.1-1:** External Data-to-Information correspondence

Both accuracy assessment and predicted accuracy concern geolocation accuracy, either directly as in a 3d geolocation product, or indirectly as in the accuracy in geolocation data, such as an image and its metadata with corresponding image locations (pixels) that correspond to sensor measurements related to geolocations.

Both accuracy assessment and predicted accuracy are actually populated models, i.e., a populated accuracy assessment model and a populated predicted accuracy model, respectively, as detailed in Sections 5.3.1-5.3.3. Predicted accuracy is typically “tuned” using corresponding accuracy assessments consisting of sample statistics of geolocation error for the same type or class of data/product. Use of the subsequent populated predicted accuracy model enables optimal and informed exploitation of the corresponding data/product. In addition, even though the accuracy assessment model and the predicted accuracy model are applicable to Commodities data, they can also be applied to NSG-internally generated data/products when applicable.

A populated accuracy assessment model is based on and applicable to at least one and typically many past realizations or specific instances of the data/product from the same type or class of data/product, whereas a populated predicted accuracy model is applicable to an arbitrary realization or instance of the same type or class of data/product. The contents of the populated predicted accuracy model are predictive statistics that were typically initialized and/or “tuned” based on the sample statistics contained in the corresponding populated accuracy assessment model. The contents of the populated predicted accuracy model are recommended for inclusion in accompanying metadata or its equivalent when a data/product is made available to the user community by its provider, or thereafter, if necessary, at which time it becomes the predicted accuracy of a specific data/product.

Empirical quality is a combination of assessment and prediction regarding the quality of data/products generated by Crowd-sourcing. Empirical quality is actually conveyed as a populated empirical quality model for each general type or class of Crowd-sourcing data/product of interest, as detailed in Section 5.3.6.

The difference between one of the above models and a corresponding populated model is as follows: the model defines applicable statistics and related data, whereas the populated model includes their corresponding values. In addition, see Section 3.1 for more formal definitions of the various models as well as the definition of a data/product and its realization.

The host organization in charge of the management of the Quality Assessment task implements the Quality Assessment Management function described in Section 5.2 which is supported by the Quality Assessment Analysis function described in Section 5.3.

### 5.1.1 Examples of External Data

Prior to presenting further details, some examples of External Data are presented below as a further introduction as well as to illustrate the wide-range of corresponding data/products.

#### 5.1.1.1 Small-Sat Imagery

Figure 5.1.1.1-1 illustrates a Planet Dove Small-Sat and Figure 5.1.1.1-2 a corresponding image – a representative example of Commodities data.

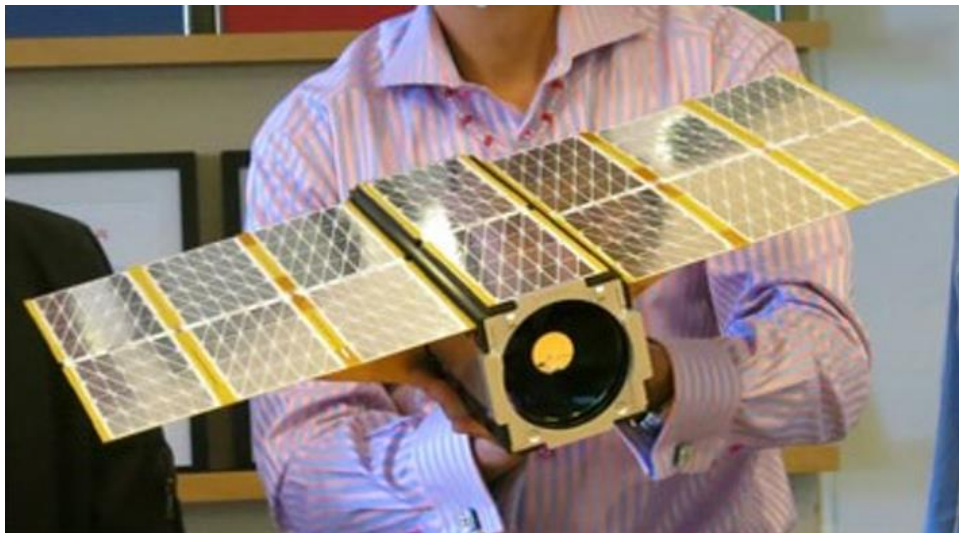


**Figure 5.1.1.1-1:** One of approximately 200 Planet Dove Small-Sats; 3-5 m ground-sample distance [1]; additional permission to use via “Source:@Year, Planet Labs Inc, Contract HM0476-18-C-0044”



**Figure 5.1.1.1-2:** Planet Dove Image of El-Alamein Egypt, Aug 28. 2016; from Planet Lab’s web-site [17]; permission to use via “Source:@Year, Planet Labs Inc, Contract HM0476-18-C-0044”

In general, a single image and its metadata (sensor pose, etc. or a ground-to-image polynomial) allow for the extraction of 3d geolocations given an external elevation, such as a DEM. However, even if an image looks “sharp”, this does not imply that the extraction of an arbitrary geolocation of a feature of interest in the image is accurate nor does it imply that there is a reasonable estimate of the accuracy available.

In addition, both absolute accuracy and relative accuracy are of interest. Typically, even if geolocation error is large corresponding to an arbitrary geolocation of interest identified and measured in the image, when that geolocation is differenced with another geolocation identified and measured in the same image, the error in their difference is typically small, such as is applicable when measuring the length of a feature such as an airport runway. The two corresponding geolocation errors are positively correlated and their common error cancels when the geolocations are differenced – the remaining or residual error corresponds to their relative error; hence, corresponding relative accuracy is typically better than absolute accuracy, at least for relatively short distances between the two geolocations.

All of the above issues are relevant to this document; in particular, the characterization and prediction of both geolocation accuracy and relative accuracy given little if any corresponding information from the image provider, as typically the case with Small-Sat imagery.

### 5.1.1.2 3d Point Clouds

Figures 5.1.1.2-1 illustrates a 3d Point Cloud – a representative example of Commodities data. An individual element in the EO-derived Point Cloud corresponds to a dot in the figure and to a specific 3d geolocation.

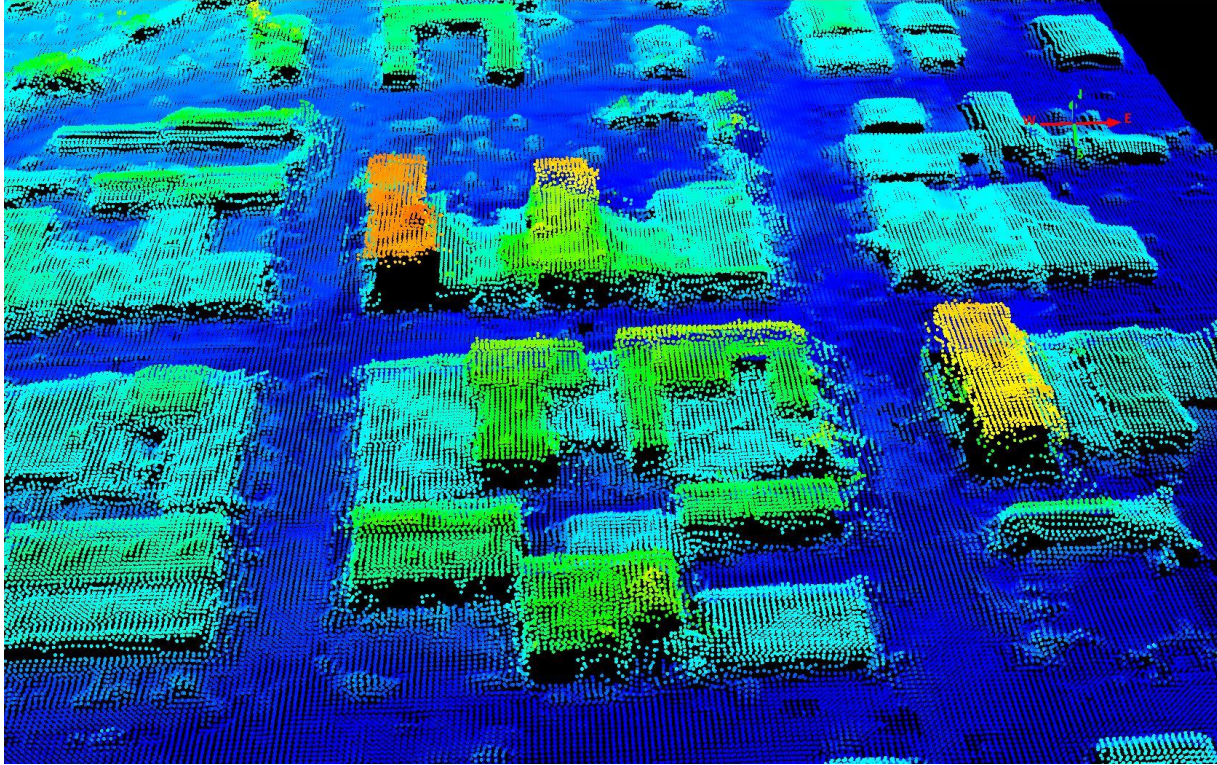


**Figure 5.1.1.2-1:** A portion of a 3d Point Cloud of an urban scene at a specific viewing orientation and zoom-factor; color-coded based on height; generated using aerial imagery from the National Agriculture Imagery Program (NAIP); public domain.

In general, geolocation accuracy degrades to varying degrees at building roof-top edges in an EO-derived Point Cloud, corresponding to “melted” roof-top edges (see Appendix G). This particular example is reasonably “well-behaved” regarding roof-top-edges; in general, a function of both the generation algorithm and the imaging geometry of the multiple images that are used to generate the Point Cloud. Multiple images with varied imaging geometry are required in order to provide “stereo” or 3d geolocation information.

Again, this document is interested in the characterization and prediction of both absolute and relative accuracy of 3d geolocations in the Point Cloud with little if any corresponding information from the provider. This time, the 3d geolocations of interest are explicitly in the data/product and correspond to each point or “dot” as opposed to being computed from an image and its metadata as in the Small-Sat example.

Figure 5.1.1.2-2 presents an example of a 3d Point Cloud derived using LIDAR instead of EO imagery; in particular, using Geiger-mode LIDAR. It is an example of a very high resolution product.

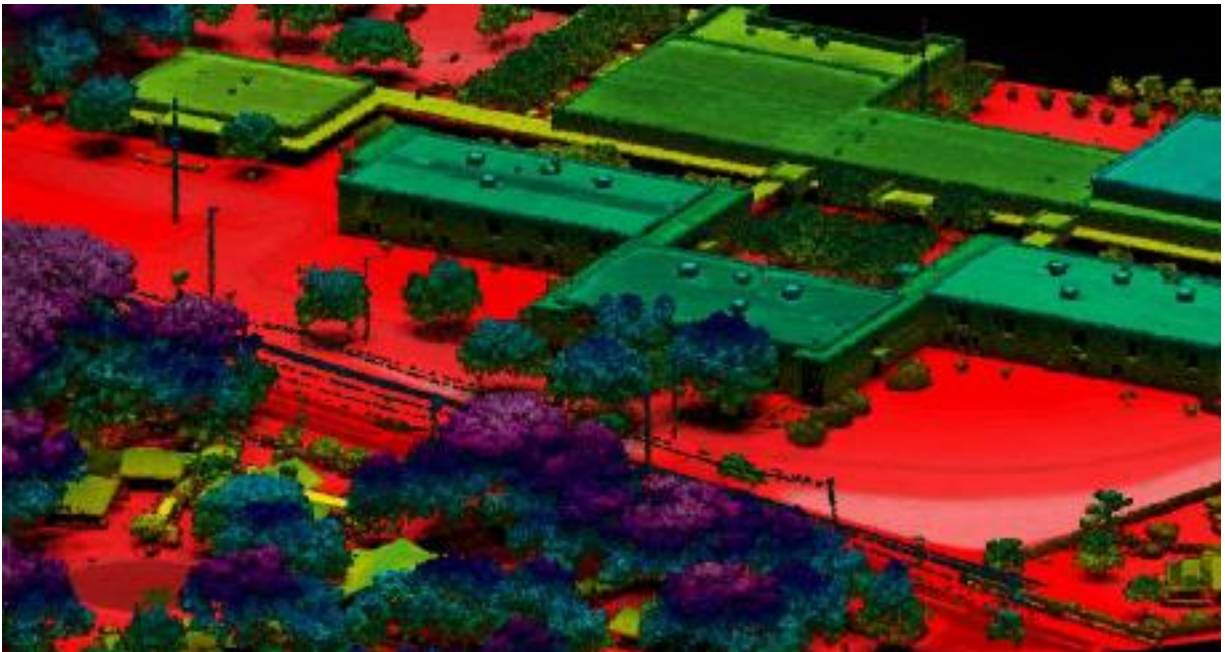


**Figure 5.1.1.2-2:** A portion of a 3d Point Cloud of an urban scene (utilities) at a specified viewing orientation and zoom-factor; color-coded based on height and intensity; Harris Geiger-mode LIDAR, permission for use courtesy of Harris Corporation

In general, LIDAR-derived 3d Point Clouds are significantly more accurate than EO-derived 3d Point Clouds, although corresponding predictions of accuracy and relative accuracy are typically not provided with products from most providers. However, “melted” roof-top edges are typically no longer an issue; that is, accuracy is typically reasonably uniform across the product. This is illustrated in the above figure.

### **5.1.1.3 Crowd-sourcing Digital Maps**

Figure 5.1.1.3-1 presents an example of a Crowd-sourcing data/product – a Digital Map from the OpenStreetMap provider. It corresponds to a region in Nepal and was generated using the publicly available OpenStreetMap service for a user-specified location and specified Area-of-Interest (AOI) or scale. It corresponds to a standard map format, without the optional overlay over imagery that was also available and without the optional printout of various keys defining annotations.

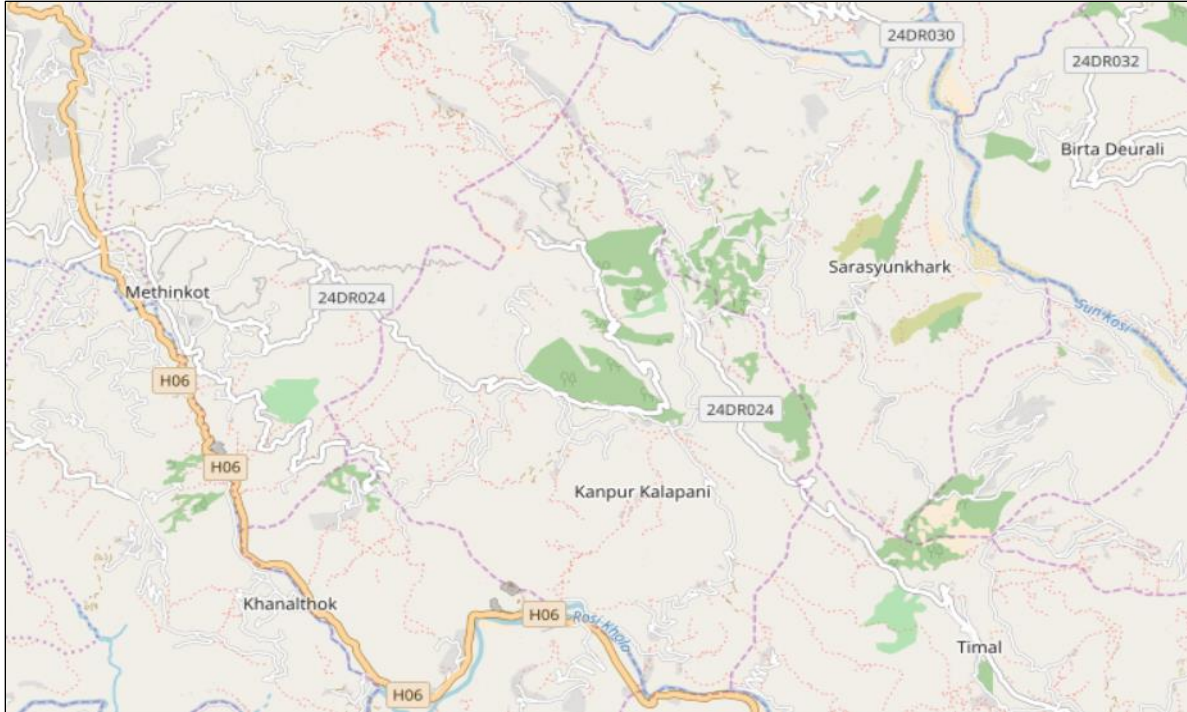


**Figure 5.1.1.3-1:** A Crowd-sourcing Digital Map via OpenStreetMap (05 July 2018) with a general-use license; an approximately 60 square mile AOI and 15 miles from downtown Kathmandu, Nepal

The Digital Map appears of reasonable quality, although we do not know: (1) its geolocation accuracy, (2) whether or not it contains all relevant features and annotations, and (3) whether or not it contains any blunders or mis-information. This is a general problem regarding the use of Crowd-sourcing data. One approach for its mitigation is the comparison of different maps from different providers over the same AOI.

However, it is also worth pointing out that Crowd-sourcing Digital Maps can be of real value in the NSG, particularly when there are no reliable standard maps of known quality over the AOI that are both available and reasonably current. For example, Crowd-sourcing Digital Maps can be invaluable during humanitarian crises with frequent updates by volunteers over the AOI.

## 5.2 Quality Assessment Management Function

The Quality Assessment Management function performs the following tasks, and is assumed implemented by the “host” NSG organization per the Section 5.1 discussion:

- 1) Receive inputs from various NSG organizations corresponding to a subset of the following:
  - a. “raw” data and products
  - b. Populated accuracy assessment models
  - c. Populated predicted accuracy models
  - d. Populated empirical quality models
- 2) Generate a subset of the following based on the “host” organization’s independent access to “raw” data and products:

- a. Populated accuracy assessment models
  - b. Populated predicted accuracy models
  - c. Populated empirical quality models
- 3) Compile, collate, integrate all of the above and compute corresponding Quality Assessment Summaries
- 4) Generate an explicit, combined, and latest overall Quality Assessment Summary, populated accuracy assessment model, populated predicted accuracy model, and populated empirical quality model for each applicable type or class (category) of geospatial data/product when possible
  - a. Include a dated history and access to (1) and (2) used to perform (3) and (4)
- 5) Provide access to all of the above to all appropriate organizations/personnel across the NSG.

In summary, the corresponding top-level charter of the Quality Assessment Management function is to provide “One-stop shopping” for the best, latest, and consistent information regarding the quality, geospatial accuracy, and geospatial predicted accuracy corresponding to the various External Data (geospatial data and products) used across the NSG.

#### **Further details and recommendations per subsection**

The following subsections go on to provide further details and recommendations regarding the Quality Assessment Management function:

- Section 5.2.1 details the content of the top-level Quality Assessment Summary (file/report); its subsections discuss:
  - The predicted accuracy summary metrics
  - The data/product reliability metric
- Section 5.2.2 cautions that Quality Assessment for some data/products may take a long time to complete
- Section 5.2.3 discusses exceptions – some data/products require minimal Quality Assessment as reliable predicted accuracy models are already available from the vendor/provider; its subsections discuss:
  - Specific examples
  - Common characteristic
- Section 5.2.4 discusses the encouragement for and potential future availability of data/product accuracy specifications from the provider; its subsections discuss related issues:
  - verification of any “advertised” accuracies from the vendor/provider
  - the need to specify and validate the accuracy of geolocation extraction tools
- Section 5.2.5 presents the top-level functional flow of the Quality Assessment Management function and its relationship with the Quality Assessment Analysis function.

Details regarding the specific implementation of the Quality Assessment Management function by the NSG “host” organization are not within the charter of this document.

### 5.2.1 Quality Assessment Summary file/report

A Quality Assessment Summary (file/report) is recommended for generation by the Quality Assessment Management function for each type or class of data/product of interest. It contains a general and primarily textual summary of the data/product as well as recommendations for its use or non-use based on the contents of populated accuracy assessment, predicted accuracy, and/or empirical quality models generated by the Quality Assessment Analysis function. The recommended content of the top-level Quality Assessment Summary is presented in Table 5.2.1-1.

**Table 5.2.1-1:** Quality Assessment Summary – recommended content (Part 1)

<ul style="list-style-type: none"> <li>• <b>Textual overview of data/product and its generation:</b> <ul style="list-style-type: none"> <li>○ Data/product type                             <ul style="list-style-type: none"> <li>• E.g., Small-Sat imagery/metadata, Digital Map: Crowd-Sourcing, etc.</li> </ul> </li> <li>○ Provider                             <ul style="list-style-type: none"> <li>• E.g., specific NSG organization, commercial vendor, Crowd-Sourcing provider, etc.</li> <li>• Links, if available</li> </ul> </li> <li>○ Applicable sensors and related generation overview</li> <li>○ Date range</li> <li>○ Geographic range or “product footprint”</li> </ul> </li> <li>• <b>Predicted Accuracy Summary Metrics:</b> <ul style="list-style-type: none"> <li>○ <b>CE90 (meters) and/or LE90 (meters)</b> or similar metrics                             <ul style="list-style-type: none"> <li>• Provided if metrics are available</li> <li>• Based on populated Predicted Accuracy Model with its corresponding confidence rating applicable as well</li> <li>• Description of geolocation extraction scenario(s) if data/product is “data” instead of a geolocation “product” per se: ... ..</li> </ul> </li> </ul> </li> <li>• <b>Recommended use/non-use of data/product:</b> <ul style="list-style-type: none"> <li>○ Data/product reliability metric                             <ul style="list-style-type: none"> <li>• Not available, or</li> <li>• Approximate <i>a priori</i> probability that an arbitrary but specific product contains some anomalous data: xx%</li> </ul> </li> <li>○ Qualifiers regarding recommended use/applications of data/product</li> <li>○ Summary of issues</li> </ul> </li> </ul>
--

**Table 5.2.1-1:** Quality Assessment Summary – recommended content (Part 2)

<ul style="list-style-type: none"> <li>• <b>Confidence in populated Accuracy Assessment Model (Commodities):</b> <ul style="list-style-type: none"> <li>○ Populated model not available</li> <li>○ Low</li> <li>○ Medium</li> <li>○ high</li> </ul> </li> <li>• <b>Confidence in populated Predicted Accuracy Model (Commodities):</b> <ul style="list-style-type: none"> <li>○ Populated model not available</li> <li>○ Low</li> <li>○ Medium</li> <li>○ high</li> </ul> </li> <li>• <b>Confidence in populated Empirical Quality Model (Crowd-Sourcing):</b> <ul style="list-style-type: none"> <li>○ Populated model not available</li> <li>○ Low</li> <li>○ Medium</li> <li>○ high</li> </ul> </li> <li>• <b>Accuracy-related metadata included with data/product from provider?</b> <ul style="list-style-type: none"> <li>○ If yes, summary of contents and available pointers/links to details</li> </ul> </li> <li>• <b>Underlying Accuracy Specification available from data/product provider?</b> <ul style="list-style-type: none"> <li>○ If yes, summary of contents and available pointers/links to details</li> </ul> </li> <li>• <b>If populated Accuracy Assessment and/or Predicted Accuracy Model available, are the summary contents of the previous two bullets compatible?</b> <ul style="list-style-type: none"> <li>○ Not applicable</li> <li>○ Yes</li> <li>○ No</li> </ul> </li> </ul>
---

The contents of the above table are primarily qualitative as opposed to quantitative which facilitates the use of the Quality Assessment Summary file/report as an easy-to-read summary or “quick guide”; however, it does “point to” further details when they are available, such as populated models, provider specifications, etc. The quality/confidence rankings of populated models included in the table are qualitative-quantitative and correspondingly labeled as “low”, “medium”, or “high”, with more definitive definitions of these ranks to be provided.

Most of the entries in the above Quality Assessment Summary table (Table 5.2-1) are self-explanatory other than: (1) “Predicted Accuracy Summary Metrics” and (2) “Data/product reliability metric” in Part 1 of the table and which are summarized as follows:

#### 5.2.1.1 Predicted Accuracy Summary Metrics

The estimated top-level values of predicted accuracy of the data/product in the Quality Assessment Summary report (Table 5.2.1-1) are expressed as scalar accuracy metrics CE90 and/or LE90 in meters if the data/product corresponds to a geolocation product per se, such as a geolocation Point Cloud. These metrics are approximate but provide convenient “bottom-line” predicted accuracies for the product. They are based on and available only if a populated predicted accuracy model is available (see Part 2 of table) which is used for their computation. Thus, they are typically unavailable if the data/product corresponds to Crowd-sourcing data.

CE90 (meters) corresponds to the radius of a circle such that, if the circle is centered at the horizontal location of an arbitrary geolocation in the product, there is an approximate 90% probability that the geolocation’s true horizontal location resides within it (Figure 5.2.1.1-1). LE90 (meters) corresponds to one-half the length of a vertical line segment centered at the vertical location of an arbitrary geolocation in the product such that there is an approximate 90% probability that the geolocation’s true vertical location resides along the line segment.

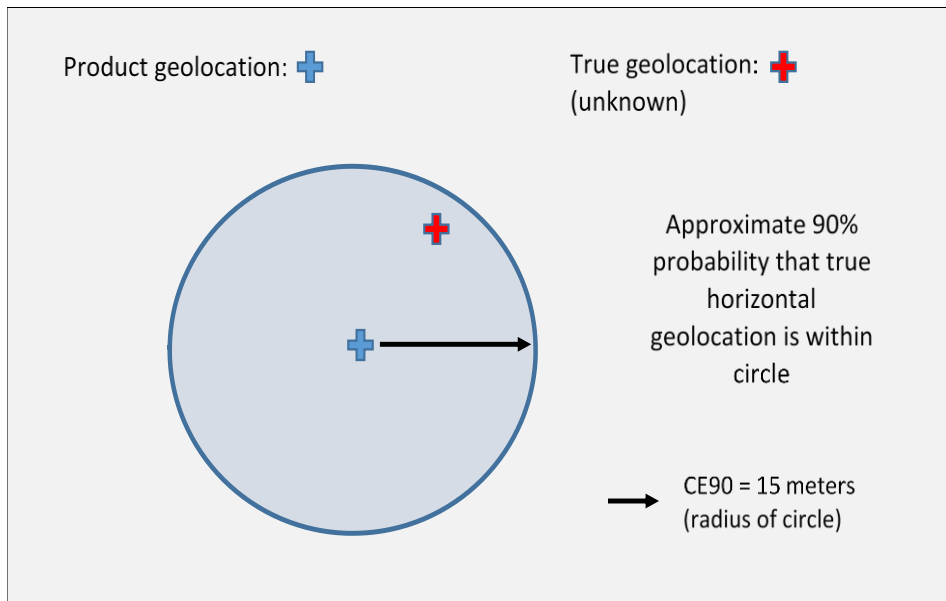


**Figure 5.2.1.1-1:** Example of CE90; value equal to 15 meters is hypothetical; geolocation coordinates assumed relative to local tangent plane coordinate system (e.g., East-North-Up)

If the data/product is data (e.g. image/metadata) instead of a product per se (e.g. 3d Point Cloud), the values of CE90 and/or LE90 are based on both a populated predicted accuracy model and an assumed and typical geolocation extraction scenario which is described in the Quality Assessment Summary as well.

For example, if the data corresponds to an image, either monoscopic (single image) extraction with external elevation source (and its predicted accuracy) or two-image stereo extraction. The approximate range of imaging angles are included as part of the overall description of the extraction scenario.

See TGD 2a (Predictive Statistics) for details on recommended methods for the Quality Assessment Management Function's computation of the Predictive Accuracy Summary Metrics, CE90 and LE90, that are contained in Table 5.2.1-1. They are computed from the predictive statistics contained in the corresponding populated predicted accuracy model. In addition, if the data/product is "data" instead of a "product", its corresponding predictive statistics are first propagated to ground-space; either directly via partial derivatives and an assumed elevation or via a "covariance-only" Multi-Image Geopositioning (MIG) solution or its equivalent if not an image. A MIG solution can actually involve one or more images and is discussed later in this document and is detailed in TGD 2d (Estimators and their Quality Control). A "covariance-only" solution only computes the solution's *a posteriori* error covariance matrix; the actual measurements used by the solution proper are immaterial.

**It must be emphasized** that although the scalar accuracy metrics that make-up the Predicted Accuracy Summary Metrics are convenient, they are only top-level summaries. Optimal and fully informed use of the data/product can only be achieved if the corresponding and much more detailed predicted accuracy model is available to the "down-stream" NSG user or application (see Section 5.3.1.2), typically via the Quality Assessment processing per this document.

Furthermore, as detailed later, a populated predicted accuracy model is typically "tuned" using a populated accuracy assessment model(s) which contains sample statistics of the error of representative data/products of the same general type or class of data/product to which the Quality Assessment Summary file/report (Table 5.2.1-1) refers.

In terms of predicted accuracy, the remainder of this document concentrates on the predicted accuracy model – its contents (predictive statistics), population, and geolocation applications. The Predicted Accuracy Summary Metrics contained in Table 5.2.1-1 are not specifically discussed in the remaining portions of this document.

### **5.2.1.2 Data/product reliability metric**

The data/product reliability metric is a scalar probabilistic-based metric defined to have a value within the interval  $[0,1]$ , or is specified as "unknown", if need be. Its top-level definition: the approximate *a priori* probability that an arbitrary instance of the data/product does not contain anomalous data which is unsuitable for use and does not have missing data.

For example, anomalous data includes 3d geolocations with extremely large errors due to problems in the generation of a 3d geolocation product. Missing data corresponds to significant voids in a 3d Geolocation product or to a missing delineation of a major feature in a portion of a Digital Map. For Small-Sat image/metadata, anomalous data includes incorrect (blundered) metadata that yields flawed metadata-based image-to-ground relationships, images that are extremely blurred, etc. That is, (portions) of the

data that are not suitable for use due to corresponding and underlying generation issues. This does not include inherent issues associated with the raw data itself, such as cloud cover.

### 5.2.2 Quality Assessment may take a long time to complete for some data/products

As discussed earlier, the Quality Assessment Summary (file/report) associated with a specific type of data/product of interest summarizes the amount of information available regarding its corresponding quality and geolocation accuracy. It also “points” to available and populated models: accuracy assessment, predicted accuracy, and/or empirical quality models. A populated accuracy assessment model contains various *a posteriori* sample statistics of error, which are the basis for the selection of the appropriate type of predicted accuracy model and the “tuning” of the *a priori* predictive statistics that it contains. The Empirical quality model for Crowd-sourcing is a lower-fidelity combination of these two models that also emphasizes the quality of data content, e.g., area of coverage and the reliability of content of a digital map.

Prior to detailing the above models in Section 5.3, it is important to point out that the “time-line” for gathering an adequate amount of information may vary significantly for different types of data/products. However, the recommended techniques in this document are designed to mitigate this as much as possible by gathering and processing information in a sequential manner. That is, it may take *xx* months to gather a sufficient amount of information and perform corresponding processing in order to reach a “high” level of confidence in results for a type of data/product of interest, but only *yy*  $\ll$  *xx* months to gather initial information to reach a lower level of confidence in results. This is better than no information/confidence at all as long as information is labeled as such. The Quality Assessment Summary (file/report) provides the applicable “status”.

It may also be true that for some types of data/products, this information will never become available, at least in a reasonable amount of time. This should be apparent by either: (1) the corresponding low confidence level in the models or their complete lack of availability as specified in the Quality Assessment Summary (Table 5.2.1-1) or (2) the complete non-availability of the Quality Assessment Summary (file/report) itself. Of course, this in itself is a form of information – it indicates to potential users of this type of data/product that it is unsuitable for certain applications and that they should assess the suitability of other types of data/products for potential use instead. To facilitate this process, it is also recommended that a catalogue of available Quality Assessment Summaries, indexed by data/product type, be generated and made available by the Quality Assessment Management function.

### 5.2.3 An Exception – Some Commodities data require minimal Quality Assessment

A relatively small subset of Commodities data requires minimal Quality Assessment because the providers of the data/products already include reliable predicted accuracies. Correspondingly, the Quality Assessment Management function needs only to ensure the occasional population of an accuracy assessment model, no population of a predicted accuracy model, and an abbreviated Quality Assessment Summary that essentially documents this situation.

The occasional populated accuracy assessment model provides a quality check regarding the predicted accuracy from the provider. The Quality Assessment Summary includes the Predicted Accuracy Summary

Metrics (CE90 and LE90) assumed available from the provider, as is typical and via their corresponding web-sites. The applicable populated predicted accuracy model or its equivalent is also available directly from the provider as described in the representative examples below.

#### ***5.2.3.1 Examples and why they are preferred***

The following are examples of data/products with reliable predicted accuracy models directly available from the vendor/provider, which is preferred whenever possible:

##### (1a) Imagery with a complete physical sensor model:

An example of the above corresponds to non-Small-Sat commercial satellite imagery/metadata available for some imaging systems from some providers. Corresponding image/metadata includes access to a complete physical sensor model: physical sensor model (invertible ground-to-image function), adjustable sensor parameters (pose, calibration), and their corresponding predicted accuracy or uncertainty (adjustable parameters' *a priori* error covariance matrix, etc.).

The complete physical sensor model's predicted accuracy is typically reliable, and along with the adjustable parameters, enables computation of the predicted accuracy of an extracted geolocation using the image(s), and optionally, adjustment of the image (metadata) for subsequent improved geolocation accuracy.

Thus, there is no need for the population of a predicted accuracy model by the Quality Assessment Management function – there is already a model from the provider that is both reliable and typically of higher fidelity.

More about (complete) physical sensor models and other sensor models is provided later in this document: an overview in Section 5.3.1.1 and further details in Section 5.3.2. All data/products considered in this document are assumed to have a sensor model of some kind in order to enable a ground-to-data/product relationship, e.g., ground-to-image function.

##### (1b) Above “mapped” to RPC:

A (sub)example of the above is a “complete RPC sensor model”, which is generated by the data/product provider by fitting the complete physical sensor model's ground-to-image function to a Rational Polynomial Coefficient (RPC) polynomial, defining adjustable parameters for the polynomial (low order coefficients), and mapping the complete physical sensor model's predicted accuracy to RPC predicted accuracy. The “complete physical sensor model”-to-“complete RPC model” mapping must be performed per the appropriate algorithm/procedure - see reference [8].

##### (2) 3d Point Clouds with a Generic Point Cloud Model (GPM):

Another example corresponds to some types of 3d Point Clouds that have an accompanying Generic Point-Cloud Model (GPM) – see reference [16]. There are two versions of GPM: GPM (sensor-space) and GPM (ground-space). Both have complete sensor models:

- GPM (sensor-space): an identity sensor model (ground-to-ground or identity transformation), adjustable sensor parameters (sensor pose, etc.), and their predicted accuracy (error covariance matrix, etc.), where the mapping of error covariance matrices from sensor-space to ground-space is accomplished by knowledge of the complete physical sensor model (sensor pose, etc.)
- GPM (ground-space): an identity sensor model (ground-to-ground or identity transformation), adjustable parameters for a grid of 3d anchor points, and their predicted accuracy.
- In both of the above cases, reference [16] terms the (invertible) sensor model the “ground-to-model” and the “model-to-ground” transformation.

Both of the above GPM versions include the optional addition of the effects of sensor-mensuration (aka “unmodeled”) errors to predicted accuracy.

The resultant predicted accuracy is reliable, contained in the product’s metadata, and computed directly by the provider.

#### 5.2.3.2 *Common characteristic*

All of the above examples in Section 5.2.3.1 have additional information for the generation of predicted accuracy not available to the Quality Assessment Management/Analysis function: internal predicted accuracies of various steps in the product generation process for each specific data/product, such as (1) an estimate and its *a posteriori* error covariance matrix of sensor pose and calibration parameters computed by a Kalman Filter Smoother implemented at an imaging-system’s ground station, and (2) an estimate and its *a posteriori* error covariance matrix of sensor pose and calibration parameters computed by a Weighted Least Squares solution (block adjustment) and propagated to ground-space as appropriate and implemented at the data provider’s Point Cloud’s generation facility. As such, the provider-supplied predicted accuracy can also be “custom-tailored” to each specific instance of the data/product, including the effects of sensor-to-ground geometries specific to each element in the data/product. In addition, based on the above additional information, not only are the predicted accuracies reliable, their values are relatively small (e.g., small error covariances or “sigmas”) indicating good accuracy associated with (near) optimal solutions.

Of course, there is no guarantee that the above providers’ predicted accuracies are always reliable, and that is why it is recommended that the Quality Assessment Management/Analysis function periodically populate an accuracy assessment model for comparison.

#### 5.2.4 **Encouraging Explicit Accuracy Specifications**

The Quality Assessment Summary (Table 5.2.1-1) referenced the possible availability of metadata and/or specifications of accuracy made available by the data/product provider. These are currently unavailable for most External Data of interest to NSG organizations, but are certainly desired by many such organizations. In addition, some providers (vendors), such as those associated with Small-Sat data, have requested corresponding guidance for their availability, particularly if they supply data/products to various organizations in the NSG by contract. It is recommended that applicable NSG organizations take a “pro-active” approach in enabling such guidance including recommended accuracy specifications as follows:

Recommended specifications for the data/product provided by the vendor/provider are to include accuracy of the data/product (e.g. CE90 and LE90). The actual specified accuracy values (e.g.  $CE90 \leq 15$  meters) are not to be recommended by the NSG; they are provided solely by the provider and based on their system design and corresponding business model.

Another recommended specification for the provider is the availability of a populated predicted accuracy model or its equivalent with the data/product or for a specified class or type of data/products.

Any such specifications should also be verified as well by the provider, and more formally validated in concert with the NSG if associated with an NSG contractual relationship. This includes validation of predicted accuracy as well as validation of accuracy. TGD 2c (Specification and Validation) presents recommended content for accuracy and predicted accuracy requirements and processing for their validation. An “easy-to-read” summary of TGD 2c is also recommended [6]. See TGD 1 [Overview and Methodologies] for a discussion regarding the difference between accuracy and predicted accuracy – “think” sample-statistics of error in previous specific data/products versus predictive statistics of error in arbitrary (“future”) data/products of a similar type or class of data/product, respectively.

It is worth noting that receptive providers may be concerned about risk associated with providing such information, including specifications, with their data/product. Correspondingly, they may feel that future contracts with NSG organizations should reflect this concern accordingly.

#### **5.2.4.1 Any Advertised Accuracy should be verified**

In addition, any “advertised” accuracy that is made available by the providers of External Data should be “verified” by the NSG via the Quality Assessment Management Function regardless the availability of corresponding specifications from the vendor/provider or not. Results of an NSG Quality Assessment should take precedence. There are examples of some provider web-sites providing accuracy results that are clearly optimistic for some of their specific data/products, i.e., present accuracy results for seemingly “best case” scenarios.

#### **5.2.4.2 Specifications for exploitation tools**

Accuracy Specifications are encouraged to be made available by External Data (product) providers as discussed in Section 5.2.4. The Quality Assessment of such products/data should also be performed by NSG Quality Assessment, per this document. In addition, NSG internally generated data/products should be subject to accuracy and predicted accuracy specification and validation, as detailed in TGD 2c (Specification and Validation). Furthermore, regardless the source of the data/products used by the NSG, they are typically processed by exploitation tools and applications for the generation of various “end” products. These tools/applications can induce additional errors of significant magnitude, and as such, it is recommended that the NSG levy and/or encourage specifications on such tools/applications regarding these errors and corresponding accuracy.

### **5.2.5 Functional Flow of the Quality Assessment Management Function**

Figure 5.2.5-1 presents the top-level functional flow and major interfaces of the Quality Assessment Management function. Major interfaces are with the other organizations in the NSG and with the Quality Assessment Analysis function. The populated models are files/reports, i.e., not s/w code or modules.

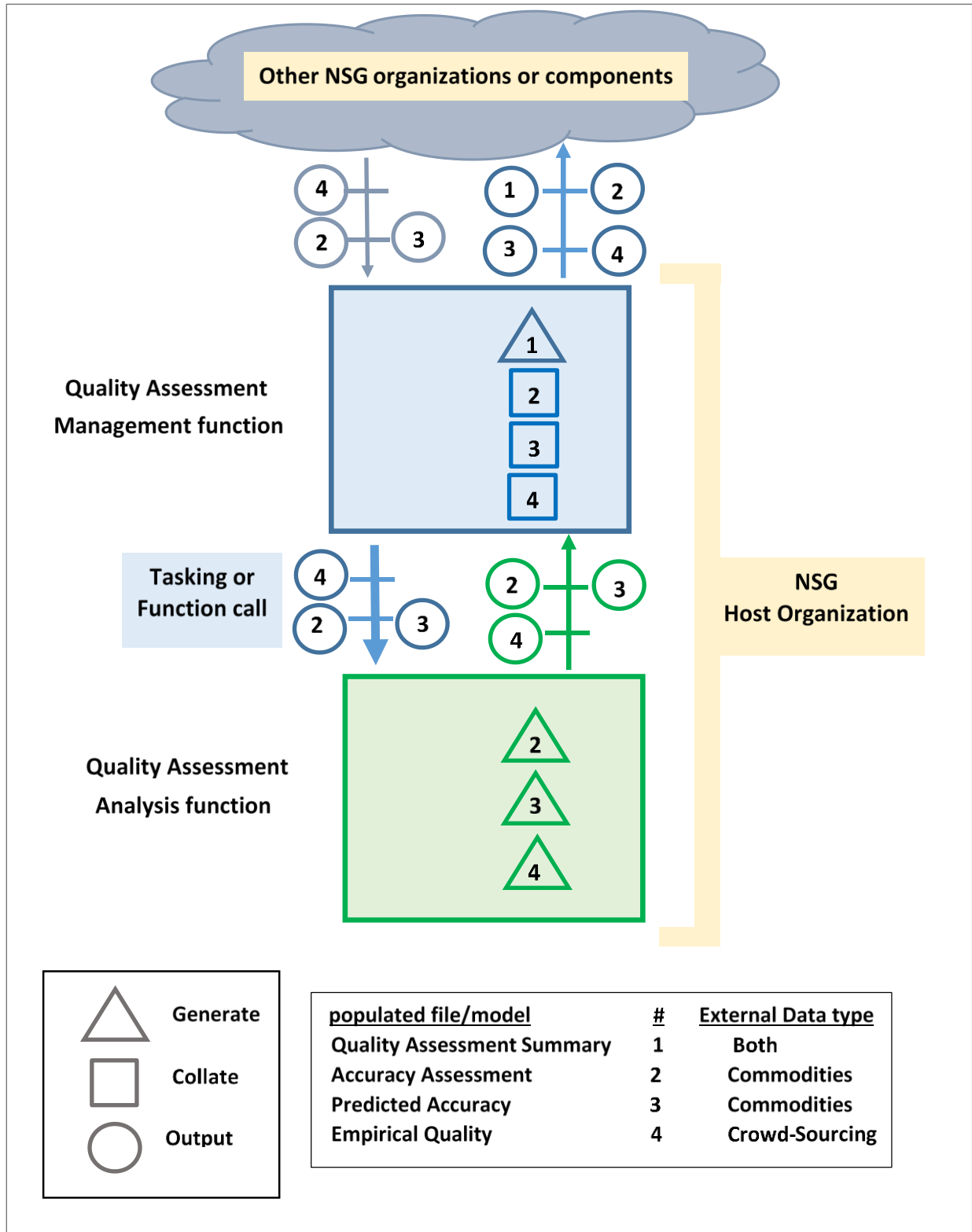


**Figure 5.2.5-1:** Functional flow and major interfaces of the Quality Assessment Management function

As indicated by the above figure, the Quality Assessment Analysis function supports the Quality Assessment Management function. More specifically, the Quality Assessment Management function “calls” the Quality Assessment Analysis function. Their actual interrelationship is dictated by the host organization’s detailed design. The Quality Assessment Analysis function is documented in Section 5.3.

Also, as mentioned previously, other organizations in the NSG may input populated models to the Quality Assessment Management function for subsequent collation and for the possible extension of ensemble statistics via the Quality Assessment Analysis function. These inputs are indicated by the upper left gray arrow in Figure 5.2.5-1. Corresponding inputs can also include “raw” data for analysis as opposed to populated models.

### 5.3 Quality Assessment Analysis Function

The Quality Assessment Analysis function primarily selects and populates applicable accuracy assessment models, predicted accuracy models, and/or Empirical quality models for each specific type of geolocation data or product of interest in support of the Quality Assessment Management function.

Like the Quality Assessment Management function, the Quality Assessment Analysis function is implemented by the “host” organization. However, unlike the Quality Assessment Management function, it may also be implemented by other NSG organizations with corresponding outputs to the Quality Assessment Management function as appropriate.

A top-level summary of various categories of External Data that the Quality Assessment Analysis function addresses is presented in Table 5.3-1, and is further categorized by the type of models it populates.

**Table 5.3-1:** Summary of the External Data addressed by the Quality Assessment Analysis function

<b>Accuracy Assessment and Predicted Accuracy Models for the following Commodities Data:</b>
<p>Small-Sat imagery/metadata                              term used generically to include                              "micro" and "nanosatellites"</p> <p>Air-borne imagery/metadata          Space-borne imagery/metadata          Full-motion video/metadata          Orthophotos and Orthomosaics          3d Point Clouds          Digital Maps          Vector Data          Hand-held devices          Digital Elevation Model (DEM)          Digital Surface Model (DSM)          ...</p>
<b>Emperical Quality Models for the following Crowd-Sourcing Data:</b>
<p>Digital Maps                              Map-based and/or image-based data                              OpenStreetMap, Wikimapia, Google MyMaps, ...          Orthophotos and Orthomosaics          ...</p>

Reference [10] presents a brief summary of the use/definitions of various classes of “Small-Sats” that are referenced in Table 5.3-1.

The various analyses performed by the Quality Assessment Analysis function are summarized in Table 5.3-2.

**Table 5.3-2:** Summary of the Quality Assessment function’s analysis tasks and techniques

Analysis Tasks and Techniques
<p><b>Population of Accuracy Assessment Model</b></p> <p>Based on Sample Statistics</p> <p>Requires access to error samples based on ground-truth or equivalent</p> <p>Model detailed in Section 5.3.2</p> <p>Population/analytic techniques discussed in Section 5.3.5</p> <p><b>Population of Predicted Accuracy Model</b></p> <p>Based on analytic error-propagation modeling</p> <p>Requires insight and tuning based on populated Accuracy Assessment Model</p> <p>Model detailed in Section 5.3.2</p> <p>Population/analytic techniques discussed in Section 5.3.5</p> <p><b>Based on the above populated models:</b></p> <p>Comparison to any accuracy descriptions/specifications available from vendor/provider</p> <p>Generation of reliability metric in the Quality Assessment Summary (Table 5.2.1-1)</p> <p><b>Population of Empirical Quality Model</b></p> <p>Based on statistics of comparisons to similar data and other techniques</p> <p>Model and population techniques discussed in Section 5.3.6</p>

As summarized in Table 5.3-2, the contents and population of the accuracy assessment model and the predicted accuracy model are discussed in Sections 5.3.2 and 5.3.5, which also contain various references to appendices for further details, such as explicit equations/algorithms for their population.

Although not listed in Table 5.3-2, a top-level overview of the interrelationship between the accuracy assessment model and the predicted accuracy model is also presented in Section 5.3.1, with corresponding subsections that also discuss their interrelationship with sensor models and the importance of the predicted accuracy model in general.

As summarized in Tables 5.3-1 and 5.3-2, the use and population of accuracy assessment and predicted accuracy models are not applicable to Crowd-sourcing data. This is due to difficulties in obtaining sufficient ground truth for sample error statistics, the frequency of missing data and blunders in the data/product, and/or significant variations in its quality over different realizations of the same data/product type. A lower-fidelity but more general empirical quality model is used and populated instead as discussed in Section 5.3.6.

### 5.3.1 Accuracy assessment and predicted accuracy models and interrelationships

An overview of the relationship between populated accuracy assessment models and predicted accuracy models, as well as their relationship to the Quality Assessment Summary (Table 5.2.1-1) are presented in Figure 5.3.1-1.

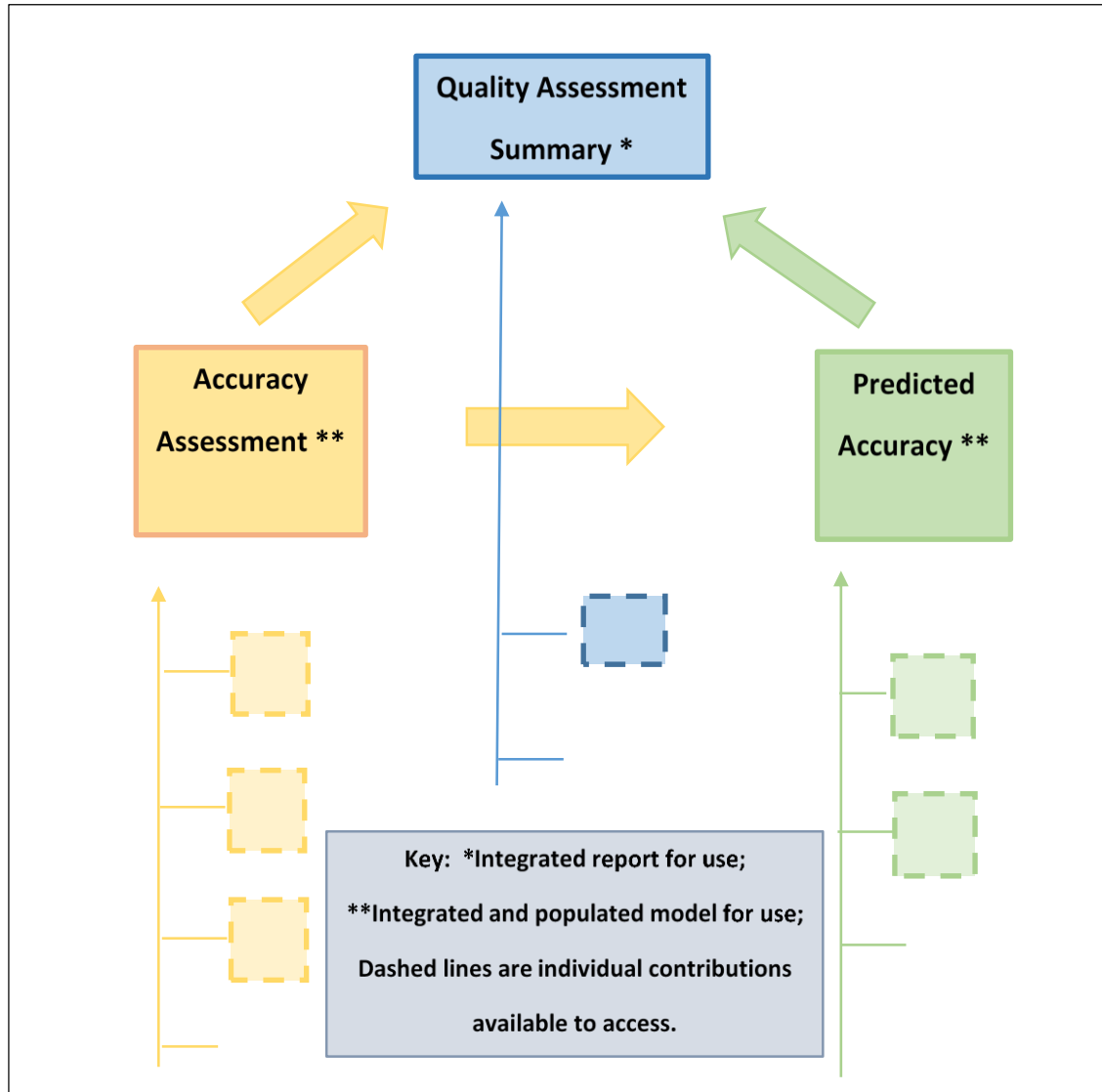


**Figure 5.3.1-1:** The relationship between Quality Assessment Summary, Accuracy Assessment, and Predicted Accuracy for each specific data/product of interest

The Quality Assessment Summary file/report, the populated accuracy assessment model, and the populated predicted accuracy model are updated periodically or every time a new individual contribution is available corresponding to a specific type or class of data/product of interest. In particular, the populated accuracy assessment model's underlying ensemble statistics are updated, and therefore the

populated predicted accuracy model and possibly the Quality Assessment Summary file/report may be updated as well.

The Accuracy Assessment “update process” essentially performs the same processing as performed for the generation of an individual contribution but is based on the use of an ensemble collection of sample statistics over all relevant individual contributions. This results in an integrated and representative populated accuracy assessment model and then a corresponding integrated and representative populated predicted accuracy model (solid rectangles in Figure 5.3.1-1). These populated models are then made available to NSG personnel/organizations upon request, along with pointers to the individual contributions or populated models (dashed rectangles in Figure 5.3.1-1).

More specifically, an initial accuracy assessment and corresponding populated accuracy assessment model are used to select/confirm a particular predicted accuracy model and its defining contents for the corresponding type or class of geolocation data/product of interest. The sample statistics in the accuracy assessment are also used to compute the initial values of the predictive statistics contained in the now populated predicted accuracy model. Subsequent accuracy assessments (ensemble statistics) are then used to periodically update the accuracy assessment model, which, in turn, is used to update the populated predicted accuracy model, i.e., modify or “tune” the values of its predictive statistics. Note that, even though the ensemble statistics are used to generate/modify the predictive statistics, the two sets of statistics are somewhat different, as appropriate and as detailed later.

Section 5.3.2 details the definitions/contents of accuracy assessment models and the predicted accuracy models, Section 5.3.3 discusses various companion and optional components to these models, Section 5.3.4 “points to” related appendices, and Section 5.3.5 discusses the corresponding analysis techniques for the population of models. Section 5.3.2 is necessarily “summary” in nature, but specific details and examples follow in Sections 5.3.3 – 5.3.5 and the related appendices.

However, prior to proceeding with Section 5.3.2, the relationship of predicted accuracy model to the corresponding data/product’s sensor model is presented (Section 5.3.1.1) followed by a description of the importance of a populated predicted accuracy model to the end-user of the data/product (Section 5.3.1.2). These descriptions provide important background information for context.

#### ***5.3.1.1 Relationships to the data/product’s sensor model and corresponding terminology***

Virtually all data/products considered in this document are assumed to include or have available a “basic sensor model” which provides a ground-to-data/product relationship or function (e.g., ground-to-image function), otherwise the data/product is not relevant, i.e., is not a geolocation-related data/product of interest. The basic sensor model and its associated metadata are directly associated with (come with) the geospatial data/product from the producer or vendor.

Figure 5.3.1.1-1 illustrates such a function for an Electro-optical (EO) image, and is assumed to correspond to a ground-to-image polynomial in this particular example. The ground-to-image polynomial provides the ground-to-image relationship, or more generally, the geolocation-to-data relationship.

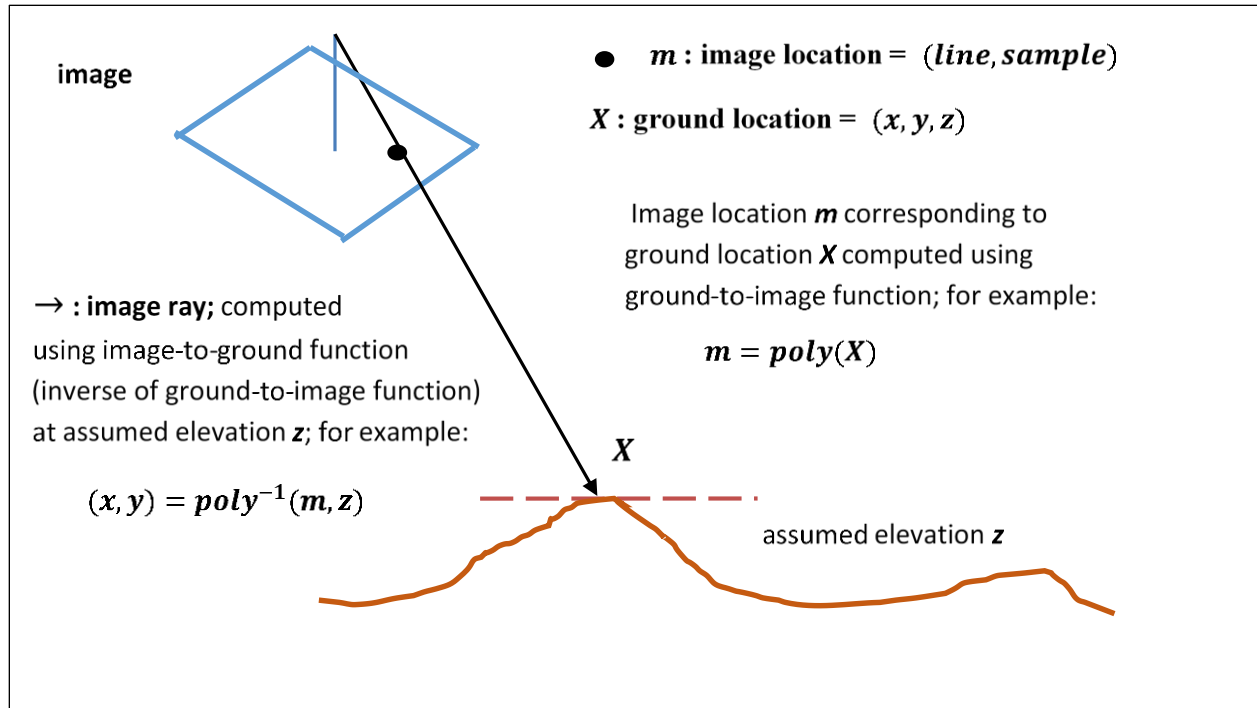


**Figure 5.3.1.1-1:** The ground-to-image function provided by the basic sensor model for the image; image location and ground location vectors are represented as row vectors instead of column vectors in the figure for convenience

The additional availability of a (populated) predicted accuracy model represents the uncertainty in the basic sensor model, i.e., the uncertainty or error in the output of its ground-to-data/product function. The availability of a predicted accuracy model transforms the basic sensor model into a “complete sensor model”, or simply a “sensor model”. A (complete) sensor model enables rigorous error propagation. It also enables optional adjustment of the data/product for improved accuracy using control information.

For most Commodities data, the predicted accuracy model is not available with the data/product from the producer or vendor, but it is defined, populated, and made available by the methods recommended in this document. A predicted accuracy model represents the uncertainty in the data/product, and is also relative to a set of adjustable parameters that affect or parameterize the ground-to-data/product function, and therefore its output. These adjustable parameters are either explicit or implicit as detailed in Sections 5.3.2.1, 5.3.2.3, and 5.3.2.4. In particular, they are explicit and defined as follows for a specific type of sensor model termed a “physical sensor model”.

A relatively small subset of sensor models applicable to Commodities data are termed “physical sensor models” because their ground-to-data/product relationship is a direct function of the sensor’s physical parameters, such as sensor pose (position and attitude) and possibly sensor calibration parameters. The ground-to-data/product function is also parameterized by adjustable parameters corresponding to a subset of these physical parameters, such as corrections to the sensor position that is provided in the data/product’s metadata. The corresponding predicted accuracy model represents the accuracy or

uncertainty in the *a priori* values of these adjustable parameters which are equal to zero; and hence, also represent the accuracy of the original metadata for the data/product. In this particular case, the predicted accuracy model represents errors in sensor-space instead of data/product-space; however corresponding error covariance matrices are readily propagated to data/product-space and then to ground-space, if need be, via appropriate partial derivatives. These partial derivatives are computed using the physical sensor model (ground-to-data/product function) and are typically numerical and are computed about an assumed operating point.

Most sensor models corresponding to Commodities data are not physical sensor models. Typical examples include sensor models with ground-to-data/product relationships as follows: (1) polynomial ground-to-image functions for an image, and (2) a direct ground-to-ground (identity) function for a 3d geolocation product.

The predicted accuracy models referenced throughout the remainder of this document are assumed to be those that are not available with data/product from the producer or vendor, but are defined and populated by the NSG per the methods detailed in this document. Correspondingly, these predicted accuracy models are applicable to the vast majority of Commodities data.

#### **5.3.1.2 *The importance of the predicted accuracy model***

A populated accuracy assessment model corresponds to at least one specific realization or instance of a data/product from a type or class of data/products that is of interest, and typically corresponds to an ensemble collection of such realizations. On the other hand, a populated predicted accuracy model is applicable to an arbitrary realization of the data/product, past or future, from the same type or class of data/product that is of interest, and is typically provided as part of accompanying metadata or its equivalent.

The contents of a populated predicted accuracy model are considered predictive statistics whereas those for a populated accuracy assessment model are sample statistics. When a populated predicted accuracy model is assigned or “attached” to a specific data/product by the Quality Assessment Management function it becomes its predicted accuracy.

The predictive statistics in a predicted accuracy model, in conjunction with the corresponding sensor model enable an entire “suite” of error propagation capabilities which are listed later in this (sub) section. A key predictive statistic is the error covariance matrix which statistically quantifies the predicted accuracy of an arbitrary  $3 \times 1$  geolocation, assuming a geolocation product.

The  $3 \times 3$  error covariance matrix is illustrated in Figure 5.3.1.2-1 for an arbitrary geolocation in the product, along with related information, such as its statistical relationship to geolocation error as well as a derived predictive statistic computed from the available error covariance matrix: a 90% confidence ellipse. The 90% confidence ellipse is computed using the upper left 2x2 of the error covariance matrix, is relative to horizontal geolocation error, and assumes a Gaussian distribution of error.

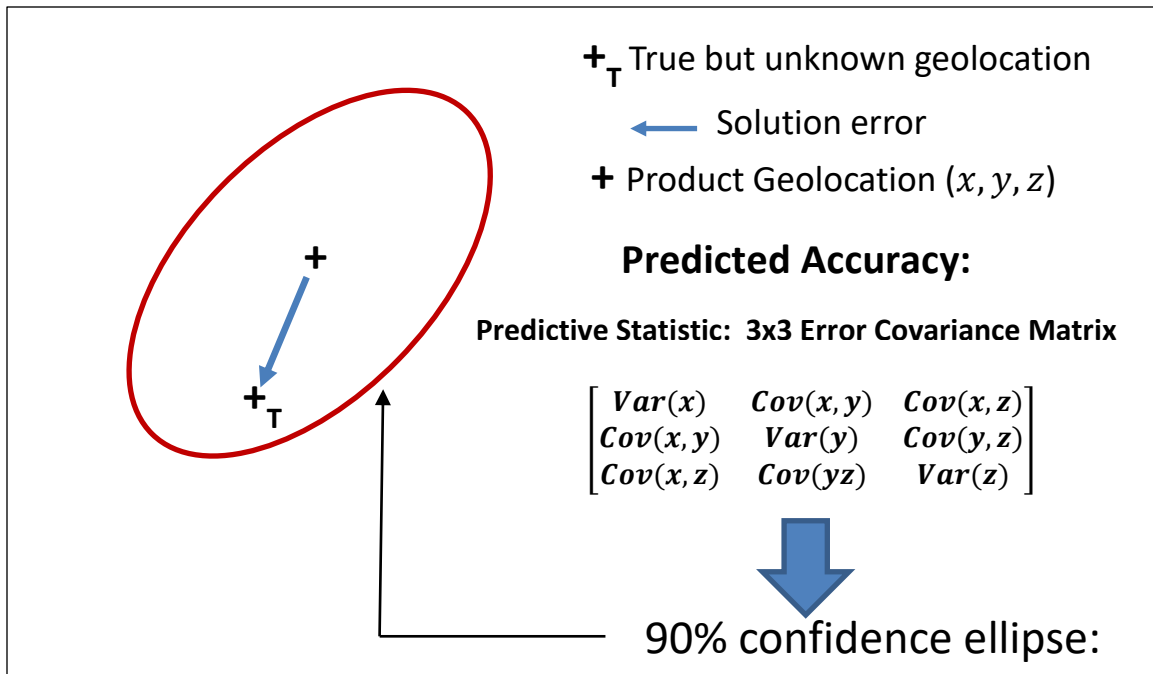


**Figure 5.3.1.2-1:** Horizontal error corresponding to product’s 3d geolocation; 90% confidence ellipse generated from the key predictive statistic: 3x3 error covariance matrix (upper left 2x2)

We are 90% confident that the true horizontal geolocation is within the ellipse which is centered at the product’s geolocation. If the geolocation were centered at zero instead, we are 90% confident that the (unknown) error is within the ellipse. This latter ellipse is also termed a 90% probability error ellipse.

In addition, using the entire 3x3 error covariance matrix, a 90% confidence 3d error ellipsoid (or some other specified level of confidence or probability) can also be computed – see TGD 1 and TGD 2a for details. Of course, the 90% confidence-level is also predicated on reliable predictive statistics, in this case, the error covariance matrix, as well as the assumption of a Gaussian distribution of error. The 90% confidence ellipse (or ellipsoid) is a derived predictive statistic and is not contained in the predicted accuracy model per se.

The error covariance matrix can also be used to compute scalar accuracy metrics, such as CE90 – the radius of a circle such that there is a 90% probability that horizontal error resides within (see TGD 1 and TGD 2a for details). CE90 is a very convenient and useful predictive statistic but contains less information than does the 90% error ellipse as it contains no directivity regarding the x and y components of horizontal error. Scalar accuracy metrics are derived predictive statistics but are typically contained in the predicted accuracy model for the convenience of the down-stream user/application.

Predictive statistics also typically correspond to an *a priori* mean-value of error equal to zero, not to a non-zero sample-based mean-value of error applicable to a specific realization and which typically varies in sign and/or magnitude from one realization to another. This reasonable assumption is applicable in Figure 5.3.1.2-1.

Strictly positive definite correlation functions (spdcf) are also predictive statistics that are contained in predicted accuracy model; more specifically, their defining parameters (typically four) are contained in the model. They characterize the spatial correlation of errors across an arbitrary realization of the data/product. If the data/product corresponds to a geolocation product (e.g., 3d Point Cloud), spatial correlation is a function of the difference between two geolocations (ground coordinates) in the same product. If the data/product corresponds to an image, spatial correlation is a function of the difference between two locations in the same image (image coordinates). The spatial correlation of errors significantly affects relative accuracy.

Spdcf are not sample-based autocorrelation functions corresponding to a specific realization of the data/product or their low-fidelity alternative – a non-zero mean-value relative to the sample-based root-sum-square of error. However, spdcf are typically “tuned” using samples of autocorrelation (or samples of relative accuracy versus distance) contained in accuracy assessments.

Finally, the predictive statistics contained in predicted accuracy model are assumed to correspond to errors contained in a wide-sensor homogeneous random field(s) for a combination of practicality and rigor. These predictive statistics are invariant to the actual location of a geolocation or data point in the data/product; more specifically, absolute accuracy is invariant to location and the relative accuracy between two geolocations or data points is a function of the distance between them. Sample statistics that are contained in corresponding accuracy assessments are used to “tune” the predictive statistics and are also organized consistent with this assumption.

Note: a populated predicted accuracy model can also contain a non-zero mean-value of error if applicable and as detailed later.

### **Suite of error propagation capabilities**

The predictive statistics contained in a populated predicted accuracy model enable an entire suite of “error propagation” capabilities which are not possible with a populated accuracy assessment model:

- Predicted accuracy of an arbitrary geolocation (or image pixel location, etc.) in the data/product
  - Mean-value of error (typically zero)
  - Error covariance matrix about the mean-value
  - Various scalar accuracy metrics (CEXX, LEXX,...)
- Predicted relative accuracy of an arbitrary pair of geolocations in the data/product
  - Mean-value of error (almost always zero)
  - Error covariance matrix about the mean-value
  - Various scalar accuracy metrics (rel\_CEXX, rel\_LEXX,...)
- Full error covariance matrix for an arbitrary set of geolocations in the data/product
  - Proper weighting/error propagation of these geolocations as control points in other data/product
- Optimal adjustment or correction of the data/product using additional information, such as surveyed data or control imagery

- Optimal fusion of the data/product with other data/products – an extension of the above data/product adjustment to the simultaneous adjustment of multiple data/products

### **Summary**

In summary, an accuracy assessment applicable to an arbitrary realization of a data/product type, past or future, instead of a specific and specified realization(s), is not possible. It would require an adequate number of error samples from corresponding ground-truth which is either not available (typical) or its subsequent comparison to the product too time-consuming. A populated predicted accuracy model is used instead. It is applicable to an arbitrary realization of the type or class of data/product of interest.

In addition, a populated predicted accuracy model enables an entire suite of error propagation capabilities not possible with an accuracy assessment. Of course, as mentioned earlier and as detailed later in this document, a populated predicted accuracy model is typically tuned using a populated accuracy assessment model, the latter based on past and specific realizations.

### **5.3.2 Accuracy assessment and predicted accuracy model definitions and content**

The following definitions and their content correspond to accuracy assessment models and to predicted accuracy models in support of External Data and its Quality Assessment. The definitions reference common statistical terms and are somewhat functionally based, with implicit and explicit inputs and outputs. Figure 5.3.2-1 provides an overview followed by related definitions. The various analysis techniques discussed in Section 5.3.5 are used to populate these models, which are then maintained and disseminated by the Quality Assessment Management function as discussed earlier in Section 5.2.

As indicated by Figure 5.3.2-1, models are first categorized by accuracy assessment or by predicted accuracy and then subcategorized.

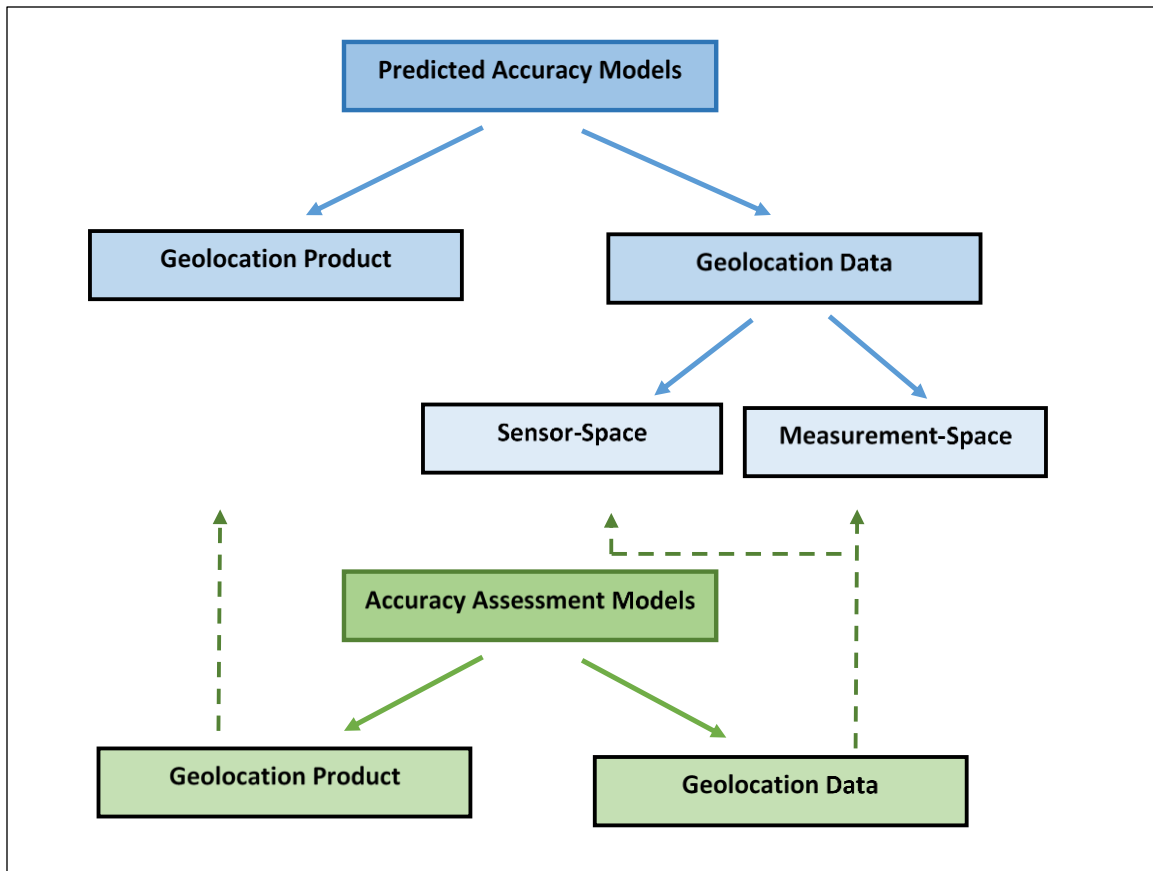


**Figure 5.3.2-1:** Predicted accuracy models and their relationships with accuracy assessment models; dashed lines represent feedback to “tune” predicted accuracy models from populated accuracy assessment models

There are three subcategories of predicted accuracy models and two subcategories of accuracy assessment models. For example, a “Geolocation Product Predicted Accuracy Model” is recommended for 3d Point Clouds while a “Geolocation Data Predicted Accuracy Model: Measurement-space” is recommended for Small-Sat images.

The various models illustrated in Figure 5.3.2-1 are described in Sections 5.3.2.1 through 5.3.2.5, including content and the recommended correspondence between type of geolocation data/product and appropriate model(s). The descriptions are relatively high-level, but specific details, including population, applications, and related examples, follow in Sections 5.3.3 - 5.3.5, Section 5.3.7, and in related appendices in order to facilitate further insight and specificity.

However, prior to proceeding with the descriptions of the various models, some background information is presented first: (1) underlying principles for the various models, (2) reasoning for their explicit names, and (3) the “assignment” or applicability of the appropriate model to the data/product of interest.

#### **Principles based on an extension of photogrammetry**

Photogrammetry is defined as the process of deriving metric information of an object through measurements made on photographs (images) of the object and is the foundation for the extraction of geolocation information from most geolocation data/products of interest, and is also closely related to various concepts of computer vision. See reference [15] for further details regarding photogrammetry.

The various models presented in Figure 5.3.2-1, their associated population, and their use for the extraction of geolocation information are based on the principles of photogrammetry, but are also extended to non-imagery and the use of modern estimation theory and probabilistic concepts (e.g., strictly positive definite correlation functions, random fields, order statistics, etc.) in order to mitigate the effects of minimal accuracy pedigree associated with most External Data.

### **Terminology: data vs. product; categories of predicted accuracy models**

The following presents the reasoning for the specific names given to the various models depicted in Figure 5.3.2-1. In order to do so, a more detailed explanation of the term “data/product” is presented first.

- Relative to the term “data/product” which is used frequently throughout this document: “product” corresponds to a geolocation product, such as a 3d Point Cloud, and “data” corresponds to data gathered by a sensor(s) or subsequently formed from it (e.g., images). A subset of this data is then measured by an NSG user/application in order to extract geolocations and/or generate geolocation products.
- Regarding the term “data”, it is further subcategorized based on the corresponding sensor model that it is associated with:
  - “sensor-space” data is associated with a physical sensor model since its adjustable parameters directly correspond to sensor metadata (e.g., sensor pose)
  - “measurement-space” data is associated with a (standard) sensor model since its output is to be measured (e.g., image coordinates) in order to extract geolocations and/or subsequently generate geolocation products
- As such, the following three names are used to represent the applicable categories of predicted accuracy models:
  - “Geolocation Product Predicted Accuracy Model”
  - “Geolocation Data Predicted Accuracy Model: Sensor-space”
  - “Geolocation Data Predicted Accuracy Model: Measurement-space”
- The reasoning for the names of only the various predicted accuracy models is presented above, as the names for the accuracy assessment models follow in accordance.
- Note: the more general term “geospatial” is sometimes substituted for “geolocation” in the names of the above models.

Although the above three names are used for the applicable predicted accuracy models in the remainder of this document, the term (geolocation) “data/product” is sometimes used to represent either “data” or “product” for convenience. The more applicable term should be apparent from context. This also helps to compensate for any possible ambiguity regarding the term “data”, which could be considered a package of data or possibly a product itself in some cases; e.g., perhaps for an image with metadata.

### **Applicability of the appropriate predicted accuracy model**

The appropriate predicted accuracy model is usually readily apparent for a given type or class of geolocation data/product of interest based on the descriptions for the models that are presented in Sections 5.3.2.1 through 5.3.2.5. For example, if a 3d Point Cloud, the Geolocation Product Predicted Accuracy Model is applicable. If an image, the Geolocation Data Predicted Accuracy Model: Measurement space or the Geolocation Data Predicted Accuracy Model: Sensor-space is applicable. The former (Measurement-space) is usually applicable since physical sensor models are not available for most Commodities data as discussed previously in Sections 5.2.3 and 5.3.1.1.

However, the appropriate correspondence of predicted accuracy model to geolocation data/product may not be so apparent for some geolocation data/products with corresponding and representative recommendations as follows:

- A Digital Elevation Model (DEM) or a Digital Surface Model (DSM) – the Geolocation Product Predicted Accuracy Model as applied to either 1d errors (only z errors are to be considered), 2d errors (only horizontal errors are to be considered), or 3d errors, as appropriate for the particular type of class of data/product of interest (e.g., vendor, date-range, possibly AOI, etc.)
- Orthophoto or ortho-image – errors are considered 2d horizontal geolocation errors, with predicted accuracy represented using either a Geolocation Product Predicted Accuracy Model or a Geolocation Data Predicted Accuracy Model: Measurement-space, whichever is most convenient:
  - If the former, errors are considered directly in terms of a geolocation product, in that the image is projected directly onto horizontal ground-space during orthophoto generation; the basic sensor model is the identity transformation, as it maps horizontal ground-space to horizontal ground-space.
  - If the later, the orthophoto is considered an image represented in (projected to) horizontal ground space; again the basic sensor model is the identity transformation, as it maps horizontal ground space to image-space which is also defined as horizontal ground-space.

Now on with the descriptions for the various models presented in Figure 5.3.2-1:

#### **5.3.2.1 Geolocation Product Predicted Accuracy Model**

The Geolocation Product Predicted Accuracy Model is applicable to geolocation products of a specific and specified type, such as a DEM, Ortho-image, or 3d Point Cloud with corresponding identified provider, date-range, etc. It is an *a priori* uncertainty (error) model for the data/product's 1d, 2d, and/or 3d geolocation errors and corresponding relative geolocation errors. It is used for predicting the accuracy and relative accuracy of the data/product's geolocations.

#### **Predictive Statistics**

The Geolocation Product Predicted Accuracy Model includes the following *a priori* predictive statistics that represent the (1d, 2d, and/or 3d) errors in an arbitrary realization of the product:

- *A priori* mean-value, covariance matrix, strictly positive definite correlation function (spdcf), and scalar accuracy metrics (e.g., CE90, LE90, relCE90, relLE90) of geolocation errors:
  - The above set of predictive statistics corresponds to the “standard” predicted accuracy model for a geolocation product
  - The inclusion of scalar accuracy metrics is optional and for the convenience of the down-stream user as they can be derived from the predicted statistics that are provided.
- As a recommended option, the above predictive statistics can also be grouped together consistent with a Mixed Gaussian Random Field (MGRF) with corresponding identified wide-sense homogeneous random fields as well as partitions and their *a priori* probability of occurrence. This allows for the representation of predicted accuracy that can vary over the product (realization):
  - There is a set of the above predictive statistics for each group or partition
  - See Section 5.3.3.3 for further details of an MGRF and its specifiable partitions and random fields.

The predictive statistics are contained in the product’s metadata or its equivalent.

The predictive statistics in a populated Geolocation Product Predicted Accuracy Model are typically tuned using the sample statistics contained in a populated Geolocation Product Accuracy Assessment Model (Section 5.3.2.2). Appendix B details this process.

#### **Relationship with the (complete) sensor model**

The Geolocation Predicted Accuracy Model is a major component of the geolocation product’s sensor model which includes the ground-to-product function (relationship). This function is simply the identity function (transformation) since an element of the product is already expressed directly in ground-space.

Note: a possible exception corresponds to any applicable ground-space coordinate system transformations of interest; considered ancillary and detailed processing and not specifically addressed in this document.

The sensor model’s adjustable parameters are “direct” adjustable parameters that modify the output of the ground-to-product function directly, i.e., are 3d geolocation offsets. For example, if an adjustable parameter  $\delta X$  is non-zero and associated with a geolocation  $X$ , it modifies the geolocation directly as follows:  $X \rightarrow X + \delta X$ . The *a priori* values of these adjustable parameters are zero and the Predicted Accuracy Model represents their uncertainty, and hence, represents the uncertainty of the geolocations in the product.

In theory, each geolocation in the product corresponds to its own adjustable parameter. However, all of the adjustable parameters share the same predictive statistics or uncertainty in their *a priori* values and there is no need to identify them (their underlying geolocations) explicitly unless the product is adjusted. Hence, they are also “implicit” adjustable parameters.

Note: because the adjustable parameters are direct, the corresponding partial derivative of an element in the product (a geolocation) with respect to its corresponding adjustable parameter is the identity matrix; therefore, there is no need to explicitly use the partial derivatives in error propagation.

The sensor model includes the optional ability to adjust the product in order to improve its geolocation accuracy prior to its subsequent use, i.e., enables adjustability of the product. The adjustment is implemented via a grid of 3d corrections across the product. The adjustment corresponds to non-zero values for the grid of adjustable parameters (corrections) which are then interpolated to adjust (correct) an arbitrary geolocation in the product, i.e.,  $X_{arbitrary} \rightarrow X_{arbitrary} + \delta X_{interpolated}$ . An overview of recommended geolocation data/product adjustment is presented in Section 5.3.3.1, and detailed specifically for a geolocation product in Appendix E.

### Applications

A populated Geolocation Product Predicted Accuracy Model enables the computation of predicted accuracy for any geolocation in the product and the computation of relative accuracy between any two geolocations in the product, i.e., enables error propagation. It also supports adjustability of the product for subsequent improved geolocation accuracy and/or fusion with other geolocation products.

### Spdcf

Finally, an spdcf is a predictive statistic that is an important part of this predicted accuracy model and many of the other models that are defined in the following subsections, and is used to represent the spatial correlation of errors corresponding to geolocations (or pixel locations if corresponding to an image) in the same arbitrary product or realization, with two examples of spdcf presented in Figure 5.3.2.1-1 as a further introduction:

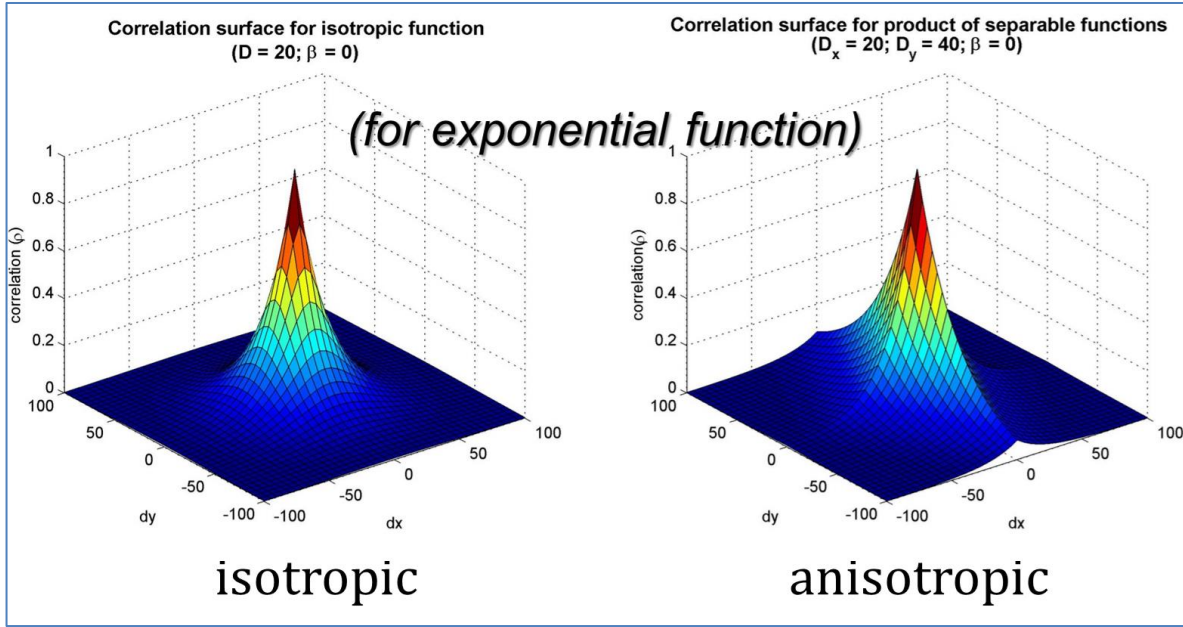


**Figure 5.3.2.1-1:** Correlation of errors (unit-less) versus 2d horizontal distance (meters) – two spdcf examples: exponential decay (isotropic) and separable exponential decay (anisotropic) as a function of horizontal distance between 3d geolocations

As a further example of spdcf, if only vertical geolocation errors are of interest with a common variance of error equal to  $\sigma_z^2$ , the variance of their relative error is equal to  $rel \sigma_z^2 = 2\sigma_z^2(1 - \rho(\Delta X))$ , where  $\rho(\Delta X)$  is the value of the applicable spdcf evaluated at the horizontal difference  $\Delta X$  between two geolocations in the same realization of the product. As correlation increases, relative error statistically decreases due to the cancellation of common error. Furthermore, applicable correlation is higher the closer the two geolocations.

In addition, an spdcf can be defined to yield an arbitrary but specifiable correlation value anywhere in the interval  $[0,1)$  for an arbitrarily small difference  $\Delta X$  and with a corresponding  $rel \sigma_z^2 > 0$ . This corresponds to a non-zero specifiable relative accuracy for two geolocations arbitrarily close together, which also increases thereafter with increasing distance. This feature is appropriate for many types of geolocation products.

An spdcf family that supports this important capability is the “CSM four parameter” family which is further detailed in Section 5.8.3.2 of TGD 1 (Overview and Methodologies) and in Appendices E and F of this document. It also supports generation of both of the correlation surfaces illustrated in Figure 5.3.2.1-1. In particular, spdcf from the “CSM four parameter” family were used that were based on the two dominant parameters only ( $A$  and  $D$ ) from the four that are available ( $\alpha = \beta = 0$ ):

- $\rho(\Delta X) = Ae^{-\sqrt{\Delta x^2 + \Delta y^2}/D}$  (isotropic;  $0 < A \leq 1, 0 < D$ )
- $\rho(\Delta X) = (A_x e^{-\sqrt{\Delta x^2}/D_x}) (A_y e^{-\sqrt{\Delta y^2}/D_y})$  (anisotropic;  $0 < A_x \leq 1, 0 < D_x; 0 < A_y \leq 1, 0 < D_y$ )

- $\rho(\Delta X) \equiv 1$  at  $\Delta X = [\Delta x \ \Delta y]^T = [0 \ 0]^T$  and  $\rho(\Delta X) < 1$  for all  $\Delta X \neq [0 \ 0]^T$
- there can be a separate spdcf for each component (x, y, or z) of geospatial error or there can be common spdcf for subsets of the components, typically for (x, y) and for (z).

### 5.3.2.2 *Geolocation Product Accuracy Assessment Model*

The Geolocation Product Accuracy Assessment Model is applicable to at least one specific geolocation product, or realization, of a specified type or class of such products, such as a specific DEM, Ortho-image, or 3d Point Cloud, via the use of ensemble statistics over the realizations. It consists of accuracy and relative accuracy metrics based on sample statistics of product 1d, 2d and/or 3d geolocation errors.

#### Sample Statistics

The Geolocation Product Accuracy Assessment Model includes the following sample statistics:

- Sample-based mean-values, covariance matrices, autocorrelation values (approximate spdcf values), and scalar accuracy metrics (e.g., CE90, LE90, relCE90, relLE90) of geolocation errors
  - If an MGRF is applicable, the above sample statistics are grouped together consistent with a Mixed Gaussian Random Field (MGRF) with corresponding identified random fields as well as partitions with their *a priori* probability of occurrence included as a statistic.
  - The inclusion of scalar accuracy metrics is optional and assumes the availability of enough independent error samples for their meaningful computation.
- Corresponding error samples consist of product geolocations minus corresponding ground truth coordinates (e.g., accurate surveyed locations).
- The number and degree of independence of the various error samples and an estimate of the accuracy of the corresponding ground truth used to compute the error samples are also included.

#### Applications

A populated Geolocation Product Accuracy Assessment Model is used to generate/tune a corresponding Geolocation Product Predicted Accuracy Model. When the latter corresponds to an MGRF representation of predicted accuracy (see Section 5.3.3.3), it is also recommended that the former categorize sample statistics by MGRF partition.

A Geolocation Product Predicted Accuracy Model is considered reliable when consistent with applicable Geolocation Product Accuracy Assessment(s), while taking into account the statistical significance corresponding to the number of underlying error samples.

### 5.3.2.3 *Geolocation Data Predicted Accuracy Model: Sensor-space*

The Geolocation Data Predicted Accuracy Model: Sensor-space is applicable to geolocation data of a specific type or class of data, such as image/metadata (2d measurements) or LIDAR/metadata (direct 3d measurements of geolocations) with corresponding identified provider, date-range, etc. It is an *a priori* uncertainty (error) model for the data. And more specifically, it is applicable to the sensor-space adjustable parameters in the data's sensor model, assumed to be a "physical sensor model". As such, it

represents the uncertainty in the sensor support data or metadata for the data, such as sensor pose (position and attitude) and calibration parameters.

### Predictive Statistics

The Geolocation Data Predicted Accuracy Model: Sensor-space includes the following *a priori* predictive statistics applicable to an arbitrary realization of the data (e.g., image):

- *A priori* mean-value, covariance matrix, and spdcf corresponding to errors (units varied) in a corresponding vector of sensor-space adjustable parameters for a set of data (data realization)
  - The spdcf represents the temporal correlation of error in the sensor-space adjustable parameters between multiple realizations of the data, when applicable; e.g., for same-pass images.
- Similar predictive statistics to the above can also be included corresponding to “sensor-mensuration” errors as an option and when applicable.
  - Sensor-mensuration (aka “unmodeled”) errors represent the high-frequency effects of sensor errors on the data (e.g., image location or mensuration errors) when present and of significant “power” – see TGD 1 (Overview and Methodologies) for further background/details.
    - As such, errors correspond directly to data errors (e.g., image locations), not errors in sensor-space adjustable parameters.
  - A corresponding spdcf represents the spatial correlation of errors within the same data realization. Sensor-mensuration errors are defined as uncorrelated between different data realizations

The predictive statistics are contained in the data’s metadata or its equivalent.

The predictive statistics in a populated Geolocation Data Predicted Accuracy Model: Sensor-space are typically tuned using the sample statistics contained in a populated Geolocation Data Accuracy Assessment Model (Section 5.3.2.5).

### Relationship with the (complete) sensor model

The Geolocation Data Predicted Accuracy Model: Sensor-space is a major component of the geolocation data’s sensor model. This physical sensor model includes a ground-to-data function (relationship) that also enables a (inverse) data-to-ground function. The sensor model is driven by the data’s metadata that contains the values of related physical sensor parameters, such as sensor pose and calibration parameters. The physical sensor model is implemented via a fairly complicated mathematical algorithm/code or via an API to the (compiled) code; for example, if the data is an image, the physical sensor model is not simply a (fitted) ground-to-image polynomial.

An identified subset of the corresponding physical sensor parameters is also adjustable. The *a priori* values of its corresponding adjustments (corrections) are equal to zero with *a priori* uncertainty as specified by the predictive statistics in the Geolocation Data Predicted Accuracy Model: Sensor-space.

The physical sensor model enables rigorous error propagation, including computation of the predicted accuracy and relative accuracy of the data (typically an image) and subsequently propagated to ground-space. It also enables adjustability of the data, i.e., the solution for non-zero adjustable parameters that affect the ground-to-data function in order to improve subsequent accuracy.

Note: the RSM replacement sensor model is also considered an equivalent of a (complete) physical sensor model, as it is derived using the latter during data/product generation with virtually identical functionality, including adjustability. See chapter 10.3 of [14] for a description of RSM.

## **Applications**

When available, use of a physical sensor model(s) in conjunction with geolocation data is generally preferred for the generation of 3d geolocation products and related geospatial objects; for example, a DEM generated using two (stereo) images and their corresponding physical sensor models. The physical sensor model and its predicted accuracy also enable the optimal extraction of geolocations via Multi-Image Geopositioning (MIG). See Section 4.1.2 and Appendix B.1 of TGD 2d (Estimators and their QC) for details regarding MIG. In addition, see [14,15] for a general description of physical sensor models associated with imagery (photogrammetry) and corresponding representation of uncertainty as well as adjustability.

The Geolocation Data Predicted Accuracy Model: Sensor-space and its corresponding physical sensor model are typically “higher fidelity” as compared to the Geolocation Data Predicted Accuracy Model: Measurement-space and its corresponding sensor model which are described in the next section, Section 5.3.2.4.

## **Caveat regarding non-use for the task at hand**

However, a Geolocation Data Predicted Accuracy Model: Sensor-space (or its equivalent) and its corresponding physical sensor model are typically not available/applicable for most Commodities data used by the NSG, in which case the Geolocation Data Predicted Accuracy: Measurement-space and its corresponding sensor model are applicable and recommended (Section 5.3.2.4). Furthermore, even if available, their predictive statistics are difficult to “tune” with accuracy assessments, as the former are in terms of sensor-space adjustable parameters and the latter in terms of sample statistics of geolocation error or equivalent image-space errors.

The (complete) physical sensor model and the population of its predicted accuracy are more applicable during data generation (Section 5.2.3) and not to the Quality Assessment Management/Analysis function. As such, the Geolocation Data Predicted Accuracy Model: Sensor-space and its corresponding physical sensor model and applications are discussed only briefly in the remainder of this document.

### ***5.3.2.4 Geolocation Data Predicted Accuracy Model: Measurement-space***

The Geolocation Data Predicted Accuracy Model: Measurement-space is applicable to geolocation data of a specific type or class of data, such as Small-Sat image/metadata (2d image measurements), RPC image/metadata (2d image measurements), or LIDAR ground data/metadata (3d geolocation

measurements) with corresponding identified provider, date-range, etc. It is an *a priori* uncertainty (error) model for the data.

The Geolocation Data Predicted Accuracy Model: Measurement-space is an *a priori* uncertainty (error) model for the approximate summed effects of sensor-space adjustable parameter errors, as represented in (projected to) measurement-space. For example, if data is an image/metadata, this is an uncertainty model for errors in the output of the sensor model's ground-to-image function, or more specifically, errors in the corresponding output of image coordinates (line,sample), due to underlying sensor pose errors.

Image coordinates are sometimes simply referred to as "image locations" and their errors as "image location errors" in this document and are also more formally represented as 2d errors in the  $2 \times 1$  vector  $m = [\text{line} \quad \text{sample}]^T$ . The superscript  $T$  corresponds to vector transpose.

The term "Measurement-space" in "Geolocation Data Predicted Accuracy Model: Measurement-space" is a reminder that the corresponding geolocation data of interest typically corresponds to a measurement, such as a measurement (location) of a pixel in an image that corresponds to an identified feature of interest.

In addition, when the geolocation data does correspond to an image, the term "Geolocation Data Predicted Accuracy Model: Image-space" is sometimes used instead for specificity.

## Predictive Statistics

The Geolocation Data Predicted Accuracy Model: Measurement-space includes the following *a priori* predictive statistics for an arbitrary realization of the data (e.g. image):

- *A priori* mean-values, covariance matrices, spdcf, and scalar accuracy metrics (e.g. CE90, LE90, relCE90, relLE90) corresponding to errors in locations or measurements in the data
  - For example, errors may correspond to 2d measurements or locations  $m = [\text{line} \quad \text{sample}]^T$  in an image, typically in terms of pixels.
  - The spdcf represents the correlation of errors between multiple measurements in the same realization of the data (e.g., same image).
  - The above predictive statistics correspond to errors associated with a wide-sense homogeneous random field for practicality and reasonable fidelity.
  - Scalar accuracy metrics are optional and for the convenience of the down-stream user as they can be computed instead from the predictive statistics that are provided.
- Sensor-mensuration (aka "unmodeled") errors can also be represented as an option, with additional *a priori* predictive statistics similar to those listed above.
- As an option, the uncertainty model and its *a priori* statistics for data errors may extend to an uncertainty model for multiple realizations of the data; e.g., the temporal correlation of errors between "same-pass" images, in which case additional spdcf are included which represent the temporal correlation. If not included, errors between different realizations of the data are assumed uncorrelated, as is typical for Commodities data.

The predictive statistics are contained in the data's metadata or its equivalent.

The predictive statistics in a populated Geolocation Data Predicted Accuracy Model: Measurement-space are typically tuned using the sample statistics contained in a populated Geolocation Data Accuracy Assessment Model (Section 5.3.2.5). Appendix C details this entire process.

### Relationship with the (complete) sensor model

The Geolocation Data Predicted Accuracy Model: Measurement-space is a major component of the geolocation data's sensor model. This sensor model is not a physical sensor model. Its ground-to-data function (relationship) also enables an inverse data-to-ground function and is driven by metadata that contains the values of the parameters that define the function, such as the coefficients of a ground-to-image polynomial.

The sensor model's adjustable parameters are "direct" adjustable parameters that modify the output of the ground-to-data function directly, e.g., are 2d image location offsets if an image. If an adjustable parameter  $\delta m$  is non-zero and associated with a data location or measurement  $m$ , it modifies the location directly as follows:  $m \rightarrow m + \delta m$ . The *a priori* values of these adjustable parameters are zero and the Geolocation Data Predicted Accuracy Model represents their uncertainty, and hence, represents the uncertainty of the locations of the elements in the data, e.g., the image-locations (pixels) in an image.

In theory, each element in the data corresponds to its own adjustable parameter. However, all of the adjustable parameters share the same predictive statistics or uncertainty in their *a priori* values and there is no need to identify them (their underlying locations) explicitly unless the data is adjusted. Hence, they are also "implicit" adjustable parameters.

Note: because the adjustable parameters are direct, the corresponding partial derivative of an element in the data with respect to its corresponding adjustable parameter is the identity matrix; therefore, there is no need to explicitly use these partial derivatives in error propagation.

The sensor model includes the optional ability to adjust the data in order to improve its accuracy prior to its subsequent use, i.e., enables adjustability of the data. If the data is an image, the adjustment is implemented via a grid of 2d corrections across the image. The adjustment corresponds to non-zero values for the grid of adjustable parameters (corrections) which are then interpolated to adjust (correct) an arbitrary image-location in the image, i.e.,  $m_{arbitrary} \rightarrow m_{arbitrary} + \delta m_{interpolated}$ . Section 5.3.3.1 presents further details.

### Applications

A populated Geolocation Data Predicted Accuracy Model: Measurement-space enables the computation of predicted accuracy for any element in the data and the computation of predicted relative accuracy between any two elements in the data, i.e., enables error propagation. It also supports adjustability of the data for subsequent improved accuracy. Some related details follow assuming that the data is an image and that errors in geolocations derived from the image(s) are of interest. Errors in the geolocations are primarily due to errors in the image(s):

An example of an image-to-ground function (inverse of the ground-to-image function) and related errors corresponding to an image (data) are depicted in Figure 5.3.3.1-1 of Section 5.3.3.1 and in Figure 5.3.5.3-1 of Section 5.3.5.3. Regarding the latter, image-space errors are included in the measured pixel location.

More generally, the (complete) sensor model, allows for the computation of a geolocation(s) and its predicted accuracy via an optimal MIG solution based on one or more images. The latter relies on the predictive statistics of the data (measurement or image location errors) contained in the predicted accuracy model to weight the measurements and correspondingly affect the solution for the geolocation(s) and its *a posteriori* error covariance matrix or predicted accuracy. Figure 5.3.4.2-1 presents an overview of MIG for a geolocation based on multiple images:

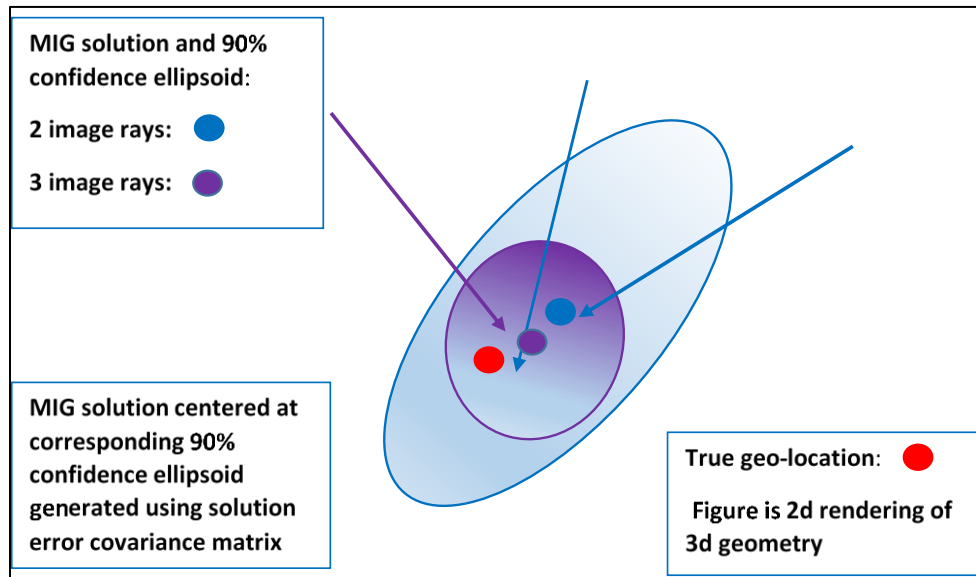


**Figure 5.3.4.2-1:** MIG 3d geolocation solution and its predicted accuracy using 2 or 3 image rays, each from a different image; rays are “image-to-ground” rays in 3d space and are computed using the basic sensor model; 2-image solution uses measurements corresponding to the 2 blue rays, the 3 image solution uses measurements corresponding to the 2 blue rays and 1 purple ray

Similarly, the sensor model can also be used for the generation of a 3d geolocation product and other geospatial objects, such as a DEM generated using two (stereo) images and that also computes the predicted accuracy of the corresponding geolocations.

#### Optional but equivalent methods to represent the predicted accuracy of data errors

Data errors (aka data location or measurement errors) may also be expressed in spaces (geometric planes) other than data-space as long as they are equivalent. For example, if an image, one of the following alternate approaches may be implemented:

- Equivalent errors in a plane perpendicular to the imaging locus at the intersection of the imaging locus and an external estimate of the geolocation’s elevation; the imaging locus is approximately

equal to the line-of-sight vector between the sensor and the geolocation if an EO image (image-to-ground function).

- As above except expressed in a local horizontal tangent plane near the intersection of the imaging locus and an external estimate of elevation
- Equivalent sensor attitude 2d errors (milliradians) about the nominal imaging locus. This method requires an estimate of an EO sensor's 3D position (often not available when only Rational Polynomial Coefficient (RPC) metadata is provided) as well as an external estimate of the geolocation's elevation.

All of the above alternatives are also associated with the (basic) sensor model, which inherently specifies the nominal imaging geometry (angles) and is required to convert errors in pixels to errors in appropriate units. The first and second alternate approaches, often associated with the RPC sensor model, listed above also require an external estimate of elevation for the conversion. See Section 5.6.1 of TGD 2a (Predictive Statistics) regarding conversion of covariance matrices of errors expressed in one coordinate system to another coordinate system based on the use of computed partial derivatives.

Figure 5.3.2.4-2 illustrates the three alternate approaches:

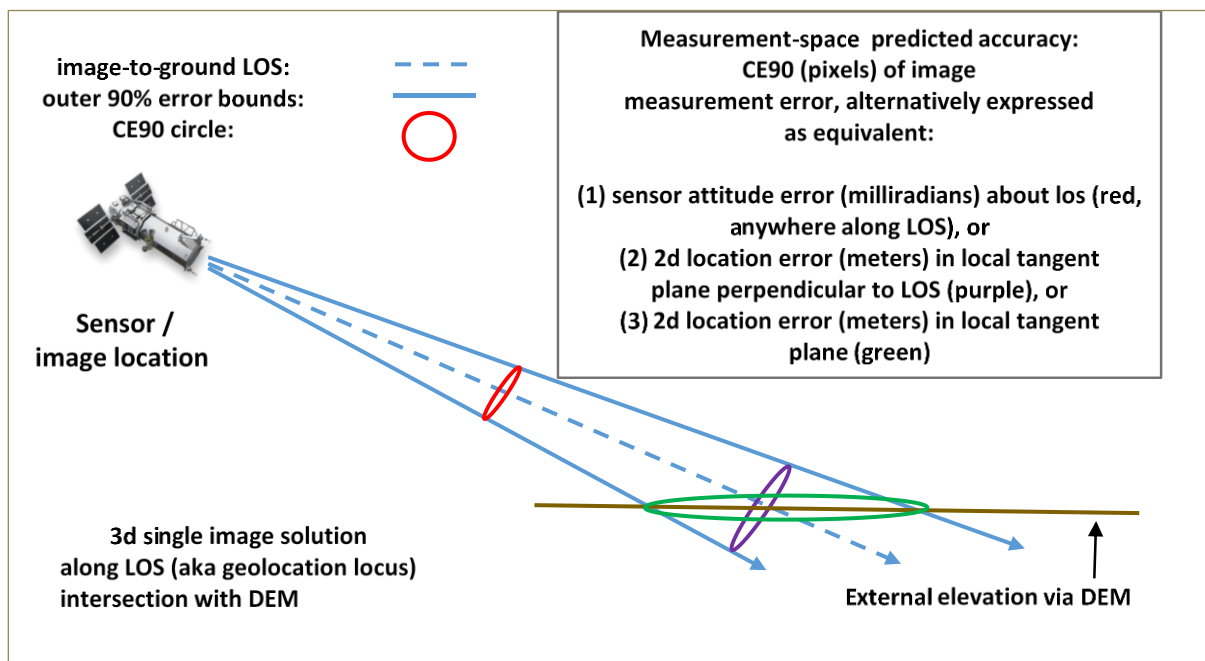


**Figure 5.3.2.4-2:** Data-space (aka Measurement-space) predicted accuracy if an EO imaging sensor; partially represented as CE90;

As noted in the title of Figure 5.3.2.4-2, CE90 is only a subset of the predictive statistics used to represent errors in the data (image); other statistics include the error covariance matrix, spdcf, etc. The CE90 circle is also equivalent to a 90% error ellipse which is also equivalent to a (scaled) error covariance matrix if the matrix is diagonal with equal variances – see TGD 1 (Overview and Methodologies) and TGD 2a (Predictive Statistics) for more details.

### 5.3.2.5 Geolocation Data Accuracy Assessment Model

The Geolocation Data Accuracy Assessment Model is applicable to at least one specific set of data, or realization, of a specified type or class of such data, such as Small-Sat images. It consists of accuracy and relative accuracy metrics based on sample statistics of errors in the data (measurements), or alternatively, errors in corresponding geolocations.

More specifically, an assessment of accuracy is based on ensemble statistics of error taken over one or more specific sets of data (realizations) using one of two possible approaches for the representation of error. The first approach is generally applicable to the standard or non-physical sensor model and a populated Geolocation Data Predicted Accuracy Model: Measurement-space. The second approach is generally applicable to the physical sensor model and a populated Geolocation Data Predicted Accuracy Model: Sensor-space.

- 1) Errors are in data-space and correspond to conjugate measurements minus ground-truth geolocations projected to data-space via the ground-to-data function and its metadata. Conjugate measurements are the identification/measurement of the ground-truth points in data-space (e.g., image).
  - a. Alternatively, if an image, the above errors can be projected to a ground-plane perpendicular to the image-locus (meters) or along the horizontal ground-plane itself as discussed in Section 5.3.2.4
- 2) Errors are in ground-space and consist of conjugate measurements projected to ground-space, using the inverse of the ground-to-data function, minus the ground-truth geolocations. Conjugate measurements are the identification/measurement of the ground-truth points in data-space (e.g., image).
  - a. 2d horizontal errors (meters) are applicable if the data and its sensor model are assumed to support the generation of horizontal geolocations at an assumed height, e.g., image-based monoscopic extraction.
  - b. 3d geolocation error (meters) are applicable if the data and its sensor model are assumed to support the generation of 3d geospatial locations, e.g., image-based stereo extraction.
  - c. The above errors or their statistics need to be subsequently “mapped” to corresponding sensor-space adjustable parameters if a physical sensor model is applicable (difficult).

### Sample Statistics

The Geolocation Data Accuracy Assessment Model includes the following sample (*a posteriori*) statistics:

- Sample-based mean-values, covariance matrices, autocorrelation values, and optional scalar accuracy metrics, e.g., CE90, LE90, relCE90, relLE90, etc., of data (measurement-space) errors or geolocation errors, whichever is applicable per the above paragraph.
  - Sample statistics are organized consistent with errors that are assumed to correspond to wide-sense homogeneous random fields for practicality with reasonable fidelity.
  - The scalar accuracy metrics are optional assuming the availability of enough independent error samples for their meaningful computation.

- Statistics regarding the number and the degree of independence of the various sampled errors and an estimate of the accuracy of the corresponding ground truth used to compute the error samples.

## Applications

A populated Geolocation Data Accuracy Assessment Model is used to initialize or subsequently “tune” either a Geolocation Data Predicted Accuracy Model: Sensor-space or a Geolocation Data Predicted Accuracy Model: Measurement-space. Also, the latter are considered reliable when consistent with the Geolocation Data Accuracy Assessment(s), while taking into account the statistical significance of the corresponding number of samples.

### 5.3.3 Companion Components

There are three important companion components to the predicted accuracy models (and sensor models) described in Sections 5.3.2.1, 5.3.2.3, and 5.3.2.4. They are described below with typically more detail than in the previous model descriptions:

- Adjustment “model”
  - Applicable to either the Geolocation Product Predicted Accuracy Model or the Geolocation Data Predicted Accuracy Model: Measurement-space
  - Briefly introduced earlier in Sections 5.3.2.1 and 5.3.2.4, and detailed further in Section 5.3.3.1 below
- Predicted accuracy model for Full Motion Video (FMV)
  - An extension of the Geolocation Data Predicted Accuracy Model: Measurement-space to Full Motion Video
  - See Section 5.3.3.2
- Mixed Gaussian Radom Field (MGRF)
  - A recommended sub-model to contain the entire *a priori* uncertainty model (predictive statistics) in a Geolocation Product Predicted Accuracy Model
  - More specifically, MGRF is recommended as the “core element” of the Geolocation Product Predicted Accuracy Model when corresponding products contain non-trivial variations in accuracy across the product. Use of an MGRF is flexible, practical, and rigorous.
  - See Section 5.3.3.3

#### 5.3.3.1 Adjustment

An adjustment “model” is an important companion component to the predicted accuracy model contained in a (complete) sensor model. The predicted accuracy models considered are either: (1) a Geolocation Product Predicted Accuracy Model, or (2) a Geolocation Data Predicted Accuracy Model: Measurement-space. Implementation of the adjustment model is optional and based on a correction grid that adjusts or corrects the corresponding data/product. The solution for the corrections or adjustments in the grid are based on additional information, such as surveyed ground control points, control imagery,

or other overlapping data/products, with subsequent improvements in the accuracy and predicted accuracy of the data/product. This concept was introduced earlier in Sections 5.3.2.1 and 5.3.2.4.

(An adjustment model is also applicable to the Geolocation Predicted Accuracy Model: Sensor-space or its equivalent contained in a (complete) physical sensor model, but it does not implement a correction grid, is well documented elsewhere [14,15], and is typically not applicable to Commodities data – hence, is only mentioned briefly in the remainder of this document.)

Corrections are either in data-space (e.g., image pixel locations if an image) or in product-space (e.g. ground locations if a 3d Point Cloud). More specifically, the correction grid is directly applicable to an underlying grid of elements in the data/product and subsequently interpolated for corrections to arbitrary elements in the data/product. If the data/product corresponds to an image, corrections are not corrections to the parameters that define the ground-to-data relationship, such as the polynomial coefficients of a ground-to-image function, but are corrections for the effects of their errors and are represented directly in image-space.

As will be detailed later in this section, the correction grid and its corresponding corrections map directly (correspond) to the predictive statistics in the predicted accuracy model, a desirable feature that is both practical and that enables (near) optimal corrections corresponding to a wide a variety of error sources. And as a reminder, the predicted accuracy model is “tuned” using actual accuracy assessments from various specific data/products from the same type of class of data/product to be adjusted.

The baseline correction grid and the corresponding adjustment process for the Geolocation Product Predicted Accuracy Model are documented in detailed in Appendix E and are summarized in a brief overview in Section 5.3.3.3. The baseline correction grid and the corresponding adjustment process for the Geolocation Data Predicted Accuracy Model: Measurement-space is further introduced below assuming that the data corresponds to an image, as is typical. The correction grid allows for a more accurate image pixel location (line,sample) for all pixels in the image.

#### **Adjustment of a specific data/product: image**

Prior to summarizing the correction grid, we first describe the pre-adjustment error, its predictive statistics, and a desired correction corresponding to an arbitrary location in the data (image). This is summarized in Figure 5.3.3.1-1.

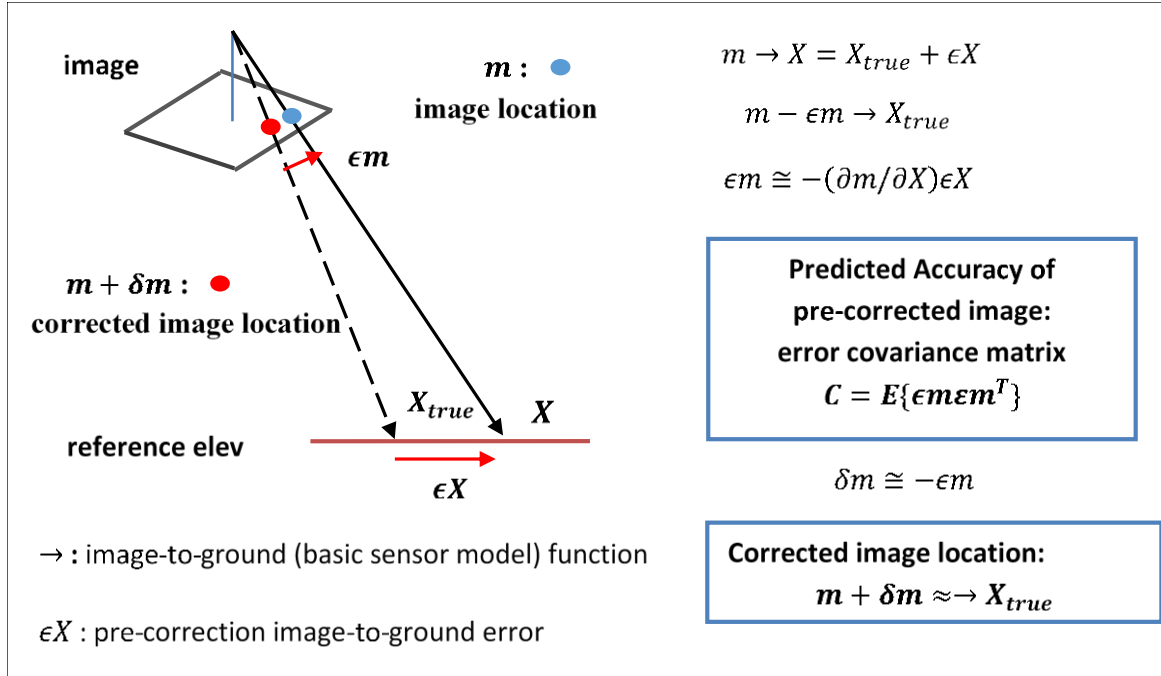


**Figure 5.3.3.1-1:** Representation of an arbitrary image pixel location ( $m = [line \ sample]^T$ ), its error ( $\epsilon m$ ), its *a priori* or pre-corrected covariance matrix ( $C$ ), and its desired correction ( $\delta m$ )

If an object of interest is identified and measured in the image at location  $m$ ,  $(m + \delta m) \rightarrow \approx X_{true}$ , where “ $\rightarrow$ ” represents the image-to-ground function evaluated at a reference elevation and using the input ( $m + \delta m$ ).

The correction  $\delta m$  is directly in image-space and compensates for the errors in the metadata but does not correct the metadata itself. Typical metadata consists of coefficients of a ground-to-image polynomial that was originally fit by the image provider to a physical sensor model’s ground-to-image function, which is a function of sensor pose (sensor position and attitude), sensor calibration parameters, etc.

Further details follow regarding the predictive statistics applicable to image location errors, followed by details of the corresponding correction grid:

### Predictive statistics

The major (*a priori*) predictive statistics in the Geolocation Data Predicted Accuracy Model: Measurement-space are defined as follows assuming an image:

- (1) Covariance matrix of the errors in an  $m = [line \ sample]^T$  image location or coordinates in the image:

$C$ , a  $(2 \times 2)$  matrix, where  $C \equiv E\{\epsilon m \epsilon m^T\}$ ,  $\epsilon m$  is the error in the location  $m$ , and  $E\{\}$  is the expected value operator.

(2) Spdcf of spatial (image-space) correlation of errors between two image locations  $m_i$  and  $m_j$ :  $\rho(\Delta m_{ij})$ , where  $\Delta m_{ij}$  is the  $2 \times 1$  vector difference in image-space between them and  $\rho(\Delta m_{ij})$  is a scalar function. The latter follows since it is assumed that correlation characteristics are the same in both the line and sample image directions in this particular example and generalized later in Appendix D.

The predictive statistics represent the error in an arbitrary image location in an arbitrary image of interest and are computed as detailed later in this document. Predictive statistics represent the underlying effects of metadata (sensor pose, etc.) errors “averaged” (root-mean-square) across image locations and across images from the type or class of images of interest. The above predictive statistics are applicable to an arbitrary image of interest prior to its adjustment.

Note: although a physical sensor model for the image is not available, if it were available, and if its ground-to-image function were parameterized by  $k$  adjustable sensor pose parameters contained in a  $k \times 1$  vector  $S$  and their corresponding  $k \times k$  error covariance matrix designated as  $C_S$ :  $C \cong \text{average} \left( \frac{\partial m}{\partial S} \right) C_S \left( \frac{\partial m}{\partial S} \right)^T$ , where  $\partial m / \partial S$  is the  $2 \times k$  partial derivative of image location with respect to sensor parameters and the average taken over representative image locations across the image. This note assumes that sensor parameter errors are the only errors of significance. In addition, and in terms of the predictive statistics, the above  $C$  is considered interim until averaged across representative images as well. Partial derivatives are typically relatively invariant across an image, and the (interim)  $C$  relatively invariant across images from a type or class of images of interest, particularly for Small-Sat images.

In addition, we assume that  $C$  is a diagonal matrix and the mean-value of error is zero ( $0_{2 \times 1}$ ), which are the standard assumptions, but not required. We also assume that optional sensor-mensuration (aka “unmodeled”) error and its corresponding predictive statistics are not applicable for simplicity of example. Based on these assumptions, the predicted accuracy for an arbitrary image location  $m$  is represented by:

(3) The *a priori* covariance matrix  $C = \begin{bmatrix} \sigma_{line}^2 & 0 \\ 0 & \sigma_{sample}^2 \end{bmatrix}$ , where  $\sigma$  represents standard deviation of error, and from which the scalar accuracy metric  $CE90$  can also be computed if so desired.

(4) Furthermore, the relative accuracy between image locations  $m_i$  and  $m_j$  is represented by the *a priori* covariance matrix  $C_{rel} = \begin{bmatrix} \sigma_{rel_{line}}^2 & 0 \\ 0 & \sigma_{rel_{sample}}^2 \end{bmatrix} = 2 \left( 1 - \rho(\Delta m_{ij}) \right) C$ , from which the scalar accuracy metric  $rel\_CE90$  can also be computed if so desired. Note that  $\sigma$  in  $C_{rel}$  represents a standard deviation or “sigma” and that  $\left( 1 - \rho(\Delta m_{ij}) \right)$  is a scalar that multiplies each element of the matrix  $C$ .

## Correction grid

A corresponding  $p \times q$  rectangular correction grid is illustrated in Figure 5.3.3.1-2 with supporting definitions – a  $3 \times 3$  grid is illustrated for clarity:

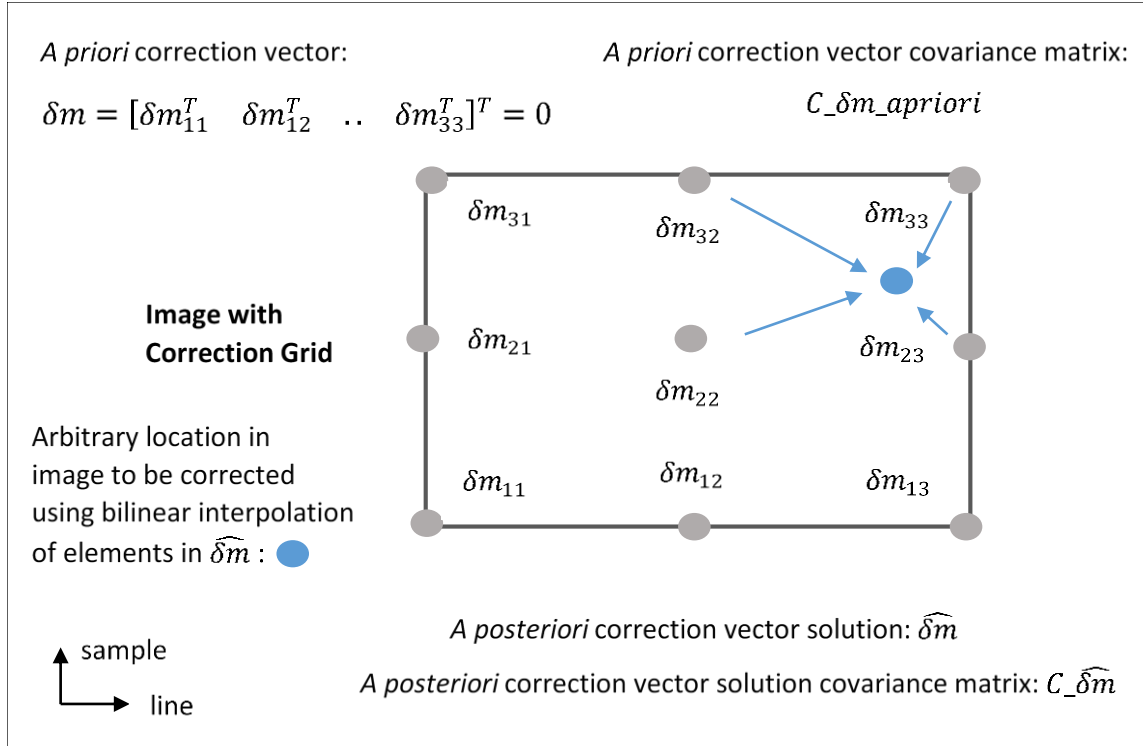


**Figure 5.3.3.1-2:** Example of a  $3 \times 3$  (square) correction grid

An element  $\delta m_{ij}$  in the correction grid is a  $2 \times 1$  vector and placed into a  $2pq \times 1$  correction or adjustment vector  $\delta m$ . The adjustment vector  $\delta m$  is represented as a column vector as is standard for vectors in these Technical Guidance Documents but can also be written as follows in order to save space:

$$\delta m = [\delta m_{11}^T \quad \delta m_{12}^T \quad \dots \quad \delta m_{1q}^T \quad \delta m_{21}^T \quad \delta m_{22}^T \quad \dots \quad \delta m_{2q}^T \quad \dots \quad \delta m_{pq}^T]^T,$$

where the superscript  $T$  represents vector transpose. The underlying image location corresponding to the correction element  $\delta m_{ij}$  is represented as a gray circle in Figure 5.3.3.1-2.

In addition, per Figure 5.3.3.1-2, the *a priori* (pre-solution) value for  $\delta m = 0_{2pq \times 1}$  and its corresponding *a priori* error covariance matrix is designated as  $C_{\delta m\_apriori}$ . The *a posteriori* (post-solution) value and its *a posteriori* error covariance matrix are designated as  $\widehat{\delta m}$  and  $C_{\widehat{\delta m}}$ , respectively.

The above notation for the elements in  $\delta m$  is cumbersome so we redefine  $\delta m$  as follows using the more generic notation  $\delta X$  for an arbitrary correction vector and single indexing for its elements, i.e.,

$$\delta X = [\delta X_1^T \quad \delta X_2^T \quad \dots \quad \delta X_{n-1}^T \quad \delta X_n^T]^T \equiv \delta m,$$

where the correction element  $\delta X_i$  is a  $2 \times 1$  vector and  $i = 1, \dots, n = pq$ . For example and regarding the correction grid in Figure 5.3.3.1-2,  $\delta X_7 = \delta m_{31}$ .

Correspondingly, we also have:  $C_{\delta X\_apriori} \equiv C_{\delta m\_apriori}$ ,  $\widehat{\delta X} \equiv \widehat{\delta m}$ , and  $C_{\widehat{\delta X}} \equiv C_{\widehat{\delta m}}$ .

The predictive statistics described earlier for errors in image locations  $m$  naturally map to the *a priori* (pre-solution) uncertainty corresponding to the elements in the correction grid. More specifically, the *a priori* (pre-solution) value or estimate for  $\delta X$  is equal to zero ( $\delta X = 0_{2pq \times 1}$ ) and its symmetric and positive definite (valid)  $2pq \times 2pq$  *a priori* error covariance matrix is equal to:

$$(5) C_{\delta X\_apriori} = E\{\delta X \delta X^T\} = \begin{bmatrix} C & \rho(\Delta m_{12})C & \dots & \rho(\Delta m_{1pq})C \\ \rho(\Delta m_{21})C & C & \dots & \dots \\ \dots & \dots & \dots & \dots \\ \rho(\Delta m_{pq1})C & \rho(\Delta m_{pq2})C & \dots & C \end{bmatrix},$$

where  $\Delta m_{ij} = (m_i - m_j)$  is the difference between the underlying image locations corresponding to corrections  $\delta X_i$  and  $\delta X_j$ , respectively, for  $i, j = 1, \dots, pq$ . This follows since the corrections are defined as minus the corresponding image location errors.

For example, if a  $2 \times 2$  grid of corrections,  $C_{\delta X\_apriori}$  is a  $8 \times 8$  matrix that contains four  $2 \times 2$  block matrices. Furthermore, the cross-block  $\rho(\Delta m_{12})C$  is the  $2 \times 2$  cross-covariance between the *a priori* values  $\delta X_1$  and  $\delta X_2$ , and the scalar function  $\rho(\Delta m_{12})$  multiplies each element of  $C$ .

The above *a priori* predictive statistics for the correction grid enable an optimal WLS solution  $\widehat{\delta X}$  for the corrections and computation of its error covariance matrix  $C_{\widehat{\delta X}}$ . The solution is also based on measurements from External Data (e.g., control images or ground control points) corresponding to conjugate image locations in the data/product (image). A measurement provides information that updates all elements in the correction grid via the *a priori* spatial correlation specified in the predictive statistics – the closer the measurement to a correction element in image-space, the “more direct” the information.

The blue circle in Figure 5.3.3.1-2 represents an arbitrary image location (measurement) to be corrected in the image. The correction is computed using bilinear interpolation of the four surrounding correction elements contained in the post-solution correction vector as indicated by the blue arrows.

The correction grid can vary in size from a  $2 \times 2$  correction grid to approximately a  $11 \times 11$  correction grid or larger, and more generally, can be an explicit rectangular grid of similar size. The number of corrections in the correction grid is recommended such that the *a priori* spatial correlation  $\rho(\Delta m_{ij})$  between adjacent corrections in the correction grid is equal to approximately 0.9 (unit-less) or greater; this will decrease for non-adjacent corrections. In addition, and as a somewhat extreme example, a  $1 \times 1$  correction grid can also be used in appropriate circumstances, with one corresponding product-wide correction and no bilinear interpolation.

See Appendix D for further details regarding adjustment based on the correction grid and the WLS solution for its values as well as detailed examples of its performance. See TGD 2d (Estimators and their Quality

Control) for a general description of WLS and corresponding quality metrics that help to ensure a reliable solution for the correction grid. Appendix D also includes a figure similar to Figure 5.3.3.1-1 of image error and its desired correction for further background. The figure includes additional details regarding true versus assumed sensor “pose” (sensor position and attitude) that affects the image metadata. In addition, see Appendix C for details regarding the generation or population of predictive statistics that are assumed available and used in the adjustment.

### Example

Figure 5.3.3.1-3 presents an example of an implementation of the correction grid based on simulated image errors and conjugate measurements. Pre-solution and post-solution errors are assessed across a check point grid that also corresponds to the 6x6 correction grid for convenience. Therefore, for example, if the image was 20k x 20k pixels in size, adjacent check point locations are 4k pixels apart.

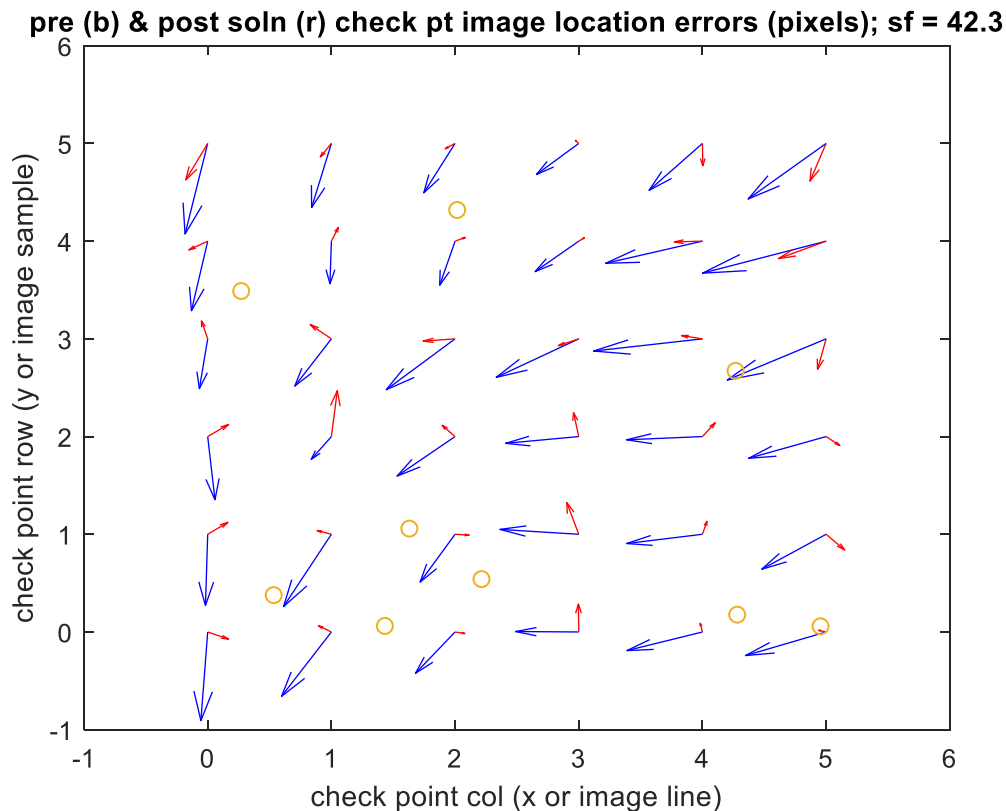


**Figure 5.3.3.1-3:** Pre-adjustment image location errors (blue arrows) and post-adjustment image location errors (red arrows) across a check point grid in the image; WLS solution for the correction grid based on 9 conjugate measurements randomly located across the image (circles); largest image location radial error (a blue arrow) equals 42.3 pixels

Nine conjugate measurements or image locations were generated randomly across the image. The conjugate measurements correspond to the identification/measurement of nine ground control points in the image for adjustment. The ground control points are either surveyed ground points or ground points

generated using control imagery. The conjugate measurements are differenced with the projections of the corresponding ground control points to image-space, the latter based on the ground-to-image function associated with the image for adjustment. This difference enables or “drives” the WLS solution for the correction grid.

Note: if control imagery is used, ground points are typically generated using stereo control images or a single control image with an accurate reference elevation.

Although not explicitly illustrated in the above figure, a post-solution correction error for an arbitrary image location in the product is approximately equal to the bilinear interpolation of the corresponding four red arrows in the check point grid.

See Appendix D for further details regarding adjustment, including other examples and also ensemble statistics across hundreds of simulated realizations of the image and its errors as opposed to the explicit results for one realization of the image and its errors as presented in Figure 5.3.3.1-3 and applicable operationally. Note that the use of random locations corresponding to the measurements in the image was implemented for the purpose of simulation only, including the computation of sample statistics across numerous realizations of the image and its errors. Operationally, locations are typically dispersed evenly across the image’s AOI or footprint as much as possible as dictated by the content of the image.

#### **Caveat regarding other possible correction approaches**

Another possible class of corrections consists of parameters that define a transformation (typically an affine or related transformation) from an arbitrary element of the data/product (e.g., 2d image-coordinates) to a correction directly applicable to that element. Corrections based on such a transformation can more directly correct for the effects of sensor pose errors (position errors and in particular, attitude or rotation errors) on the ground-to-data/product relationship (e.g., ground-to-image polynomial) than can a correction grid. This is primarily relevant for Commodities data that corresponds to images, such as Small-Sat images. Let us term the above transformation “affine” for the remainder of this section for specificity.

The appropriate predictive statistics (*a priori* error covariance matrix) corresponding to the parameters (coefficients) of the affine transformation do not directly map to the predictive statistics in the predicted accuracy model and a mapping or correspondence between the two, once derived, will only be an approximation. In addition, the applicability of such a transformation is not known *a priori* for a given type of class of data/product in general, since its ground-to-image function (metadata) and corresponding errors typically reflect additional value-added processing during data/product generation, such as image registration or possibly multiple image registrations, with accuracy that can vary significantly from data/product to data/product.

However, it is true that if the specific data/product to be adjusted does have errors consistent with the affine transformation, a well-modeled adjustment based on solving for the coefficients of such a transformation will do better than a correction grid, particularly if the ground control points (or its equivalent) are relatively sparse and are not geometrically diverse over the image. In contrast, the

correction grid can account for a more varied collection of errors, including those represented by the affine transformation, albeit with somewhat less fidelity. See Appendix D for further details and examples of performance.

The above comments are also generally applicable to yet another class of corrections that define a transformation: a low order polynomial from either ground-space or image-space to corrected image-space. Again, the appropriate predictive statistics (*a priori* error covariance matrix) corresponding to the coefficients of the low order (correction) polynomial do not directly map to the predictive statistics in the predicted accuracy model and a mapping or correspondence between the two, once derived, will only be an approximation.

For example, if there are four polynomial coefficients, an offset and a rate correction for each image coordinate, with a summed effect corresponding to a correction to each image coordinate, predicted absolute accuracy will be a function of the location of a pixel in the image. In addition, predicted relative accuracy between two locations is dependent on both of their locations in the image, not just the distance between them, assuming that the rate uncertainties (sigmas) are different for the two image coordinates components (x vs y, or alternatively, line vs sample).

Of course, if only offset coefficients are applicable to the (correction) polynomial, absolute predicted accuracy is invariant of the location of a pixel in the image and predicted relative accuracy is either equal to zero or only a function of horizontal distance between two locations if sensor-mensuration error is modeled too. However, a sparse correction grid is virtually equivalent if *a priori* spatial correlation is specified as high across the image via the spdcf.

In summary, due to its generality as well as its reasonable performance, a correction grid is recommended for the adjustment of Commodities-based data (e.g., images) that have little or no accuracy pedigree accompanying the data as provided by the vendor, i.e., data that has a populated Geolocation Data Predicted Accuracy: Measurement-space generated by the NSG.

#### **5.3.3.2 Full Motion Video**

A predicted accuracy model for Full Motion Video (FMV) is an extension of the Geolocation Data Predicted Accuracy Model: Image-space. The predictive statistics that are already included in the latter are assumed applicable to each image in the FMV image-sequence as a simple but reasonable assumption. However, the extension to FMV also requires an additional predictive statistic: the spdcf for the temporal correlation of errors between images in the image-sequence. This is illustrated conceptually in Figure 5.3.3.2-1.

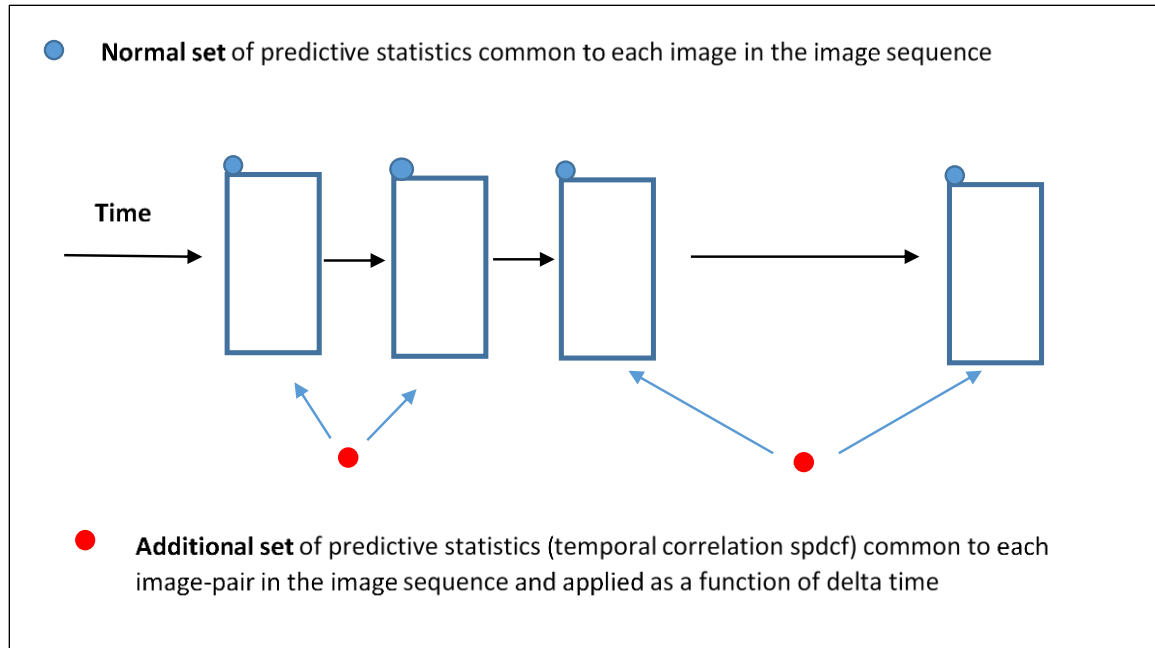


**Figure 5.3.3.2-1:** FMV image sequence and its corresponding predictive statistics representing predicted accuracy of the images; adjacent images in time have overlapping ground footprints (not depicted in figure)

The adjustment model (section 5.3.3.1) is augmented as well for FMV. Either corrections correspond to the summation of the corrections in the (baseline) correction grids corresponding to each image in the sequence, or they correspond to the summation of corrections in the correction grids corresponding to a subset of the images in the sequence, with interpolation between these correction grids for corrections applicable to arbitrary images in the sequence. Note that measurements containing external information directly applicable to a correction grid in one image are also related to the correction grids for all other images in the sequence via the *a priori* temporal correlation between it and the other images as specified by the corresponding temporal spdcf, a function of the delta time-of-applicability between image-pairs. This relationship is automatically exploited using a proper solution process, such as a correctly implemented WLS adjustment, which was previously discussed in Section 5.3.3.1 but requires augmentation in order to contain the sequence of correction grids for FMV.

A successful adjustment process, regardless the type of adjustable parameters or the estimator used to solve for them, requires the automatic/automated measurement of conjugate geolocations in adjacent image frames (“tie points”) and typically in control imagery as well (or photo-identifiable ground control points) for good resultant accuracy. This can be a challenge. For example, Figure 5.3.3.2-2 presents one frame in an FMV sequence which includes the color-coded status of the frame’s current tie points that are automatically and dynamically “tracked”, i.e., identified and measured in this frame and previous frames [7]. Tie-points are dropped and new ones added (tracked) due to changing imaging geometry and other challenges. In this particular example, WLS was implemented in order to solve for adjustable parameters associated with a physical sensor model.

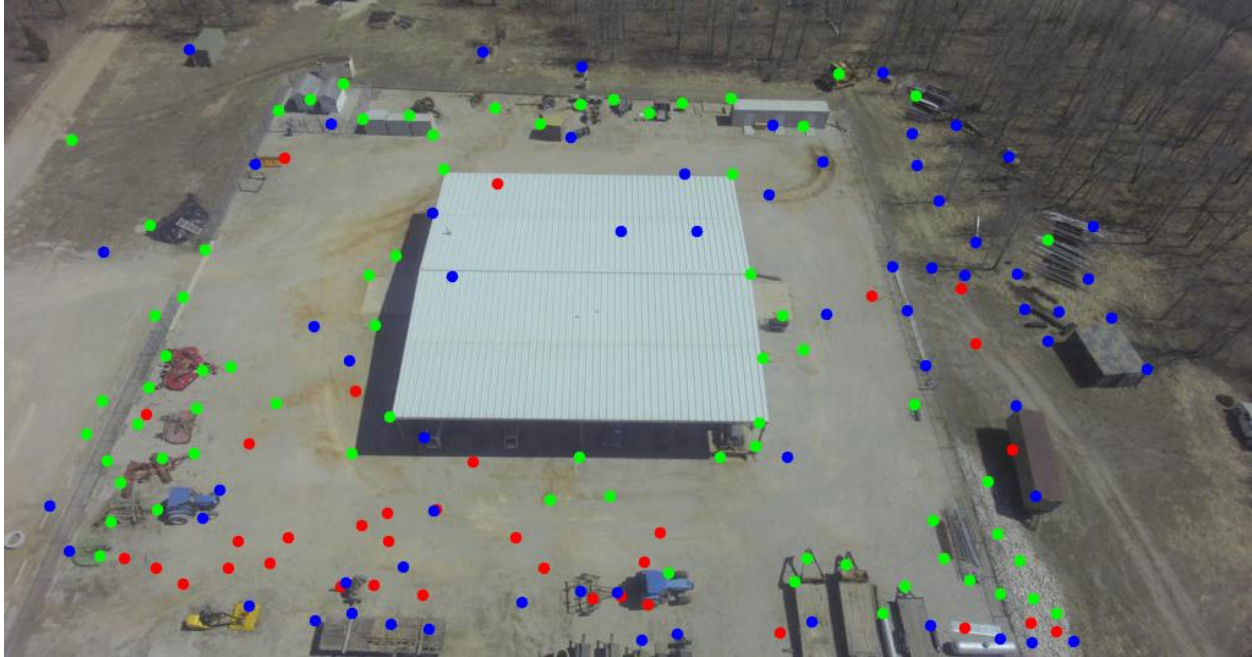


**Figure 5.3.3.2-2:** Tie points automatically measured (“tracked”) in frame #36 and their color-coded image-location and status: continues to be tracked (green), dropped this frame (red), track initialized this frame (blue); quadcopter motion imagery frame with graphic overlay

More applied research is recommended for both tie point tracking and the implementation of adjustable parameters associated with correction grids. Aspects of the latter include applied research into WLS implementation for reasonably high throughput for relatively long image sequences (use of small grid size, diagonal covariance matrices, etc.). A Kalman filter implementation should also be considered that solves for the equivalent of grid corrections in near-real time and consistent with the predictive statistics contained in the Geolocation Data Predicted Accuracy Model: Image-space (FMV).

### 5.3.3.3 *Mixed Gaussian Random Field*

A Mixed Gaussian Random Field (MGRF) is considered a companion component to the Geolocation Product Predicted Accuracy Model (Section 5.3.2.1). More specifically, it is an option to represent or “contain” the latter’s entire *a priori* uncertainty model (predictive statistics). It allows for the representation of predicted accuracy that can vary over the product (realization). If an MGRF is not included, the “standard” predicted accuracy model is applicable as summarized in Section 5.3.2.1 and detailed in Appendix B.

An MGRF is rigorous, flexible, as well as practical, and is considered ideal as the core element of a Geolocation Product Predicted Accuracy Model. It is also practical in the sense that it only requires a few predictive statistics which are easily contained in the product’s metadata or its equivalent. These statistics are also readily “mapped” to either the predicted accuracy of a geolocation of interest or to the predicted relative accuracy between geolocations of interest. The MGRF also enables an appropriate adjustment model.

An MGRF and the Geolocation Product Predicted Accuracy Model in which it resides correspond to a particular type or class of 3d geolocation product, typically categorized by vendor/producer, type of product (e.g. EO-derived 3d Point Cloud), date-range, and possibly general scene content (e.g., urban, agriculture, etc.). The contents of the MGRF are tuned by previous accuracy assessments of products from the same type or class of 3d geolocation product.

An MGRF consists of a collection of specified partitions over the geolocation product's Area of Interest (AOI) or ground "footprint". Each geolocation in the product is associated with one and only one partition. In addition, an MGRF also consists of a collection of specified random fields. Each partition in the MGRF corresponds to a specified subset of the random fields. This provides a method to group geolocations (points) with similar predicted accuracy characteristics as further described below.

A random field is a collection of spatially correlated and Gaussian distributed random errors corresponding to the underlying geolocations in the product or MGRF. The random field's predictive statistics make-up the *a priori* statistical model for these errors. The error in a geolocation associated with a particular partition in an MGRF consists of a sum of independent (uncorrelated) errors, one from each of the partition's specified random fields. As such, an MGRF can also be considered a mixture of random fields. An example of a single random field is presented graphically later in this section for further insight (Figure 5.3.3.3-2).

More specifically, an MGRF contains: (1) a description of each partition, (2) the *a priori* probability of occurrence of each partition, (3) a list of random fields corresponding to each partition, and (4) the predictive statistics defining each random field. The latter consist of the mean-value of error, the covariance matrix about this mean-value, and a strictly positive definite correlation function (spdcf) that specifies the spatial correlation of errors within the same realization of the random field. The *a priori* probability of occurrence for a partition corresponds to the approximate probability that an arbitrary geolocation in the product is associated with that partition.

There is one and only one MGRF associated with a product. A typical MGRF has between 1-5 partitions and the same number of random fields. The baseline or default "mapping" of random fields to partitions is as follows and assumes  $m$  partitions and  $m$  random fields:

Partition 1 corresponds to random field 1, and partition  $i$ ,  $1 < i \leq m$ , corresponds to random field 1 plus random field  $i$ . Random field 1 represents systematic errors applicable across the entire product, whereas random field  $i > 1$  represents additional additive errors associated with geolocations that were difficult to generate due to various issues. For example, if an EO-generated Point Cloud, geolocations corresponding to "melted roof top edges" or possibly corresponding to crop anomalies due to the effect of "corn rows" on the measurement of conjugate image points when generating the Point Cloud. The predicted accuracy of geolocations associated with or "in" partition 1 is better (smaller value indicating less uncertainty) than for geolocations in the other partitions. Figure 5.3.3.3-1 graphically illustrates the concept of the baseline Random Field-to-Partition Mapping assuming three partitions:

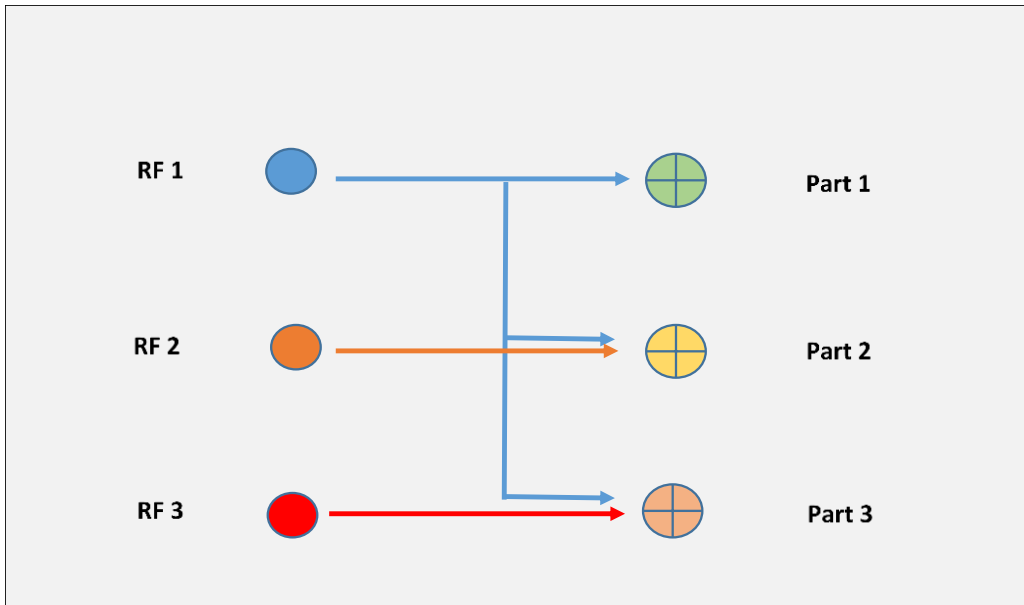


**Figure 5.3.3.3-1:** Baseline Random Field-to-Partition Mapping assuming an MGRF with three partitions

Regardless the particular random field-to-partition mapping, the first partition is the “nominal” partition defined as all geolocations in the product not associated with any other partition, and is typically applicable to most of the geolocations in the product. The other partitions are simply defined textually. For example, if the product corresponds to an EO-derived 3d Point Cloud a non-nominal partition’s description might be all geolocations corresponding to “melted roof-top edges”. (See Appendix G for an overview of melted roof-top edges.)

Typically, the geolocations associated with a non-nominal partition are not explicitly identified ahead of time prior to product dissemination. If such a geolocation is of interest to the “down-stream” user, its corresponding partition is either identified by the user based on the partitions’ textual descriptions and the user’s visualization of the product (optionally, by an automatic/automated process) or is designated as unknown by the user. As detailed in Appendix E, the MGRF contains both the predicted accuracy for geolocations known to be in a particular partition and the predicted accuracy for arbitrary geolocations in the product, i.e., those geolocations in an unknown partition. Computation of the latter utilizes the *a priori* probability of occurrence of each partition which sum to 1.

The predictive statistics for a geolocation of interest are “higher fidelity” if its associated partition is known versus unknown. Also, it is not unusual for certain types or classes of geolocation products to have only one partition specified in the MGRF, the nominal partition, which is applicable to all geolocations in the product, by definition. As such, identification of a partition is moot. A relevant example corresponds to some types or classes of LIDAR-derived 3d Point Clouds where predicted accuracy is reasonably represented as invariant across the product. The use of only one partition is equivalent to the non-use of an MGRF, i.e., corresponds to the “standard” predicted accuracy model for a geolocation product as detailed in Appendix B.

See TGD 1 (Overview and Methodologies) for an introduction to random fields in general and Appendix E for a thorough description of the MGRF for representation of predicted accuracy for a geolocation product. Appendix E also includes detailed quantitative examples and plots illustrating concepts, and also includes details of product adjustment or fusion based on MGRF. Some of these concepts are also summarized in the remainder of this section:

- The “Spatial correlation” summary provides insight into the concept of a random field and the spatial correlation of errors.
- The “Product adjustability” summary states that a product can be adjusted in a practical and near-optimal manner based on the use of MGRF, or more generally, fused with other products, and includes a summary of subsequent benefits.
- The “Scalar predicted accuracy metrics” summary provides an example of an MGRF with corresponding partitions and their associated random fields. It should help to clarify the above description of an MGRF, which may seem somewhat complicated at first reading due to the various terminology and interrelationships that were introduced. The example also details various scalar accuracy metrics, such as CE90, applicable to geolocations known to be associated with a particular partition as well as to arbitrary geolocations in the product (partition unknown). It also discusses optional additions to the MGRF (product) metadata or its equivalent.

### **Spatial correlation**

The geolocation errors in a geolocation product are spatially correlated as represented by the spdcf corresponding to each random field that is specified as part of the MGRF representation. Spatial correlation has a significant effect on the relative accuracy between two geolocations in the same product realization. The higher the correlation, the better the predicted relative accuracy corresponding to the statistical cancellation of similar errors. Correlation of geolocation errors corresponding to geolocations in different random fields in the same product, as well as to all geolocation in different products (realizations) of the same type or class of geolocation product, are reasonably assumed uncorrelated. Note that all random fields are assumed to be (wide-sense) homogeneous, analogous to (wide-sense) stationary stochastic processes. That is, a random field’s predictive error statistics are not a function of the actual value of the geolocation(s), other than their difference for relative errors. A random field is also considered multi-variate, as it corresponds to 3d geolocation errors in general.

Figure 5.3.3.3-2 presents an example of a single Gaussian random field of horizontal geolocation errors corresponding to a specific 3d geolocation product or realization that contains a collection of 3d geolocations (e.g., 3d Point Cloud) for further insight into the concept of a random field. Although geolocation errors are 3d, only horizontal geolocation errors are plotted for clarity.

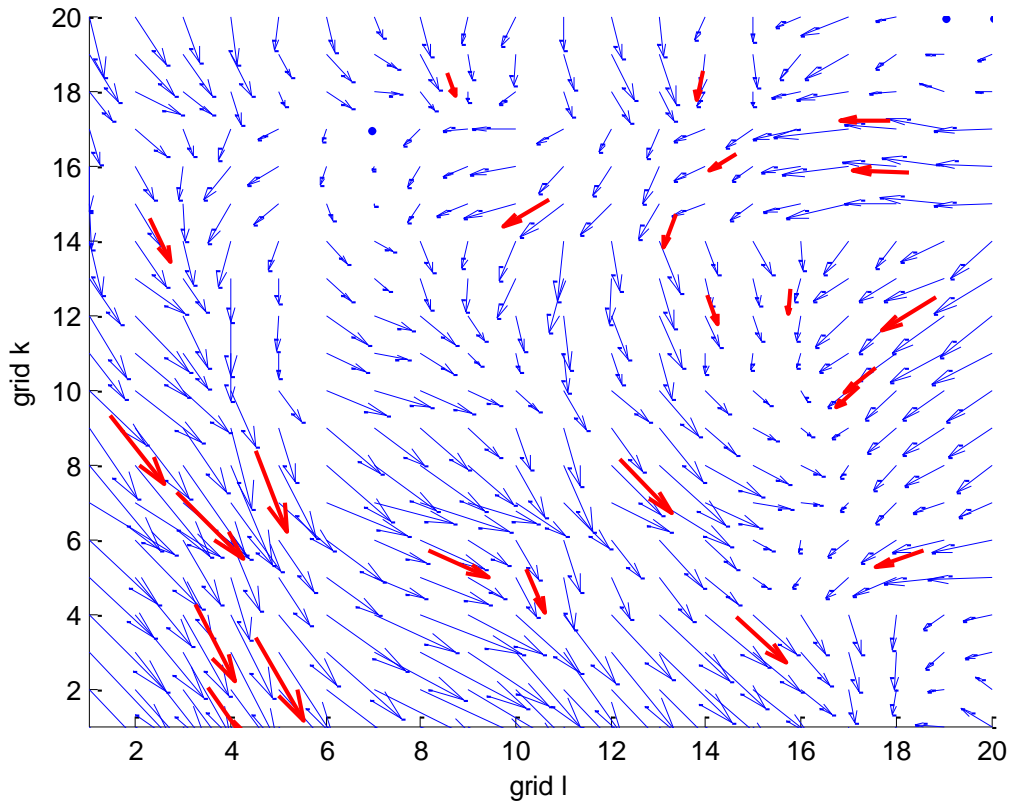


**Figure 5.3.3.3-2:** Realization of a Random Field; quiver plot of simulated horizontal errors (2d vectors) contained in a random field corresponding to a portion of a 3d geolocation product; errors are in meters and the plot is self-scaled; red 2d vectors are interpolated errors between geolocations

The errors in Figure 5.3.3.3-2 are represented across a horizontal grid corresponding to a local tangent plane in the product, where each horizontal error is located at the horizontal coordinates of its corresponding 3d geolocation. There is a “medium” level of spatial correlation of errors between most geolocations in this example, and a “high” level of correlation (similarity of errors) between nearby geolocations. This is consistent with *a priori* spatial correlation evaluated as a function of distance in the corresponding spdcf.

### **Product adjustability**

Appendix E describes the optional correction grid-based adjustment of the MGRF (product), and more generally, the fusion of the product with other products. Fusion not only improves product accuracies, but ensures the consistency of geolocations across the products. It simultaneously solves for corrections to the systematic errors in each of the products involved and then allows for the correction of each geolocation in each product. Reference [2] provides an “easy-to-read” overview of the MGRF and fusion.

Adjustment based on a correction grid is performed in conjunction with the predictive statistics (error covariance matrices and spdcf) in the MGRF that are used to represent the *a priori* predicted accuracy of the corrections, their values equal to zero prior to the adjustment. Such an adjustment can successfully

correct for geolocation errors that are very general, typically due to both the underlying sensors/metadata in the product generation process as well as the generation process itself. Errors consistent with a more “specific” or “deterministic” adjustment model, such as the coefficients of a 3d geolocation-to-corrected 3d geolocation transformation, can be absorbed by a correction grid but many types of errors consistent with MGRF predictive statistics cannot be absorbed by such a transformation.

The adjustment based on a correction grid for a geolocation product is very similar to an adjustment based on a correction grid for an image that was described earlier in Section 5.3.3.1 and illustrated by example in Figures 5.3.3.1-2 and 5.3.3.1-3. Primary differences correspond to: (1) 3d geolocations vs 2d image locations and their corrections, and (2) the predictive statistics for the geolocation product correspond to an MGRF as described above, but the predictive statistics for the image technically do not. However, regarding the latter, the predictive statistics for the image do correspond to a random field (possibly two random fields if sensor-mensuration errors are modeled separately), but not to different partitions across the image.

The above adjustment “scenario” for a geolocation product is also predicated on the non-availability of high-fidelity “complete sensor model” containing both reliable predicted accuracy and a product-specific adjustment model which are generated when the product itself is generated and subsequently made available to the NSG, such as GPM for 3d Point Clouds as discussed earlier in Section 5.2.3. However, such a high-fidelity complete sensor model is currently not available for most External Data, and for geolocation products in particular. Hence the use of MGRF-based predictive statistics and the optional adjustment of the product based on a correction grid as described in this section of the document: a practical yet theoretically rigorous approach.

### **Scalar predicted accuracy metrics**

Appendix E also details the recommended metadata or its equivalent associated with the MGRF (product), and Appendix E contains associated MATLAB pseudo-code for its generation. This includes the generation of scalar accuracy metrics CEXX and LEXX corresponding to horizontal and vertical predicted accuracy, respectively, at probability levels XX=90, 99, and optionally 999 (99.9 %), for both geolocations within a known partition and for arbitrary geolocations within the product. These scalar accuracy metrics are simple but practical and informative metrics. Correspondingly, their computations are detailed in this document and they are recommended for inclusion in the product’s predictive statistics and contained in the product’s metadata or its equivalent. They are particularly suited for the support of actionable intelligence.

A representative example involving the scalar accuracy metrics corresponding to an MGRF (product) with two partitions is summarized in Table 5.3.3.3-1. Although geolocation errors are 3d (x,y,z), only horizontal errors (x,y) and their corresponding scalar accuracy metrics are detailed in this example for ease of illustration. The scalar accuracy metrics are Circular Error CEXX, the radius of a circle such that horizontal radial error is less than or equal to CEXX with probability XX%. Three values of XX are evaluated: XX=90 (90%), XX=99 (99%), and XX=999 (99.9%).

**Table 5.3.3.3-1:** *A priori* probability of occurrence and scalar accuracy metrics for partitions 1 and 2, and scalar accuracy metrics for arbitrary geolocations (partition unknown)

Partition	prob occur	CE90 (meters)	CE99 (meters)	CE999 (meters)
1	0.9	4.3	6.1	7.5
2	0.1	13.6	19.2	23.5
arbitrary	n/a	5.2	13.6	19.2

The *a priori* probability that a geolocation is in partition 1, the nominal partition, is 0.90. The *a priori* probability that a geolocation is in partition 2 is 0.10. The errors in the geolocations in partition 1 correspond to random field 1. The errors in the geolocations in partition 2 correspond to the sum of two independent errors, one from random field 1 and one from random field 2 in this example.

Both random field 1 and random field 2 correspond to horizontal geolocation errors with an *a priori* mean-value of error equal to zero ( $0_{2 \times 1}$ ); however, the *a priori* uncertainty (standard deviations) of errors in random field 2 are three times larger than that for random field 1. More specifically, the *a priori* covariance matrices corresponding to horizontal errors in random fields 1 and 2 are equal to:

$$\begin{bmatrix} 4 & 0 \\ 0 & 4 \end{bmatrix} = \begin{bmatrix} 2^2 & 0 \\ 0 & 2^2 \end{bmatrix} \text{meters-squared and } \begin{bmatrix} 36 & 0 \\ 0 & 36 \end{bmatrix} = \begin{bmatrix} 6^2 & 0 \\ 0 & 6^2 \end{bmatrix} \text{meters-squared, respectively.}$$

Correspondingly, the *a priori* mean-value of error for geolocations residing in both partition 1 and 2 remain zero. However, the corresponding covariance matrices for geolocations in the partitions are equal to:

$$\begin{bmatrix} 4 & 0 \\ 0 & 4 \end{bmatrix} = \begin{bmatrix} 2^2 & 0 \\ 0 & 2^2 \end{bmatrix} \text{meters-squared for geolocations in partition 1 which contains random field 1, and}$$

$$\begin{bmatrix} 4 & 0 \\ 0 & 4 \end{bmatrix} + \begin{bmatrix} 36 & 0 \\ 0 & 36 \end{bmatrix} = \begin{bmatrix} 40 & 0 \\ 0 & 40 \end{bmatrix} \cong \begin{bmatrix} 6.3^2 & 0 \\ 0 & 6.3^2 \end{bmatrix} \text{meters-squared for geolocations in partition 2 which}$$

contains random field 1 and random field 2.

The above mean-values and covariance matrices for the partitions were used to compute the partitions' scalar accuracy metrics in Table 5.3.3.3-1 based on an assumed Gaussian distribution of corresponding geolocation errors. Their Gaussian distribution follows since errors are either from random field 1 or the sum of errors from random fields 1 and 2, all of which are assumed to be Gaussian distributed. However, the computation of the scalar accuracy metrics corresponding to an arbitrary geolocation requires additional information: the partitions' *a priori* probability of occurrence and the fact that relevant errors are considered to correspond to a probabilistic mix of errors from both partition 1 and partition 2. Correspondingly, the distribution of errors is not Gaussian distributed for this case. Appendix E details appropriate methods for the computation of the scalar accuracy metrics corresponding to both geolocations in known partitions and to arbitrary geolocations.

Partition 2 corresponds to geolocations that were “problematic” during product generation, i.e., had a large source of error (random field 2) in addition to or combined with the product-wide source of error associated with partition 1 (random field 1). The following comments also apply:

- Table 5.3.3.3-1 and the above description of corresponding partitions and underlying random fields only address absolute accuracy. Relative accuracy is also dictated by spatial correlation as specified by the spdcf associated with each random field. See Appendix E for further details regarding relative accuracy and its computation and Appendix F for corresponding MATLAB pseudo-code.
- Although the above *a priori* covariance matrices are diagonal with equal variances, they are more generally arbitrary covariance matrices (symmetric and positive definite). See Appendix E for further details.
- All scalar accuracy metric and underlying predictive statistic values are fictitious in this example and for the purpose of illustration only.

Figure 5.3.3.3-3 presents a graphical summary of a subset of the scalar accuracy metrics presented in Table 5.3.3.3-1. CE90 (blue) and CE99 (blue-dash) correspond to partition 1 and CE90 (red) and CE99 (red-dash) correspond to arbitrary geolocations (partition unknown). Two thousand independent random samples of error in correct proportion from partition 1 (blue dots) and partition 2 (magenta dots) based on their *a priori* probability of occurrence are also included in the figure for further insight.

CE arb: 90%(r),99%(-r);CE part1: 90%(b), 99%(-b);samples part1 (.b),part2(.m)

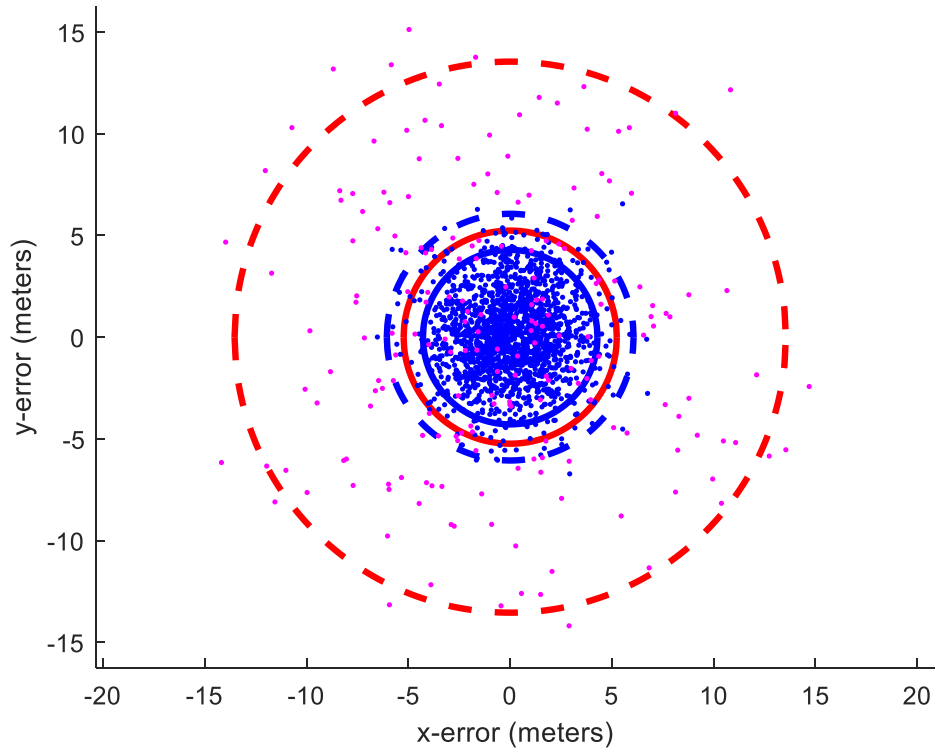


**Figure 5.3.3.3-3:** Based on an MGRF representation of Predicted Accuracy for a specific geolocation product: *CE90* (radius of blue circle) and *CE99* (radius of blue-dash circle) for geolocations known to reside in the nominal partition, partition1; *CE90* (radius of red circle) and *CE99* (radius of red-dash circle) for arbitrary geolocations in the product (partition unknown); blue and magenta dots correspond to a total of 2000 simulated independent random samples in correct proportions from partitions 1 and 2, respectively.

The *CE90* and *CE99* circles corresponding to partition 2 are not included in the figure for clarity. However, due to its low probability of occurrence but large uncertainty relative to partition 1, partition 2 has little effect on *CE90* for an arbitrary geolocation in the product but does have a significant effect on its *CE99*, as seen in the figure. That is, the red circle (*CE90* arbitrary) is only slightly larger than the blue circle (*CE90* partition 1), but the red-dash circle (*CE99* arbitrary) is significantly larger than the blue-dash circle (*CE99* partition 1) due to the possible influence of partition 2 on an arbitrary geolocation.

The corresponding scalar accuracy metrics enable actionable intelligence: If a geolocation of interest is known to be in the (nominal) partition 1, we know that it is only 1% probable that its horizontal geolocation error is greater than 6.1 meters, but if the partition in which the geolocation resides is unknown, we know that it is 1% probable that its horizontal geolocation error is greater than 13.6 meters. This significant increase in *CE99* is due to the 10% probability that the geolocation may be associated with partition 2.

The following additional comments apply:

- If partition 2's *a priori* uncertainty were significantly greater than approximately three times that of partition 1, the increase in CE99 for an arbitrary geolocation would be even larger and more dramatic than shown in Figure 5.3.2.6-3. On the other hand, if partition 2's *a priori* probability of occurrence were significantly larger, CE90 for an arbitrary geolocation would increase significantly.
- If the geolocation of interest were known to correspond to partition 2, the partition 2 scalar accuracy metrics would be directly applicable (see Table 5.3.3.3-1).
- As a reminder, the scalar accuracy metrics are predictive statistics corresponding to predicted accuracy; they are not sample-based scalar accuracy metrics. Also, each of the simulated independent random samples illustrated in Figure 5.3.3.3-3 correspond to a different realization of the product.
- Figures similar to Figure 5.3.3.3-3 are readily generated during the computation of scalar accuracy metrics per Appendix E and Appendix F, and may be considered as optional metadata content for additional insight regarding actionable intelligence and other factors of interest to the “down-stream” user. Note that independent samples of error in similar figures become even more interesting (non-symmetric pattern or distribution) when the corresponding covariance matrices have non-zero off-diagonal elements and/or the corresponding mean-values are not equal to zero (non-typical) – see TGD 2D for various examples involving up to 3 partitions in the MGRF.

It is recommended that both CE90 and CE99 are included in the product metadata or its equivalent for each partition as well as for arbitrary geolocations (partition unknown). In addition, although the underlying distribution for geolocation errors corresponding to geolocations in a specific partition are assumed to be Gaussian distributed, this is not true for the distribution of errors corresponding to arbitrary geolocations. Therefore, as detailed in Appendix E, it is also recommended that CE999 (99.9%) be included for arbitrary geolocations in order to capture any possible effects of very low probability-of-occurrence partitions with very large predicted errors. Of course, regardless which scalar accuracy metrics are included in the metadata or not, the various parameters and predictive statistics that actually define the MGRF and that were detailed earlier are always included. As such, and although not as convenient, a “down-stream” user or application can then compute any desired scalar accuracy metrics of interest based on the equations of Appendix E and/or the pseudo-code in Appendix F.

As a final comment regarding MGRF metadata: As discussed earlier, a geolocation of interest is known to correspond to a particular partition if it is identified as such by the “down-stream” user of the product or possibly by an automatic/automated process. It could also be identified as such if it were within one of a set of geographic boundaries optionally computed by the product provider and/or NSG Quality Assessment and included in the product’s metadata or its equivalent. Also, as a reminder, identification of a partition is not applicable if the MGRF has only one (product-wide) partition.

#### 5.3.4 Guide to detailed examples of accuracy assessment and predicted accuracy models

Further details, applications, and examples of accuracy assessment models, predicted accuracy models, and related components are “pointed to” in Table 5.3.4-1:

**Table 5.3.4-1:** References to further details of accuracy assessment and predicted accuracy models and their applications, including examples, contained in this document

Section	Model (or related processing)	Contents	Population (generation)	User Applications
B.1	Geolocation Product Accuracy Assessment	x	x	
B.2	Geolocation Product Predicted Accuracy	x	x	
B.3	Applications of above models			x
C.1	Geolocation Data Accuracy Assessment	x	x	
C.2	Geolocation Data Predicted Accuracy	x	x	
C.4	Applications of above models			x
D	Geolocation Data adjustment			x
E	Geolocation Product MGRF and adjustment	x	x	x
5.3.5.3	Geolocation Data Accuracy Assessment		x	

A 3d Point Cloud is an example of the applicability of Sections B.1-B.3 and (appendix) E in the above table. A Small-Sat image is an example of the applicability of Sections C.1-C.2, C.4, and (appendix) D in the above table.

The three categories of predicted accuracy models defined earlier in Sections 5.3.2.1, 5.3.2.3, and 5.3.2.4 are also discussed in v1.1 of TGD 1 (Overview and Methodologies) at a summary level, including illustrative graphics, but using slightly different terminology more generally termed “methods”. The appropriate mapping between these two documents is presented in Table 5.3.4-2:

**Table 5.3.4-2:** The relationship between predictive accuracy model definitions and corresponding methods in TGD 1

TGD 2f section #	name of model	TGD 1 section #	name of method
5.3.2.1	Geolocation Product Predicted Accuracy Model	Appendix B	Geolocation Equivalent Method
5.3.2.3	Geolocation Data Predicted Accuracy Model: Sensor-space	Appendix B	State Vector Direct Method
5.3.2.4	Geolocation Data Predicted Accuracy Model: Measurement-space	Appendix B	Sensor Direct Method

### 5.3.5 Analysis techniques for the population of models

Key to the appropriate population of both the accuracy assessment model and the predicted accuracy model is the generation of appropriate sample error statistics. More specifically, these statistics directly populate the accuracy assessment model, with corresponding results used to select and tune the appropriate predicted accuracy model. This is true for all of the models defined in Sections 5.3.2.1 through 5.3.2.5.

Appropriate sample error statistics are generated per the underlying principles presented in TGD 2b (Sample Statistics) and are summarized in Section 5.3.5.2. However, their generation relies on samples of data/product geolocation error, which in turn requires the availability of geolocation “ground truth” as discussed below:

#### 5.3.5.1 Ground truth and various alternatives

Ground truth is used to generate error samples by subtracting ground truth geolocations or their equivalent from corresponding product geolocations or their equivalent.

More specifically, ground truth (3d) is used to generate 1d, 2d, or 3d error samples in support of an accuracy assessment for a geolocation product. For example, a 3d error sample (meters) is generated by subtracting a 3d ground truth geolocation from a corresponding conjugate 3d geolocation that is measured/identified in the 3d geolocation product; corresponding sample statistics populate an applicable Geolocation Product Accuracy Assessment Model.

Ground truth (3d) is also used to generate 2d error samples in support of an accuracy assessment for geolocation data. For example, a 2d error sample (pixels) is generated in image-space for a Small-Sat image by first measuring a conjugate 2d image location of a ground-truth geolocation identified in the image. The 3d ground truth geolocation is then projected to image-space using the basic sensor model and then subtracted from the measurement; corresponding sample statistics populate an applicable Geolocation Data Accuracy Assessment Model.

(Alternatively, the resultant error is projected to a plane (2d in meters) perpendicular to the image locus (image line-of-sight, if an EO image) and that corresponds to the elevation or vertical component of the 3d ground truth point.)

Regardless the specific details for the generation of an error sample, corresponding sample statistics populate an applicable accuracy assessment model.

Ground truth can be directly available in some cases, or can be generated from corresponding highly accurate “control” imagery in other cases. The accuracy of “ground-truth” needs to be reasonably better than the data/product being assessed per TGF 2c (Specification and Validation of Accuracy and Predicted Accuracy).

However, sometimes ground truth is not available, not uncommon for some types of External Data, particularly corresponding to remote or restricted parts of the world. In this case, ground truth or its equivalent may be able to be generated by other means which take advantage of independent information from overlapping data/products as discussed in Appendix H. There are three general scenarios regarding the overlapping data/products:

- (1) Data/products generated using the same sensor
- (2) Data/products from the same type or class of data/products
- (3) Data/products from different types or classes of data/product

The above approach is not ideal as compared to obtaining surveyed ground-truth or its equivalent, but is better than no ground truth at all. Subsequent accuracy assessments based on this ground truth or its equivalent should note the generation method as well as the estimated accuracy of such ground truth.

Section 5.3.5.2 now goes on to present an overview and summary of sample error statistics, and Section 5.3.5.3 presents a real-world example and a related issue:

#### **5.3.5.2 Sample error statistics**

Sample error statistics are key to the meaningful population of accuracy assessment models and the subsequent “tuning” or population of corresponding predicted accuracy models, the latter based on both the overall characteristics as well as the detailed quantitative values of the sample statistics. The sample statistics can correspond to 2d errors for data (e.g., image location errors for an image), or to 1d errors (vertical), 2d errors (horizontal), and/or 3d errors for a product.

Sample error statistics generally consist of the following *a posteriori* (sample) statistics: mean-value of error, error covariance matrix, relative error covariance matrix, auto-correlation values (approximate spdcf values), various scalar accuracy metrics, as well as the number of independent samples and the total number of samples used in their calculations and directly related to the statistical significance or reliability of the sample statistics. The computation of predictive statistics is based on underlying sample statistics.

The above sample statistics and their predictive statistics counterparts are consistent with the practical representation of errors as a wide-sense homogenous random field in an arbitrary realization of the type or class of data/product of interest.

Correspondingly, predictive statistics are applicable to an arbitrary realization of the data/product; the predicted mean-value of error and the error covariance matrix are both assumed constant regardless the absolute locations of the elements of interest in the data/product; e.g., applicable to errors in image locations regardless their absolute locations in the image. In addition, the spatial correlation between the errors in two elements in the data/product is assumed solely a function of the distance between them, such as the distance between two geolocations in a product or the distance between two image locations in an image as represented in image-space. Also, the mean-value of relative errors is assumed zero and distance bins are characterized by the distance between two elements, not their absolute locations. In addition, as detailed later, the predicted mean-value of error is not only assumed constant, but is assumed equal to a value of zero consistent with an assumed “bias free” generation process, unless specifically demonstrated otherwise.

The above predictive statistics are relative to an arbitrary realization of the data/product, not specific realizations over which sample statistics are computed. For a specific realization, the sample mean-value will typically equal a significantly non-zero value due to the spatial correlation of errors within the data/product, but when averaged over numerous specific realizations, the average sample mean-value will approach zero assuming no system-wide bias, i.e., no bias in the data/product generation process. Hence, the applicability of a predicted mean-value of error equal to zero corresponding to an arbitrary data/product realization, past or future. And although the predicted mean-value is equal to zero, the predicted error covariance matrix will still capture the appropriate variability of errors both within and across arbitrary realizations.

Sample statistics should be computed for an accuracy assessment corresponding to multiple independent realizations of the data/product. In addition, (sub) assessments corresponding to each of these realizations also involve multiple error samples. However, the latter are not independent error samples, but are required and desired as such in order to quantify the spatial correlation of errors in a realization which is directly related to relative accuracy. Recall that the errors in different realizations of the data/product are assumed independent or uncorrelated, but errors in the same realization of the data/product are spatially correlated.

Note: The above spatial correlation is more correctly termed “intra-data/product spatial correlation”, as it is applicable to errors in the elements of the same data/product realization; e.g., the errors in two different image locations in the same image. The correlation applicable to errors in the elements from two different data/product realizations is termed “inter-data/product correlation”, and is assumed zero unless specifically designated otherwise, such as corresponding to temporal correlation for two same-pass images. The two different types of data/product correlations also correspond to representation by corresponding spdcf, simply termed “spdcf” for spatial correlation and “temporal spdcf” for same-pass images in this document.

### Absolute accuracy

The sample mean-value of error is computed over all samples of error for each data/product realization, and the sample error covariance matrix is computed for each data/product realization relative to the corresponding sample mean-value. Thus, if there are  $m$  realizations of the data/product available, there are  $m$  pairs of sample mean-values and sample error covariance matrices computed for information. In addition, the “ensemble” sample mean-value of error is computed over all samples of error over all realizations, and the “ensemble” sample error covariance matrix is computed over all samples of error over all realizations and relative to the ensemble sample mean-value. Again, these are computed for information only. Finally, the “representative” sample error covariance matrix is computed over all error samples over all realizations and relative to an assumed mean-value of error equal to zero. The representative sample error covariance matrix is equivalent to the (vector) root-mean-square error over all error samples over all realizations.

All of the above sample mean-values of error and sample error covariance matrices are contained in the populated accuracy assessment model, along with the corresponding number of data/product realizations, the number of corresponding error samples for each realization, and other supporting details.

The predicted error covariance is set equal to the above representative sample error covariance matrix and the predicted mean-value of error is set equal to zero, and both of these predictive statistics are contained in the corresponding populated predicted accuracy model.

The above is consistent with the following baseline approach that was discussed earlier: (1) the sample mean-value of error for each data/product realization is significantly non-zero due to the spatial correlation of errors in the same realization, and (2) these mean-values of error vary in both sign and magnitude over different realizations and approach an average value equal to zero. Hence, the applicable predicted mean-value of error for the corresponding type of class of data/products of interest is equal to zero unless demonstrated otherwise.

Compelling evidence that the baseline approach is not applicable relies on analysis of the various sample mean-values and sample error covariance matrices computed and contained in the populated accuracy assessment model as described above. Numerous data/product realizations must also be involved, and if applicable, the root-cause of a significant non-zero mean-value should be investigated in the data/product generation system. In the interim, the predicted accuracy model can either contain the non-zero mean-value and corresponding error covariance matrix about this mean-value, or continue with the baseline approach.

Finally, even if the true (unknown) mean-value of error were non-zero corresponding to a “system” bias in the generation of the type or class of data/products of interest, this is mitigated by the baseline approach corresponding to a predicted error covariance matrix that is equivalent to a (vector) root-mean-square error, and thus, includes the effects of a non-zero mean-value in terms of magnitude.

### Relative accuracy

The sample relative error covariance matrix is computed over all relative error samples for each data/product realization and corresponding to specified distance bins. A relative error sample consists of the difference between two error samples that are solely constrained to be within the bin's specified distance, regardless where the two geolocations are located within the product. This practical assumption is also consistent with errors modeled as a wide-sense homogeneous random field.

Consistent with the above, the sample relative error covariance matrix for each data/product realization and for each distance bin is computed relative to a mean-value of relative error equal to zero. There are nominally two distance bins: "small" corresponding to the maximum length of the majority of features of interest contained in the type or class of data/product of interest, and "large" corresponding to all distances that are larger.

For each distance bin, the above sample relative error covariance matrices are combined over all data/product realizations to yield an "ensemble" sample relative error covariance matrix for the distance bin. The average distance of all underlying relative error samples is also computed for the distance bin. The distance corresponding to a specific relative error sample is simply the distance between the two data/product elements involved; e.g., the distance in image-space between two image locations in an image.

Based on the ensemble relative error covariance matrix and the representative sample error covariance matrix (see Absolute accuracy), the corresponding sample (auto) correlation value is computed for each distance bin. The ensemble sample relative error covariance matrix, the sample correlation value, and the average distance for each distance bin are contained in the populated accuracy assessment model, along with supporting details.

The sample correlation values along with the corresponding average distances for all distance bins are then used to compute ("fit") the spdcf as part of the predictive statistics in the populated predicted accuracy model as described in Section B.2.2 in Appendix B. The spdcf is nominally from the "CSM four parameter" family of spdcf with the two dominant defining parameters  $A$  and  $D$  active. The spdcf in conjunction with the error covariance matrix that is also contained in the predicted accuracy model enable the calculation of a predicted relative error covariance matrix corresponding to any desired distance of interest.

#### Scalar accuracy metrics

Scalar accuracy metrics can be computed corresponding to errors and/or relative errors as derived predictive statistics using the contents of the predicted accuracy model per the techniques described in TGD 2a (Predictive Statistics) as well as in the various appendices of this document. They are typically computed for vertical errors as LEXX and horizontal errors as CEXX for any desired levels of probability XX, which typically include 90%.

In addition, sample scalar accuracy metrics are computed independently and contained in the populated accuracy assessment model per the techniques described in TGD 2b (Sample Statistics) as well as in the various appendices in this document. They are based on order statistics of radial error samples for

absolute error and order statistics of radial relative error samples for relative error. These are typically computed for XX=90% only, as higher values of XX require more error samples, which are typically limited in number.

**The bottom line:** Computation of sample statistics and the corresponding population of an accuracy assessment model and the subsequent population of a predicted accuracy model were summarized above and are detailed in Appendix B of this document, and to a lesser extent, in Appendix C. Related issues are also discussed and further illustrated, including why the applicable mean-value is typically zero even though a single realization of the data/product typically exhibits a systematic or bias-like error. This effect is due to “spatial” correlation and is correctly represented by an spdcf.

In addition, the computation of sample statistics and related processing summarized above and detailed in Appendices B and C correspond to the population of a “standard” predicted accuracy model, not the more general MGRF-based predicted accuracy model (Section 5.3.3.3). MGRF-based predicted accuracy is recommended for some geolocation products (e.g., EO-generated 3d Point Clouds) for a higher-fidelity representation of predicted accuracy. Processing for the population of corresponding models is based on an extension of the techniques applicable to the standard predicted accuracy model and is outlined in Section B.5.2.

Appendices B and C also take into account that External (Commodities) Data typically has relatively few error samples that are available. This is an unfortunate but realistic situation for many types of External Data that must be addressed in order to characterize accuracy as best we can.

#### ***5.3.5.3 Real-world example of accuracy assessment: initial processing and a common issue***

Finally, we close out Section 5.3.5 on “Analysis techniques for the population of models” by illustrating sample-based processing using real-data and applicable to the population of a Geolocation Data Accuracy Assessment Model along with a common issue associated with such processing. Analysis corresponds to Small-Sat imagery, in particular Planet Dove images as detailed in reference [1]. The populated Geolocation Data Accuracy Assessment Model would be used to tune a Geolocation Data Predicted Accuracy Model: Measurement-space.

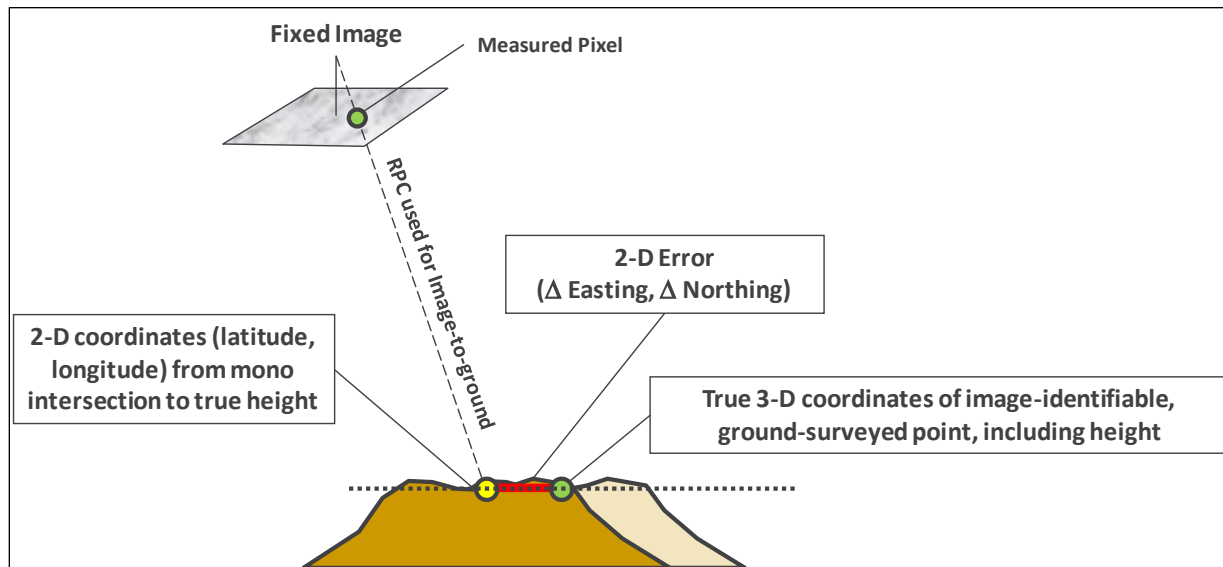
This example corresponds to initial or “first-step” processing and computes independent samples of horizontal radial error and a major sample statistic: CE90. The CE90 computation is based on the techniques recommended in TGD 2c (Specification and Validation), including the use of order statistics, the computation of confidence intervals, and the computation of representative error samples. References [6] provides an “easy-to-read” summary of TGD 2c and reference [4] provides an “easy-to-read” summary regarding the computation CE90 and other scalar accuracy metrics specifically.

The initial processing as detailed in [1] does not include the generation of other sample statistics, such as error covariance matrices, and does not address relative accuracy (error) corresponding to two geolocations extracted from the same image, both specified as needed for a complete accuracy assessment earlier in this document. Related processing for a complete accuracy assessment was

summarized in the previous section and is covered in detail in Appendices B and C, but examples included in these and the other appendices are based on simulated data.

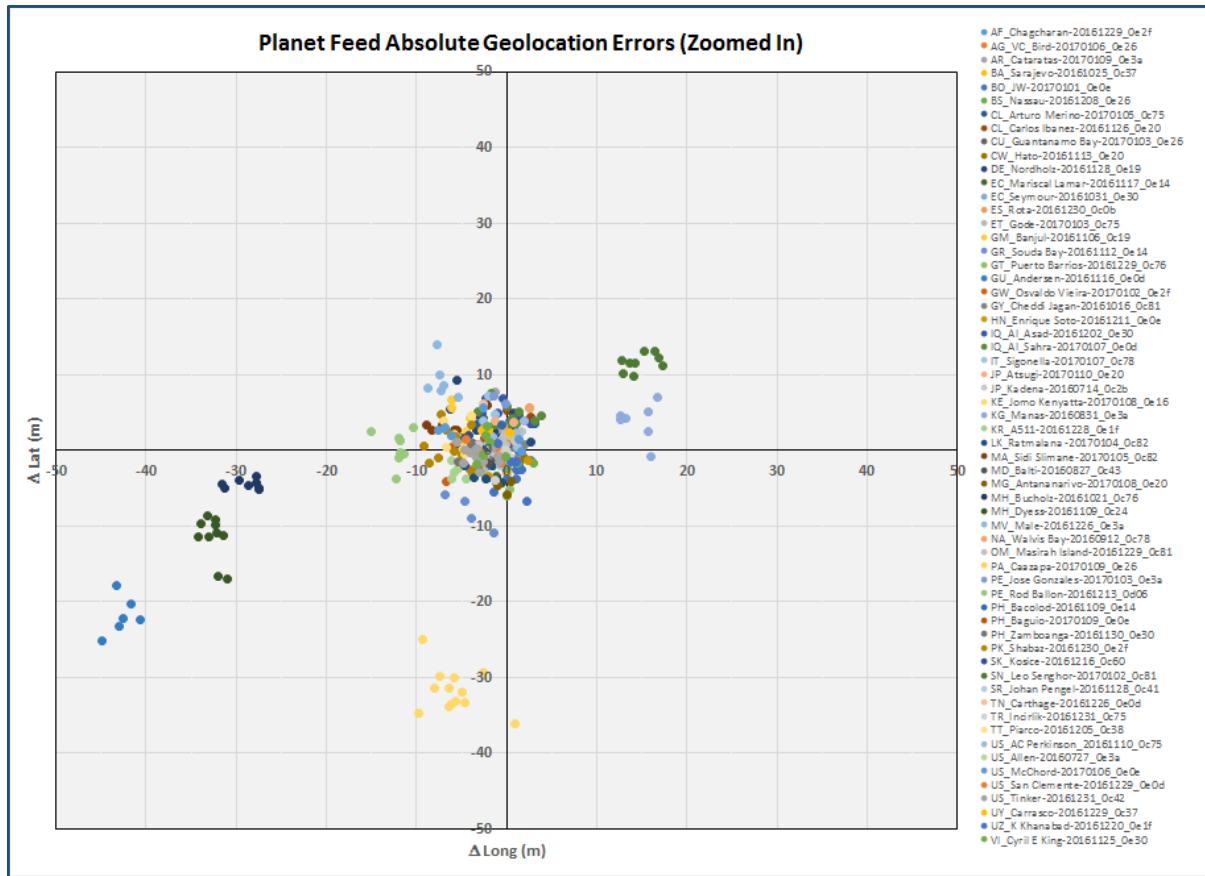
The analysis presented below is from and further detailed in reference [1]. In particular, geolocation accuracy was assessed for 60 unrectified (Basic) Dove PS2 images collected from 14 July 2016 to 10 January 2017 with correspond geo-registration of the images (metadata) performed by Planet from 21 December 2016 to 10 January 2017. Geo-registration was performed by Planet as part of their normal operations concept in order to produce reasonably accurate image metadata (RPC or sensor pose, etc.) by geo-registering individual Planet Dove images to available collections of overlapping control imagery of varied numbers and accuracy.

Various samples of horizontal geolocation error were generated based on the availability of ground truth and the process illustrated in Figure 5.3.5.3-1. Corresponding sample-based CE90 was generated based on one representative error sample from each of 60 images. For a given image, the representative error sample was the “average” of multiple individual error samples corresponding to this image per the baseline technique of Section 5.6.4 of TGD 2c (Specification and Validation).



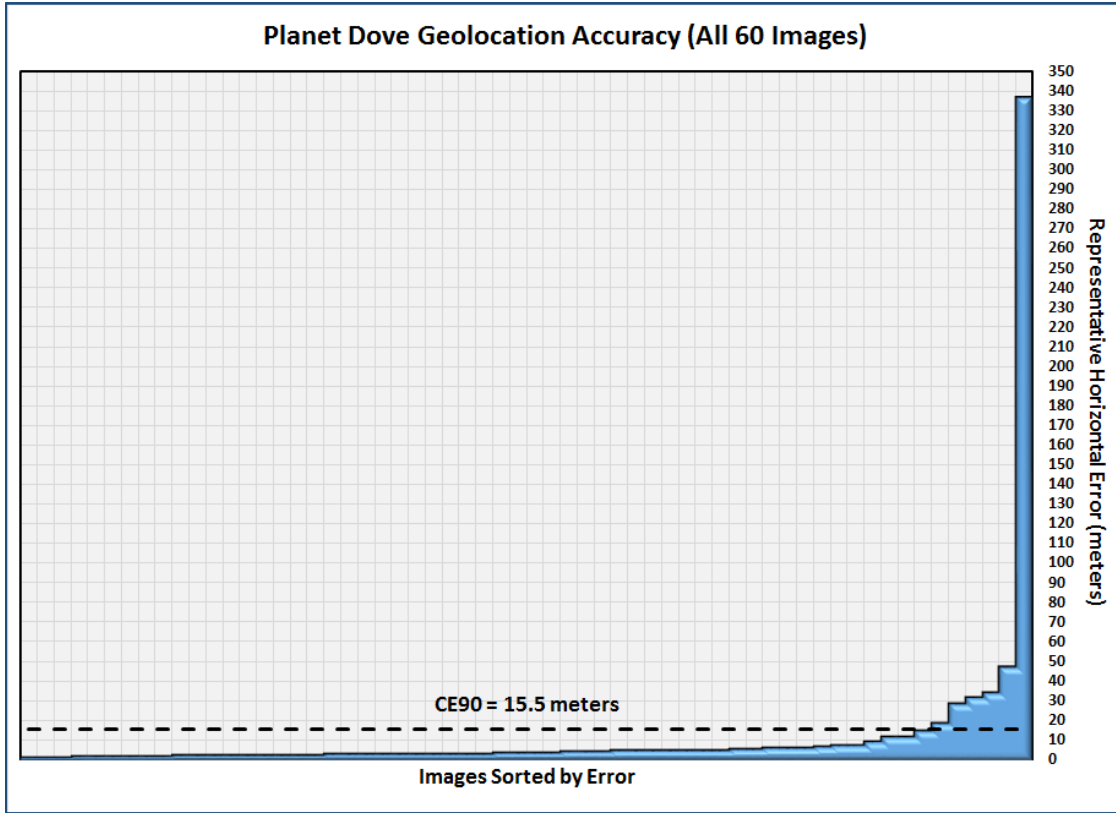
**Figure 5.3.5.3-1:** Process for the computation of a specific horizontal geolocation error

Figure 5.3.5.3-2 presents the corresponding individual error samples for 59 of the 60 images; the image that was left-out of the figure in order to keep the plot scale reasonable was over Seymour, Ecuador (Galapagos), which had a horizontal error on the order of 330 meters.



**Figure 5.3.5.3-2:** Individual representative error samples from 59 of the 60 images

As can be seen above, the majority of error samples are reasonably small and indicate relatively little bias or common error. However, 12 of the images had significantly larger errors and corresponded to images taken over small islands. It is theorized that geo-registration did not perform well over the small-islands for various reasons. Regardless, CE90 was computed over all 60 images as presented in Figure 5.3.5.3-3. 90% of all geolocation horizontal radial errors were less than or equal to 15.5 meters.



**Figure 5.3.5.3-3:** Sample-based CE90 using all 60 images

Figure 5.3.5.3-4 presents sample errors corresponding to the 48 out of 60 images that did not correspond to small islands, and Figure 5.3.3.3-5 presents the corresponding CE90 computation. With this restriction, 90% of all geolocation horizontal radial errors are now less than or equal to 11.0 meters. However, as seen in Figure 5.3.5.3-4, there are still some “groupings” of results, although certainly not as severe as when all images were included (Figures 5.3.5.3-1 and 5.3.5.3-2).

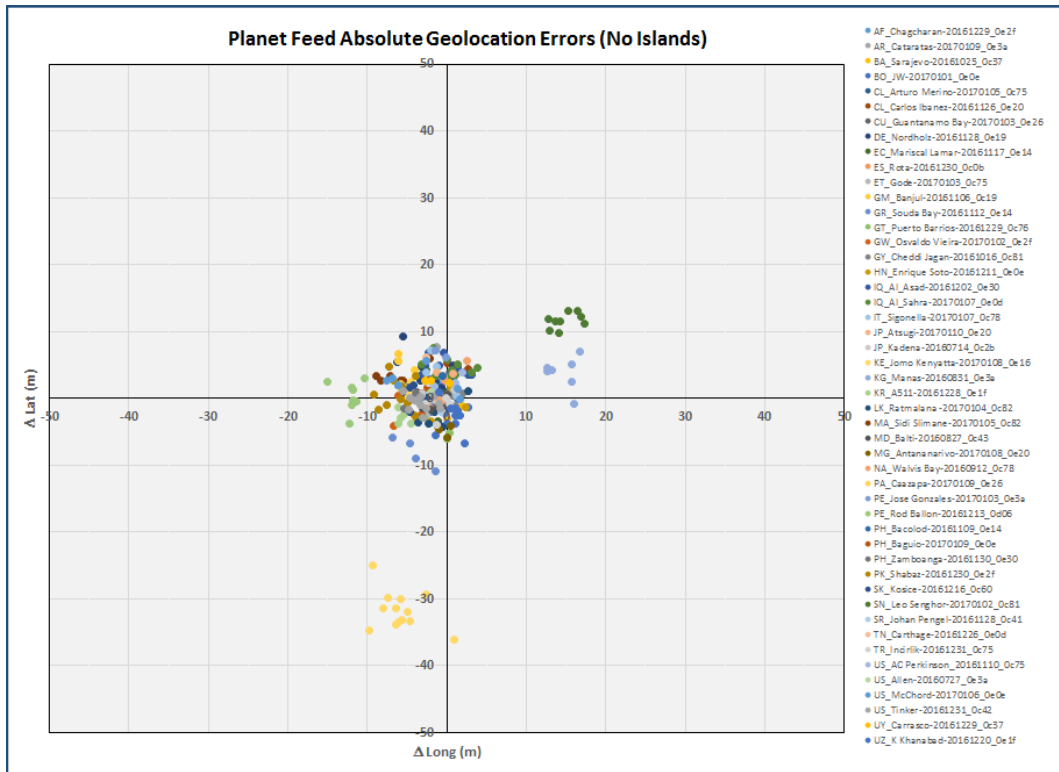


Figure 5.3.5.3-4: Individual representative error samples from 48 of the 60 images

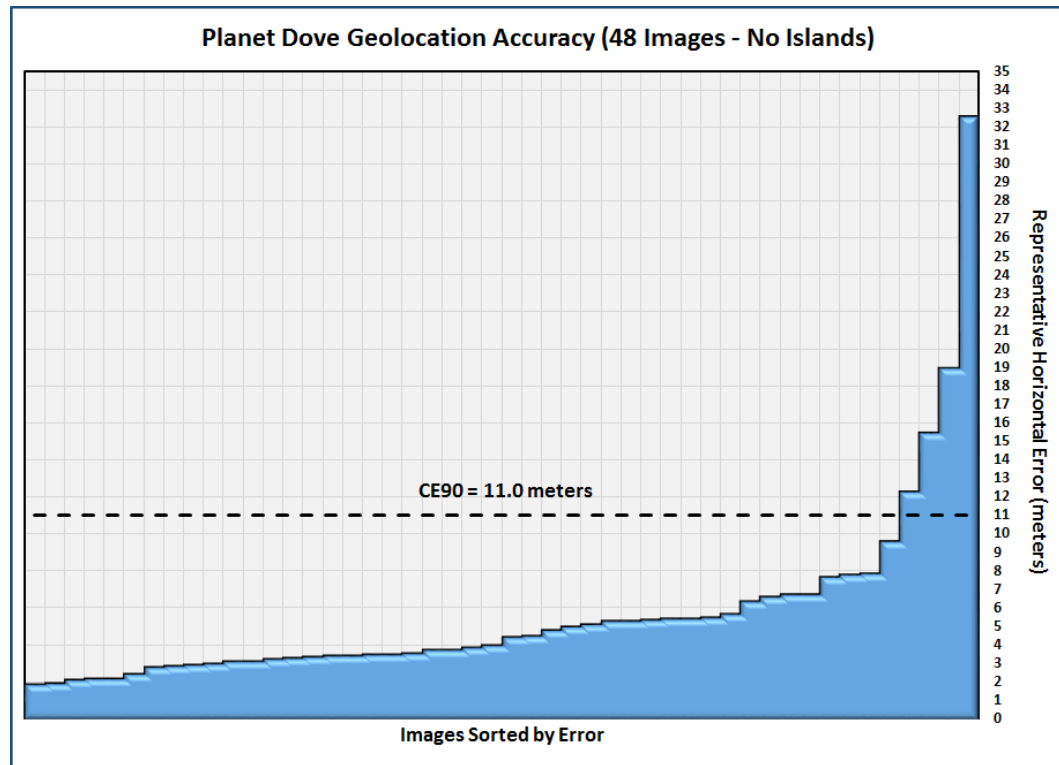


Figure 5.3.5.3-5: Sample-based CE90 using 48 images

The above example illustrates a general problem regarding the population of an accuracy assessment model and the corresponding selection and tuning (population) of an applicable predicted accuracy model – the “grouping” of errors. The following lists various alternatives:

- 1) Consider the poorer (60 image) results a temporary aberration and use the 48 image result. Of course, results are also qualified as such, i.e., sample statistics correspond to the 48 images not associated with small islands. This is applicable to the populated accuracy assessment model explicitly and will affect/tune the populated predicted accuracy model in a similar manner.
- 2) Include all results in the statistics. As such, the big gap between results, although present, will not be apparent, i.e., the computed CE90 is pessimistic for most images. This will affect/tune the predicted accuracy model in a similar manner.
- 3) Break results into the two camps for the accuracy assessment model statistics: (1) small-islands and (2) excluding small islands. This additional detail will be placed in the populated accuracy assessment model, but the predicted accuracy model will be tuned using the ensemble (all samples) statistics, i.e., a predicted accuracy model that is pessimistic for most images. Perform additional accuracy assessments as soon as possible to determine whether results were based on initial processing “problems”, and hence, not applicable to imagery qualified as corresponding to later dates with changes to populated models in accordance.
- 4) Break the results into the two camps for the accuracy assessment model, and possibly generalize the predicted accuracy model to include the MGRF-concept of Section 5.3.3.3, but tailored to imagery instead of to a 3d geolocation product; or more easily, directly as a 3d geolocation product for orthoimages when generated as products. This is a future applied research topic, and could reasonably account for any inherent “variability” of the geo-registration process for an arbitrary image and hence, for an arbitrary geolocation, in a probabilistic and theoretically correct manner.

Until future information and/or applied research is available, Method 3 is recommended.

### 5.3.6 The Empirical Quality Model for Crowd-sourcing data/products

This section of the document describes an empirical quality model for Crowd-sourcing data/products, and as such, is termed an “Empirical Quality Model”. It is used instead of an accuracy assessment model and a predicted accuracy model due to the following characteristics of Crowd-sourcing data/products:

- little if any underlying quality pedigree
- data varies significantly in terms of “quality” over different realizations of the data/product
  - consistency
  - geolocation accuracy
  - completeness
  - blunders
- ground-truth is difficult to obtain
- geospatial coordinates are also associated with specific features and corresponding delineations
- missing data in the data/product is common, e.g., missing portions of a road.

Crowd-sourcing data/products are usually based on Volunteered Geographic Information (VGI) for applications of interest. It is this underlying source of data that yields some of the negative characteristics

listed above, and correspondingly, the use of the “lower fidelity” empirical quality model as compared to the other models previously described.

However, before proceeding with a description of the Empirical Quality Model, it is first worth pointing that there are “positives” associated with Crowd-sourcing data. In particular, they usually contain more recent information than “standard” reference maps of known pedigree, assuming the latter are even available in some remote areas.

A prime example of Crowd-sourcing data is a digital map. Figures 5.3.6-1 and figure 5.3.6-2 present two representative examples over the same AOI near Kathmandu, Nepal using OpenStreetMap and Google MyMaps. Both examples correspond to standard map format, with options available to interactively read-out geolocations, zoom-in and zoom-out, overlay with satellite imagery, etc., if so desired. Figure 5.3.6-1 was also discussed earlier in Section 5.1.1.3.

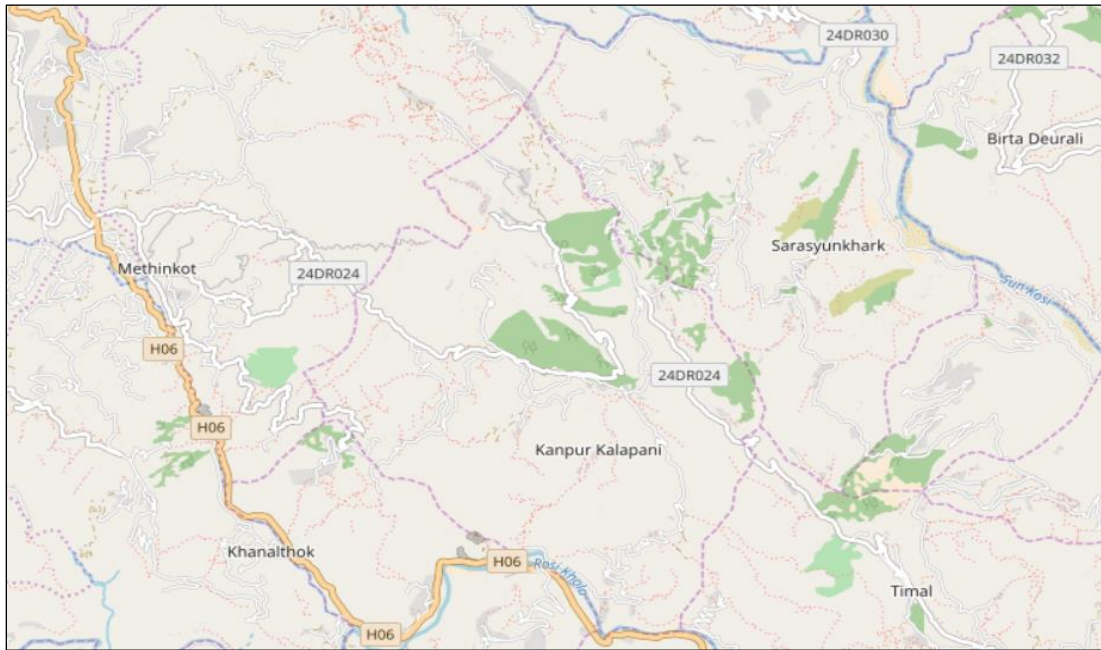


**Figure 5.3.6-1:** Area of Interest near Kathmandu, Nepal: OpenStreetMaps (general use license)



**Figure 5.3.6-2:** Area of Interest near Kanpur, Nepal: Google MyMaps (general use license)

Notice the differences in general content including some of the names in the above two figures. There are also some differences in feature shapes (geolocations) apparent for some of the features delineated. However, in general, these two maps are reasonably consistent.

#### 5.3.6.1 *Model contents/definition*

The specifics regarding contents of the Empirical Quality Model require further applied research, but are recommended to include functions or look-up tables based on important characteristics of the data/product type if available, such as:

- number of volunteers
  - type of volunteers, if possible
  - may not be explicitly available
- product scene content
- general geographic area
- date range

Corresponding quantities modeled by the above functions include a subset of the following:

- geolocation accuracy: CEXX, LEXX
- % of missing data
- % blunders
- Consistency of data across a realization
  - Ranked as low, medium, high
    - More specific definitions to be provided

- Consistency of data across similar scene content (geographic area and date range) by different product types
  - Ranked as low, medium, high
    - More specific definitions to be provided
- Data description/dates used to estimate the above, including number of samples

References [11-13,18] discuss Crowd-sourcing in general as well as the assessment of the quality of VGI which specifically illustrate general challenges. For example, reference [11] discusses various assessments of the quality of OpenStreetMap, such as one that corresponds to a digital map of London roads that contains 80% of desired coverage and approximately 6 meter (no further details) geolocation accuracy as compared to a high-quality reference map. This is for one realization or specific instance of OpenStreetMap, and probably represents a “better” example based on the use of VGI data from many volunteers over a very important AOI. The same reference presents other examples that have significantly less quality regarding coverage, geolocation accuracy, etc., further illustrating issues and difficulties.

### ***5.3.6.2 Analysis techniques for population of models for Crowd-sourcing***

If enough ground-truth is available, sample statistics similar to those in a populated accuracy assessment model can be generated in support of the characterization of geolocation accuracy in the Empirical Reliability Model. However, this will not be applicable in many situations, although the analysis techniques which correspond to a ground-truth substitute (Section 5.3.5.1) may be applicable.

However, the above cannot be counted on in general, and it does not address the other quantities of interest in the Empirical Model, such as coverage or % of missing data. As such, methods/algorithms for the comparison of geolocations and corresponding features/delineations across different realizations over the same AOI from different data/product types (e.g., OpenStreet Map, Wikimapia, etc.) are applicable when possible. In terms of geolocation accuracy, such comparisons can also compute upper bounds for accuracy by analysis of multiple samples of the relative difference in geolocation coordinates between different data/product types – low-fidelity, but needed information none-the-less. A corresponding issue of note regarding geolocation comparisons: two maps may have been generated using common underlying information (surveys, satellite imagery, etc.), therefore geolocation difference statistics will not include the error in their shared information.

It will not be uncommon for a specific Crowd-sourcing data/product type that its Empirical Quality Model will be available but will only be partially populated, i.e., some specified content will contain “not available” entries. However, some reasonably reliable information is better than none at all.

The above recommendations for analysis techniques for population of the Empirical Quality Model require further detail; corresponding applied research is recommended.

### **5.3.7 The data/product is needed now, but accuracy assessments are not available**

Occasionally it may be necessary in the NSG to utilize a data/product that does not have a populated predicted accuracy model available due to the lack of previous accuracy assessments for data/products from the same corresponding type or class of product. It could be a data/product that corresponds to either Commodities data or Crowd-sourcing data and that essentially has no accuracy pedigree or has an

unreliable pedigree. The relevant point: this data/product is needed “now” for an NSG application and there is neither the time nor the data to perform an accuracy assessment and populate a subsequent predicted accuracy model – relevant details follow:

A populated predicted accuracy model is essential for the corresponding predicted accuracy associated with an arbitrary element in the data/product in question but is unavailable. Also, the data/product may correspond to very poor accuracy that needs to be improved prior to its reasonable use.

The following is a recommended approach for the mitigation of this situation and requires some external control information. The control information does not have to be extremely accurate but it should include corresponding predicted accuracies. Of course, the techniques presented earlier in this document that rely on previous accuracy assessments and subsequent populated predicted accuracy models are superior and preferred whenever possible. In particular, they are applicable to an arbitrary data/product of a specific type or class of data/products and do not utilize/require control information. The approach presented below is applicable to the individual and specific data/product and requires overlapping control information. In addition, the control information is typically not nearly as accurate as the “ground truth” used in accuracy assessments.

The recommended approach is as follows:

**Representative Example: data/product is an image**

Select an (unpopulated) predicted accuracy model applicable to the data/product in question (image, 3d geolocation product, etc.). For example, if an image, select the Geolocation Data Predicted Accuracy Model: Measurement-space. Set the corresponding *a priori* predictive statistics to represent very large uncertainty. This is illustrated below with subsequent steps assuming an image for specificity. It is further assumed that the image metadata is available, although possibly of very poor quality, as well as the availability of a basic sensor model (image-to-ground function).

(1) Predictive statistics for  $2 \times 1$  image location(s)  $m$ :

(a) *A priori* mean-value equals zero ( $0_{2 \times 1}$ ).

(b) *A priori* covariance matrix  $C = \begin{bmatrix} \sigma_{large}^2 & 0 \\ 0 & \sigma_{large}^2 \end{bmatrix}$ , a  $2 \times 2$  matrix, where  $\sigma_{large}$  is an appropriately large standard deviation of error, such as 500 pixels assuming a relatively large image and relatively large sensor height. Its use stabilizes the subsequent WLS solution in step (2) below.

(c) Parameters defining the spdcf of intra-image correlation set to values that nominally yield approximately 0.8 correlation (unit-less) across the width of the image as well as a value at very small distances between image locations such that the corresponding relative accuracy  $\sigma_{rel_{large}}$  is reasonably large; for example, 5 pixels. The latter may also be accomplished using

the predictive statistics (*a priori* covariance matrix and spdcf) corresponding to optional sensor-mensuration or “unmodeled” error – see Section C.3.1.

(2) Perform a data/product WLS adjustment using external control information:

Utilize the solution to correct arbitrary image locations in the image and the solution’s *a posteriori* error covariance to represent corresponding predicted accuracy. The solution is assumed to correspond to a correction grid in this representative example – see Section 5.3.3.1 and Appendix B.2.2.

(3) Compute various quality control metrics (e.g., normalized *a posteriori* measurement residuals) corresponding to the WLS solution, and based on their expected range of values, edit the measurements and/or adjust the above *a priori* predictive statistics as appropriate and re-perform the solution.

See Sections B.2.2 and E.3.1.1 for related discussions, and more generally, TGD 2d (Estimators and their Quality Control) for further details regarding quality control metrics and related processing.

(4) Perform QC on the corresponding iterated solution and then iterate the entire solution process again if necessary:

Utilize the various quality metrics listed in TGD 2d corresponding to a WLS solution to help to ensure the reliability of the solution.

If iteration is necessary, modify parameters that affect the WLS solution, such as the covariance matrix for *a priori* measurement error, the number of measurements corresponding to the External Data (e.g., control images) – increase if possible, the size of the correction grid, and the spdcf.

The best way to do the above requires further applied research, particularly for automated methods.

#### **Modification of method if metadata is not available:**

Metadata to support the data/product-to-ground relationship may not be available in some more extreme situations. This is not applicable for a geolocation product because such a relationship is direct (the identity function), and hence, is always available. However, it may be applicable to other External Data such as imagery. Regardless, whether predicted accuracy is available or not, a ground-to-image (and inverse image-to-ground) relationship is needed for geolocation-related processing. Therefore, before proceeding with processing to control the data/product, such as that described in the previous paragraphs, a ground-to-image or “basic” sensor model must first be derived.

There are various techniques to do so, all also requiring control information in order to generate an applicable ground-to-image function. Some require more control information (e.g., ground control points) than others, and some are more rigorous than others. One example is an image resection which estimates sensor physical parameters and is used with a corresponding physical sensor model when

identified as applicable for the data/product in question. Others estimate more generic ground-to-image functions, which are also invertible yielding an image-to-ground function. Such transformations or “mappings” include Orthographic and Direct linear transforms (DLT) – see [15] and [14] for details. This general topic as applicable to External Data is also recommended as an applied research topic.

## **5.4 Summary**

This document presented specific recommendations for the Quality Assessment of External Data in the NSG. Section 5.4.1 presents an overview of key recommendations and Section 5.4.2 presents recommended applied research.

### **5.4.1 Key Recommendations**

Table 5.4.1-1 presents key recommendations for External Data and its Quality Assessment based on this document.

Table 5.4.1-1: Key recommendations

Key Recommendations or "Take-Aways"
<b>Outsourcing:</b> contracts should include requirements for contractor to include Quality Assurance/Quality Control metrics with delivery of the product for review by appropriate NSG organization to help ensure quality/reliability of the product to the end user.
<b>Quality Assessment</b> should consist of two major functions: Quality Assessment Management and Quality Assessment Analysis:
<b>Quality Assessment Management function</b> should be implemented by one NSG "host" organization if possible with appropriate and dedicated funding to input/collate/summarize the individual assessments from various NSG organizations, as well as from itself, and make available to all authorized organizations/personnel.
<b>Quality Assessment Management function</b> should provide "one-stop shopping" for for the best, latest, and consistent information regarding the quality, geolocation accuracy, and geolocation predicted accuracy corresponding to the various External Data (geolocation data and products) used across the NSG.
<b>Quality Assessment Management function</b> should generate a Quality Assessment Summary report based on inputs from the supporting Quality Assessment Analysis Function. It should make both the summary and these inputs available to the NSG in general. These inputs are generated as follows:
<b>Quality Assessment Analysis function</b> should include the generation of: (1) populated Accuracy Assessment Model(s), (2) populated Predicted Accuracy Model(s), and/or (3) populated Empirical Quality Models(s), the latter for Crowd-Sourcing data/products when applicable.
<b>Quality Assessment Analysis function</b> should populate the above models as soon as possible and update them periodically. These models are applicable to most External data due to its lack of accuracy pedigree and/or physical sensor models, or their equivalent, with appropriate metadata.
<b>Quality Assessment Analysis function</b> models are practical and based on accuracy assessments of error from multiple realizations of the same type or class of data/product of interest. These models support all aspects of geolocation: predicted absolute and relative accuracy, optimal extraction, and optimal adjustment of the data/product. They also enable Actionable Intelligence.

**Table 5.4.1-1:** Key recommendations (continued)

Key Recommendations or "Take-Aways" (continued)
<b>Inorder to minimize</b> the Quality Assessment effort summarized above, utilize (but verify) any accuracy pedigree available from the geolocation data/product vendor or producer as follows:
<b>Encourage use</b> of reliable Predicted Accuracy Models if already available from External Data vendor ( <b>rare</b> ), usually includes associated (higher fidelity) physical sensor model; example: Generic Point Cloud Model
<b>Encourage development/availability</b> of appropriate accuracy and predicted accuracy specifications from the geolocation data/product vendor or producer; "work with them"

#### 5.4.2 Recommended future applied research

Future applied research in support of Quality Assessment of External Data in the NSG is recommended to include that listed in Table 5.4.2-1:

**Table 5.4.2-1:** Recommended Applied Research

Further details for the recommended content of the Empirical Quality Model for Crowd-Sourcing data as well as techniques for its population
Automation for the population of recommended models in general
Details regarding computation/population of the scalar reliability metric contained in the Top-level Quality Assessment file/report
Possible use of contour plots to represent various reliability and/or geolocation accuracy metrics for a specific data/product type over an Area of Interest
Underlying and more specific definitions for “low”, “medium” and “high” rankings contained in the Top-level Quality Assessment file/report and in the Empirical Quality Model
Extension of the use of MGRF in the Geospatial Product Predicted Accuracy Model to other Predicted Accuracy Models as appropriate
Development and population of accuracy and predicted accuracy summary metrics for features considered as a whole( e.g., a building as a collection of nodes, edges, etc.), including feature attributes (e.g., centroid, area, volume)
Integration of recommended predicted accuracy and adjustment models in appropriate APIs, such as the Community Sensor Model (CSM)
Obtain additional error samples of real geolocation data/products and assess performance of recommended methods for the population of corresponding models
Non-technical applied research: ways to best mobilize and organize the NSG in support of the Quality Assessment of External Data in the NSG
General but unknown modifications to current recommendations based on feedback from their initial implementation across the NSG

## 6 Notes

### 6.1 Intended Use

This information and guidance document provides technical guidance to inform the development of geospatial data accuracy characterization for NSG GEOINT collectors, producers and consumers -- accuracy characterization as required to describe the trustworthiness of geolocations for defense and intelligence use and to support practices that acquire, generate, process, exploit, and provide geolocation data and information based on geolocation data. This document is part of a series of complementary documents. TGD 2f provides technical guidance for methods, practices, and algorithms regarding External Data in the NSG and its Quality Assessment as of part of a series of information and guidance documents titled Accuracy and Predicted Accuracy in the NSG. Other documents in this series address a more generalized overview of accuracy and predicted accuracy and additional topic specific technical guidance in predictive statistics, sample statistics, specification and validation, estimators and their quality control, and Monte-Carlo simulations.

## 7 References

- [1] Bresnahan, P., et al, "Planet Dove Constellation Absolute Geolocation Accuracy, Geolocation Consistency, and Band Co-Registration Analysis", Joint Agency Commercial Imagery Evaluation (JACIE) Workshop, 19 – 21 September 2017, PA case # 17-582; <https://calval.cr.usgs.gov/wordpress/wp-content/uploads/Paul-Bresnahan-1.pdf>.
- [2] Dolloff, John, "Representation of predicted accuracy of 3d geospatial products and their subsequent fusion with other products", submitted for publication in the Proceedings of the SPIE 2019 Conference on Defense and Commercial Sensing.
- [3] Dolloff, J., Braun, A., and Theiss, H., "Generalization of the SPDCF Method for the Assembly of Multi-State Vector Covariance Matrices", NGA white paper, PA 18-158, 29 November, 2017.
- [4] Dolloff, J., and Carr, J., "Computation of scalar accuracy metrics LE, CE, and SE as both predictive and sample-based statistics", Proceedings of IGTF 2016 Annual Conference.
- [5] Dolloff, J., and Carr, J., "Geolocation system estimators: processes for their quality assurance and quality control ", Proceedings of SPIE 2018 Conference on Defense and Commercial Sensing.
- [6] Dolloff, John, and Carr, Jacqueline, "Methods for the specification and validation of geolocation accuracy and predicted accuracy ", Proc. SPIE 10199, Geospatial Informatics, Fusion, and Motion Video Analytics VII, 1019908 (May 1, 2017); doi:10.1117/12.2263855; <http://dx.doi.org/10.1117/12.2263855>, last accessed 30 May 2017.
- [7] Dolloff, J., Hottel, B., Edwards, D., Theiss, H, and Braun, A., "Geopositioning with a quadcopter: Extracted feature locations and predicted accuracy without a priori sensor attitude information", PA case # 17-289; Proceeding of SPIE 2017 Conference on Defense and Commercial Sensing.
- [8] Dolloff, J., Theiss, H., and Lee, S., "Generation and Application of RPC Uncertainty Parameters," NGA report, PA case # 11-463, January 2012.
- [9] Doucette, P., Dolloff, J., Lenihan, M., "Geostatistical modeling of uncertainty, simulation, and proposed applications in GIScience", Proceedings of the SPIE Defense and Security Conference, 2015.
- [10] Geospatial World's web-site;

<https://www.geospatialworld.net/blogs/nanosatellites-or-Small-Satellites-are-going-to-play-a-big-role/>;  
accessed 10 December 2018.

[11] Goodchild, M., 2007. Citizens as sensors: the world of volunteered geography.  
GeoJournal 69 (4), 211–221.

[12] Goodchild, M.F. and Li, L., 2012. Assuring the quality of volunteered geographic information.  
Spatial Statistics, 1, 110–120. doi:10.1016/j.spasta.2012.03.002.

[13] Heipke, C., “Crowd-sourcing geospatial data”, ISPRS Journal of Photogrammetry and remote Sensing,  
65 2010.

[14] McGlone, J.C., et al, Manual of Photogrammetry, 6<sup>th</sup> edition, ASPRS, 2013.

[15] Mikhail E., Bethel, J., and McGlone C., Modern Photogrammetry, John Wiley and Sons, 2001.

[16] NSG-unique Standards, “The Generic Point-cloud Model (GPS): Implementation and Exploitation,  
Version 1.0;

<https://nsgreg.nga.mil/doc/view?i=4197>; accessed 05 August 2018.

[17] Planet Lab’s web-site;

[www.planet.com/gallery/el-alamein-20160828/](http://www.planet.com/gallery/el-alamein-20160828/); accessed 02 July 2018.

[18] Senaratne, H., et al, “A review of volunteered geographic information Quality Assessment methods”,  
International Journal of Geospatial Information Science, 31 (2017).

## Appendix A: Additional Terms and Definitions

There are a number of authoritative guides as well as existing standards within the NSG and Department of Defense for definitions of the identified additional terms used in this technical guidance document. In many cases, the existing definitions provided by these sources are either too general or, in some cases, too narrow or dated by intended purposes contemporary to the document's development and publication. The definitions provided in this document have been expanded and refined to explicitly address details relevant to the current and desired future use of accuracy in the NSG. To acknowledge the basis and/or lineage of certain terms in Section 3.1, we reference the following sources considered as either foundational or contributory:

[a] Anderson, James M. and Mikhail, E., Surveying: Theory and Practice, 7<sup>th</sup> Edition, WCB/McGraw-Hill, 1998.

[b] DMA-TR-8400.1, DMA Technical Report: Error Theory as Applied to Mapping, Charting, and Geodesy.

[c] Defense Mapping Agency, Glossary of Mapping, Charting, and Geodetic Terms, 4<sup>th</sup> Edition, Defense Mapping Agency Hydrographic/Topographic Center, 1981.

[d] ISO TC/211 211n2047, Text for ISO 19111 Geographic Information - Spatial referencing by coordinates, as sent to the ISO Central Secretariat for issuing as FDIS, July 17, 2006.

[e] Joint Publication (JP) 1-02, Department of Defense Dictionary of Military and Associated Terms, November 8, 2010 as amended through January 15, 2016.

[f] MIL-HDBK-850, Military Handbook: Glossary of Mapping, Charting, and Geodetic Terms, January 21, 1994.

[g] MIL-STD-2401, Department of Defense Standard Practice; Department of Defense World Geodetic System (WGS), January 11, 1994

[h] MIL-STD-600001, Department of Defense Standard Practice; Mapping, Charting and Geodesy Accuracy, February 26, 1990.

[i] *National System for Geospatial Intelligence* [Brochure] Public Release Case #15-489.

[j] NGA.STND.0046\_1.0, The Generic Point-cloud Model (GPM): Implementation and Exploitation, Version 1.0, October 03, 2015.

[k] Oxford Dictionaries ([www.oxforddictionaries.com/us/](http://www.oxforddictionaries.com/us/)) copyright © 2016 by Oxford University Press.

[l] Soler, Tomas and Hothem, L., "Coordinate Systems Used in Geodesy: Basic Definitions and Concepts", Journal of Surveying Engineering, Vol. 114, No. 2, May 1988.

**A priori** - Relating to or denoting reasoning or knowledge that proceeds from theoretical deduction rather than from observation or experience. [k]

- For typical NSG accuracy and predicted accuracy applications, *a priori* refers to a mathematical statistical model of errors and/or the corresponding state vector containing those errors prior to its adjustment using additional information.

**A posteriori** - Relating to or denoting reasoning or knowledge that proceeds from observations or experiences to the deduction of probable causes. [k]

- For typical NSG accuracy and predicted accuracy applications, *a posteriori* refers to a refined mathematical statistical model of errors and/or the corresponding state vector containing those errors following its adjustment using additional information.

**Absolute Horizontal Accuracy** - The range of values for the error in an object's horizontal metric geolocation value with respect to a specified geodetic horizontal reference datum, expressed as a radial error at the 90 percent probability level (CE). [b],[f],[j]

- There are two types of absolute horizontal accuracy: *predicted* absolute horizontal accuracy is based on error propagation via a statistical error model; and *measured* absolute horizontal accuracy is an empirically derived metric based on sample statistics.
- The term "horizontal accuracy" is assumed to correspond to "absolute horizontal accuracy".
- The 90% probability level (CE) is the default; 95% and 50% probability levels are optional, i.e., CE\_95 and CE\_50, respectively.

**Absolute Vertical Accuracy** - The range of values for the error in an object's metric elevation value with respect to a vertical reference datum, expressed as a linear error at the 90 percent probability level (LE). [b],[f],[j]

- There are two types of absolute vertical accuracy: *predicted* absolute vertical accuracy is based on error propagation via a statistical error model; and *measured* absolute vertical accuracy is an empirically derived metric based on sample statistics.
- The term “vertical accuracy” is assumed to correspond to “absolute vertical accuracy”.
- The 90% probability level (LE) is the default; 95% and 50% probability levels are optional, i.e., LE\_95 and LE\_50, respectively.

**Accuracy (augmented definition)** - The range of values for the error in an object’s metric value with respect to an accepted reference value expressed as a probability. [f]

In an NSG Geolocation System a typical object of interest is an arbitrary 3d geolocation extracted by the system, with a more specific definition of accuracy as follows:

- Accuracy
  - The probability of error corresponding to an arbitrary 3d geolocation extracted by the system. The probability of error is typically expressed as CE90=XX meters, the 90% probability that horizontal circular or radial error is less than XX meters, as well as LE90=YY meters, the 90% probability that vertical linear error is less than YY meters. In general, the error is represented as a 3d random vector and its corresponding CE90 and LE90 values are typically specified and/or evaluated based on sample statistics of independent samples of error.
    - The accuracy requirements for a Geolocation System are typically specified as horizontal radial error and vertical linear error of an arbitrary but specific 3d geolocation are less than specCE90 with a probability of 90% and less than specLE90 with a probability of 90%, respectively.
    - An “accurate geolocation” is defined as the geolocation of a specific extraction that satisfies the specified accuracy requirements of the Geolocation System.

**Bias Error** - A category of error; an error that does not vary from one realization (trial or experimental outcome) to the other. When error is represented as a random variable, random vector, stochastic process, or random field, a bias error corresponds to a non-zero mean-value. [f],[j]

- Caution: a given realization of a mean-zero stochastic process with typical temporal correlation and over a reasonable finite time interval appears to have a non-zero sample mean-value; however, when sample statistics are taken over enough multiple (independent) realizations, the sample mean-value approaches zero in accordance with the true mean-value. This characteristic extends to random fields as well.

**CE-LE Error Cylinder** - A 3D cylinder made up of CE and LE such that there is between 81-90% probability that the 3d error resides within.

**Circular Error (CE)** – See **Scalar Accuracy Metrics**.

**Confidence Ellipsoid** - An ellipsoid centered at an estimate of geolocation such that there is a 90% probability (or XX% if specified specifically) that the true geolocation is within the ellipsoidal boundary (ellipsoid interior). A confidence ellipsoid is typically generated based on an error covariance matrix, an assumed mean-value of error equal to zero, and an assumed multi-variate Gaussian probability distribution of error in up to three spatial dimensions.

**Confidence Interval** - A type of interval estimate of an unknown population parameter in statistics. More specifically, if  $X$  is a vector of random samples from a probability distribution with statistical parameter  $\theta$  which is to be estimated with confidence-level (confidence coefficient)  $\gamma$ :

- $prob\{a(X) < \theta < b(X)\} = \gamma$ , where  $a(X)$  and  $b(X)$  are random end-points and functions of  $X$ .
- Note that the probability distribution need not be specified, but typically is, e.g., a Gaussian (Normal) distribution, a commonly assumed continuous probability distribution.
- Typical parameters represented by  $\theta$  are the distribution's (or corresponding random variable's) mean-value, standard deviation, or percentile.
- The above confidence interval is a two-sided confidence interval; a one-sided confidence interval involves only  $a(X)$  or  $b(X)$  and is bounded on one side, e.g.,  $prob\{\theta < b(X)\} = \gamma$ .

**Correlated Error** - A category of errors; errors that are correlated with other errors, and typically represented in the NSG as a random vector, stochastic processes, or random field. A correlated error is independent (uncorrelated) with itself and other errors from one realization (trial or experimental outcome) to the next. However, within a given realization, it is correlated with other errors of interest:

- If a random vector, the various elements (random variables) which make it up are correlated with each other (intra-state vector correlation).
- If a stochastic process, the collection of random vectors which make up the stochastic process are correlated with each other (inter-state vector correlation). That is, the elements of one random vector are correlated with the elements of another random vector, typically the closer the two random vectors in time, the greater the correlation. A similar concept is applicable to random fields.

**Correlated Values** - Values (of random variables) which are related by a statistical interdependence. For two random variables, this interdependence is represented by their covariance and typically expressed as a correlation coefficient – both have non-zero values. This interdependence is relative to deviations about their respective mean-values. [f]

**Covariance** - A measure of the mutual variation of two random variables, where variations (deviations or dispersions) are about their respective mean-values. If the covariance between two random values is zero, they are uncorrelated. [b]

**Cross-covariance Matrix** - An  $n \times m$  matrix containing the covariance between each pair of elements (random variables) of an  $n \times 1$  random vector and an  $m \times 1$  random vector.

**Degree of freedom** - The number of scalar measurements  $m$  minus the number of state vector components  $n$  for solution in a NSG Estimator.

**Deterministic Error** - An error that is not random or dependent on “chance” – a “known” value, such as the specific realization of an error of an estimated geolocation as compared to “ground truth”, i.e., their difference, where “ground truth” is assumed error-free.

**Elevation** - Vertical distance from a datum, usually mean sea level, to a point or object on the Earth’s surface; not to be confused with altitude which refers to points or objects above the Earth’s surface. In geodetic formulas, elevations are heights:  $h$  is the height above the ellipsoid;  $H$  is the height above the geoid or local datum. Occasionally  $h$  and  $H$  may be reversed. [c], [f]

**Error (augmented definition)** - The difference between the observed or estimated value and its ideal or true value. [f] There are a number of different categories of errors applicable to the NSG: Bias Error, Random Error, and Correlated Error. In general, an error of interest may be a combination of errors from these categories. Their combination is typically represented as either a random variable, random vector, stochastic process, or random field:

- A random variable represents a bias error plus a random error. The former corresponds to the random variable’s mean-value, and if equal to zero, the random variable represents random error only, which is uncorrelated from one realization of the random variable to the next realization.
- A random vector, stochastic process, and random field can represent all three categories of error. The random variables that make-up (are elements of) random vectors are uncorrelated from one realization to the next by definition. However, within a given realization, they can also be correlated with each other:
  - For a random vector per se, this correlation is also termed “intra-state vector correlation”.
  - For a stochastic process, which consists of a collection of random vectors, random variables in one random vector can also be correlated with random variables in another random vector, this is also termed “inter-state vector” correlation. The same concept is applicable to random fields.

**Fusion** - A process that combines or relates different sources of (typically independent) information.

**Linear Error (LE)** – See Scalar Accuracy Metrics

**Local Tangent Plane Coordinate System** - A local X,Y,Z right-handed rectangular coordinate system such that the origin is any point selected on a given reference ellipsoid, its XY plane is tangent to the reference ellipsoid at the point of origin, and the Y-axis is typically directed to the North Pole (an East-North-Up (ENU) system). [a]

**Mean-Value** - The expected value of a random variable. Given a collected sample of measurements, the sample mean-value is the average of the values of the sample measurements. The mean-value of a predictive error is typically assumed zero unless specifically stated otherwise. If correctly modeled, the

predictive mean-value should be closely approximated by the sample mean-value taken over a large number of independent and identically distributed samples.

- The concept of mean-value readily extends to random vectors and is the vector of the mean-values of the individual components or random variables making up the random vector. It readily extends to stochastic processes and random fields as well, since they are collections of random vectors. If (wide-sense) stationary or (wide-sense) homogeneous, respectively, their corresponding mean-value is a constant random vector mean-value.

**Multi-Image Geopositioning (MIG)** - An optimal solution for a “target’s” geolocation (state vector) with reliable predicted accuracies based on the (weighted) measurements of the geolocation in one or more images. A batch process which minimizes the sum of weighted *a posteriori* measurement residuals, where the latter may also include measurements equivalent to *a priori* estimates of geolocation. MIG can also correspond to the simultaneous solution for the geolocation of multiple targets. In general, a MIG solution’s predicted accuracies correspond to or are derived from the solution’s *a posteriori* error covariance matrix.

**Monte-Carlo Simulation** - A technique in which a large number of independent sample inputs for a system are randomly generated using an assumed *a priori* statistical model to analyze corresponding system output samples statistically and support derivation of a statistical model of the system output. This technique is valuable for complex systems, non-linear systems, and those where no insight to internal algorithms is provided (“black box” systems).

**Multi-State Vector Error Covariance Matrix** - An error covariance matrix corresponding to multiple state vector errors (random error vectors) “stacked” one on top of the other as one large state vector error (random error vector), e.g. to represent the position and attitude errors of multiple images’ adjustable parameter errors that impact the solution and predicted accuracy of a subsequent MIG. The multi-state vector error covariance matrix is sometimes termed the joint covariance matrix for a collection of multiple state vector errors.

**Predicted Accuracy (augmented definition)** - The range of values for the error in a specific object’s metric value as expressed by a statistical or predictive error model, and may also be expressed as a probability if a specific probability distribution is specified or assumed, typically a Gaussian (or Normal) probability distribution.

In an NSG Geolocation System a typical object of interest is an arbitrary but specific 3d geolocation extracted by the system, with a corresponding definition of predicted accuracy as follows:

- Predicted accuracy
  - A statistical description of the error in a specific geolocation extracted by the system. The error is expressed as a 3d random vector and the statistical description consists primarily of an error covariance matrix of the random vector about a mean-value typically assumed equal to zero unless specifically stated otherwise. The probability of error can also be computed if either a probability distribution is also specified or a multi-

variate Gaussian probability distribution of error is assumed. The probability of error is expressed as a probability or confidence ellipsoid at a specified probability or confidence level, respectively, and may also be expressed as CE90 and LE90.

- The estimate of geolocation is usually performed by an estimator, such as a Weighted Least Squares estimator, with a corresponding solution error that is a function of measurement errors that are random from one solution or realization to the next as well as sensor-to-ground geometry at different geolocations.
- The term “predicted” in predicted accuracy does not correspond to a prediction of accuracy applicable to the future since the corresponding error corresponds to a geolocation already generated or extracted by the NSG Geolocation System.
- “Reliable predicted accuracy” is defined as predicted accuracy that is consistent with solution error(s).

**Principal Matrix Square Root** - The principal matrix square root of a valid error covariance matrix is a valid error covariance matrix itself of the same dimension such that when multiplied with itself yields the original error covariance matrix. The calculation of principal matrix square root is based on Singular Value Decomposition.

**Probability density function** - A function that defines the probability distribution of a random variable. If continuous, its integral is the (cumulative) probability distribution function.

**Probability distribution** - Identifies the probability of a random variable’s values over an applicable range of values. There are many different types of probability distributions: Gaussian or Normal, uniform, exponential, etc.

- In most NSG applications for accuracy and predicted accuracy, the random variable and its probability distributions are assumed continuous.
- The probability distribution is specified by either a probability density function or a (cumulative) probability distribution function; either based on an *a priori* model or sample statistics.

**Probability distribution function (cdf)** - The (cumulative) probability distribution function defines the probability that a random variable’s value is less than or equal to a specified number in the interval [0,1].

**Radial Error** - A generalization of two horizontal error components ( $x, y$ ) or three dimensional (horizontal and vertical error components –  $x, y, z$ ) error components to a distance value (magnitude) as measured along the radius of a circle or sphere, respectively.

**Random Error** - A category of error; a measure of deviation from an ideal or true value which results from an accidental and unknown combination of causes and varies from one measurement to the next. Not deterministic. For NSG applications, a random error is typically represented as a random variable, random

vector, stationary process, or random field. And more specifically, as deviations about their mean-values, the latter considered biases. [b],[f]

- The random error corresponding to a random variable or the random error corresponding to (the elements of) a random vector are independent (uncorrelated) from one realization to the next, by definition.
- The random error corresponding to (the elements of) a random vector can also be correlated between the various elements for a given realization (intra-state vector correlation); hence this error is also a correlated error.
- The random error corresponding to a stochastic process corresponds to the collection of random errors associated with the collection of random vectors making up the stochastic process. Random error is independent (uncorrelated) from one realization to the next. However, within a specific realization, the individual random error vectors are typically temporally correlated amongst themselves (inter-state vector correlation); hence, random error is also correlated error. This same characteristic extends to random fields.
- The probability distribution for a random variable representing a random error is arbitrary – not necessarily Gaussian.

**Random Error Vector** - An error represented by a  $n \times 1$  random vector, and in the NSG, typically corresponds to the error in a state vector's value. The error itself could correspond to a combination of errors from different error categories: bias error, random error, and/or correlated error. That is, the term "random error vector" does not imply the corresponding category of error is necessarily (only) "random error".

**Random Field** - A random field (RF) is a collection of random vectors (RV), parameterized by an N-dimensional spatial vector  $q$ . In general, two different random vectors from the same realization of the random field are correlated. In the NSG, when error is represented by a random field, its corresponding statistics are specified by a statistical error model. A general descriptor of a given random field is as follows: a ("scalar" or "multi-variate") ("homogeneous" or "non-homogeneous") "ND random field".

- Scalar ( $n=1$ ) or multi-variate ( $n>1$ ) refers to the number of elements  $n$  that each random vector contains and is sometimes described as "(nd)", e.g. (2d) corresponds to 2 elements (random variables) per random vector.
- Homogeneous or non-homogeneous refers to whether the corresponding statistics are invariant or vary over spatial location  $q$ .
- ND refers to the number of spatial dimensions (number of elements in  $q$ ), e.g. 3D corresponds to 3 spatial dimensions. Each random vector corresponds to a unique value of  $q$ .
- As an example of terminology, "a multi-variate homogeneous 3D random field" or more specifically "a homogeneous 3D random field (2d)" corresponds to a multi-variate homogeneous random field over 3 spatial dimensions ( $q$  is a vector with 3 elements). The random vectors contain 2 elements.

- Spatial dimensions are general. For typical NSG applications, they correspond to some combination of geolocation directions and time. Note that a stochastic process is also a random field with  $N=1$ .
- In general, the collection of random vectors is infinite for a random field; however, only a finite subset are of interest for most applications, i.e., random vectors associated with a finite set of spatial locations.
- For typical NSG applications, the spatial correlation of a random field is specified by one of more strictly positive definite correlation functions (spdcf) contained in the corresponding statistical error model.

**Random Variable** - A variable whose value varies by chance, i.e., non-deterministic. Somewhat more formally, a random variable is a mapping from the space of experimental outcomes to a space of numbers. In the NSG, when error is represented by a random variable (a random vector with one component or element, i.e.,  $n=1$ ), its corresponding statistics are specified by a statistical error model.

- For most NSG applications, the space of experimental outcomes is already a number. For example, the x-component of sensor position can be considered a random variable. Equivalently, it can be defined as the true x-component of sensor position plus x-component of sensor position error, the former a deterministic (typically unknown) value and the latter a random variable.
- A random variable is statistically characterized by its mean-value, variance, and (more completely) its probability density function (pdf). The probability density function (pdf) is typically unknown and not included, but if needed for the calculation of probabilities, assumed Gaussian distributed with the pdf completely characterized by the mean-value and variance.

**Random Vector** - A random vector (RV) is an  $n \times 1$  vector which contains  $n$  random variables as components or elements. In the NSG, when error is represented as a random vector, its corresponding statistics are specified by a statistical error model. The corresponding random vector is also sometimes termed a random error vector.

- The realization of a Random Vector corresponds to a specific value of the vector (components or elements) for a given event such as a trial or experiment. Important descriptive statistics of a RV are its mean (vector) value and the error covariance matrix about the mean, and optionally, a multi-variate probability density function. These statistics can be predictive or sample-based.

**Realization** - For NSG accuracy and predicted accuracy applications, a specific trial or experimental outcome or independent sample involving a random error (category of error).

**Relative degree of freedom** - The degree of freedom divided by the number of state vector elements  $n$  for solution in an NSG Estimator; essentially the average degree of freedom per component for solution, or the average measurement redundancy.

**Relative Horizontal Accuracy** - The range of values for the error in the difference between two objects' horizontal metric geolocation values with respect to a specified geodetic horizontal reference datum; e.g., expressed as a radial error at the 90 percent probability level (CE90). There are two types of relative

horizontal accuracy: predicted relative horizontal accuracy is based on error propagation via a statistical error model(s); and measured relative horizontal accuracy is an empirically derived metric based on sample statistics.

**Relative Vertical Accuracy** - The range of values for the error in the difference between two objects' vertical metric geolocation values with respect to a specified geodetic vertical reference datum; e.g. expressed as a linear error at the 90 percent probability level (LE90). There are two types of relative vertical accuracy: predicted relative vertical accuracy is based on error propagation via a statistical error model(s); and measured relative vertical accuracy is an empirically derived metric based on sample statistics.

**Scalar Accuracy Metrics (augmented definition)** - convenient one-number summaries of geolocation accuracy and geolocation predicted accuracy expressed as a probability: [b],[f], and [h]

- Linear Error (LE) - LE is an unsigned value that corresponds to the length of a vertical line (segment) such that there is a 90% probability that the absolute value of vertical error resides along the line. If the line is doubled in length and centered at the target solution, there is a 90% probability that the true target vertical location resides along the line. LE\_XX corresponds to LE at the XX % probability level.
- Circular Error (CE) - CE is an unsigned value that corresponds to the radius of a circle such that there is a 90% probability that the horizontal error resides within the circle; or equivalently, if the circle is centered at the target solution, there is a 90% probability the true target horizontal location resides within the circle. CE\_XX corresponds to CE at the XX % probability level.
- Spherical Error (SE) - SE is an unsigned value that corresponds to the radius of a sphere such that there is a 90% probability that 3d error resides within, or equivalently, if the sphere is centered at the target solution, there is a 90% probability that the true target location resides within the sphere. SE\_XX corresponds to SE at the XX % probability level.

For the above scalar accuracy metrics:

- It is assumed that the underlying  $x$ - $y$ - $z$  coordinate system is a local tangent plane system, i.e.,  $x$  and  $y$  are horizontal components and  $z$  the vertical component.
- CE-LE corresponds to the CE-LE error cylinder. There is a probability between 81 to 90 percent that 3d radial error resides within the cylinder. The former value corresponds to uncorrelated horizontal and vertical errors, the latter value to highly correlated horizontal and vertical errors.
- LE\_XX, CE\_XX, and SE\_XX (aka LEXX, CEXX, and SEXX, respectively) are also called XX percentiles for absolute vertical errors, horizontal radial errors, and spherical radial errors, respectively. XX is expressed as an integer greater than zero and less than 100.

**Spatial Correlation** - The correlation between the elements (random variables) of two random vectors at two different spatial locations associated with the same realization of a random field.

**Spherical Error (SE)** - See **Scalar Accuracy Metrics**.

**Standard Deviation** – The square root of the variance of a random variable. A measure of deviation or dispersion about the random variable’s mean-value.

**State Vector** - A vector of parameters or variables that describe a system’s state.

**State Vector Error** - A vector of errors corresponding to an estimate of a state vector relative to a (typically unknown) true state vector; a random vector of errors, or random error vector.

**Statistical Error Model** - Information which describes the error data corresponding to a given state vector. The information includes the type of corresponding error representation (random variable, random vector, stochastic process, or random process), the category of statistics (predictive or sample), and associated statistical information including at a minimum the mean-value and covariance data.

**Stochastic Process** - A stochastic process (SP) is a collection of random vectors (RV), parameterized by a 1D quantity, typically time. For a given realization of the stochastic process, the individual random vectors are correlated with each other. If the random vectors consist of one element or component ( $n=1$ ), the stochastic process is sometimes called a scalar stochastic process, and if greater than one, a multi-variate stochastic process. A stochastic process is also a random field with one spatial (or time) dimension, i.e.,  $N=1$ . In the NSG, when error is represented as a stochastic process, its corresponding statistics are specified by a statistical error model.

**Strictly positive definite correlation function (spdcf)** - function which models the statistical correlation between random vectors (random variables), typically applied in the NSG to describe the temporal correlation and/or spatial correlation between various random vectors which are part of a stochastic process or random field, i.e., the spdcf is a function of delta time or delta distance (possibly in each of multiple directions) between random vectors. The proper use of an spdcf ensures assembly of a valid multi-state vector error covariance matrix, i.e., positive definite and symmetric.

**Temporal Correlation** - The correlation between the elements (random variables) of two random vectors at two different times associated with the same realization of a stochastic process.

**Uncorrelated Error** - At an intuitive level, an error that is statically unrelated to all other relevant errors. More precisely, if two random variables represent two uncorrelated errors (about their respective mean-values), their covariance and their corresponding correlation coefficient are zero. A random variable is uncorrelated (with itself) from one realization to the next by definition. This latter property is also true for the random variables making up random vectors, stochastic processes, and random fields. However, these three representations typically include correlated errors within the same realization.

**Variance** - The measure of the dispersion of a random variable about its mean-value, also the standard deviation squared. [b]

**Vertical Error** - As applied to geospatial measurements and processes, vertical error is a signed and one dimensional (linear) error value typically observed in the direction of the z-axis of a local right-handed

coordinate system where the  $x, y$  plane is defined as tangent to the defined reference surface at the point of origin and the  $z$ -axis is normal to the  $x, y$  plane and positive in the up direction.

## **Appendix B: Geolocation Product Accuracy Models – the basics**

This appendix describes the basics of the Geolocation Product Accuracy Assessment Model and the Geolocation Product Predicted Accuracy Model:

- their corresponding contents
- methods for their population based on the computation of sample-statistics and predictive statistics
- applications
- performance or populated model “fidelity”

The models that are detailed in this appendix are illustrated in Figure B.1 in red. The populated Geolocation Product Accuracy Assessment Model is used to populate the corresponding Geolocation Product Predicted Accuracy model. Both models correspond to specific type or class of geolocation product.

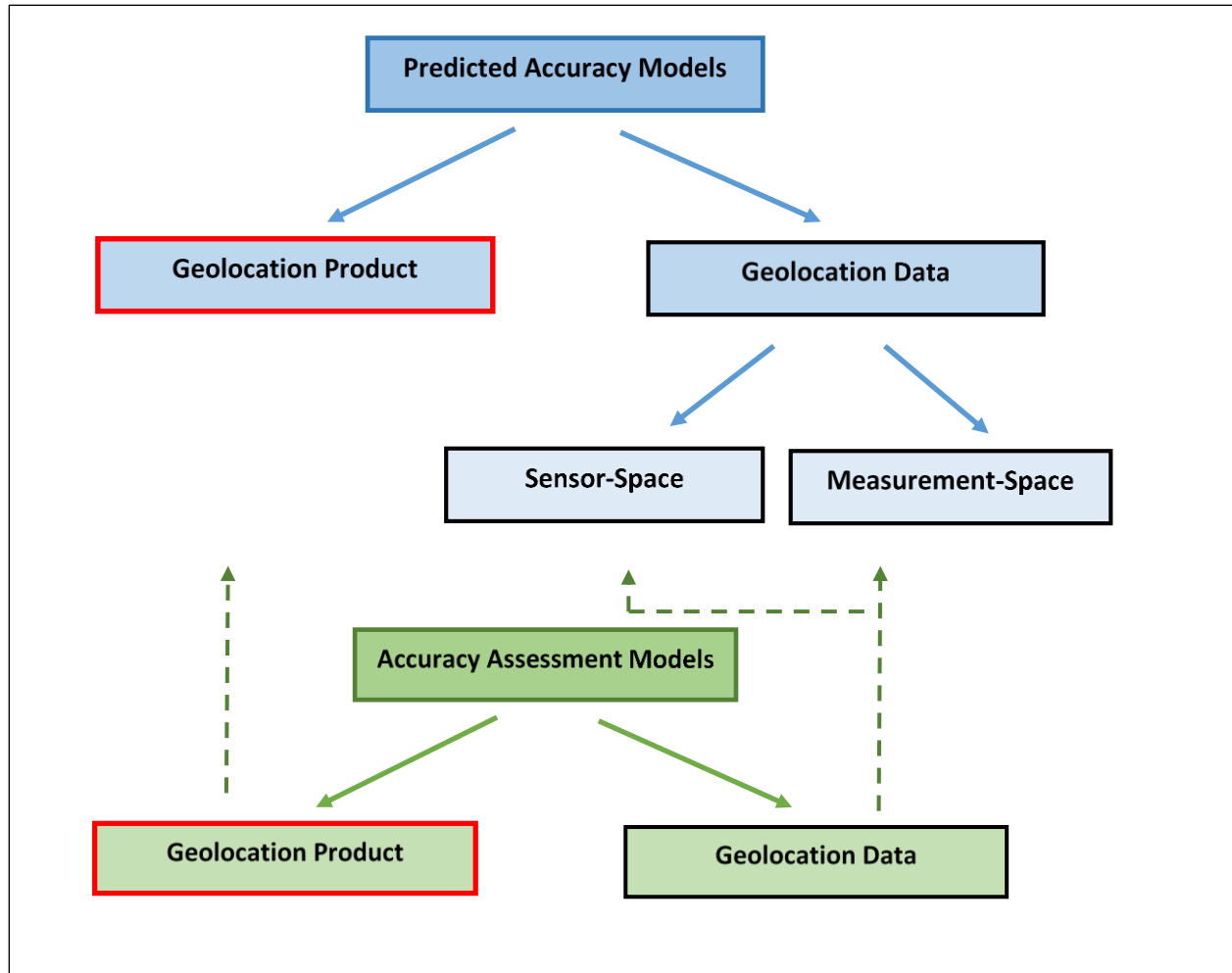


Figure B-1: Models described in this appendix (red)

For many types of External Data it is not uncommon to have relatively few samples of error available to populate an accuracy assessment model. This appendix presents corresponding methods to compute sample statistics in order to populate an accuracy assessment model, followed by methods to populate a corresponding predicted accuracy model. Because of the availability of relatively few samples, both populated models would typically be “ranked” as either “low” or “medium” quality in corresponding references to them in the Quality Assessment Summary described in Section 5.2.1 of the main body of this document.

Although the methods presented in this appendix are relatively simple, they are reasonable as well as practical. As such, they do not include more comprehensive statistical methods that typically require more samples, such as the computation of confidence intervals, a heavy reliance on order statistics, etc. However, they can also be applied to a larger number of samples when they are available for convenience, with corresponding quality ranked “medium” or “high”. For a description of additional and more comprehensive methods, see TGD 2a (Predictive Statistics) and TGD 2b (Sample Statistics).

For a subset of the External Data described above, it is also not unusual to know virtually nothing *a priori* about their geolocation accuracy as well as have very few error samples available. Correspondingly, although the quality or confidence in the processing results will be ranked “low”, such results are significantly better than no knowledge at all as long as the quality rankings are readily apparent.

For example, there may be a type of geolocation product with geolocation accuracy that could be within the range of from ten meters of error to hundreds of meters of error, i.e., error characteristics are virtually unknown. Using the methods described in this appendix, and assuming that the true (unknown) accuracy is on the order of 30 meters (one sigma), an estimate of accuracy ranging from 15 meters to 60 meters (one sigma) might be computed with very few samples – still significant information given that virtually nothing was known previously and considering that results are tempered by a “low” ranking for quality. Of course, if more than a very few error samples are available, a better estimate of accuracy is achievable – as good as ranging from 27 to 33 meters per the Section B.4 experiments parameterized by number of samples. Furthermore, regardless the number of initial error samples, additional samples may be made available in the future that can be pooled with this first set for a better estimate of geolocation accuracy and a higher quality ranking.

Sections B.1 and B.2 of the appendix describes the processing required to populate an accuracy assessment model and corresponding predicted accuracy model, respectively, for a geospatial product. Both models assume that 2d horizontal geolocation errors are of interest for convenience. Processing is readily extendable in a straightforward manner to 3d geolocation errors, either horizontal and/or vertical errors separately or combined together as a 3d error vector. Section B.3 provides a brief summary of user applications of the populated predicted accuracy model. Section B.4 presents a performance assessment of the overall process of model population based on an extensive set of simulated examples/experiments and includes various plots illustrating underlying concepts. Section B.5 discusses extension of the documented processing.

In general, the processing described in this appendix is based on the following: predictive statistics correspond to the representation of geolocation errors as a wide-sense homogeneous random field, and sample statistics are in accordance with this assumption. As such, the mean-value of error and the error covariance matrix about this mean-value are assumed constant across an arbitrary realization of the product, and the spatial correlation of errors is only a function of distance between two geolocations. That is, these predictive statistics are independent of the absolute locations of geolocations of interest in the product. As such, relative errors also have a mean-value of zero and corresponding distance bins are a function of the distance between two geolocations only, and not the geolocations’ absolute locations. Furthermore, the random field is assumed Gaussian distributed, and therefore the mean-value and error covariance matrix completely characterize the multi-variate probability distribution of geolocation errors.

The above corresponds to the “standard” predicted accuracy model and not to an assumed MGRF representation of geolocation uncertainty, as the latter represents geolocation errors as a mixture of multiple Gaussian wide-sense homogeneous random fields. However, an MGRF representation: (1) is not required in general for Commodities data, and (2) typically requires more than a relatively few error

samples for adequate population. On the other hand, this appendix is consistent with an MGRF representation that contains only one partition and one random field – the nominal partition and its random field that were discussed previously in Section 5.3.3.3.

Computation of sample statistics in support of the population of an MGRF based on the techniques presented in this appendix is discussed further in Section B.5.2. Appendix E describes the MGRF concept, contents, and applications in detail.

This appendix (Appendix B) is referenced in Section 5.3.4 of the main body of this document as well as in various other appendices that refer to the basic processing regarding the computation of sample statistics and predictive statistics presented here. A roadmap to the remainder of Appendix B is as follows:

### **Roadmap to Appendix B sections**

#### **B.1 Population of the accuracy assessment model**

##### **B.1.1 Absolute accuracy**

##### **B.1.2 Relative accuracy**

##### **B.1.3 Outputs**

#### **B.2 Population of predicted accuracy model**

##### **B.2. Absolute Accuracy**

##### **B.2.1 Relative Accuracy**

##### **B.3.1 Outputs**

#### **B.3 Applications**

#### **B.4 Performance assessment of populated models: quantitative results**

#### **B.5 Extension of results**

### **B.1 Population of the accuracy assessment model**

Let us assume that errors of interest are 2d horizontal geolocation errors for simplicity and ease of notation. The processing described below can be simplified to 1d vertical errors and performed separately, if so desired, or horizontal error samples can instead be combined with the vertical error samples for a subsequent 3d analysis by straight-forward extensions. Error samples correspond to a product geolocation minus “ground truth” coordinates.

The following assumes that relatively few horizontal error samples are available – on the order of from 4 to 10 samples of 2d error from each of from 3 to 20 product realizations. Multiple realizations of the product are required in order to assess absolute accuracy, and multiple samples of geolocation error in the same realization are also required in order to assess relative accuracy. The processing described is reasonably flexible and can even support the availability of only one error sample in some product realizations as long as other product realizations have multiple samples.

The more samples available, both within a product and across products, the better (statistically significant) the results. As a general “rule of thumb”, at least 10 product realizations are preferred, with most having

samples of error corresponding to at least 7 geolocations at varied distances between pairs. In addition, a significant number of these distances should also be “small” regardless the number of product realizations, where a “small” distance corresponds to the typical length of a feature of interest in the product and for which predicted relative accuracy is of particular importance. Section B.4 characterizes performance results based on fewer product realizations and fewer error samples per realization.

Error samples are also assumed individual error samples from a product (realization), not one “representative” error sample from the product that was used in the analysis described in Section 5.3.5.3 of the main body of this document. Representative error samples do not support the assessment of relative errors and/or the characterization of the spatial correlation of errors.

Finally, the processing in this section computes the various sample statistics of interest based on the equivalent of WLS solutions for the statistics of interest using the samples from each product weighted by the number of samples in that product – the greater the number of samples from a product, the higher its relative weight or influence it has on the various solutions.

This approach to weighting is practical and also reasonable given that the errors in a product are not 100% spatially correlated and can also include non-negligible mensuration errors that is almost always uncorrelated between samples. If these two characteristics were not applicable, a product’s errors would be a bias (only) and the same bias for all products; correspondingly, one sample from a product would contain the same information as a hundred samples. If this were the case, optimal weighting would be the same weight for all products regardless their number of samples.

Note: theoretical statistical significance is not quantified explicitly in this appendix, but is detailed in TGD 2a and TGD 2b for various statistics as a function of the number of independent samples. A somewhat crude but convenient “rule of thumb” for predicted accuracy in general:  $pred\_σ \cong true\_σ + /- true\_σ/\sqrt{n}$ , where  $n$  is the number of independent samples of error. This is similar to a confidence interval for predicted accuracy but without an explicit level-of-probability specified. In addition, statistical significance is quantified empirically in Section B.4.

Caution: in the following documentation, the index  $i$  represents a different realization  $i$  of the data/product, not an MGRF partition  $i$ , as an MGRF representation of uncertainty is not used as explained earlier in the introduction to this appendix.

### **B.1.1 Absolute accuracy**

#### **Introduction and initial definitions**

Define  $\epsilon X_{ij}$  as a  $2 \times 1$  sample of horizontal error corresponding to from  $j = 1, \dots, n_i$  geolocations in from  $i = 1, \dots, m$  data/product independent realizations. In general, geolocation errors corresponding to geolocations in the same realization are spatially correlated, but independent (uncorrelated) with geolocations from different realizations.

It is required that the number of realizations ( $m$ ) is greater than or equal to two and that at least two of those realizations have at least two samples of geolocation error in order to proceed.

If the above requirement regarding the number of samples in the same realization of the product is not met, statistics corresponding to absolute geolocation accuracy can still be computed but those corresponding to relative geolocation accuracy cannot.

### **Processing – sample mean and covariance**

Using the above samples, compute the sample mean-value  $\bar{X}_i$  and the sample covariance matrix  $C_i$  for each realization  $i = 1, \dots, m$ :

$$\bar{X}_i = (1/n_i) \sum_{j=1}^{n_i} \epsilon X_{ij} \quad 2 \times 1 \quad (\text{B.1.1-1})$$

$$C_i = (1/n_i) \sum_{j=1}^{n_i} (\epsilon X_{ij} - \bar{X}_i) (\epsilon X_{ij} - \bar{X}_i)^T \quad 2 \times 2 \quad (\text{B.1.1-2})$$

Because the error samples in a given realization are spatially correlated, we expect their 2d vector mean-value  $\bar{X}_i$  to be significantly different than zero. The corresponding covariance matrix  $C_i$  is computed relative to this mean-value. Both  $\bar{X}_i$  and  $C_i$  are computed for general information and for use in the computation of corresponding sample statistics taken over all realizations as follows:

Compute the sample mean-value  $\bar{X}$  and the sample covariance matrix  $C$  over all realizations  $m$ , where the total number of error samples is defined as  $n_{tot} \equiv \sum_{i=1}^m n_i$ :

$$\bar{X} = \sum_{i=1}^m w_i \bar{X}_i, \text{ where the scalar weight } w_i = (n_i/n_{tot}) \quad 2 \times 1 \quad (\text{B.1.1-3})$$

$$C = \sum_{i=1}^m w_i (C_i + \bar{X}_i \bar{X}_i^T) \quad 2 \times 2 \quad (\text{B.1.1-4})$$

The covariance matrix  $C$  is computed equivalent to the assumption of a mean-value of error equal to zero and corresponds to a mean-square error.  $\bar{X}$  is computed for “information only” and in support of a “reasonableness check” that a significant product-wide error bias is not applicable, i.e. that the absolute values of its components are reasonably smaller than their corresponding sigmas (standard deviations) in  $C$ . As detailed in Section C.2, predictive statistics in a corresponding predicted accuracy model set the *a priori* mean-value of error equal to zero and the *a priori* covariance matrix equal to the above  $C$  which corresponds to an *a priori* mean-square error. This is a reasonable (conservative) course of action given that error samples are from a relatively few number of realizations and is consistent with an assumed non-biased product until demonstrated otherwise. Also, even if the correct (unknown) mean-value were non-zero (biased), its effect is still included in the magnitude of  $C$  as computed in Equation (C.1.1-4).

It is recommended that a single plot of all of the individual error samples be made with different colors used for samples from each of the  $i = 1, \dots, m$  different product realizations.  $m$  individual plots of all error samples in each product realization  $i = 1, \dots, m$ , with their mean-value  $X_i$  removed, are also recommended, as well as a single plot of all  $m$  color-coded mean values. If the mean-values are all non-trivial and approximately the same value, the corresponding type of class of geolocation product may have a systematic bias that should be investigated. The plot axes correspond to the x-component and the y-component of geolocation error and an individual error sample is represented as a dot in the corresponding 2d “error-space”.

### **Processing – scalar accuracy metrics**

Each radial error sample corresponding to sample  $j$  from realization  $i$  is computed as follows:

$$r_{ij} = \sqrt{\epsilon X_{ij}^T \epsilon X_{ij}} \quad (\text{B.1.1-5})$$

The  $r_{ij}$  are ranked by increasing magnitude over all samples and all realizations and a sample CE90 is computed as follows:

sample CE90 equals the smallest ranked radial error sample such that at least 90% of the ranked radial error samples are smaller; computed assuming a total of at least 15 samples and a total of at least 3 product realizations, otherwise set to “n/a”. (B.1.1-6)

Samples between realizations are assumed uncorrelated (independent) but those within the same realization are spatially correlated to some degree. Independent samples are preferred in general; hence, Equation (B.1.1-6) is an approximation. This approximation is simple to implement and provides at least minimal statistical significance for the computation of sample-based CE90 for Commodities data.

### **B.1.2 Relative accuracy**

#### **Introduction and initial definitions**

The following processing is somewhat more complicated in that it deals with relative differences between error samples in a given data/product realization, with corresponding sample statistics subsequently compiled over all realizations in order to characterize geolocation relative accuracy. In addition, the corresponding (auto) correlation values of spatial error are computed since they are used to generate or fit an spdcf when populating a corresponding Geolocation Product Predicted Accuracy Model as detailed in Section B.2.

The following is based on the definition of the random samples as defined previously in Section B.1.1:  $\epsilon X_{ij}$  as a  $2 \times 1$  sample of horizontal error, for  $j = 1, \dots, n_i$  samples in each of  $i = 1, \dots, m$  realizations of the data/product.

For convenience in the following documentation, we now assume that  $n_i \geq 2$ , i.e., each product realization contains at least two samples of horizontal geolocation error. We further assume that the previous value for  $m$  and corresponding realization numbering are adjusted accordingly, if necessary.

For each data/product realization  $i$ , identify and compute the number of unique pairs of samples  $p_i \geq 1$  in that realization. A unique pair is defined as corresponding to two error samples that have at most only one sample in common with any other pair of samples in the same data/product realization.

### **Processing – relative covariance matrices and spatial correlation values**

Identify each unique pair of error samples, the sample numbering associated with that pair, (B.1.2-1) and the total number of such pairs  $p_i$  in realization  $i = 1, \dots, m$ .

Define/compute the relative error sample  $k$  corresponding to each unique pair of geolocation errors in the data/product realization  $i$  as follows:

$$\Delta X_{ik} = \epsilon X_{ij1} - \epsilon X_{ij2}, \quad (B.1.2-2)$$

$k = 1, \dots, p_i, i = 1, \dots, m$ , and where  $j1, j2 \in \{1, \dots, n_i\}, j1 \neq j2$ .

There are  $p_i$  relative error samples in realization  $i$ , where  $p_i = \binom{n_i}{2}$  or “ $n_i$  choose 2”.

Note: the definition/convention for the difference between two error samples was specified in Equation (C.1.2-2) as  $\Delta X_{ik}$  instead of the possibly more logical  $\Delta \epsilon X_{ik}$  in order to keep symbology from getting too cumbersome.

Define/compute the relative error samples’ corresponding horizontal distances as:

$$dX_{ik} = |X_{ij1} - X_{ij2}| \equiv \sqrt{(X_{ij1}(1) - X_{ij2}(1))^2 + (X_{ij1}(2) - X_{ij2}(2))^2}, \quad (B.1.2-3)$$

$k = 1, \dots, p_i, i = 1, \dots, m$ , and where  $j1, j2 \in \{1, \dots, n_i\}, j1 \neq j2$ .

In general,  $X_{ij}$  is the 3d geolocation associated with horizontal error sample  $\epsilon X_{ij}$ , and  $X_{ij}(1)$  and  $X_{ij}(2)$  are its two horizontal coordinates. (If the error samples of interest were 3d instead of horizontal error samples, horizontal distances are still generally applicable.)

Define the total number of relative error samples over all data/product realizations as:

$$p = \sum_{i=1}^m p_i. \quad (B.1.2-4)$$

### **Example**

As an example, assume that we have the following 10 individual error samples taken over  $m = 3$  data/product realizations (relatively few samples/realizations are used for ease of example only):

$$\epsilon X_{11}, \epsilon X_{12}, \epsilon X_{13}, \epsilon X_{14}; \epsilon X_{21}, \epsilon X_{22}, \epsilon X_{23}; \epsilon X_{31}, \epsilon X_{32}, \epsilon X_{33}$$

Thus, we have a total of  $p = 12$  relative error samples over three data/product realizations:

$$\begin{aligned} \Delta X_{11} &= \epsilon X_{11} - \epsilon X_{12}, \Delta X_{12} = \epsilon X_{11} - \epsilon X_{13}, \Delta X_{13} = \epsilon X_{11} - \epsilon X_{14}, \\ \Delta X_{14} &= \epsilon X_{12} - \epsilon X_{13}, \Delta X_{15} = \epsilon X_{12} - \epsilon X_{14}, \Delta X_{16} = \epsilon X_{13} - \epsilon X_{14}, \text{ with } p_1 = 6; \\ \Delta X_{21} &= \epsilon X_{21} - \epsilon X_{22}, \Delta X_{22} = \epsilon X_{21} - \epsilon X_{23}, \Delta X_{23} = \epsilon X_{22} - \epsilon X_{23} \text{ with } p_2 = 3; \\ \Delta X_{31} &= \epsilon X_{31} - \epsilon X_{32}, \Delta X_{32} = \epsilon X_{31} - \epsilon X_{33}, \Delta X_{33} = \epsilon X_{32} - \epsilon X_{33}, \text{ with } p_3 = 3. \end{aligned}$$

### ... End example

Allocate the various horizontal distances  $dX_{ik}$ ,  $k = 1, \dots, p_i$ ,  $i = 1, \dots, m$ , and their corresponding relative error samples into two distance bins: “small” and “large”. A reasonable definition of “small” is product-use dependent and consistent with distances spanning typical features of interest in the product on the order of  $d1$  meters or less. Correspondingly, the two distance bins have corresponding distance intervals equal to  $bin\_small = (0, d1]$  and  $bin\_large = (d1, d2)$ , where  $d2$  is essentially  $\sqrt{2}$  times the product width if a square product.  $bin\_small$  and  $bin\_large$  are sometimes referred to as “bin1” and “bin2”, respectively, for generality.

Note: if too few samples with varied distances are available across the products for the applicability of both “small” and “large” distance bins, only one distance bin can be used. It is termed “bin\_all” and contains all error samples from a given product, with corresponding processing for the population of the Geolocation Product Accuracy Assessment Model and the subsequent Geolocation Product Predicted Accuracy Model (Section B.2.2) modified accordingly.

Note: if enough samples are available with varied distances, more than two distance bins can be defined for higher fidelity, with corresponding processing for population of both the accuracy assessment model and the subsequent predicted accuracy model (Section B.2.2) modified accordingly. This is typically not applicable for Commodities data.

Compute the corresponding distance boundary separating the two distance bins and also the average distance for both bins taken over all relative error samples over all realizations: (B.1.2-5)

$$d\_bndry = d1$$

$$d\_avg\_small = \text{average distance between all geolocation pairs in the small distance bin over all realizations}$$

$d_{avg\_large}$  = average distance between all geolocation pairs in the large distance bin over all realizations

For each data/product realization  $i$ , compute the following:

For all relative error samples  $\Delta X_{ik}$ , with distances corresponding to the “small” distance bin, compute the corresponding relative error sample covariance matrix about an assumed mean-value of relative error equal to zero (if there were a non-zero mean-value of error it would cancel out):

$$rel\_C_{i\_small} = (1/p'_i) \sum_{k'=1}^{p'_i} \Delta X_{ik'} \Delta X_{ik'}^T \quad 2 \times 2, \quad (B.1.2-6)$$

where  $p'_i$  is the appropriate number of relative error samples in the “small” distance bin and  $k'$  their appropriate index. If  $p'_i = 0$ , set  $rel\_C_{i\_small}$  to zero, i.e., to the matrix  $0_{2 \times 2}$ .

For all relative error samples  $\Delta X_{ik}$ , with distances corresponding to the “large” distance bin, compute the corresponding relative error sample covariance matrix about an assumed mean-value of relative error equal to zero:

$$rel\_C_{i\_large} = (1/p''_i) \sum_{k''=1}^{p''_i} \Delta X_{ik''} \Delta X_{ik''}^T \quad 2 \times 2, \quad (B.1.2-7)$$

where  $p''_i$  is the appropriate number of relative error samples in the “large” distance bin and  $k''$  their appropriate index. If  $p''_i = 0$ , set  $rel\_C_{i\_large}$  to zero.

### **Example (continues)**

Assume the following categorization by distance bin for the previous example:

The “large” distance bin corresponds to horizontal point-pair distances greater than 200 meters, and the “small” distance bin for point-pair distances greater than zero and less than or equal to 200 meters (values for illustrative purposes only).

Further assume, for “convenience of example”, that:

$dX_{11} = |X_{11} - X_{12}|$ ,  $dX_{12} = |X_{11} - X_{13}|$ ,  $dX_{13} = |X_{11} - X_{14}|$  are within distance bin “large”,  
 $dX_{14} = |X_{12} - X_{13}|$ ,  $dX_{15} = |X_{12} - X_{14}|$ ,  $dX_{16} = |X_{13} - X_{14}|$  are within distance bin “small”,  
 $p''_1 = 3$ , and  $p'_1 = 3$ ;

$dX_{21} = |X_{21} - X_{22}|$ ,  $dX_{22} = |X_{21} - X_{23}|$  is within distance bin “large”;  
 $dX_{23} = |X_{22} - X_{23}|$ , is within distance bin “small”,  
 $p''_2 = 2$ , and  $p'_2 = 1$ ;

$dX_{31} = |X_{31} - X_{32}|$ ,  $dX_{32} = |X_{31} - X_{33}|$  is within distance bin “large”;  
 $dX_{33} = |X_{32} - X_{33}|$ , is within distance bin “small”,  
 $p''_3 = 1$ , and  $p'_3 = 1$ ;

Therefore, after associating relative error samples with corresponding horizontal distances, the following is applicable:

$$rel\_C_{1\_large} = (1/3) \sum_{k''=1}^3 \Delta X_{1k''} \Delta X_{1k''}^T, \quad rel\_C_{1\_small} = (1/3) \sum_{k'=4}^6 \Delta X_{1k'} \Delta X_{1k'}^T;$$

$$rel\_C_{2\_large} = (1/2) \sum_{k''=1}^2 \Delta X_{2k''} \Delta X_{2k''}^T, \quad rel\_C_{3\_small} = (1/1) \sum_{k'=3}^3 \Delta X_{2k'} \Delta X_{2k'}^T.$$

$$rel\_C_{3\_large} = (1/2) \sum_{k''=1}^2 \Delta X_{3k''} \Delta X_{3k''}^T, \quad rel\_C_{3\_small} = (1/1) \sum_{k'=3}^3 \Delta X_{3k'} \Delta X_{3k'}^T.$$

The above has relatively simple indexing regarding  $k''$  due to “convenience of example”.

### ... End example (continues)

The reasonable assumptions that  $p'_i \geq 1$  and  $p''_i \geq 1$  for all realizations  $i = 1, \dots, m$ , are made for simplicity of the following equations (otherwise reduce the value of  $m$  in the appropriate equation accordingly):

Compute the relative error sample covariance matrix for each distance bin over all realizations:

$$rel\_C\_small = \sum_{i=1}^m w_i rel\_C_{i\_small} \quad (B.1.2-8)$$

$$rel\_C\_large = \sum_{i=1}^m w_i rel\_C_{i\_large}, \quad (B.1.2-9)$$

where the scalar weight  $w_i$  was defined earlier as  $w_i = (n_i/n_{tot})$ , i.e., the total number of error samples in realization  $i$  relative to the total number of samples over all realizations.

Compute the corresponding representative spatial correlation values for each distance bin:

$$\rho_{small} = 1 - \frac{(rel\_C\_small(1,1) + rel\_C\_small(2,2))}{2(C(1,1) + C(2,2))} \quad (B.1.2-10)$$

$$\rho_{large} = 1 - \frac{(rel\_C\_large(1,1) + rel\_C\_large(2,2))}{2(C(1,1) + C(2,2))} \quad (B.1.2-11)$$

Recall that  $C$  used in the above equations is the sample covariance matrix computed previously in Equation (C.1.1-4).

**Comment:** Formulas B.1.2-10 and B.1.2-11 are based on the following relationship between relative errors, their relative and absolute covariance matrices, and their spatial correlation coefficient, assuming scalar errors for simplicity and corresponding to an arbitrary realization of a wide-sense stationary process (random field):

$$E\{(\epsilon x_1 - \epsilon x_2)(\epsilon x_1 - \epsilon x_2)^T\} = rel\_sigma^2 = 2\sigma^2(1 - \rho). \quad (B.1.2-12)$$

### Processing – scalar relative accuracy metrics

Each radial relative error sample  $k$  from realization  $i$  is defined as follows:

$$rel\_r_{ik} = \sqrt{\Delta X_{ik}^T \Delta X_{ik}} \quad (B.1.2-13)$$

They are further subcategorized as relative error samples from the small and large distance bins,  $rel\_r_{ik\_small}$  and  $rel\_r_{ik\_large}$ , respectively. They are then ranked by increasing magnitude over all relevant samples and all realizations and sample  $rel\_C90$  computed as follows: (B.1.2-14)

(1) Sample  $rel\_CE90\_small$  equals the smallest ranked radial error sample such that at least 90% of the ranked radial relative error samples in the small distance bin are smaller; computed assuming at least a total of 15 samples over at least 3 product realizations, otherwise set to “n/a”.

(2) Sample  $rel\_CE90\_large$  equals the smallest ranked radial error sample such that at least 90% of the ranked radial relative error samples in the large distance bin are smaller; computed assuming at least a total of 10 samples from at least 3 product realizations, otherwise set to “n/a”.

### **B.1.3 Outputs**

#### Contents of the Accuracy Assessment Model (file/report): absolute accuracy

Based on the above, the following are included in the populated Accuracy Assessment Model (file/report): (B.1.3-1)

- The number of realizations  $m$  and the number of samples  $n_i$  in each realization
- The sample statistics (B.1.1-1 through B.1.1-4):
  - For each product (realization)  $i$ , the mean-value  $\bar{X}_i$  (meters) and the covariance matrix about the mean-value  $C_i$  (meters-squared)

- Combined over all product realizations, the mean-value  $\bar{X}$  (meters) and the covariance matrix about an assumed mean-value of zero  $C$  (meters-squared)
- Sample scalar accuracy metric, assuming enough realizations (products) were available (B.1.1-6):
  - $CE90$  (meters)
- Listing of all error samples for each realization and optional plot over all product realizations
- Listing of all radial error samples for each realization and optional plot over all product realizations
- Any applicable comments/observations related to the above analyses.

### **Contents of the Accuracy Assessment Model (file/report): relative accuracy**

Based on the above, the following are also included in the populated Accuracy Assessment (file/report): (B.1.3-2)

- The number of realizations  $m$  and the number of samples  $n_i$  in each product realization
- The total number of relative error samples  $p_i$  used in each realization  $i = 1, \dots, m$  (B.1.2-1)
- Distances associated with the two (“small” and “large”) distance bins (B.1.2-5):
  - $d_{bndry}$  (meters)
  - $d_{avg\_small}$  (meters)
  - $d_{avg\_large}$  (meters)
- Sample-based relative error covariance matrices for the two distance bins for each product realization  $i$  (B.1.2-6 through B.1.2-7):
  - $rel\_C_{i\_small}$  (meters-squared)
  - $rel\_C_{i\_large}$  (meters-squared)
- Supporting absolute sample-based error covariance matrix  $C$  (B.1.1-4)
- Sample-based relative error covariance matrices for the two distance bins averaged over all realizations (B.1.2-8 and B.1.2-9):
  - $rel\_C\_small$  (meters-squared)
  - $rel\_C\_large$  (meters-squared)
- Sample-based (auto) correlation coefficients  $\rho_{small}$  and  $\rho_{large}$  for spatial error for both distance bins (B.1.2-10 and B.1.2-11):
  - $\rho_{small}$  (unit-less)
  - $\rho_{large}$  (unit-less)
- Sample based scalar relative accuracy metrics corresponding to the two distance bins, assuming enough relative error samples and realizations available (B.1.2-14):
  - $rel\_CE90\_small$  (meters)
  - $rel\_CE90\_large$  (meters)
- Listing of all relative error samples and their distances for each realization; optional plots of relative error samples over all realizations in various formats
- Any applicable comments/observations related to the above analyses.

## **B.2 Population of the predicted accuracy model**

The following describes population of a Geolocation Product Predicted Accuracy Model for an arbitrary geolocation product of the same type or class as that associated with the populated Geolocation Product Accuracy Assessment Model described in Section B.1. The population of the former is based on the latter, and refers to the related data of Section B.1.

The following assumes 2d horizontal errors consistent with Section B.1 but can be easily modified for vertical errors or even 3d errors if so desired. In particular, if for vertical errors, covariance matrices are  $1 \times 1$  instead of  $2 \times 2$ , and the sdpcf is a scalar function applicable to z errors instead of both x and y errors, but is still a function of horizontal location of the corresponding geolocations in the product.

### B.2.1 Absolute accuracy

#### Processing – mean value and covariance

The following *a priori* predictive statistics are computed corresponding to the horizontal geolocation error of an arbitrary geolocation in an arbitrary realization of the data/product. They formally correspond to a single random field (Random Field 1 in the nominal partition if for an MGRF representation). The sample statistics used in the computations are via Equation (B.1.1-4).

The 2d vector mean-value of error:

$$\bar{X} = 0 \quad 2 \times 1 \quad (\text{B.2.1-1})$$

$$C_X = \text{diag}(C) \quad 2 \times 2, \quad (\text{B.2.1-2})$$

$C_X$  is set to a diagonal matrix corresponding to the diagonals of the sample-based covariance matrix  $C$  as is reasonable for Commodities data, but is not required in general. Also, as a reasonable alternative for some types of product,  $C_X$  is set to a diagonal matrix with each diagonal entry equal to  $\text{trace}(C)/2$  or average eigenvalue. This essentially removes any azimuth dependent effects as captured by the sample statistics, and which may not be applicable to future (arbitrary) product realizations.

#### Processing – scalar accuracy metrics

The scalar accuracy metric  $CE90$  is computed as follows:

$$CE90 = 2.1460\sqrt{\text{trace}(C_X)/2} \quad 1 \times 1 \quad (\text{B.2.1-3})$$

The above computation of the predictive statistic  $CE90$  is a reasonable approximation and is also based on an assumed Gaussian distribution of geolocation errors. Its inclusion in the following file/report is for the convenience of the down-stream user as it is a statistic that can be derived from  $C_X$  which is always included.

As an option,  $CE90$  can be computed instead based on the ratio of its eigenvalues of  $C$  as detailed in TGD 2a (Predictive Statistics) for “higher fidelity”. As another option,  $CEXX$  for other probability levels other than  $XX=90$  can be computed and included as well.

### B.2.2 Relative accuracy

The following predictive statistics correspond to the relative geolocation error between an arbitrary pair of geolocations in the realization of the data/product. Those statistics that correspond to distance bins further assume that the distance between geolocations making up a geolocation pair is within the distance bin. Again, all geolocations in the product (realization) correspond to the nominal partition with error specified by the predictive statistics of a random field (random field 1). The sample statistics used in the computations of the following predictive statistics are via the associated populated Accuracy Assessment file/report (Equations B.1.3-1 and B.1.3-2).

#### Processing – mean-value and covariance for relative errors

Relative distances associated with the two distance bins “small” and “large”:

$$d_{avg\_small} \text{ and } d_{avg\_large}. \quad (B.2.2-1)$$

The mean-value of relative error and the associated covariance matrix for each of the distance bins are computed as follows:

$$rel\_X = 0 \quad 2 \times 1, \quad (B.2.2-2)$$

$$rel\_C_{X\_small} = diag(rel\_C\_small) \quad 2 \times 2, \quad (B.2.2-3)$$

$$rel\_C_{X\_large} = diag(rel\_C\_large) \quad 2 \times 2, \quad (B.2.2-4)$$

where in general, “ $diag(E)$ ” corresponds to a diagonal matrix with diagonal elements equal to those of matrix  $E$ . Diagonalization of the matrix is not required but is typically done corresponding to the availability of relatively few error samples.

Note that  $rel\_X = 0$  is compatible with the representation of geolocation errors as a wide-sense homogenous random field with a constant mean-value  $\bar{X}$ . This is seen as follows: the relative error  $\Delta X$  between two geolocations  $i$  and  $j$  is  $\Delta X = \epsilon X_i - \epsilon X_j$ , and therefore its mean-value is equal to  $E\{\epsilon X_i - \epsilon X_j\} = \bar{X} - \bar{X} = 0$ .

#### Processing – spdcf parameters (spatial correlation) and scalar accuracy metrics of relative error

A strictly positive definite correlation function (spdcf) from the “CSM 4-parameter” family of spdcf is assumed applicable for the representation of spatial correlation across the product, or more specifically, across each individual realization of the product. This spdcf is very general and is reasonably assumed applicable *a priori*. In addition, as a reasonable and simplifying assumptions, it is further assumed that:

- Only the two major parameters of the four parameters ( $A, \alpha, \beta, D$ ) that define the specific spdcf are “active” or non-zero:  $A$  and the distance constant  $D$ .
  - The baseline assumption that  $\alpha = 0$  inherently assumes that the system that generates the geolocation products is unbiased, i.e.,  $\alpha A$  is the floor or minimum value for decorrelation ( $0 \leq \alpha < A$ , where both parameters are unit-less)
  - A non-zero  $\beta$  tends to decrease the rate of decorrelation at small values of distance, i.e., change the shape of the spdcf somewhat ( $0 \leq \beta < 10$  and is unit-less)
- The corresponding spdcf is assumed isotropic and applicable (common) to both the x and y horizontal components of error, i.e.,  $\rho(dX) = Ae^{-dX/D}$ , where  $dX$  is the distance between two geolocations separated by  $\Delta X$ , i.e.,  $dX = |\Delta X|$ . Note that the correlation function could have also been written in an equivalent and more general form  $\rho(\Delta X) = Ae^{-|\Delta X|/D}$ .

The spdcf parameters are computed based on the sample statistics contained in the populated Accuracy Assessment file/report, and in particular, are based on two equations for two unknowns ( $A$  and  $D$ ):

$$\rho_{small} = Ae^{-d_{avg\_small}/D} \text{ and } \rho_{large} = Ae^{-d_{avg\_large}/D} \quad (\text{B.2.2-5})$$

The corresponding solution is:

$$D = (d_{avg\_small} - d_{avg\_large}) / \ln(\rho_{large} / \rho_{small}),$$

$$A = e^z, \text{ where } z = (d_{avg\_large}/D + \ln(\rho_{large})). \quad (\text{B.2.2-6})$$

$\ln$  represents the natural logarithm and it is assumed that  $0 < \rho_{large} < \rho_{small} \leq 1$  prior to implementing Equation (C.2.2-6).

If the above inequality is not met, perform the following steps in sequential order prior to implementing Equation (C.2.2-6): (B.2.2-7)

- If  $\rho_{small} > 1$ , set  $\rho_{small} = 1$
- If  $\rho_{large} \leq 0$ , set  $\rho_{large} = 0.01$
- If  $\rho_{large} \geq \rho_{small}$ , set  $\rho_{small} = (\rho_{small} + \rho_{large})/2$  and then  $\rho_{large} = \rho_{small} - .01$
- If  $0 < \rho_{large} < \rho_{small} \leq 1$  is still not met, the spdcf is not applicable/available, i.e., set  $A$  and  $D$  to “n/a”.

The above adjustment of the correlation values  $\rho_{small}$  and  $\rho_{large}$  is performed in order to mitigate the possible adverse effects of very few product realizations and/or error samples per realization, or to mitigate the adverse effects of grossly incorrect *a priori* assumptions regarding error modeling, and in

particular, spatial correlation characteristics. When the above adjustment is performed, related details should be noted in the predicted accuracy model (file/report): relative accuracy (Equation B.2.3-2).

The spdcf corresponding to Equation (C.2.2-6) is a function of the horizontal distance  $dX$  between geolocations:  $\rho(dX) = Ae^{-dX/D}$ . Furthermore,  $\rho(dX) \equiv 1$  when  $dX = 0$ .

Representative scalar predicted relative metrics are computed for both distance bins as follows:

$$\begin{aligned} rel\_CE90\_small &= 2.1460\sqrt{trace(C_x) (1 - \rho(dX))}, \text{ where } dX = d\_avg\_small; \\ rel\_CE90\_large &= 2.1460\sqrt{trace(C_x) (1 - \rho(dX))}, \text{ where } dX = d\_avg\_large. \end{aligned} \quad (B.2.2-8)$$

The spatial correlation values  $\rho(dX)$  are evaluated using the spdcf. In addition, the computation/inclusion of  $rel\_CE90\_small$  and  $rel\_CE90\_large$  is optional and for the convenience of the down-stream user as they are derived predictive statistics and can be computed by the down-stream user if so desired.

Note: if only one distance bin is applicable (“bin\_all”) with corresponding representative correlation value  $\rho\_all$  in the populated accuracy assessment model, as an approximation, set  $\rho\_small \equiv 0.99$  and  $\rho\_large \equiv \rho\_all$  and evaluate Equation (C.2.2-6) accordingly for the spdcf parameters  $A$  and  $D$ .

#### **Optional generalization of the spdcf #1 (not recommended):**

The processing that was described above is applicable to an spdcf that is assumed common to each component of horizontal error and that is also assumed isotropic in form, which are reasonable assumptions for a geolocation product. The processing and output of sample statistics in Section B.1 were compatible with these assumptions.

However, this processing can be readily generalized to compute a different isotopic spdcf for the different components of horizontal geolocation error, such as  $\rho_x(dX)$  for errors in the x-component and  $\rho_y(dX)$  for errors in the y-component, if so desired. This is done by providing two sets of sample-statistics for relative error in the populated accuracy assessment model – one set for relative x-error and one set for relative y-error, both categorized by 2d horizontal distance. The corresponding processing in Section B.2 is modified accordingly, i.e., the two spdcf are generated independently.

This generalization is not required for a separate assessment/prediction of 2d horizontal errors and 1d vertical errors. Simply perform the baseline processing/outputs of Sections B.1 and B.2 twice – once for horizontal errors and once for vertical errors. The predictive statistics for horizontal error will necessarily be different than the predictive statistics for vertical errors. In particular, the predictive statistics for horizontal error will include a common spdcf for both the x and y components of error, and the predictive statistics for vertical errors will include a different spdcf.

#### **Optional generalization of the spdcf #2 (not recommended and typically not feasible):**

If an anisotropic spdcf is to be computed instead of an isotropic spdcf, the parameters defining two separate spdcf must be generated:  $A_x$  and  $D_x$  for the spatial correlation of horizontal errors in the x-direction and  $A_y$  and  $D_y$  for the spatial correlation of horizontal errors in the y-direction. The resultant anisotropic spdcf is the product of these two spdcf, i.e.,  $\rho(\Delta X) = A_x e^{-|\Delta x|/D_x} A_y e^{-|\Delta y|/D_y}$ . This spdcf is also assumed common to both components of horizontal error, i.e.,  $\rho(\Delta X) = \rho_x(\Delta X) = \rho_y(\Delta X)$ , but can be generalized to two separate spdcf per the previous paragraph. The computation of an anisotropic spdcf is not recommended for a geolocation product, as it is: (1) typically not applicable as a general error model, and (2) too complicated to generate, requiring too many samples of error that are typically unavailable, and also requires the “fitting” of four major spdcf parameters ( $A_x$ ,  $D_x$ ,  $A_y$ , and  $D_y$ ) instead of the deterministic computation of only two ( $A$  and  $D$ ).

**Comment: Future applied research**

Further applied research regarding the best method(s) to populate both an accuracy assessment model and corresponding predicted accuracy model regarding relative errors is warranted. Subareas of research include effects regarding the number of samples, the use of non-zero mean-values, and the identification of the appropriate spdcf family and the best methods for the computation of its defining parameters.

**Comment: What if only sample-based scalar accuracy metrics are available for computation of predictive statistics?**

The previous methodology/equations of Sections CB2.1 and B.2.2 assumed the availability of the sample statistics that are recommended in a populated accuracy assessment model. In some circumstances, only their scalar accuracy metrics counterparts, such as CE90, may be available (see Section 5.3.5.3). If so, the methodology/equations in Sections C.2.1 and C.2.2 can be “reversed engineered” for “lower fidelity” results if need be. More specifically, and assuming that absolute accuracy is of interest (Section B.2.1) for specificity, the scalar accuracy metrics are converted to a corresponding error covariance based on the assumption that the components of geolocation error are uncorrelated and of equal magnitude. For example, given CE90 and LE90:

$$C_X = \begin{bmatrix} \left(\frac{CE90}{2,1460}\right)^2 & 0 & 0 \\ 0 & \left(\frac{CE90}{2,1460}\right)^2 & 0 \\ 0 & 0 & \left(\frac{LE90}{1.6449}\right)^2 \end{bmatrix},$$

where the multipliers correspond to the 90% probability level of the scalar accuracy metrics and the latter’s values are detailed in Sections 5.4.1 and 5.4.2 of TGD 2a and can be modified accordingly for any other probability levels of interest.

On the other hand, if CE and LE are given as samples of radial horizontal and radial (absolute value of) vertical error directly (as opposed to CE90 and LE90), corresponding  $C_X$  samples can be computed and then averaged if multiple samples are available:

$$C_X = \begin{bmatrix} CE^2 & 0 & 0 \\ 0 & CE^2 & 0 \\ 0 & 0 & LE^2 \end{bmatrix}.$$

The statistical significance of the error covariance matrix corresponding to use of the CE90 and LE90 values is typically greater than that based on an individual horizontal radial error sample and/or vertical error sample, since a collection of individual samples were used to generate the former's values.

The above only addressed contingencies for absolute accuracy. Similar processing for relative accuracy would require the availability of relCE90 for various distance bins.

### B.2.3 Outputs

#### **Contents of the predicted accuracy model (file/report): absolute accuracy**

Based on the above, the following are included in the populated accuracy assessment model (file/report): (B.2.3-1)

- The applicable definitions and the computed values of the predictive statistics and related quantities presented in Equations (B.2.1-1) through (B.2.1-3):
  - The mean-value  $\bar{X}$  (meters), nominally set to zero
  - The covariance matrix about an assumed mean-value of zero  $C_X$  (meters-squared)
  - The scalar accuracy metric  $CE90$  (meters)
- Any applicable comments/observations related to the above analyses.

#### **Contents of the predicted accuracy model (file/report): relative accuracy**

Based on the above, the following are included in the populated Predicted Accuracy Model (file/report): (B.2.3-2)

- The applicable definitions and the computed values of the predictive statistics and related quantities presented in Equations (B.2.2-1) - (B.2.2-6), (B.2.2-8):
  - Relative (average) distances associated with the two distance bins "small" and "large":
    - $d_{avg\_small}$  (meters)
    - $d_{avg\_large}$  (meters)
  - The mean-value  $rel\_X$  (meters), nominally set to zero
  - The relative error covariance matrices associated with the two distance bins:
    - $rel\_C_{X\_small}$  (meters-squared) and  $rel\_C_{X\_large}$  (meters-squared)
  - The correlation coefficients associated with the two distance bins:
    - $\rho_{small}$  (unit-less) and  $\rho_{large}$  (unit-less)
  - The spdcf defining parameters:
    - $A$  (unit-less) and  $D$  (meters)
  - The scalar accuracy metrics associated with the two distance bins:
    - $rel\_CE90\_small$  (meters) and  $rel\_CE90\_large$  (meters)
- Any applicable comments/observations related to the above analyses.

### B.3 Applications

The section of the appendix presents a brief overview of some of the more important applications of the predictive statistics that are contained in a populated Geolocation Product Predicted Accuracy Model.

Given the predictive statistics contained in the predicted accuracy model (file report) of Equations (B.2.3-1) and (B.2.3-2) and computed via Equations (B.2.1-2) and (B.2.2-6), the user of the populated predicted accuracy model can compute, in conjunction with the applicable sensor model, the following items:

The full error covariance (symmetric and positive definite) matrix corresponding to horizontal errors in multiple geolocations from the same but arbitrary data/product realization. This is illustrated in the following example corresponding to 3 geolocations, where  $dX_{ij}$  corresponds to the horizontal distance between arbitrary geolocations  $i$ ,  $1 \leq i \leq 3$ , and  $j$ ,  $1 \leq j \leq 3$ , in the realization:

$$C_{X\_full} = \begin{bmatrix} C_X & \rho(dX_{12})C_X & \rho(dX_{13})C_X \\ . & C_X & \rho(dX_{23})C_X \\ . & . & C_X \end{bmatrix} \text{meters-squared} \quad 6 \times 6, \quad (\text{B.3-1})$$

and where  $\rho(dX_{ij})$  multiplies each term of the  $2 \times 2$  diagonal error covariance matrix  $C_X$ .

(If two geolocations were in different products, their corresponding off-diagonal block or cross-covariance matrix in Equation (B.3-1) would be defined as identically equal to zero.)

In addition, the actual best estimate of the 3 geolocations are those geolocations that are actually identified/measured in the product; hence, corresponding errors typically include mensuration errors associated with these geolocations. Thus, if the three  $2 \times 1$  geolocation (horizontal) vectors are placed into a  $6 \times 1$  column vector as the best estimate  $\hat{X}$ , the corresponding  $6 \times 6$  error covariance matrix equals:

$$C_{X\_full} \rightarrow C_{X\_full} + C_{mens\_full} \quad 6 \times 6 \quad (\text{B.3-2})$$

$C_{mens\_full}$  is a  $6 \times 6$  block diagonal matrix with each  $2 \times 2$  block the corresponding error covariance matrix  $C_{mens}$  for the mensuration error associated with measuring/identifying the corresponding geolocation.

In general,  $C_{mens}$  is a diagonal matrix and typically common to each of the three geolocations and typically containing the same variance of error for both the geolocation's x-coordinate and the y-coordinate:

$$C_{mens} = \begin{bmatrix} \sigma_{mens}^2 & 0 \\ 0 & \sigma_{mens}^2 \end{bmatrix} \text{meters-squared} \quad 2 \times 2 \quad (\text{B.3-3})$$

However, the above can vary per geolocation as well as per geolocation coordinate, if applicable.

The computation of CE90 for a geolocation of interest is computed as follows: (B.3-4)

- (1)  $CE90 = 2.1460\sqrt{\text{trace}(C_X)/2}$ .
- (2) If mensuration error is to be included, as above except that  $C_X \rightarrow C_X + C_{\text{mens}}$ .

The computation of rel\_CE90 for two geolocations of interest separated by  $dX$  is computed as follows: (B.3-5)

- (1)  $rel\_CE90 = 2.1460\sqrt{\text{trace}(C_X) (1 - \rho(dX))}$ .
- (2) If mensuration error is to be included:  $rel\_CE90 \rightarrow r_{ss}\{rel\_CE90, 2.1460\sqrt{\text{trace}(C_{\text{mens}})}\}$ , where  $r_{ss}$  is root-sum-square.

See TGD 2a (Predictive Statistics) for more exact methods than Equations (B.3-4) and (B.3-5) for different levels of probability.

## B.4 Performance assessment of the populated models

Experiments (studies) were performed based on simulated data in order to further illustrate and assess the performance of the concepts and equations presented in Sections B.1 through B.3. In particular, accuracy assessments were performed followed by the population of corresponding predicted accuracy models. In addition, the resultant predicted accuracy as represented in the populated predicted accuracy model was compared to the “true” predicted accuracy model. The simulated error samples were generated consistent with the predictive statistics contained in the “true” predicted accuracy model per the techniques detailed in TGD 2e (Monte-Carlo Simulation).

### B.4.1 Descriptions of the performance assessment experiments

#### The true predicted accuracy model:

Prior to describing the various experiments and corresponding results, we first “set the stage” by describing the baseline values for the true predictive statistics applicable to the products in the experiments with a common product width equal to 10 grid-units:

- (1) The true covariance matrix for horizontal errors:  $C_{\text{true}} = \begin{bmatrix} 10^2 & 0 \\ 0 & 15^2 \end{bmatrix}$  meters-squared

- (2) The true spdcf parameters:  $A_{\text{true}} = 0.98$  (unit-less) and  $D_{\text{true}} = 30$  grid-units, or

$spdcf_{\text{true}} = 0.98e^{-d/30}$ , where  $d$  is horizontal distance in grid-units. This spdcf is isotropic and common to both product x-component errors and y-component errors.

$C_{true}$  specifies the expected magnitude of errors in an arbitrary product (realization) and  $spdcf_{true}$  specifies the spatial correlation or degree of similarity of errors in the same product realization as a function of distance between the errors' corresponding horizontal locations.

The true spdcf is illustrated in Figure B.4.1-1 as a function of horizontal distance across an arbitrary line in the horizontal plane for convenience – see Figure 5.3.2-1-1 for the rendering of a similar isotropic spdcf as a function of distance across the entire horizontal plane. The spdcf parameter  $A_{true}$  essentially specifies the correlation at very small distances and the spdcf parameter  $D_{true}$  specifies its exponential decay as a function of increasing horizontal distance.

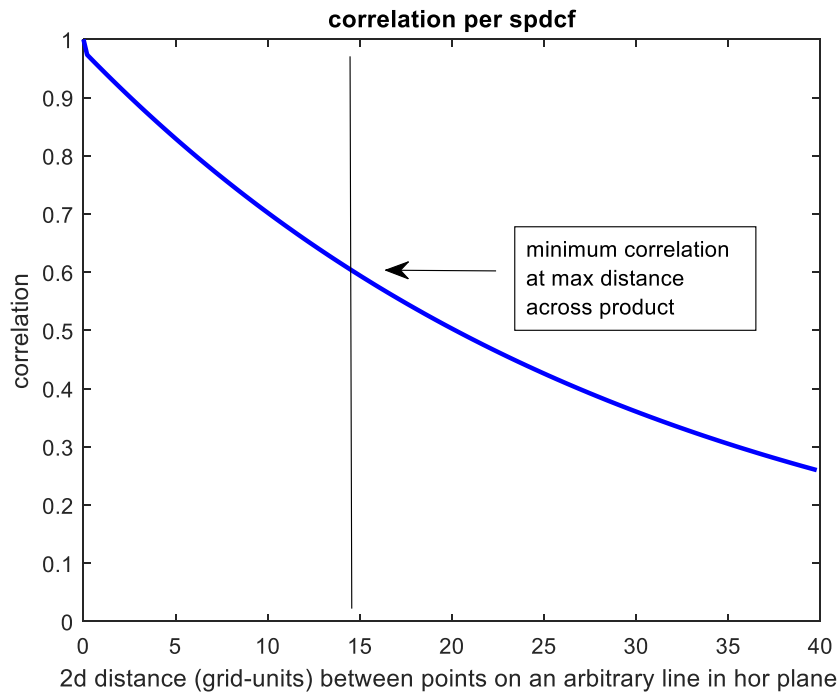


**Figure B.4.1-1:** strictly positive definite correlation function (spdcf)

Figures B.4.1-2 and B.4.1-3 present the horizontal errors (2d vectors or quivers) across a grid in the product's horizontal plane for two different product realizations. In both of the figures, the errors were generated consistent with the above true predictive statistics ( $C_{true}$  and  $spdcf_{true}$ ). The value of "sf" in the title of each figure is the magnitude in meters of the maximum horizontal error in the grid.

As seen in the figures, errors are spatially correlated (similar) within the same product but independent (uncorrelated) between products. This is per desired modeling and can be observed in numerous examples of actual 3d Point Clouds with corresponding errors generated from available "ground truth".

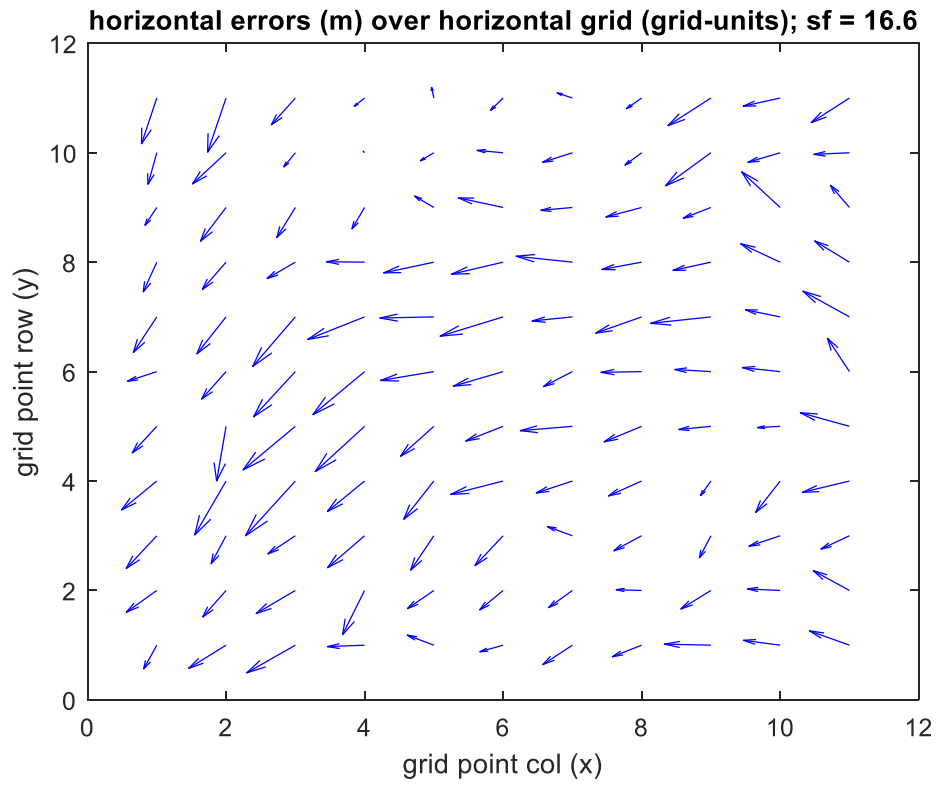


**Figure B.4.1-2:** Product realization #1: horizontal errors across a horizontal grid

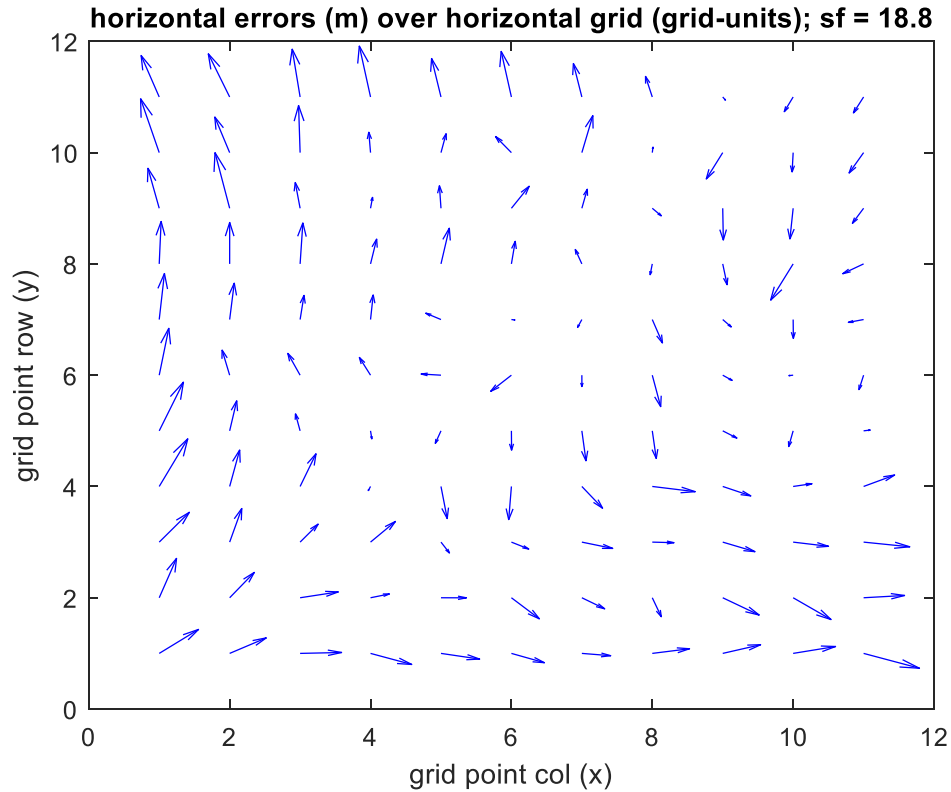


**Figure B.4.1-3:** Product realization #2: horizontal errors across a horizontal grid

**Definition of an experiment:**

Each experiment corresponds to a specified scenario implemented over 1000 independent Monte-Carlo trials with resultant performance metrics computed as an “ensemble” average over the trials.

**Definition of a scenario:**

A scenario is specified by the number of products (product realizations) and the number of error samples per product. A Monte-Carlo trial consists of the generation of corresponding error samples for each of the products, a subsequent populated accuracy assessment model generated from the samples from all of these products, and finally, a subsequent populated predicted accuracy model based on the accuracy assessment. As mention earlier, all error samples are generated consistent with the true predicted accuracy model. Also, all products are assumed to have a common AOI or ground footprint with a width of 10 grid- units.

A scenario consists of either 3, 10, or 100 products. The number of geolocation error samples per product is common over all products and is equal to either 4, 7, or 10 samples. The underlying geolocations associated with each error sample in each product are generated randomly.

**Geolocations corresponding to error samples in a product:**

(1) Geolocations are grouped into local groups that contain either two or three geolocations. There are multiple local groups in each product, their number dependent on the total number of error samples per product (4, 7, or 10) for the specified scenario.

(2) The geolocations in a local group are randomly generated and separated uniformly from each other from between 0 to 0.15 grid units. The first local group is centered in the products' footprint and the other local groups are separated randomly and uniformly from the first local group. Distances between the local groups are between 0 to 1/2 the product's width.

(3) If 4 geolocation error samples are specified per product, there are two local groups in each product, each containing two error samples. If 7 error samples are specified per product, there are three local groups, two containing two error samples each and one containing three error samples. If 10 error samples are specified per product, there are four local groups, two containing two error samples each and two containing three error samples each.

Distances between geolocation pairs in a local group correspond to the "small" distance bin with a nominal width of 0.25 grid units. Distances between geolocation pairs consisting of geolocations in different local groups correspond to the "large" distance bin with a nominal width between 0.25 and approximately 15 grid-units, the latter the maximum distance possible for two geolocations in a product.

If a specified scenario contains a total of  $m$  error samples per product, there are " $m$ -choose-2" different relative error samples per product. For example, if there are 7 error samples, there are 21 relative error samples. Thus, if the specified scenario also contains 10 products, there are a total of 70 error samples and a total of 210 relative error samples computed and used to populate the accuracy assessment models and subsequent predicted accuracy model for one Monte-Carlo trial.

The relative error samples corresponding to each sample-pair are computed by differencing the corresponding error samples, i.e., relative error samples are not really measured, neither in the simulation nor operationally in the real-world – only individual error samples require measurement based on differencing the underlying geolocation from corresponding "ground truth". Note also that if the product width is equivalent to 10,000 meters, 0.1 grid units is equivalent to 100 meters which is assumed to be the typical length of interest for features in the product, and the corresponding relative error sample corresponding to the measurement of the feature's length is within the "small" distance bin or "bin1".

#### **The Monte-Carlo ensemble performance metric:**

Predicted CE90 and rel\_CE90 at various distance bins are derived statistics computed using the populated predicted accuracy model. They were selected as convenient measures of performance. In particular, the "ensemble error" is computed over the 1000 Monte-Carlo trials as follows for the CE90 predictive statistic as a representative example:

Average of  $\frac{|CE90_{pred_i} - CE90_{true}|}{CE90_{true}}$ , computed over  $i = 1, \dots, 1000$  Monte-Carlo trials, expressed as a % (0 to 100).

See equations B.3-1 and B.3-2 for the computation of CE90\_pred and rel\_CE90\_pred, respectively.

CE90\_true and rel\_CE90\_true for various distance bins are common to each trial and these “true” derived predictive statistics are computed using the true predicted accuracy model that was specified earlier.

In addition, all true CE90 and rel\_CE90 values are computed with virtually no approximation error per the techniques of TGD 2a (Predictive Statistics) regardless if non-zero mean-values are included or not in the additional experiments that are described later. However, a Gaussian distribution of errors is assumed as is reasonable for these experiments.

Finally, the experiments presented in Section B.4.2 do not include any simulated ground truth errors or mensuration errors associated with the error samples. Section B.4.3 quantifies their effects when they are not negligible compared to geolocation product errors per se.

## B.4.2 Performance results

Table B.4.2-1 presents the performance results for the first set of experiments. There were three experiments, each of them corresponding to a scenario with 7 geolocation errors per product. The number of products in the corresponding scenario varied per experiment. 10 products correspond to the “baseline” scenario (column highlighted light gold in table).

**Table B.4.2-1:** Performance results for set 1 of the experiments

<b>Predicted Accuracy Performance Results for 3 different experiments (set 1)</b> <b>1000 trials per experiment</b> <b>Each experiment corresponds to a different scenario</b> <b>(light gold corresponds to experiment with baseline scenario)</b> <b>Error in scalar accuracy metrics "averaged" over all trials</b> <b>error in metric: populated model's metric relative to true metric (%)</b>			
<b>Number of samples per product:</b>	<b>7</b>		
<b>Number of products:</b>	<b>3</b>	<b>10</b>	<b>100</b>
<b>error in CE90 (%):</b>	21.5	11.9	3.8
<b>error in rel_CE90(%):</b>			
d=0.15 distance units	11.7	7.5	3.0
d=1	13.7	7.6	2.9
d=5	18.4	10.2	3.4
d=10	18.5	10.2	3.4
d=15	18.4	9.9	3.3

Based on the above and for an arbitrary trial in “the future” that corresponds to the baseline scenario, we expect that the derived statistics CE90 and rel\_CE90 computed from the populated predicted accuracy model will differ from their true (unknown) counterparts by approximately 11.9 % and 7.5 to 10.2 %, respectively. For example, if true\_CE90 were equal to 27 meters, we expect that the CE90 computed

based on the populated predicted accuracy model would equal approximately 27 +/- 3 meters. For the baseline scenario, the populated predicted accuracy model is generated based on 10 realizations of the product, each with 7 samples of geolocation error.

Note: the scenario with 100 products was included in the above table in order to quantify asymptotic performance, as the availability of this large of number of products for accuracy assessment is not realistic for External Data.

Note: for the experiment applicable to the scenario with 3 products in the above table, one of the 1000 trials required modification of the sample correlation values  $\rho_{small}$  and/or  $\rho_{large}$  per Equation (B.2.2-7): the original  $\rho_{large}$  was slightly less than 0 and adjusted to a value of 0.01 prior to proceeding. No other trials for the other scenarios in the table required adjustment. In addition, no other trials for other scenarios in additional tables presented later in this appendix required adjustment unless specifically stated otherwise.

Note: for each experiment, the sample “ensemble” mean was also computed over all trials and was equal to approximately zero as expected. For example, the sample ensemble mean for the experiment with the baseline scenario (light gold column) in the above table was equal to -.06, and -0.13 for the x and y components of error, respectively. However, as mentioned earlier and for an individual trial, the sample mean-value is typically and significantly non-zero for a given product (realization) due to the spatial correlation of errors within the product. The sample-mean value taken over all product realizations in the trial is closer to zero due to the subsequent averaging of independent errors (mean-values). And when further averaged over all trials, the ensemble mean-value of error approaches zero.

Prior to presenting the performance results for another set of experiments, Table B.4.2-2 first presents details of one of the 1000 trials that made-up the experiment corresponding to the baseline scenario in Table B.4.2-1. It refers to various statistics referenced in Sections B.1 through B.3. The predictive statistics corresponding to the error covariance matrix, CE90, and rel\_CE90 are presented for both the populated predicted accuracy model and the corresponding “true” predictive accuracy model, and highlighted light gold. Applicable units are meters for errors and “distance units” or “grid-units” for all relevant distances. The latter units are arbitrary as long as consistent across all distances, including the spdcf distance constants (D). Listed data in the table correspond to the “outputs” of the populated Accuracy Assessment and the predicted accuracy models.

**Table B.4.2-2:** Details corresponding to one trial of the experiment corresponding to the baseline scenario

	TRUE	Accuracy Assessment (sample statistics)	Predicted Accuracy (predictive statistics)	Corresponding Equations
<b>SIMULATION PARAMETERS</b>				
Product width (distance units)	10			
Number of products (realizations)		10		
Number of error samples per product		7		
total number of error samples		70		
total number of relative error samples		210		
<b>ABSOLUTE ACCURACY</b>				
Mean Value (2x1):				
mean-value x (m)	0	0.7 (info only)	0	//B.1.1-3/B.2.1-1/
mean-value y (m)	0	2.1 (info only)	0	
Error Covariance (2x2), diagonal:				
corresponding sigma x (m)	10	7.8	7.8	//B.1.1-4/B.2.1-2/
corresponding sigma y (m)	15	17.3	17.3	
CE90 (m)	27.6	24.5	28.9	//B.1.1-6/B.2.1-3/
<b>RELATIVE ACCURACY</b>				
specified distance range of interest				
bin 1 aka "small" (distance units)		0<dist<=0.25		
bin 2 aka "large" (distance units)		0.25<dist<=15		
total number of rel error samples per bin				
bin 1		50		
bin 2		160		
average distance per bin				
bin 1 (distance units)		0.11		
bin 2 (distance units)		5.3		
correlatin at average distance per bin				
bin1		0.98		
bin2		0.78		
spdcf parameter A (unitless)	0.98	n/a	0.982	//B.2.2-6/
spdcf parameter D (distance units)	30	n/a	22.9	
rel_CE90_bin 1 (m)		5.6	6.1	//B.1.2-8/B.2.2-8/
rel_CE90_bin 2 (m)		20.4	19.2	
Derived : rel_CE90 (m) for distance d				
d=0.15 (distance units)	6.1	n/a	6.4	//B.3-1/
d=1 (distance units)	8.9	n/a	10.0	
d=15 (distance units)	24.8	n/a	28.6	

Table B.4.2-3 presents the performance results for a second set of experiments. There were three experiments, each of them corresponding to a scenario with 10 products. The number of error samples per product varied per experiment. 7 error samples per product corresponds to the “baseline” scenario (column highlighted light gold in table).

**Table: B.4.2-3:** Performance results for set 2 of the experiments

<b>Predicted Accuracy Performance Results for 3 different experiments (set 2)</b> <b>1000 trials per experiment</b> <b>Each experiment corresponds to a different scenario</b> <b>(light gold corresponds to experiment with baseline scenario)</b> <b>Error in scalar accuracy metrics "averaged" over all trials</b> <b>error in metric: populated model's metric relative to true metric (%)</b>			
<b>Number of products:</b>	<b>10</b>		
<b>Number of samples per product:</b>	<b>4</b>	<b>7</b>	<b>10</b>
<b>error in CE90 (%):</b>	12.6	11.9	11.8
<b>error in rel_CE90 (%):</b>			
d=0.15 distance units	9.3	7.5	6.5
d=1	10.2	7.6	6.8
d=5	13.6	10.2	8.5
d=10	13.5	10.2	8.5
d=15	13	9.9	8.3

As can be seen by comparison of Table B.4.2-3 to Table B.4.2-1, given a reasonable number of error samples per product, the big driver regarding performance is the number of products. Of course, if only 1 or 2 error samples per product are available, performance of predicted relative accuracy will degrade appreciably and possibly not be computable, i.e., the number of samples per product would be the big driver.

### B.4.3 Additional sensitivity and robustness experiments

Table B.4.3-1 presents the performance results for additional experiments in order to assess the sensitivity or robustness of the methods presented in Section B.1 and B.2 to more extreme situations and/or the presence of non-trivial mismodeling. The scenarios are described in the table as changes relative to the baseline scenario described earlier (7 error samples in each of 10 products) and possibly changes relative to the true predictive statistics described earlier. Each of these additional experiments also consisted of 1000 Monte-Carlo trials.

The more challenging experiments correspond to experiments #7 and #9 in the table, the latter the most challenging as it corresponds to significant mismodeling. In the real-world, mismodeling is always present to some degree in that true predictive statistics never correspond to each product exactly.

**Table B.4.3-1:** Performance results for robustness/sensitivity experiments

<b>Predicted Accuracy Performance Results for different robustness experiments</b> <b>1000 trials per experiment</b> <b>Error in scalar accuracy metrics "averaged" over all trials</b> <b>error in metric: populated model's metric relative to true metric (%)</b>		
<b>Experiment #</b>	<b>Description: changes relative to baseline scenario</b>	<b>Results</b>
<b>1</b>	<b>included sample mensuration error:</b> 1.0 m (one sigma)  independent errors per error sample; can include the effects of uncorrelated and non-negligible "ground truth" errors; baseline scenario assumes negligible mensuration error, or if non-negligible, considered part of product (use) error	<b>error in CE90 (%):</b> 11.9  <b>error in rel_CE90 (%):</b> d=0.15 distance units 12.3 d=1 7.8 d=5 9.7 d=10 9.9 d=15 9.7
<b>2</b>	<b>added non-zero true mean-value of error:</b> x_component=-5 m and y_component=5 m  resultant sample mean-value over all product realizations over all trials: x_component=-4.9 m and y_component=5.2 m	<b>error in CE90 (%):</b> 12.1  <b>error in rel_CE90r (%):</b> d=0.15 distance units 7.4 d=1 7.7 d=5 9.9 d=10 9.8 d=15 9.4
<b>3</b>	<b>different A_true:</b> A_true=1.0  recall that baseline A_true=0.98	<b>error in CE90 (%):</b> 11.9  <b>error in rel_CE90 (%):</b> d=0.15 distance units 9.5 d=1 10.7 d=5 10.5 d=10 10.0 d=15 9.6
<b>4</b>	<b>different A_true:</b> A_true=0.95  recall that baseline A_true=0.98	<b>error in CE90 (%):</b> 11.8  <b>error in rel_CE90 (%):</b> d=0.15 distance units 6.6 d=1 6.2 d=5 9.4 d=10 10.0 d=15 9.9
<b>5</b>	<b>different D_true:</b> D_true=120  recall that baseline D_true=30	<b>error in CE90 (%):</b> 12.9  <b>error in rel_CE90 (%):</b> d=0.15 distance units 6.8 d=1 5.8 d=5 8.4 d=10 9.9 d=15 10.5

Table B.4.3-1: (continued)

Experiment #	Description: changes relative to baseline scenario	Results
6	<p><b>different D_true:</b> D_true=7</p> <p>recall that baseline D_true=30</p>	<p><b>error in CE90 (%):</b> 9.6</p> <p><b>error in rel_CE90 (%):</b></p> <p>d=0.15 distance units 8.0</p> <p>d=1 11.6</p> <p>d=5 10.7</p> <p>d=10 9.3</p> <p>d=15 8.9</p>
7	<p><b>different true spdcf (CSM 4-parameter)</b> alpha_true=0.0, A_true=0.98, beta_true=10, D_true=7</p> <p>baseline spdcf's alpha_true=0 and beta_true=0</p>	<p><b>error in CE90 (%):</b> 12.9</p> <p><b>error in rel_CE90 (%):</b></p> <p>d=0.15 distance units 10.6</p> <p>d=1 18.1</p> <p>d=5 11.8</p> <p>d=10 15.0</p> <p>d=15 23.0</p>
8	<p><b>different true spdcf (CSM 4-parameter)</b> alpha_true=0.3, A_true=0.98, beta_true=10, D_true=120</p> <p>resultant cor for bin1&lt;=cor for bin2 for 48% of ensemble runs; subsequently and successfully adjusted a small amount per Equation (B.2.2-7)</p>	<p><b>error in CE90 (%):</b> 10.0</p> <p><b>error in rel_CE90 (%):</b></p> <p>d=0.15 distance units 6.4</p> <p>d=1 6.0</p> <p>d=5 5.7</p> <p>d=10 8.8</p> <p>d=15 8.6</p>
9	<p><b>baseline truth statistics change every third product (realization) to:</b> sigma_x=15 m, sigma_y=20 m, A_true=0.98, D_true=20</p> <p>contrary to baseline assumption that the same true predictive statistics are applicable to each product; truth is weighted average</p>	<p><b>error in CE90 (%):</b> 19.0</p> <p><b>error in rel_CE90 (%):</b></p> <p>d=0.15 distance units 21.9</p> <p>d=1 27.0</p> <p>d=5 28.4</p> <p>d=10 27.2</p> <p>d=15 26.0</p>
10	<p><b>true covariane has non-zero x-y correlation</b> x-y correlation = 0.5 resulting in non-diagonal covariance matrix</p>	<p><b>error in CE90 (%):</b> 13.0</p> <p><b>error in rel_CE90 (%):</b></p> <p>d=0.15 distance units 7.9</p> <p>d=1 8.5</p> <p>d=5 11.3</p> <p>d=10 11.3</p> <p>d=15 11.0</p>
11	<p><b>10th product has only 2 error samples</b> 2 samples instead of the baseline 7 for the other 9 product (realizations)</p>	<p><b>error in CE90 (%):</b> 12.6</p> <p><b>error in rel_CE90 (%):</b></p> <p>d=0.15 distance units 7.6</p> <p>d=1 8.0</p> <p>d=5 10.6</p> <p>d=10 10.7</p> <p>d=15 10.5</p>

The results presented in the above table indicated that the methods presented in Sections B.1 and B.2 for the population of an Accuracy Assessment and predicted accuracy model are reasonably robust. A summary of the majority of the experiments is presented below.

Robustness experiment #1: Added mensuration error

The baseline scenario assumes no “additional” mensuration errors or ground truth errors associated with the error samples. However, this robustness experiment does so as follows:

Simulated mensuration errors of 1 meter (one-sigma) are added to the error samples that are used to populate the Accuracy Assessment and subsequently the predicted accuracy model. They are modeled as uncorrelated between error samples, or more specifically, as uncorrelated errors in the identification/measurement of geolocations conjugate to known ground truth locations. The added errors can also be considered to include uncorrelated ground truth errors as well.

Results of the experiment are as expected relative to the baseline scenario – primarily a moderate increase in the error in the computation of  $rel\_CE90$  relative to its true value at a distance  $d=0.15$  due to the addition of the mensuration errors to the errors in the product per se. This increase is apparent at very small distances since mensuration error is uncorrelated between error samples or measurements.

If “additional” mensuration errors were instead to be considered as inherent or applicable to the use of the product in general and not added explicitly, their effect could be approximated as a corresponding slight increase in the error covariance matrix  $C_X$  and a slight decrease in the spdcf parameter  $A$  for the predicted accuracy model that are computed per Section B.2. Correspondingly, if such changes were made to the true predicted accuracy model and the experiment performed again, there would be little difference in the results between it and the (revised) baseline scenario.

Robustness experiment #2: True mean-value of geolocation product error not equal to zero

Results are as expected – essentially no change relative to the baseline scenario. This is due to: (1) computation of the error covariance matrix in the predicted accuracy model based on a sample error covariance matrix computed as a mean-square error in the accuracy assessment, and (2) the cancellation of a common non-zero mean value of error in relative error. Of course, overall performance could be improved (smaller predicted accuracy) if the corresponding bias associated with the non-zero mean-value was detected and removed from the system that generates the products.

Robustness experiments #3-6: Extreme values for the true spdcf parameters  $A_{true}$  and  $D_{true}$

Results are as expected – essentially no change relative to the baseline scenario. This comes as no surprise since the fundamental assumptions of the predicted accuracy model remain applicable. Results also indicate reasonable robustness or non-sensitivity to more extreme values for the true spdcf parameters

that affect the error samples and their spatial correlations that are used to populate the accuracy assessment model and subsequent predicted accuracy model.

Robustness experiments #7-8: Use of all parameters in the “CSM four parameter spdcf” for the true spdcf

Results indicate an increase in the error in the computation of rel\_CE90 at the larger distances when the true value of D is small in conjunction with the true value of beta large (max value allowed) for experiment #7. However, the degradation in performance is not extreme. Results for experiment #8 actually improve overall performance due to actual errors (samples) that are more spatially correlated – it is easier to solve for their predictive statistics. In particular, due to the non-zero value of the true alpha, there is actually a corresponding common error (“bias”) in all of the products for a given trial, although it does not make up all of the error. Recall that for both experiments, the spdcf that is solved for as part of the predicted accuracy model is limited to solving for the spdcf parameters A and D only, i.e., alpha and beta are assumed to equal zero in the populated predicted accuracy model.

Robustness experiment #9: Extreme mismodeling

The errors in the computation of CE90 and rel\_CE90 in experiment #9 relative to their true counterparts are approximately twice as large for CE90 and three times as large for rel\_CE90 as compared to the experiment with the baseline scenario presented in Section B.4.2. For example, the error in the computation of CE90 for the baseline scenario is 11.9% in Tables B.4.2-1 and B.4.2-3 and is 19.0% for the robustness experiment #9 in Table B.4.3-1 above. This is as expected due to the relatively extreme mismodeling corresponding to this particular robustness experiment – the true predicted error model changes dramatically every third product. There is essentially no way around this “degradation” of performance. However, the “good news” is that the predicted accuracy model “averages” the results as is reasonable and as long there are a reasonable number of products that are available.

Of course there are other possible forms of non-trivial mismodeling. For example, if the true predicted accuracy model corresponds to errors represented by an affine transformation with significant scale and/or rotational parameters (see Section D.3 for further details applicable to image errors instead of geolocation product errors). This true predicted accuracy model does not correspond to a homogenous random field for the representation of errors since corresponding predicted accuracies vary per corresponding location(s) in the product, contrary to the assumptions inherent to the Geolocation Predicted Accuracy Model. However, the latter’s performance should still do reasonably well for External (Commodities) Data. For example, one possible significant effect of the affine model is the reduction of relative errors corresponding to large distances in the product due to the possible cancellation of errors of large magnitudes in opposite directions – that is, spatial correlation becomes significantly negative. However, this is mitigated by ensuring that the representative sample correlation value corresponding to the large distance bin for relative error is non-negative and close to zero (hence, the distance constant D very large) via Equation B.2.2-7 used in the population of the Geolocation Product Predicted Accuracy Model.

#### **B.4.4 Summary**

In summary, Tables B.4.1-1, B.4.1-3, and B.4.3-1 illustrate that the methods for the population of Accuracy Assessment and predicted accuracy models presented in Sections B.1 and B.2 work well given relatively few products (product realizations) and relatively few samples of error per product that is typical for External (Commodities) Data. Of course, the more products and the more error samples available per product, the better the results as parameterized in Tables B.4.1-1 and B.4.1-3. Results are also reasonably robust to more extreme scenarios including mismodeling as detailed in Table B.4.3-1.

## B.5 Extension of results

The following presents various extensions to the methods/equations presented in the previous sections of Appendix B.

### B.5.1 All components of 3d geolocation error

Sections B.1 and B.2 addressed accuracy assessment and predicted accuracy for horizontal geolocation errors only. A reasonable and practical approach to address 3d errors assumes that horizontal and vertical errors are uncorrelated and is outlined as follows:

- (1) Perform the processing of Section B.1 and B.2 for horizontal errors – term the resultant predicted error covariance matrix and spdcf (common to both x and y errors) as  $C_{X\_hor}$  and  $\rho_{hor}(dX)$ , respectively.
- (2) Perform the processing of Section B.1 and B.2 again but modified such that errors are vertical errors, i.e., all error samples, sample statistics, and predictive statistics correspond to 1d errors; for example, all error covariance matrices are 1x1 and the spdcf is applicable to z errors (vertical or elevation errors) only. Thus, corresponding processing is even simpler than for horizontal errors. Term the resultant predicted error covariance matrix and spdcf as  $C_{X\_vert}$  and  $\rho_{vert}(dX)$ , respectively.
- (3) Various derived statistics, such as CE90 and rel\_CE90 can be computed using the outputs of (1). Various derived statistics, such as LE90 and rel\_LE90 can be computed using the outputs of (2). In addition, the  $3 \times 3$  predicted error covariance matrix and the  $3 \times 1$  predicted spdcf  $\rho_{3d}(dX)$  that are applicable to all components of 3d error are computed and output as follows:

$$C_{X\_3d} = \begin{bmatrix} C_{X\_hor} & 0_{2 \times 1} \\ 0_{1 \times 2} & C_{X\_vert} \end{bmatrix}, \text{ and} \quad (\text{B.5.1-1})$$

$$\rho_{3d}(dX) = [\rho_{hor}(dX) \quad \rho_{hor}(dX) \quad \rho_{vert}(dX)]^T.$$

From these outputs, the down-stream user or application can compute the full 3d error covariance for an arbitrary set of points in the product as follows, assuming two points for convenience that are separated by a horizontal distance  $dX_{12}$ :

$$C_{X\_full\_3d} = \begin{bmatrix} C_{X\_3d} & S(C_{X\_3d}) \\ . & C_{X\_3d} \end{bmatrix}, \text{ a } 6 \times 6 \text{ error covariance matrix, where the} \quad (\text{B.5.1-2})$$

$$3 \times 3 \text{ matrix } S = \begin{bmatrix} \rho_{hor}(dX_{12}) & 0 & 0 \\ 0 & \rho_{hor}(dX_{12}) & 0 \\ 0 & 0 & \rho_{vert}(dX_{12}) \end{bmatrix}.$$

The assumption that horizontal and vertical errors are uncorrelated used in the above approach is both reasonable and straight-forward, but not required. Explicit 3d error samples and “full” 3d sample and predictive statistics (e.g., a full  $C_{X\_3d}$  in Equation B.5.1-1) are possible with the extension of Sections B.1 and B.2 processing and outputs from 2d to explicit 3d. However, processing will become more complicated.

### B.5.2 Support of MGRF representation of predicted accuracy

The predicted accuracy model detailed in Section B.2 assumes that an MGRF representation of predicted accuracy is not applicable, i.e., that there are either no partitions in the product or that there is only one (“nominal”) partition that is applicable to all geolocations in the product. This is also true for the accuracy assessment model detailed in Section B.1. Together, such accuracy assessment and predicted accuracy models are “standard” or baseline models for a geolocation product.

The MGRF extends predicted accuracy such that it can vary over the product, i.e., a different set of predictive statistics or their combination is applicable to different collections of geolocations in the product. The MGRF is documented in Appendix E, but its explicit population is not covered in detail. Such population relies on the techniques presented in Sections B.1 and B.2 for the population of an accuracy assessment and subsequent predicted accuracy model, but extended to or categorized by relevant partitions in the product. The partitions also need to be identified (textually described) and include a corresponding and approximate *a priori* probability of their occurrence, i.e., the probability that an arbitrary geolocation in the product corresponds to that partition. In particular, the accuracy assessment model groups sample statistics by corresponding and identified partition or collection of geolocations, and the predicted accuracy model groups corresponding predictive statistics in a similar manner.

This, in turn, requires initial sample-based statistical analysis to identify said partitions. One possible approach is based on the MATLAB function “fitgmdist”, available in the Statistics and Machine Learning toolbox. It can be used to identify partitions corresponding to a fit of the entire set of error samples to a Gaussian Mixed probability distribution. A more straightforward approach is to view the error samples across a rendering of the geolocation product(s), and group errors with similar characteristics.

The “nominal” partition corresponds to the nominal group of error samples that are typical and is designated as partition #1. Geolocations in a product correspond to this partition by default. If a group of error samples exhibits large errors as compared to the nominal group, underlying and similar geolocations correspond to a unique partition #m>1. For example, if a certain type or class of products of interest contains EO-derived 3d Point Clouds, such a partition corresponds to geolocations that were difficult to generate due to various anomalies as described in Appendices E and G. The partition is also described textually, such as “all geolocations corresponding to ‘melted roof-top edges’”. Correspondingly,

the down-stream user/application can readily identify any such geolocation of interest by visualization of the product and possibly by automated or automatic means. Correspondingly, the predictive statistics corresponding to partition #m are applicable to this geolocation and to any other geolocations associated with the partition.

### **B.5.3 Recommended applied research**

Additional methods to populate the accuracy assessment and predicted accuracy models are of interest, including the fitting of the spdcf based on more relative accuracy bins when enough error samples are available. This also includes generalization of the spdcf to the use of all parameters in the “CSM four parameter” spdcf family for possible higher fidelity regarding the representation of spatial correlation. In addition, possible methods for population of an anisotropic spdcf are of interest.

The detection/editing of outliers in the error samples based on techniques similar to those detailed in TGD 2d (Estimators and their Quality Control) are of interest and are to be included as part of Section B.1 processing.

Applied research regarding support for the population of an MGRF per the above discussion in Section B.5.2 is of interest.

## **Appendix C: Geolocation Data Accuracy Models – the basics**

This appendix describes the basics of the Geolocation Data Accuracy Assessment Model and the Geolocation Data Predicted Accuracy Model: Measurement-Space:

- their corresponding contents
- methods for their population based on the computation of sample-statistics and predictive statistics
- applications

The models that are detailed in this appendix are illustrated in Figure C.1 in red. The populated Geolocation Data Accuracy Assessment Model is used to populate the corresponding Geolocation Data Predicted Accuracy Model: Measurement-space. Both models correspond to a specific type or class of geolocation data assumed to be an image and its metadata (e.g., Small-Sat image) as is typical and also for convenience of description.

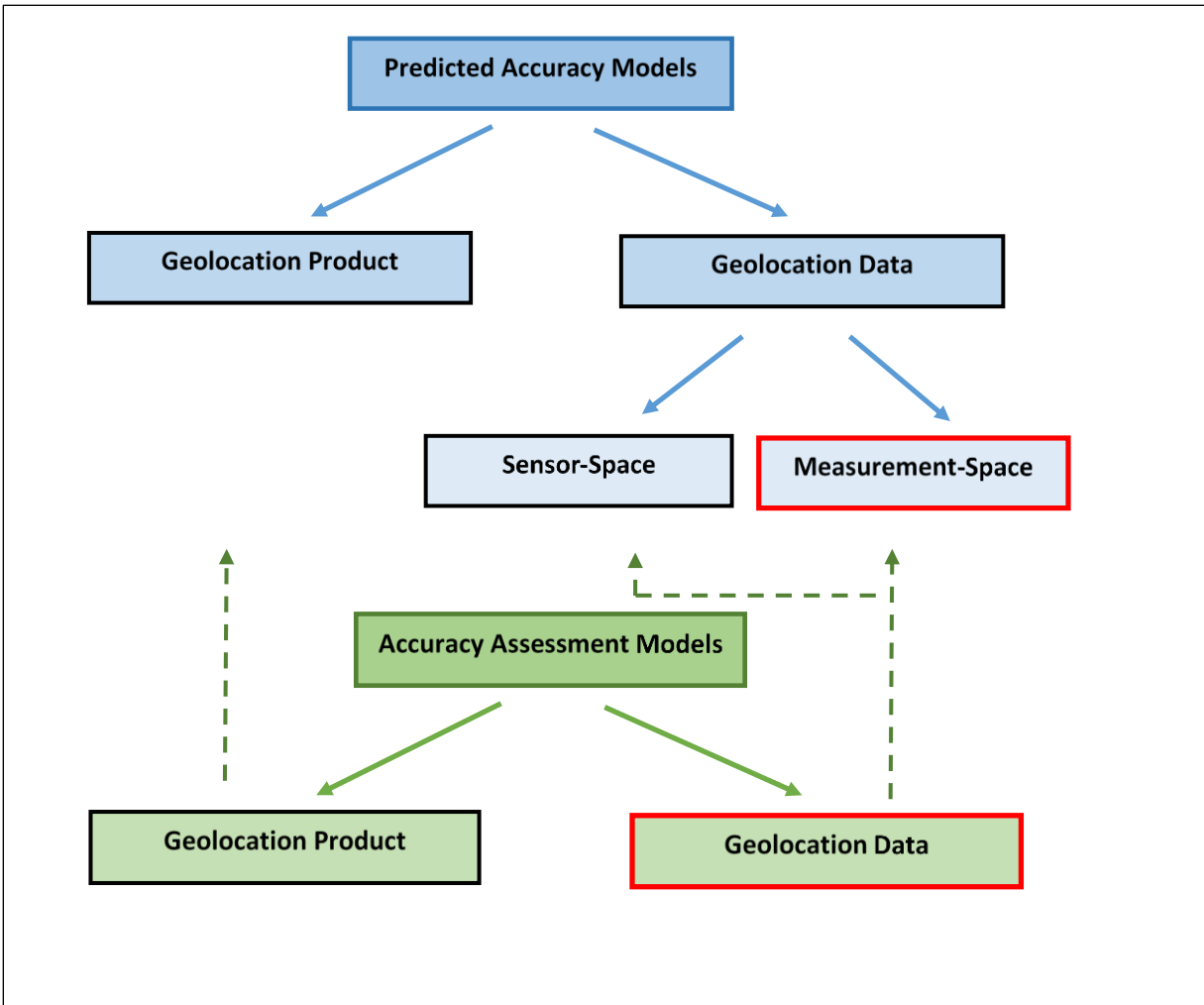


**Figure C-1:** Models described in this appendix (red)

In particular, Sections C.1 and C.2 of the appendix describes the processing required to populate an accuracy assessment model and corresponding predicted accuracy model, respectively, for Geospatial Data assumed to be an image and its metadata for specificity. Both of these models assume that errors are 2d image location errors that represent the summed and equivalent effects of various error sources on the ground-to-image transformation as represented by the image meta-data, primarily underlying errors in sensor pose. It is also assumed that there are relatively few samples of image location errors available. Processing is also extendable in a straightforward manner to 2d image errors alternatively expressed in horizontal ground-space as was previously discussed in Section 5.3.2.4.

Processing in both Sections C.1 and C.2 are virtually the same as described in Sections B.1 and B.2 for a geolocation product, respectively, where errors of interest were assumed to be horizontal ground-space errors – just substitute 2d image location errors for 2d horizontal geolocation errors. Thus, sections C.1

and C.2 essentially just “point to” the corresponding sections B.1 and B.2, respectively, and where the latter also include their various subsections.

Note: image location error samples can be computed in a straight-forward manner as follows: Identify/measure a 3d ground truth geolocation in an image of interest as a measured image location (line, sample). Compute the corresponding image location using the ground truth location and the ground-to-image function. The horizontal error sample is simply the difference between these two image locations.

In addition, the notation for the basic  $2 \times 2$  error covariance matrix in the predicted accuracy model changes from  $C_X$  in Section B.2 to simply  $C$  in Section C.2 with the removal of the geolocation subscript  $X$  in order to further document that errors now correspond to image location errors instead of geolocation errors. In addition, the functional notation for an spdcf changes as well: from  $\rho(dX)$  in Section B.2 to  $\rho(\Delta m)$  in Section C.2, where  $\Delta m$  corresponds to the difference in image locations instead of  $dX$  which corresponds to the difference in geolocations. The notation for the parameters  $A$  and  $D$  which detail an spdcf remain the same for both sections and should be clear from context.

However, there can be some differences between predicted accuracy model processing for an image and predicted accuracy model processing for a geolocation product, as opposed to just their symbology, as described in Section C.3. In particular, Section C.3 describes optional processing and corresponding outputs for the inclusion of predictive statistics associated with sensor-mensuration error for an image. It also includes optional processing for the inclusion of predictive statistics that represent the temporal correlation of errors between images. If applicable, such images are typically same-pass images with times of applicability on the order of a few minutes.

Section C.4 discusses application for the predicted accuracy model for image data. It differs from the corresponding Section B.3 due to inherent difference between applications for a geolocation product (e.g., 3d Point Cloud) and applications for geolocation image data. The latter requires additional processing in order to generate corresponding geolocations and predicted accuracies. The resultant error covariance matrices and related quantities are represented as  $C_X$ , where the subscript “ $X$ ” now corresponds to a geolocation(s) computed from an images(s), not a geolocation contained in a geolocation product per se as in Appendix B.

This appendix (Appendix C) is referenced in Section 5.3.4 of the main body of this document as well as in various other appendices that refer to the basic processing regarding the computation of sample statistics and predictive statistics presented in Appendix C. In particular, it is referenced in Appendix D that describes adjustment of an image based on a correction grid and that relies on the populated predicted accuracy model that is described in Section C.2. A roadmap to the remainder of Appendix C is as follows:

### **Roadmap to Appendix C sections**

#### **C.1 Population of the accuracy assessment model**

C.2 Population of predicted accuracy model

C.3 Optional processing

C.3.1 Sensor-mensuration error and predicted accuracy

C.3.2 Predicted accuracy regarding temporal correlation (same-pass images)

C.3.3 Generalization of the *spdcf*

C.4 Applications

## C.1 Population of the accuracy assessment model

Processing and outputs for the same type or class of images is essentially identical to that described in Section B.1 for the same type or class of geolocation products. Processing/outputs includes the accuracy assessment of both absolute errors and relative errors.

Simply redefine error samples as follows:

Define  $\epsilon X_{ij}$  as a  $2 \times 1$  sample of image location error corresponding to from  $j = 1, \dots, n_i$  image locations in from  $i = 1, \dots, m$  images (independent realizations). In general, image location errors corresponding to image locations in the same image are spatially correlated, but are independent (uncorrelated) with image location errors from different images. Spatial correlation is function of the distance (typically units of pixels) between image locations (line,sample) in the same image. (See Section C.3 for a possible exception regarding the correlation of errors between same-pass images.)

Error samples are also assumed individual error samples from an image (realization), and not “representative” error samples from the image used in the analysis described in Section 5.3.5.3 of the main body of this document. Representative error samples are essentially average (rms) error samples and do not support the assessment of relative errors and/or the spatial correlation of errors.

## C.2 Population of the predicted accuracy model

Processing and outputs for the same type or class of images is essentially identical to that described in Section B.2 for the same type of class of geolocation products per the redefinition of error samples described above in Section C.1. Processing/outputs includes the accuracy assessment of both absolute errors and relative errors.

In addition, recall that notation changes somewhat for an image as described in the introduction to this appendix. In particular, the two key predictive statistics for an image computed per Section C.2 are as follows:

$$C, \tag{C.2-1}$$

which represents the  $2 \times 2$  error covariance matrix for an image, and is applicable to an arbitrary image location in the image; and the functional notation for the *spdcf*:

$$\rho(\Delta m), \quad (C.2-2)$$

which represents the scalar-valued spdcf for an image, and is applicable to the spatial correlation of errors in the same image with corresponding image locations separated by the  $2 \times 1$  difference vector  $\Delta m$  in image-space. The *spdcf* is also assumed applicable to (common to) errors in both the image line coordinates and the image sample coordinates unless specifically designated otherwise.

### C.3 Optional processing

If the general reader is not interested in optional processing, please proceed to Section C.4 for applications of the populated predicted accuracy model for an image.

The various categories of optional processing are all related to modification or extension of the key predictive statistics computed and output via Section C.2:

(1) The  $2 \times 2$  error covariance matrix  $C$  with units of pixels-squared, and about an assumed mean-value of error equal to zero – see Equation (C.2-1).

(2) The spdcf which is represented functionally as  $\rho(\Delta m)$  – see Equation (C.2-2). It is assumed that the spdcf is of the form  $\rho(\Delta m) = Ae^{-|\Delta m|/D}$ , where  $\Delta m$  is the difference between two image locations in the same image and  $|\Delta m|$  is the corresponding distance. The spdcf is isotropic and assumed applicable to the spatial correlation of errors in both the line coordinates and the sample coordinates in the image (both components of error) unless specifically designated otherwise.

Note:  $\rho(\Delta m = 0_{2 \times 1}) \equiv 1$ , and if  $A < 1$ , then  $(1 - A)C$  equals the covariance matrix of the subcomponent of image error that is spatially uncorrelated, i.e., “totally” random.  $(1 - A)$  is a scalar that multiplies each element of the covariance matrix  $C$ .

The above summarized the baseline key predictive statistics. Their optional modifications are as described below:

1. Generalization of the spdcf: (a) there is a different spdcf for each component of error, (b) the spdcf is anisotropic, and (c) the spdcf is from the “CSM four parameter” family and utilizes all four of the defining parameters. These various suboptions are independent, e.g., there can be a different spdcf for errors in the image line direction and for errors in the image sample direction, in addition, they can be either be isotropic or anisotropic in form. See Section C.3.1 for further details.
2. The addition of predictive statistics for additive sensor-mensuration error. See Section C.3.2 for further details.
3. The addition of an spdcf for the representation of the temporal correlation of errors between same-pass images. See Section C.3.3 for further details.

#### C.3.1 Generalization of spdcf

The baseline processing described in Appendix C assumes an isotropic spdcf of the general form  $\rho(\Delta m) = Ae^{-|\Delta m|/D}$  as is reasonable assuming that relatively few samples of error are available and that the processing is to be relatively simple. It is further assumed that the spdcf is applicable to errors in both the line and sample coordinates of an image. However, various options can change these assumptions:

(a) Regarding a different (non-common) spdcf for different components of error – see Section B.2.2 which outlined a relatively straight-forward option to solve for a different (isotropic) spdcf for different components (x and y) of horizontal errors: one spdcf for x-errors and one spdcf for y-errors. This is directly applicable to image errors, if so desired – just substitute errors in the line coordinate for x-errors and errors in the sample coordinate for y-errors. This option should only be utilized if underlying design analysis or detailed accuracy assessments indicate its suitability and corresponding positive impact (increased fidelity).

(b) Regarding an anisotropic spdcf – see Section B.2.2 which also outlined another option to compute spdcf that are not isotropic, i.e., if applied to image errors, would compute an anisotropic spdcf that is the product of two spdcf, one a function of distance in the line direction and one a function of distance in the sample direction:

$$\rho(\Delta m) = A_l e^{-|\Delta l|/D_l} A_s e^{-|\Delta s|/D_s}. \quad (C.3.1-1)$$

This above spdcf is also assumed common to both the line coordinate and the sample coordinate of image errors. See figure 5.3.2.1-1 for a comparison between isotropic and anisotropic spdcf.

However, computation of an anisotropic spdcf is more difficult than the baseline computation of an isotropic spdcf in that four dominant parameters must be fit ( $A_l$ ,  $D_l$ ,  $A_s$ ,  $D_s$ ) instead of the deterministic solution for only two dominant parameters ( $A$  and  $D$ ). However, when applicable, *a priori* knowledge of the imaging system may be included that allows for an easier solution of the four parameters, such as: (1) *a priori* estimates for some of the parameters, such as  $A_l$  and  $D_l$ , or (2) if errors are more highly correlated in the sample direction than in the line direction,  $D_l = (0.1)D_s$ , for example.

In general, computation of parameters applicable to both the line direction and the sample direction also require the availability of more error samples for more “observability” into the spatial correlation along both of these directions in the image.

(c) Assuming that candidate spdcf are from the four-parameter CSM family, as is reasonable and also supported by many current APIs, there is another generalization possible for an (isotropic) spdcf: the spdcf utilizes all four of the parameters ( $A$ ,  $\alpha$ ,  $\beta$ , and  $D$ ):

$$\rho(\Delta m) = A(\alpha + \frac{(1-\alpha)(1+\beta)}{\beta + e^{|\Delta m|/D}}). \quad (C.3.1-2)$$

However, the added complexity of solving for all four of these parameters instead of just two ( $A$  and  $D$ ) is typically not considered warranted – the dominant parameters ( $A$ , and  $D$ ) are considered more than adequate for reasonable fidelity, i.e., parameters  $\alpha$  and  $\beta$  are not solved for (set to zero).

### Summary regarding spdcf generalizations:

In summary, optional generalizations of spdcf are difficult, particularly those corresponding to options (b) and (c) above, given the constraints regarding a limited number of error samples and the desire for relatively simple processing as deemed appropriate for Commodities data. However, they can be done, typically with additional *a priori* knowledge embedded into the processing. Option b, which generates an anisotropic spdcf, could be particularly useful for images that are scanned images and that may have significantly different spatial correlation characteristics in the line direction than in the sample direction. This requires future applied research. However, it is important that designers of applications take into account that these generalizations may become available.

### C.3.2 Sensor-mensuration error and predicted accuracy

Sometimes it is convenient to separate the predictive statistics into two groups applicable to two different types of errors when the geolocation data is an image: strictly image errors and sensor-mensuration (high frequency errors, aka “unmodeled errors”). This may also be of use when utilizing APIs that expect such a separation.

In general, image errors are represented by a  $2 \times 2$  error covariance matrix  $C$  and by an spdcf  $\rho(\Delta m)$ , where the latter is represented by parameters  $A$  and  $D$ , and sensor-mensuration errors are represented by a  $2 \times 2$  error covariance matrix  $C_{sm}$  and by an spdcf  $\rho_{sm}(\Delta m)$ , where the latter is represented by two parameters  $A_{sm}$  and  $D_{sm}$ . Correspondingly, the resultant error for an arbitrary location in the image is the sum of these two types of errors which are also assumed to be uncorrelated with each other.

Note: The above assumes a common and isotropic spdcf for image errors and a common and isotropic spdcf for sensor–mensuration errors, but both can be generalized per the optional processing described in Section C.3.1.

If given the original image errors and their predictive statistics only, and if the (original) spdcf parameter  $A$  is less than 1 as is typical, these predictive statistics can be “separated” into (1) a modified set of predictive statistics for the image errors per se, and (2) a set of predictive statistics corresponding to sensor-mensuration error as follows:

Sensor-mensuration error predictive statistics: (C.3.2-1)

$C_{sm} = (1 - A)C$ , in pixels-squared, where the scalar  $(1 - A)$  multiplies each element of the (original) covariance matrix  $C$ ;

$\rho_{sm}(\Delta m) = (A_{sm})e^{-|\Delta m|/D_{sm}}$ , where  $A_{sm} = 1$  and  $D_{sm} \ll 1$ , i.e., essentially representing spatially uncorrelated errors, where  $A_{sm}$  is unit-less and  $\Delta m$  and  $D_{sm}$  have units of pixels.

The set of predictive statistics for image errors are then modified as follows: (C.3.2-2)

$C \rightarrow (A)C$ ;

$\rho(\Delta m) = (A)e^{-|\Delta m|/D}$ , where  $A = 1$  and  $D$  remains unchanged.

The outputs corresponding to the processing of Section C.2 are modified and identified accordingly: (C.3.2-3)

Original outputs  $\{C \text{ and } \rho(\Delta m)\}$  become  $\{C \text{ and } \rho(\Delta m) \text{ from Equation (C.3.2-2), } C_{sm} \text{ and } \rho_{sm}(\Delta m)\}$  from Equation (C.3.2-1).

Another option consists of obtaining a populated *a priori* sensor-mensuration error model by other means. In this case, instead of “backing them out” from the predictive statistics for image error, a somewhat conservative sub-option is to leave the baseline key predictive statistics unmodified and to append the sensor-mensuration error predictive statistics in a manner similar to Equation (C.3.2-3).

### C.3.3 Temporal correlation

If it is determined that the errors in “same-pass” images are correlated, such temporal correlation can be optionally modeled as such via an spdcf functionally represented as  $\rho_{time} = (A_{time})e^{-dt/T}$ , where  $0 < A_{time} \leq 1$ ,  $T$  is the time constant in seconds, and  $dt$  is the absolute value of the difference in the image times of applicability in seconds. This spdcf, typically termed a “temporal spdcf”, can then be used to compute the appropriate correlation of errors between multiple image measurements in a MIG extraction of a common ground location, such as a stereo extraction.

Note: The above assumes a common and isotropic temporal spdcf for image errors, but can be generalized per the optional processing described in Section C.3.1.

In order to estimate the parameters  $A_{time}$  and  $T$  defining such an spdcf, the processing described in Section C, and thus Section B, would require augmentation in order to compute sample-values of the temporal correlation (coefficient) corresponding to either one or two “time bins”. This processing requires grouping images into appropriate “image-pairs” based on their times of applicability.

Such processing is not detailed further in this document. However, it is important that designers of applications take into account that such a temporal spdcf may be made available.

## C.4 Applications

The following utilizes the two key predictive statistics contained in a populated predicted accuracy model for an image as computed per Section C.2: the  $2 \times 2$  error covariance matrix  $C$  and the scalar-valued spdcf  $\rho(\Delta m)$ . The spdcf is also assumed common to both line and sample errors.

With the availability of these two predictive statistics, numerous geolocation applications and derived predictive statistics can be computed in conjunction with the applicable sensor model. Some of them are illustrated below:

The full (symmetric) error covariance matrix correspond to multiple image locations corresponding to multiple ground location (features) measured in the same image is computed as follows assuming two image locations for convenience:

$$C_{full} = \begin{bmatrix} C & \rho(\Delta m_{12})C \\ \cdot & C \end{bmatrix} \text{ pixels-squared} \quad (\text{C.4-1})$$

where  $\Delta m_{12}$  is the distance (pixels) in image-space between the two image locations and the above scalar-valued  $\rho(\Delta m_{12})$  multiplies each element of the error covariance matrix  $C$ .

Note: If the two image locations are from two different images that are assumed uncorrelated, as is typical,  $C_{full}$  is a block diagonal matrix, i.e., has a zero  $2 \times 2$  cross-covariance block. This supports a MIG stereo solution, and not detailed in the appendix.

Note: See Equation D.2.1-1 in Appendix D for a generalization of Equation (C.4-1) if the applicable spdcf is different for each coordinate, i.e., is an anisotropic spdcf.

Equation (C.4-1) supports a MIG (mono) solution for two ground locations assuming an external elevation source. This is done by generalizing image errors to “total” image errors or “image measurement” errors, which include mensuration errors and sensor-mensuration errors when applicable. The mensuration errors correspond to errors in the user/application’s measurement of image locations corresponding to ground locations of features of interest “seen” in the image.

Correspondingly: (C.4-2)

(1)  $C_{meas} = C + C_{sm} + C_{mens}$ , a  $2 \times 2$  error covariance matrix, and if sensor-mensuration errors are not modeled,  $C_{sm} = 0_{2 \times 2}$ . All error covariance matrices are in units of pixels-squared.

(2)  $C_{meas\_full} = \begin{bmatrix} C_{meas} & (\rho(\Delta m_{12})C + \rho_{sm}(\Delta m_{12})C_{sm}) \\ \cdot & C_{meas} \end{bmatrix}$ , a  $4 \times 4$  full error covariance matrix.

(3) Perform the MIG solution for the two ground point locations in the image using their two image locations,  $C_{meas\_full}$ , and the reference elevation – see TGD 1 and TGD 2d for details regarding a MIG (mono) solution – resulting in:

$\hat{X}$  with corresponding  $4 \times 4$  *a posteriori* error covariance matrix  $C_{X\_full}$  in meters-squared,

assuming that only horizontal coordinates are solved for and easily generalized to 3d ground coordinates.

The  $4 \times 4$  *a posteriori* error covariance matrix  $C_X$  can be represented as follows for the two horizontal geolocations from the MIG solution:

$$C_{X\_full} = \begin{bmatrix} C_{X11} & C_{X12} \\ \cdot & C_{X22} \end{bmatrix}. \quad (\text{C.4-3})$$

This is used to compute the corresponding  $2 \times 2$  covariance matrix  $rel\_C_X$  for relative error between the two horizontal locations as follow:

$$rel\_C_X = C_{X\ 11} + C_{X\ 22} - 2C_{X\ 12}, \text{ in meters-squared.} \quad (C.4-4)$$

And given the above  $rel\_C_X$ , the corresponding scalar accuracy metric  $rel\_CEXX$  (meters) can be computed for any desired level of probability  $XX$  assuming a Gaussian distribution of errors.

Note: the above  $C_{X\_full}$  can also be approximated as  $C_{X\_full} = F(C_{meas\_full})F^T$ , where

$F = \begin{bmatrix} \partial(x,y)/(l,s) & 0_{2 \times 2} \\ 0_{2 \times 2} & \partial(x,y)/(l,s) \end{bmatrix}$  and  $\partial(x,y)/(l,s)$  are the  $2 \times 2$  numerical partial derivatives of horizontal ground location with respect to image location applicable at a nominal location in the image and computed using the image-to-ground function (typically the iterative inverse of the ground-to-image function) at the reference elevation.

Appendix D that follows describes a different type of application of the populated predicted accuracy model: its use in the adjustment of the image for a corresponding reduction in its errors. When performed, the processing described above modified accordingly will yield more accurate results.

## Appendix D: Adjustment of Geolocation Data

A populated Geolocation Data Predicted Accuracy Model also supports an adjustment or correction of the corresponding data. An example of such a populated predicted accuracy model was detailed in Appendix C for an image.

This appendix (Appendix D) describes a corresponding adjustment model and related processing assuming the availability of control information. In particular, it provides further details regarding the WLS solution for a correction grid that was initially described in Section 5.3.3.1 in the main body of this document. It also provides further insight regarding image errors such that corresponding predictive statistics represent the summed effects of underlying errors, such as error in the ground-to-image function due to sensor pose (sensor position and attitude) errors. This appendix also presents a simulation-based assessment of correction grid performance.

### Roadmap

#### D.1 Background information

#### D.2 The correction grid, its solution, and subsequent adjustment of the image

##### D.2.1 Detailed definitions and their related processing

##### D.2.2 WLS solution

##### D.2.3 Correction of an arbitrary measurement or location in the image

##### D.2.4 Summary: Why a correction grid?

### D.3 Correction grid performance and comparison to an affine-transformation based correction

#### D.3.1 Simulation based performance

## D.1 Background information

Prior to detailing the correction grid for a corresponding image, the solution for its content, and its applications, further background information is presented that complements Figure 5.3.3.1-1 of Section 5.3.3.1 (Adjustment) in the main body of this document. In particular, Figure D.1-1 below illustrates true sensor pose versus sensor pose assumed and contained (represented) in the image metadata and their effects on computed geolocations. The blue dot in the figure represents an arbitrary image location  $m = (line, sample)$  that is observed/measured in the image, and the red dot represents its corrected image location. Recall that this approach to image adjustment does not correct for the metadata per se, but for its effects in image-space.

The image-to-ground function and its inverse are also represented by green and gold arrows in the figure, corresponding to both the assumed sensor pose (metadata with the image) and the true (unknown) sensor pose, respectively. The colors for the arrows were selected arbitrarily.

Note: there are two image planes illustrated in the Figure D.1-1 (blue and black line segments), which are physically one in the same but are indicated separately per associated sensor/image pose. The two blue dots in the figure are at the same measured image location or  $(line, sample)$  values.

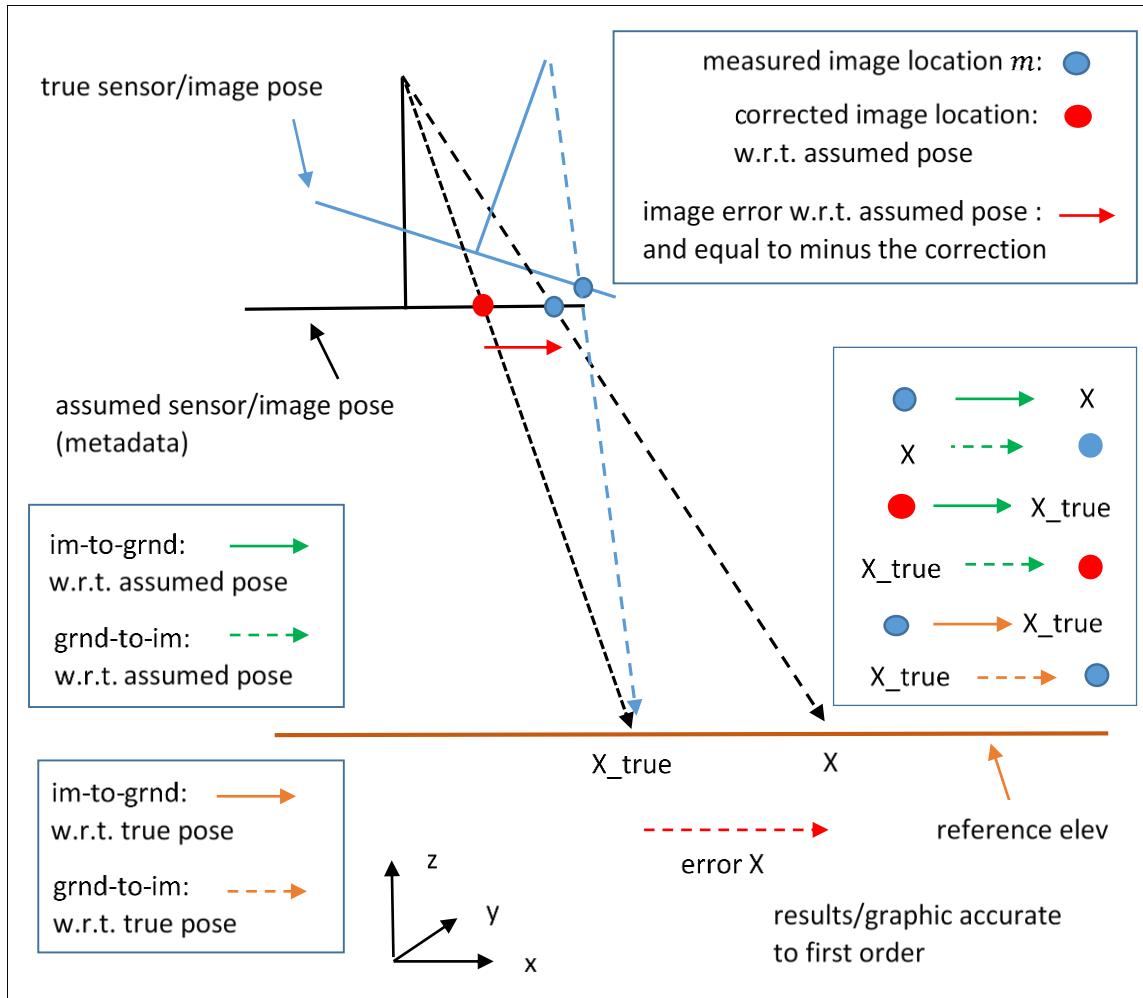


**Figure D.1-1:** Background information regarding true vs. assumed sensor pose (metadata): an arbitrary image measurement  $m$  (blue dot), its error (red arrow) due to errors in the assumed sensor pose, its correction (minus the error), and the corrected measurement  $\hat{m}$  (red dot); figure is a 2d rendering of 3d space for convenience/clarity

The correction grid detailed below represents the desired correction in the figure, and is solved for using observed/measured locations in the image relative to external control information.

## D.2 The correction grid, its solution, and subsequent adjustment of the image

A correction grid is presented in Figure D.2-1 and corresponds to a specific  $3 \times 3$  correction grid for clarity and ease of example. Once computed, it is used to correct an arbitrary location or measurement  $m$  in the image (blue circle) for the effects of image metadata errors. The corrected measurement  $\hat{m}$  is indicated by the red circle in the figure. The blue and red circles are analogous to those presented earlier in Figure D.1-1.

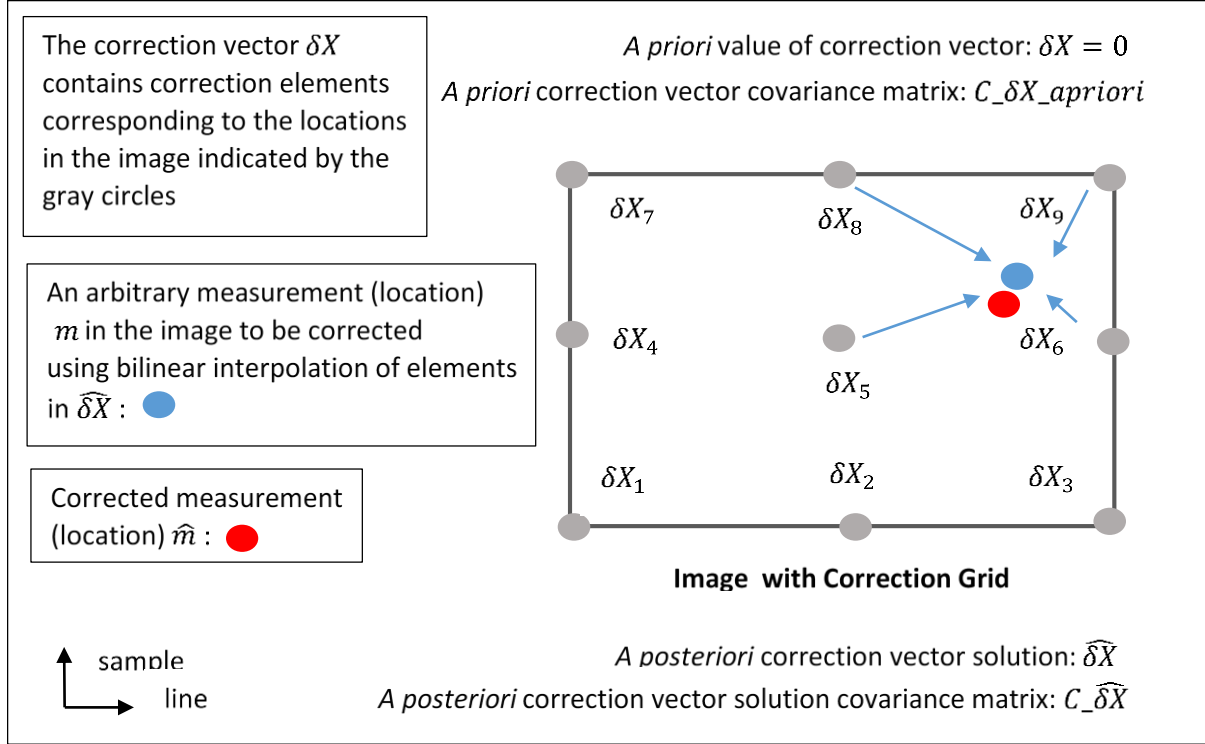


**Figure D.2-1:** An example of a  $3 \times 3$  correction grid and its application for an arbitrary measurement or location  $m = (line, sample)$  in the image

The following goes on to describe the recommended process for computation of the correction grid using external control information. The subsequent application of the correction grid is then described.

### D.2.1 Detailed definitions and their related processing

This section of the appendix presents necessary definitions and related processing require to compute the correction grid and then apply it to arbitrary locations in the image.

#### Initial definitions and *a priori* statistics for the correction grid for solution:

Correction vector for solution:  $\delta X = [\delta X_1^T \ \dots \ \delta X_9^T]^T$ , where each  $2 \times 1$  element  $\delta X_j$  corresponds to an (underlying) image location  $m_j$  in the image (gray circles in Figure D.2.1-1). The *a priori* statistics for  $\delta X$  are equivalent to the key statistics in the populated predicted accuracy model for the image that were detailed in Appendix C. Their correspondence is as detailed below:

The *a priori* value of  $\delta X$  is equal to zero, i.e.,  $\delta X = 0_{2(9) \times 1} = 0_{18 \times 1}$ . Its corresponding *a priori* error covariance matrix is an  $18 \times 18$  matrix and is equal to:

$$C_{\delta X\_apriori} = E\{\delta X \delta X^T\} = \begin{bmatrix} C & \rho(\Delta m_{12})C & \dots & \rho(\Delta m_{19})C \\ \rho(\Delta m_{21})C & C & \rho(\Delta m_{23})C & \dots \\ \vdots & \vdots & \vdots & \vdots \\ \rho(\Delta m_{91})C & \rho(\Delta m_{92})C & \dots & C \end{bmatrix}, \quad (D.2.1-1)$$

which also corresponds to Equation (C.5-1) extended to multiple image locations and with a slight change in notation, i.e.,  $C_{\delta X\_apriori} \equiv C_{full}$ .

If the spdcf  $\rho(\Delta m_{ij})$  is not common to errors in both the line and sample coordinates, simply replace it with two spdcf  $\rho_l(\Delta m_{ij})$  and  $\rho_s(\Delta m_{ij})$  and replace the term  $\rho(\Delta m_{ij})C$  in  $C_{\delta X\_apriori}$  with  $SC \equiv \begin{bmatrix} \rho_l(\Delta l_{ij}, \Delta s_{ij}) & 0 \\ 0 & \rho_s(\Delta l_{ij}, \Delta s_{ij}) \end{bmatrix} C$ , since  $C$  is a diagonal matrix in this example; otherwise, replace the term with  $C^{1/2}SC^{1/2}$ , where superscript  $1/2$  represents matrix principal square root and the superscript  $T$  represents matrix transpose.

### Measurements:

Assume that there are  $p \ 2 \times 1$  measurements  $m_l^*$ ,  $l = 1, \dots, p$ , in the image that correspond to  $p$  ground control points that are available and in the image AOI or footprint:

#### Equation/Processing

(D.2.1-2)

- Given a ground control point with *a priori* ground location  $X\_cntrl$  and accompanying description
- $X\_cntrl \rightarrow m\_cntrl_l$  in the image for adjustment using its ground-to-image function
  - red square in Figure D.2.1-1 below
- $m_l^*$  corresponds to the ground control point identified/measured in the image for adjustment
  - blue square in Figure D.2.1-1 below

This is represented graphically in Figure D.2.1-1, essentially a repeat of Figure D.2-1 but with information only directly applicable to a ground control point and its measurement used in the solution for the correction grid. In this relatively simple figure, the blue square represents  $m_l^*$  and the red square represents  $m\_cntrl_l$ . The *a priori* ground control point location is represented as  $X\_cntrl$  in the figure.

Note: an explicit control image can be used instead of ground control points for external control of the image as detailed later.

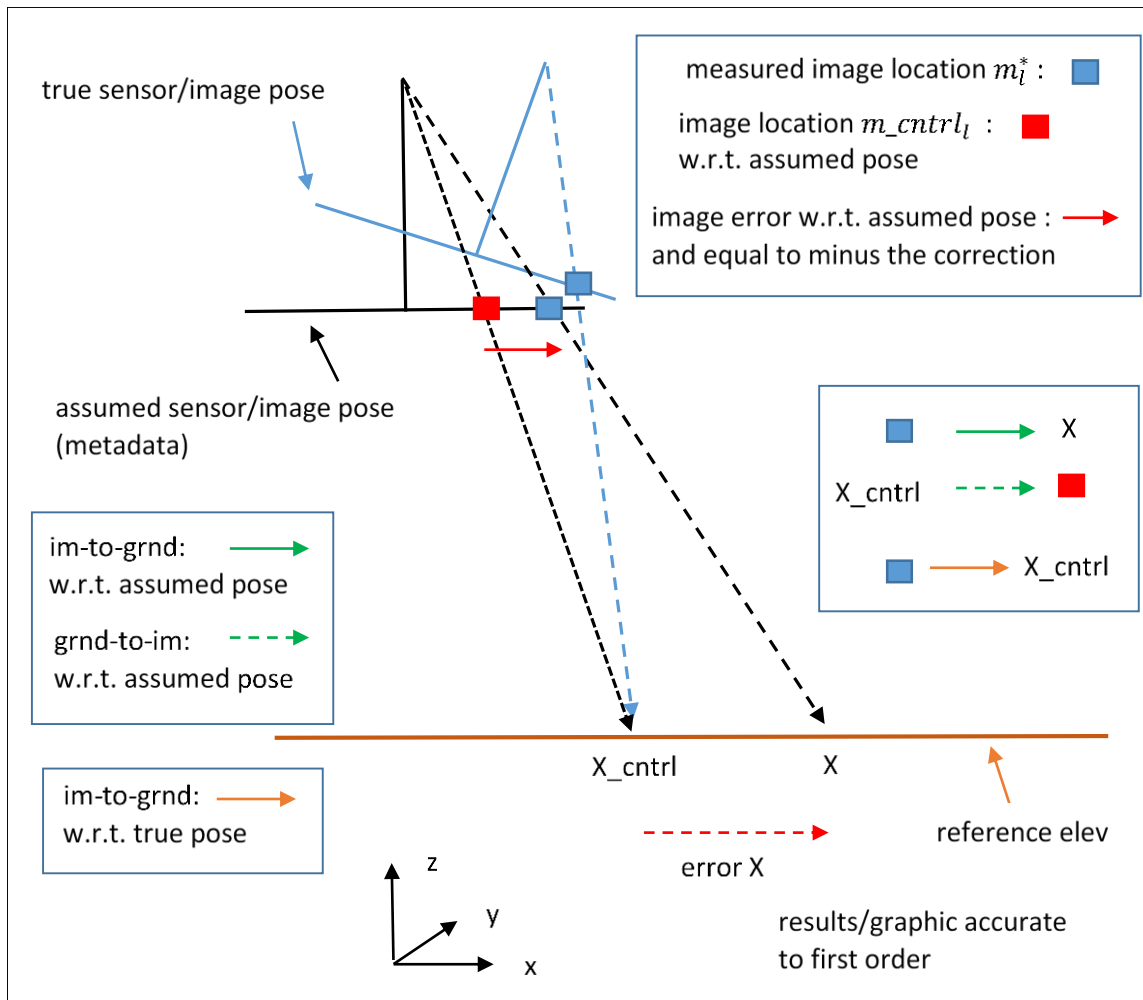


**Figure D.2.1-1:** Measurement  $m_l^*$  of a ground control point in the image and related quantities

For further perspective,  $m_l^*$  and  $m_{cntrl_l}$  are also illustrated in the correction grid in Figure D.2.1-2. Note that both Figures D.2.1-1 and D.2.1-2 correspond to the same image, but the former relative to a 1d or “side” perspective and the latter relative to a 2d or “top-down” perspective.

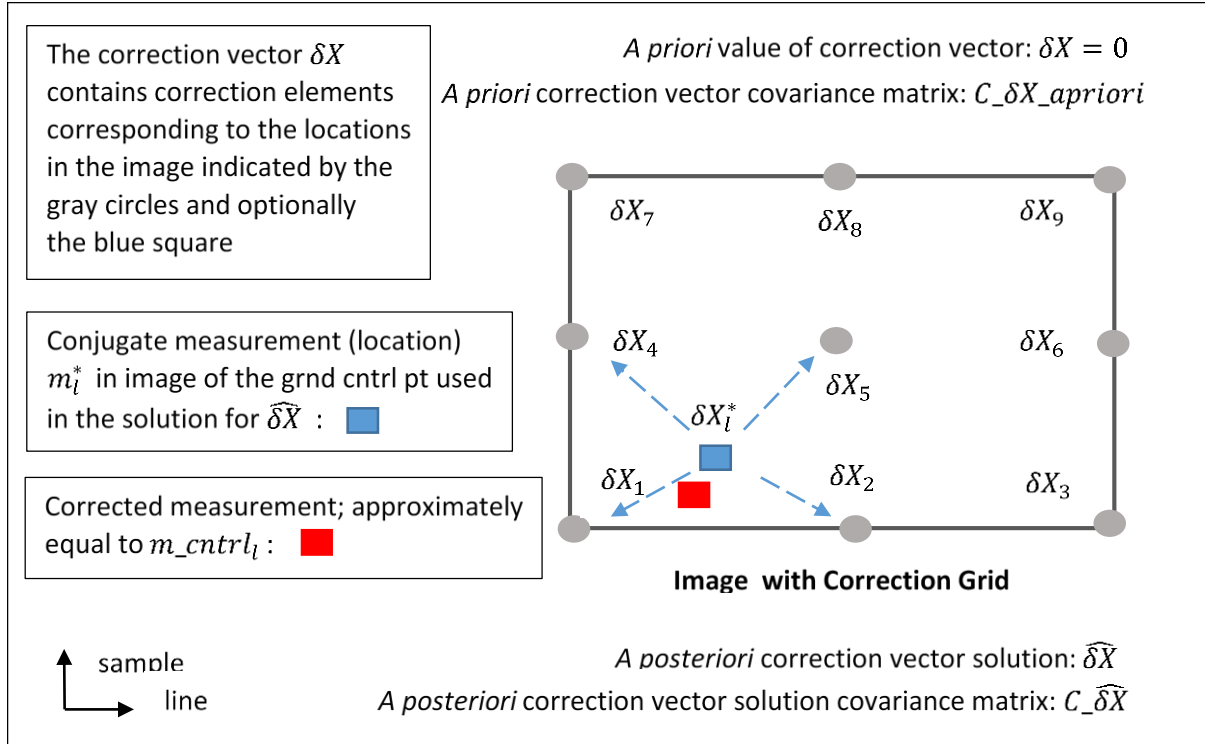


**Figure D.2.1-2:** Measurement  $m_l^*$  of a ground control point in the image and related quantities as illustrated relative to the correction grid for solution

The dashed blue lines in Figure D.2.1-2 represent the flow of information from the measurement  $m_l^*$ , in conjunction with  $m_{cntrl_l}$ , into the solution for the elements ( $\delta X_i$ ) of the correction grid. In addition, even though only the closest elements of the correction grid are “pointed to” in the figure, information actually flows into all of the elements due to the spatial correlation (spdcf) specified in their *a priori* statistics. The correction element  $\delta X_l^*$  is not an explicit member of the correction grid but is an optional and explicit member of the correction vector  $\delta X$  for solution, as detailed later.

#### Detailed definitions associated with the measurements and their errors:

Referring to Equation/Processing D.2.1-2 and to Figure D.2.1-2, and with “ $\epsilon$ ” representing a designated type of error:

$m_{cntrl_l} = m_{true_l} + \epsilon_{sys\_cntrl_l}$ , the red square in the figure,

where  $m_{true_l}$  is the “true” image location of the ground control point based on the ground-to-image function using the current metadata or (incorrect) sensor pose.  $m_{cntrl_l}$  is equal to  $m_{true_l}$  plus the systematic error  $\epsilon_{sys\_cntrl_l}$  associated with errors in the *a priori* location  $X_{cntrl}$  of the ground control point projected to image-space.

$m_l^* = m\_true_l - \delta X_l^* + \epsilon\_mens_l^*$ , the blue square in the figure,

where  $m_l^*$  is the actual measured location of the ground control point in the image.  $\delta X_l^*$  is the desired correction in image-space and  $\epsilon\_mens_l^*$  is the mensuration error associated with the identification/measurement of the ground control point in the image.

$\Delta m_l \equiv m\_cntrl_l - m_l^* = \delta X_l^* + \epsilon\_sys\_cntrl_l - \epsilon\_mens_l^*$ , or

$\Delta m_l \equiv \delta X_l^* + \epsilon\_meas\_ \Delta m_l$ .

In the above:

- The actual systematic error to be removed via solution for the correction grid and its subsequent application corresponds to the correction  $\delta X_l^*$  per Figure D.2.1-2 (correction grid)
- $\epsilon\_mens_l^*$  is defined as the random mensuration error due the identification/measurement of the ground control point in the image for adjustment and is assumed to be uncorrelated with measurements corresponding to other ground control points, e.g.,  $\epsilon\_mens_{l1}^*$  and  $\epsilon\_mens_{l2}^*$ ,  $l1 \neq l2$ , are uncorrelated. Correspondingly, a block diagonal  $2m \times 2m$  error covariance matrix is applicable for the measurements of  $p$  ground control points in the image, and is typically a diagonal matrix.
- $\epsilon\_sys\_cntrl_l$  is the systematic error in image-space due to errors in the ground control point location that was provided; in general, it is spatially correlated in image-space with the systematic errors associated with other ground control points and a full  $2p \times 2p$  error covariance matrix in image-space is applicable for  $p$  ground control points. This error covariance matrix is generated by the propagation of a full ground location error covariance matrix to image-space, performed by the latter's pre and post multiplication by a block diagonal  $2p \times 3p$  partial derivative matrix  $(\partial(l,s)/\partial(x,y,z))$  and its transpose, respectively. This partial derivative matrix is applicable to all ground control points and typically generated numerically using the ground-to-image function for the image at the appropriate operating points or *a priori* ground control point locations associated with linearization of the problem.
- $\Delta m_l$  is the difference between  $m\_cntrl_l$  and  $m_l^*$  and is the actual measurement into the WLS solution process.
- The total measurement error  $\epsilon\_meas\_ \Delta m_l = \epsilon\_sys\_cntrl_l - \epsilon\_mens_l^*$

Finally, we have:

$\Delta M \equiv [\Delta m_1^T \ \dots \ \Delta m_p^T]^T$ , a  $2p \times 1$  vector, the measurement vector into the WLS solution process.

Note: If control imagery or its equivalent is used instead of a ground control point, it is assumed to have been aligned with (resampled or mapped to) the image coordinate system of the image to be adjusted for the purposes of identification of the same object (only). Also, the above equations change somewhat:

- $\Delta m_l \equiv \delta X_l^* + \epsilon\_meas\_ \Delta m_l$  but is computed as follows:

- Identify/measure an arbitrary ground location in the control image (m1) and in the image to be adjusted (m2); using the control image's image measurement (m1) and its image-to-ground function, compute the corresponding geolocation; using this geolocation and the ground-to-image function of the image to be adjusted, compute the conjugate geolocation image location (m3);  $\Delta m_l = m2 - m3$ .
- Also,  $\epsilon_{meas\_}\Delta m_l$  has an additional additive mensuration error associated with the measurement in the control image, and an additional additive error associated with the error in the assumed reference elevation used in the image-to-ground projection.

#### Measurement error vector and predictive statistics:

The measurement error vector corresponding to  $\Delta M$  is defined as:

$\epsilon_{meas\_}\Delta M \equiv [\epsilon_{meas\_}\Delta m_1^T \ \dots \ \epsilon_{meas\_}\Delta m_p^T]^T$ , a  $2p \times 1$  vector, with an assumed *a priori* mean-value equal to zero and an *a priori* error covariance matrix equal to:

$C_{meas\_}\Delta M = C_{mens\_}\Delta M + C_{sys\_}cntrl$ , a  $2p \times 2p$  matrix, where:

- $C_{mens\_}\Delta M$  is a  $2p \times 2p$  diagonal matrix assumed to have common block diagonals (although this can be generalized, if applicable)
- $C_{sys\_}cntrl$  is a  $2p \times 2p$  matrix that is generally full, i.e., contains cross-covariance blocks due to spatial correlation
- Unlike, Equation (C.4-2) in Appendix C describing applications of a populated accuracy model for an image,  $C_{meas\_}\Delta M$  does not include the equivalent of predictive statistics for *a priori* errors in the image since these are for solution via  $\delta X$ .

#### Partial derivatives:

Define the partial derivative of the measurement vector with respect to the state vector (adjustment or correction vector  $\delta X$ ) for solution as follows for the example described earlier, i.e. a  $3 \times 3$  correction grid with  $p$  conjugate measurements corresponding to ground control points:

$$B \equiv \partial(\Delta M)/\partial(\delta X) = \begin{bmatrix} B_1 \\ \vdots \\ B_l \\ \vdots \\ B_p \end{bmatrix}, \text{ where } B_l \text{ is a } 2 \times 2(9) \text{ matrix associated with component } l \text{ of the}$$

measurement vector  $\Delta M_l = \Delta m_l$ .

$B_l$  is defined as follows based on the image location  $m_l^*$  that corresponds to the blue square in Figure B.2.2.2-2, and more specifically, to the blue square in Figure D.2.1-2 and its corresponding correction for solution  $\delta X_l^*$ . However, in this solution approach,  $\delta X_l^*$  is not in the adjustment vector and is approximated by the four adjustment elements  $\{\delta X_1, \delta X_2, \delta X_4, \text{ and } \delta X_5\}$  in the correction grid cell that are defined as follows:

Let  $a_1 - a_4$  represent the adjustment elements' corresponding scalar bilinear interpolation coefficients, respectively, computed based on the 2d distances between  $m_j^*$  and  $m_1, m_2, m_4$ , and  $m_5$ , respectively.

Define  $A_k = a_k I_{2 \times 2}$ , for  $k = 1, \dots, 4$ . (Note: the  $a_k$  are non-negative and sum to 1.)

Therefore:

$\delta X_l^* \cong A_1 \delta X_1 + A_2 \delta X_2 + A_3 \delta X_4 + A_4 \delta X_5$ , and the

corresponding entry in the  $B$  matrix is equal to:

$$B_l = [A_1 \quad A_2 \quad 0_{2 \times 2} \quad A_3 \quad A_4 \quad 0_{2 \times 2} \quad 0_{2 \times 2} \quad 0_{2 \times 2} \quad 0_{2 \times 2}].$$

### D.2.2 WLS solution

Define the measurement weight matrix as  $W = (C_{meas} \Delta M)^{-1}$ , a  $2p \times 2p$  matrix.

The WLS solution for the correction vector is as follows:

$$\widehat{\delta X} = (C_{\delta X}) B^T W \Delta M,$$

where the *a posteriori* solution error covariance matrix is equal to:

$$C_{\delta X} = (C_{\delta X_{apriori}}^{-1} + B^T W B)^{-1}.$$

Note that in the solution process, the measurement  $\Delta M_l$  updates  $\delta X_1, \delta X_2, \delta X_4$ , and  $\delta X_5$  directly (dashed blue lines in Figure D.2.1-2), but in addition also updates all of the other adjustment elements indirectly via the spatial correlation contained in the adjustment vector's *a priori* covariance matrix  $C_{\delta X_{apriori}}$ .

Note that  $\Delta M$  can also be considered equal to the *a priori* measurement residual vector, i.e.,  $\Delta M \rightarrow \Delta M + \Delta M_0$ , where  $\Delta M_0$  is the *a priori* (pre-solution) prediction of the value of  $\Delta M$  and is equal to zero. The *a priori* measurement residual is not to be confused with the *a posteriori* (post solution) measurement residual, typically analyzed to help ensure a valid WLS solution.

It is recommended that the WLS solution includes processing for quality control of the solution, such as measurement editing and examination of the *a posteriori* (post-solution) measurement residuals normalized by their predicted accuracy. If these residuals are outside their expected range, modify the solution vector's *a priori* error covariance matrix  $C_{\delta X_{apriori}}$  accordingly and re-perform the WLS solution as needed. General "rules of thumb" for the modification of  $C_{\delta X_{apriori}}$  are as follows regarding the parameters used to compute it:

- If the normalized residuals are too large, increase the correction vector's *a priori* error covariance matrix by a positive scale factor greater than 1 and/or reduce the *a priori* spatial correlation via modification of the spdcf, e.g., decrease the distance constant(s) if a CSM four parameter spdcf.

- If the normalized residuals are too small, reduce the correction vector's *a priori* error covariance matrix by a positive scale factor less than 1 and/or increase the *a priori* spatial correlation via modification of the spdcf, e.g., increase the distance constant(s) if a CSM four parameter spdcf

As mentioned above, the above are only general rules of thumb and involve the modification of  $C_{\delta X_{apriori}}$  only, which are assumed the most likely *a priori* predictive statistics requiring modification. However, the *a priori* measurement error covariance matrix  $C_{meas\_DM}$  may also need modifications (scaled up or down).

See TGD 2d (Estimators and their Quality Control) for further details regarding a WLS solution in general and methods for its quality control.

### An optimal solution:

The above solution process is near optimal, but not theoretically optimal, due to the use of interpolation associated with the conjugate measurements. An optimal solution process (assuming correct *a priori* modeling) is recommend as a simple extension to the above solution process that does not require the interpolation. It is the baseline method and is defined as follows:

Augment the state (correction) vector for solution with  $2 \times 1$  corrections that are explicitly associated with the conjugate measurements (locations) in the image for correction, i.e.,  $\delta X_l^*$  associated with  $m_l^*$ ,  $l = 1, \dots, p$  (see Figure B.2.2-4):

$$\delta X \equiv [\delta X_1^T \quad \dots \quad \delta X_9^T \quad \delta X_1^{*T} \quad \dots \quad \delta X_p^{*T}]^T, \text{ a } (18 + 2p) \times 1 \text{ vector.}$$

Augment the *a priori* covariance matrix as well:  $C_{\delta X_{apriori}}$ , a  $(18 + 2p) \times (18 + 2p)$  matrix.

The same method that was originally used to compute the *a priori* covariance matrix in the first place is used to augment it in order to reflect the augmented correction vector for solution. That is,  $C$  and  $\rho(\Delta m_{ij})$  are still applicable, but are also applied to the augmented elements in  $\delta X$  and for the evaluation of the spdcf at all image location differences  $\Delta m_{ij}$ , i.e., applicable to all pairs of the underlying locations in the original elements  $\delta X_j$ ,  $j = 1, \dots, 9$ , the augmented elements  $\delta X_l^*$ ,  $l = 1, \dots, p$ , and between these two sets of locations.

Redefine the partial derivative matrix  $B$  as follows:

$$B = [0_{2p \times 18} \quad I_{2p \times 2p}].$$

The remaining steps in the solution are identical to those for the first solution, yielding an  $(18 + 2p) \times 1$  *a posteriori* solution  $\widehat{\delta X}$  and a  $(18 + 2p) \times (18 + 2p)$  *a posteriori* solution error covariance matrix  $C_{\widehat{\delta X}}$ .

This optimal solution method updates the new elements in the augmented correction vector directly via the measurements, whereas the original elements are now updated via their spatial correlation with the new elements as specified in the corresponding cross-covariance block in the augmented  $C_{\delta X\_apriori}$ .

Note: in general, the predicted accuracies for grid corrections in the optimal solution method are slightly larger (worse) than their counterparts in the standard solution, the latter using bilinear interpolation to relate the measurements to the grid corrections instead of *a priori* spatial correlation exclusively. This effect becomes even more pronounced if the *a priori* spatial correlation is less than 0.9 per adjacent grid point. However, the standard solution's predicted accuracy is only theoretically valid (consistent with actual solution errors) if local grid errors are indeed bilinearly related to the measurements, which is only an approximation in general for errors corresponding to a random field, i.e., corresponding to the *a priori* predictive statistics for image errors.

The augmented elements in the optimal solution can be removed from  $\widehat{\delta X}$  and their corresponding covariance block and cross-block from  $C_{\widehat{\delta X}}$  if so desired, making the subsequent processing for the correction of an arbitrary image measurement (location) in the corrected image identical for both solution methods, and defined as follows:

### D.2.3 Correction of an arbitrary measurement or location in the image

For an arbitrary image location (measurement)  $m$  in the image (see blue circle in Figure D.2-1), compute its correction as the bilinear interpolation of the four elements in  $\widehat{\delta X}$  that correspond to the correction cell in which it resides, i.e.,  $\widehat{\delta X}_5$ ,  $\widehat{\delta X}_6$ ,  $\widehat{\delta X}_8$ , and  $\widehat{\delta X}_9$  for the example in Figure D.2.1-2. The correction is added to the image location to yield a corrected location  $\widehat{m}$  (red circle):

$$\widehat{m} = m + A_1 \widehat{\delta X}_5 + A_2 \widehat{\delta X}_6 + A_3 \widehat{\delta X}_8 + A_4 \widehat{\delta X}_9, \text{ where}$$

$a_k, k = 1, \dots, 4$ , are the scalar non-negative bilinear coefficients that sum to 1 and  $A_k = a_k I_{2 \times 2}$ .

The  $2 \times 2$  error covariance matrix for  $\widehat{m}$  is defined as the bilinear interpolation of the  $2 \times 2$  diagonal blocks in  $C_{\widehat{\delta X}}$  corresponding to  $\widehat{\delta X}_5$ ,  $\widehat{\delta X}_6$ ,  $\widehat{\delta X}_8$ , and  $\widehat{\delta X}_9$ , respectively, and that also corresponds to a mean-value of error equal to zero ( $0_{2 \times 1}$ ). The same bilinear coefficients used for the computation of  $\widehat{m}$  are applicable.

Such a correction and its predicted accuracy are approximate due to the interpolation, but are reasonable. Furthermore, they are virtually optimal if the *a priori* spatial correlation between adjacent corrections in the correction grid is high, approximately 0.9 or higher.

A theoretically optimal correction for an arbitrary location in the image would require an additional augmented correction  $\delta X_k^{**}$ , for each location  $m_k$  in the image of interest, similar to the augmented corrections  $\delta X_l^*$  associated with the optimal solution for the correction vector that were defined earlier. Optimality is defined as the smallest solution errors possible (minimization of the WLS cost function), given the set of available control image measurements, and that includes reliable predicted accuracy.

### D.2.4 Summary: Why a correction grid?

A correction grid with associated *a priori* statistics was selected to represent the adjustment of an image for the effects of incorrect image metadata. The image is assumed to correspond to Commodities data with little or no accuracy pedigree available at the time of image/metadata generation and subsequent (initial) dissemination. Correspondingly, the *a priori* statistics used in the solution for the correction grid are generated per the techniques detailed in Appendix C, and essentially represent the “average” (root-mean-square) effect of underlying sensor pose errors on image location errors across an image. The *a priori* statistics are populated based on sample statistics corresponding to multiple realizations of the type or class of images of interest. The summed effects of other less-dominant underlying sources of error are included and represented as well. In summary, the *a priori* statistics represent image location errors for an arbitrary image from the type or class of images of interest.

The correction grid approach is very general and can account for the summed effects of “deterministic” sensor pose errors, “random” sensor pose/image formation errors (e.g., sensor-mensuration error), and the effects of residual errors associated with possible multiple control procedures applied to the image/metadata by the generator/provider prior to its dissemination to the user community. For an arbitrary, but specific image, these summed effects will typically vary across the image in a systematic manner consistent with spatial correlation – hence, the solution for a grid of corrections across the image.

“Deterministic” sensor pose errors were illustrated in Figures D.1-2 and D.2.1-2 and are essentially the difference between “assumed” and “true” sensor/image pose, where sensor/image pose includes sensor location, attitude, and focal length. Both sets of poses, and therefore the errors in the assumed pose, are deterministic for a given or specific image, and their equivalent effects on image locations in the image are similar for adjacent or near-by locations in the image. However, sensor pose errors and their equivalent effects on image location errors vary from image to image.

Correspondingly, and with respect to the predictive statistics which are applicable to image location errors in an arbitrary image from the type or class of images of interest, errors are considered random. More specifically, they are uncorrelated from image to image and spatially correlated as a function of image-location distance within the same image. This is also true for the practical representation of the summed effects of all error sources listed in the paragraphs above.

The spatial correlation of image location error is represented by an (intra-image) spdcf. The greater the corresponding spatial correlation, the less density required in terms of the number of grid points in the correction grid. The *a priori* spatial correlation and other *a priori* statistics for the image are contained in a populated Geolocation Data Predicted Accuracy Model: Image-space, and are typically tuned based on accuracy assessments (sample statistics of actual errors) corresponding to images from the same type or class of image.

#### **Examples:**

Examples of the correction grid based on simulated data are presented in Section D.3 below including comparisons to corrections based on affine transformations. The latter can better model

“deterministic” sensor pose errors than can a correction grid, but cannot effectively model any of the other sources of error discussed in the paragraphs above.

### **D.3 Correction grid performance and comparison to an affine-transformation based correction**

Section D.2 detailed the generation and use of a correction grid for an image. This section of the appendix details corresponding performance results that were initially discussed in Section 5.3.3.1. An alternate affine transformation-based correction and its performance are also detailed in this appendix that were initially discussed in Section 5.3.3.1 as well. The affine-transformation-based correction can yield better results than a correction grid if errors are known to be consistent with such a transformation, which is not true in general for a Commodities data image.

#### **Correction grid**

The correction grid is used to adjust or correct the image locations of all pixels in an image. It is solved via a WLS solution using conjugate control image measurements or their equivalent. The *a priori* statistics for the correction grid (errors) used in the WLS solution correspond to the predictive statistics contained in the Predicted Accuracy Model: Measurement space, as discussed in Section 5.3.3.1 and as detailed in Section D.2. In particular, the predictive statistics correspond to errors represented as a random field.

The correction grid is the recommended or “baseline” correction or adjustment method for a Commodities data image. It includes the optimal WLS solution variant that includes an augmented state vector as detailed in Section D.2.

#### **Affine-transformation**

An affine transformation is an invertible transformation  $y = Mx + t$  that transforms a vector  $x$  into a vector  $y$ , and can represent a combination of translation, rotation, skew, and two scale factors (see chapter A.4 of reference [15]). Note that for the 2d example discussed in this section, the affine transformation has no skew and only a single scale factor and as such, is also a conformal transformation.

The ground-to-image function for the image may be represented by a ground-to-image polynomial. The image-to-corrected image transformation is represented by the affine transformation. The corrections correspond to errors in the underlying ground-to-image function.

A representative image-to-corrected image affine transformation is as follows using capital  $X$  for the 2d (original) image location and  $(X + \Delta X)$  for its corrected value:

$$X + \Delta X = (1 + s) \begin{bmatrix} 1 & \alpha \\ -\alpha & 1 \end{bmatrix} X + X_0,$$

where  $\alpha$  represents a small angle rotation about the center of the image,  $s$  a scale factor correction, and  $X_0$  a 2d offset correction.

Therefore, the correction itself (not necessarily affine) is represented as:

$$\Delta X \cong \begin{bmatrix} s & \alpha \\ -\alpha & s \end{bmatrix} X + X_0,$$

with a corresponding partial derivative matrix used in a WLS solution for the state parameters  $[s \ \alpha \ x_0 \ y_0]^T$  equal to:

$\frac{\partial \Delta M}{\partial state} = \begin{bmatrix} x & y & 1 & 0 \\ y & -x & 0 & 1 \end{bmatrix}$ , where  $state \equiv [s \ \alpha \ x_0 \ y_0]^T$  and  $\Delta M$  is the difference between conjugate image measurements, one in the “control image” and one in the product image. Note that the image coordinate system  $(x, y)$  has an origin at the center of the image, but that previous plots in this document show the origin at the corner of the image since that is the convention used when illustrating image coordinates in terms of rows and columns.

Note: an affine-based correction model containing only parameter state elements  $x_0$  and  $y_0$  is equivalent to a RPC polynomial correction model for two polynomial offset coefficients. In addition, both are equivalent to a correction grid adjustment model if the latter’s *a priori* spatial correlation of image location errors is specified as very high ( $\geq \approx 0.98$ ) across the image.

### D.3.1 Simulation results

A simulation was performed that generates image errors and then solves for their corrections via a WLS solution using conjugate image measurements. Both the above correction grid and affine solution approach were implemented, i.e., their corresponding corrections and state parameters were solved for via WLS.

#### D.3.1.1 Definitions and *a priori* values

Errors were simulated consistent with either the (*a priori*) predictive statistics in the Geolocation Data Predicted Accuracy Model: Image-space or the (*a priori*) predictive statistics of an Affine-based error model, termed “Pred Acc” and “Affine”, respectively, for convenience.

“Pred Acc” corresponds to a 2x2 error covariance matrix for image-location errors and an spdcf that specifies their spatial correlation across image-space. The spdcf was assumed a scalar isotropic function applicable to both x (image line) and y (image sample) errors across the image as a function of horizontal image-space distance between image locations.

“Affine” corresponds to the standard deviation (sigma) of each of the four elements in the state vector  $[s \ \alpha \ x_0 \ y_0]^T$ , with each of their corresponding errors assumed uncorrelated with the others. A 4 × 4 covariance matrix with the above standard deviations-squared down the diagonal is equivalent. Note that both the “Affine” as well as the “Pred Acc” errors are reasonably assumed to have mean-values equal to zero and to be Gaussian distributed.

Errors were corrected based on two different WLS solutions: (1) one for a correction grid and termed “cor grid” with *a priori* uncertainty assumed consistent with the above “Pred Acc” error model, and (2) one for the affine parameter  $state \equiv [s \ \alpha \ x_0 \ y_0]^T$  and termed “affine” with *a priori* uncertainty assumed consistent with the above “Affine” error model.

The actual predictive statistics for the two error models are specifiable in the pseudo-code (presented later in this appendix), and are equal to the following:

**“Pred Acc”:**

$$cov = \begin{bmatrix} \sigma^2 & 0 \\ 0 & \sigma^2 \end{bmatrix} = \begin{bmatrix} 20^2 & 0 \\ 0 & 20^2 \end{bmatrix} \text{ pixels-squared,}$$

and spdcf represented as a CSM four parameter spdcf, with corresponding parameters equal to

$A = 1$  (unit-less),  $\alpha = \beta = 0$ , and  $D = 10$  or  $20$  grid units,

where a grid unit is one-fifth the width (distance) of the image in this simulation. A grid unit is also equal to the distance between adjacent corrections in the  $6 \times 6$  correction grid also assumed applicable to the “cor grid” solution. Therefore, if the image is  $25k \times 25k$  pixels, a grid unit is equal to  $5k$  pixels.

Note that the correlation of errors between two image locations is equal to  $\rho(dist) = Ae^{-dist/D}$ , where  $dist$  is the distance between the two geolocations in grid units. Thus, if distance is equal to the distance between two adjacent corrections in the correction grid and  $D = 10$ ,  $\rho(dist) = (1.0)e^{-0.1} \cong 0.90$ . If  $D = 20$ ,  $\rho(dist) = (1.0)e^{-0.05} \cong 0.95$ .

Also, the value of  $A$  is sometimes set to a value slightly less than 1, such as 0.98, in order to approximate the contributions of “sensor-mensuration” error, if applicable, and/or to put a lower limit on pre and post-solution relative accuracy (sigma) between two image locations that are very close together.

**“Affine”:**

$$cov\_affine\_state = \begin{bmatrix} 4^2 & 0 & 0 & 0 \\ 0 & 6^2 & 0 & 0 \\ 0 & 0 & 12^2 & 0 \\ 0 & 0 & 0 & 12^2 \end{bmatrix}, \text{ with corresponding } a \text{ priori standard deviations of error for}$$

the affine state vector parameters  $s$ ,  $\alpha$ ,  $x_0$ , and  $y_0$  equal to 4 pixels/grid unit, 6 pixels/grid unit, 12 pixels, and 12 pixels, respectively.

### ***D.3.1.2 Specific results***

The simulation (image realization) was performed 200 times or “trials” for each applicable combination of the above. Errors were generated independently for image-location errors (or affine state errors, as applicable) and for conjugate measurement errors for each of the 200 realizations.

A specified number of measurements was also generated for each realization, with control image errors consistent with a standard deviation of 1 pixel for each image coordinate and assumed independent for convenience. The locations of the conjugate measurements in the image were also generated randomly for each realization.

Results are categorized assuming two different degrees of spatial correlation when actual errors correspond to the “Pred Acc” error model:  $D = 10$  and  $D = 20$ . The latter corresponds to somewhat higher spatial correlation or similarity of image location errors across the image, although both are reasonable and their applicability dictated by accuracy assessments of different images from the same class or type of image of interest. Also, regardless the actual error model (“Pred Acc” vs “Affine”), the “cor grid” solution method (correction grid) assumes the appropriate value for  $D$ . Note that the sensitivity of results to this and other assumption is address in Section D.1.3.

### ***D.3.1.3 Distance constant specifies relatively high spatial correlation***

Results are presented in Table D.3.1.3-1 for a 6x6 grid of check points that align with the “cor grid” solution’s correction grid for convenience, and where “pred sigma” is the corresponding *a posteriori* standard deviation of error (predicted accuracy) based on the corresponding WLS solution. Results are presented in terms of image radial location errors, i.e., the root-sum-square of image x (line) errors with image y (sample) errors with units of pixels. A value of the distance constant  $D = 20$  grid units was used to simulate (actual) errors if they were specified to be consistent with “Pred Acc” and was also used in the WLS “cor grid” solution if applicable.

**Table D.3.1.3-1:** Monte-Carlo results regarding image location radial errors and their predicted accuracy (sigma); root-mean-square results in pixels over 200 simulated independent realizations per actual error model and corresponding to a 6x6 check point grid;  $D = 20$  grid units

Actual Error Model	# conjugate msmnts	Pre-soln errors (pixels)	Post- soln errors: cor grid (pixels)	Post-soln errors: affine (pixels)	Post-soln pred sigma: cor grid (pixels)	Post-soln pred sigma: affine (pixels)
"Pred Acc"	5	27.8	9.3	11.7	9.2	1.2
	15	28.4	6.9	10	6.8	0.6
	150	28.2	3.9	9.2	3.8	0.2
"Affine"	5	24.8	10.4	1.2	9.2	1.2
	15	23.7	4.6	0.6	6.9	0.6
	150	24.5	1.4	0.2	3.9	0.2

Note the sensitivity of post-solution errors to the number of randomly located conjugate measurements.

The following presents examples of specific realizations of the above corresponding to actual errors consistent with “Pred Acc” followed by those consistent with “Affine”. 15 conjugate measurements at random locations in the image (circles) are applicable for each realization. As a reminder, the errors consistent with “Pred Acc” correspond to a random field. Pre-adjustment and post-adjustment 2d errors are represented by blue and red 2d vectors or quivers, respectively, across a grid of check points in the plots that follow.

**Actual Error Model: “Pred Acc”**

In the following, the actual error model used to generate image errors in the realization was “Pred Acc”.

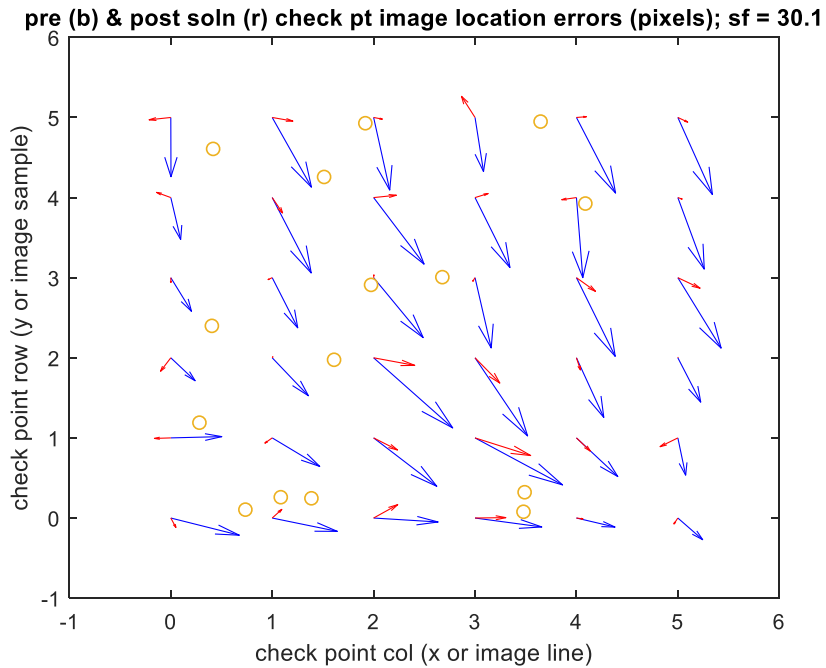


**Figure D.3.1.3-1:** WLS solution “cor grid” applicable; largest image location radial error equals 30.1 pixels

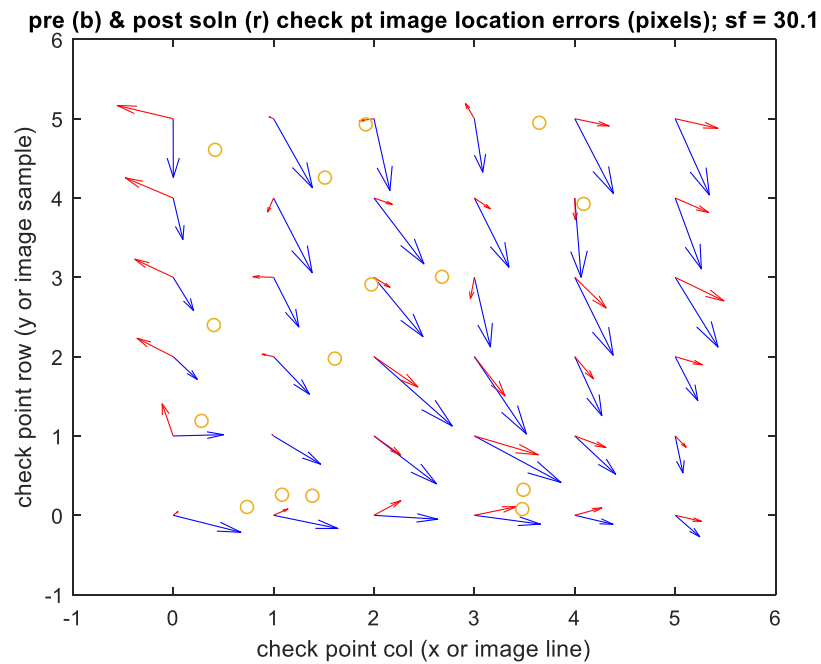


**Figure D.3.1.3-2:** WLS solution “affine” applicable; largest image location radial error equals 30.1 pixels; same realization of errors and measurements as in Figure D.3.1.3-1

### Actual Error Model: Affine

In the following, the actual error model used to generate image errors in the realization was “Affine”.

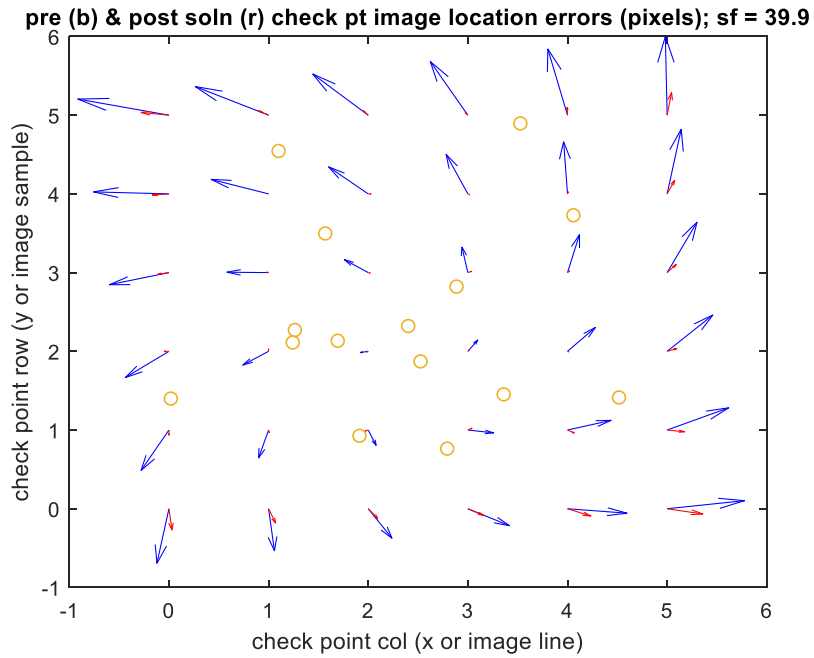


**Figure D.3.1.3-3:** WLS solution “cor grid” applicable; largest image location radial error equals 39.9 pixels

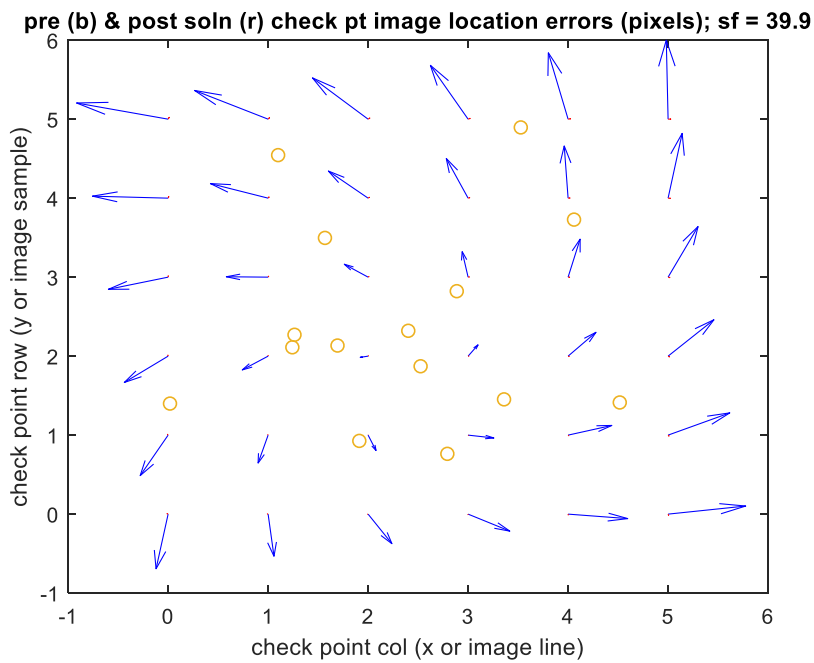


**Figure D.3.1.3-4:** WLS solution “affine” applicable; largest image location radial error equals 39.9 pixels; same realization of errors and measurements as in Figure D.3.1.3-3

As illustrated in Figure D.3.1.3-4, the “affine” WLS solution performed extremely well when errors were consistent with its assumed error model and its predictive statistics.

As illustrated in Figure D.3.1.3-3, the “cor grid” solution performed reasonably well. Note that its *a priori* predictive statistics only statistically approximate the “Affine” errors. In particular, the spdcf approximates well the spatial correlation of errors that are within a few distance units apart but does not de-correlate all the way to negative values that are possible for errors 5-7 grid units apart, i.e., in opposite “quadrants” in the above figures. This is particular true if “Affine” errors (realizations) correspond to large-valued scale and/or rotational errors.

#### ***D.3.1.4 Distance constant specifies lower spatial correlation***

Results are presented in Table D.3.1.4-1 for a 6x6 grid of check points that align with the “cor grid” solution’s correction grid for convenience, and where “pred sigma” is the corresponding *a posteriori* standard deviation of error (predicted accuracy) based on the corresponding WLS solution. Results are presented in terms of image radial location errors, i.e., the root-sum-square of image x (line) errors with image y (sample) errors with units of pixels. A value of the distance constant  $D = 10$  grid units was used to simulate (actual) errors if they were specified to be consistent with “Pred Acc” and also used in the WLS “cor grid” solution if applicable. The reduction of the distance constant  $D$  from 20 to 10 grid units corresponds to a lower degree of spatial correlation.

**Table D.3.1.4-1:** Monte-Carlo results regarding image location radial errors and their predicted accuracy (sigma); root-mean-square results in pixels over 200 simulated independent realizations per actual error model and corresponding to a 6x6 check point grid;  $D = 10$  grid units

Actual Error Model	# conjugate msmnts	Pre-soln errors (pixels)	Post- soln errors: cor grid (pixels)	Post-soln errors: affine (pixels)	Post-soln pred sigma: cor grid (pixels)	Post-soln pred sigma: affine (pixels)
"Pred Acc"	5	28.2	13.8	17.5	13.5	1.2
	15	28.7	9.9	13.7	9.9	0.6
	150	28.2	5.6	13.0	5.6	0.2
"Affine"	5	23.2	9.4	1.2	13.2	1.2
	15	24.7	5.1	0.6	10.0	0.6
	150	23.2	1.5	0.2	5.6	0.2

The following presents examples of specific realizations corresponding to actual errors corresponding to “Pred Acc” followed by those corresponding to “Affine”. Again, 15 conjugate measurements at random locations in the image are applicable for each realization and errors are presented across a grid of check points.

**Actual Error Model: “Pred Acc”:**

In the following, the actual error model used to generate image errors in the realization was “Pred Acc”.

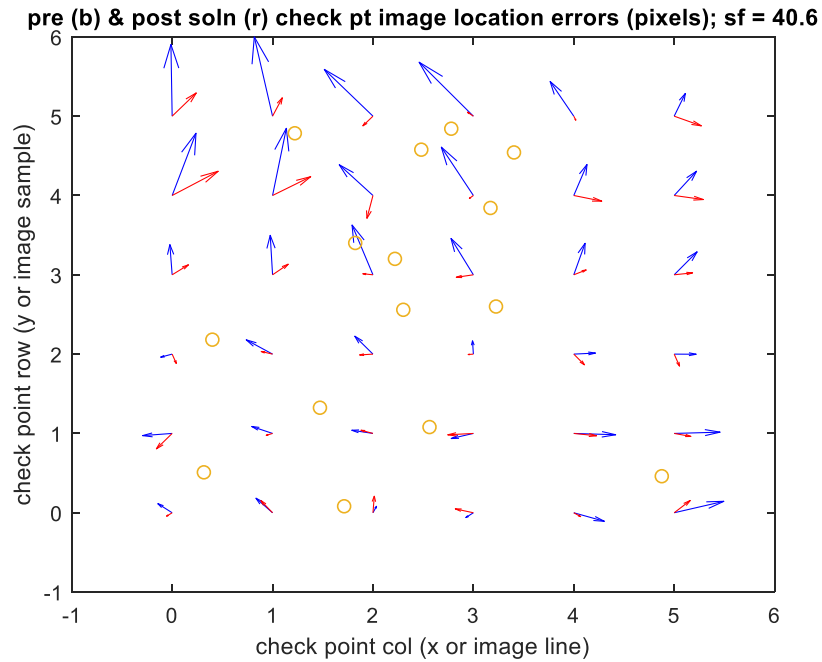


**Figure D.3.1.4-1:** WLS solution “cor grid” applicable; largest image location radial error equals 40.6 pixels

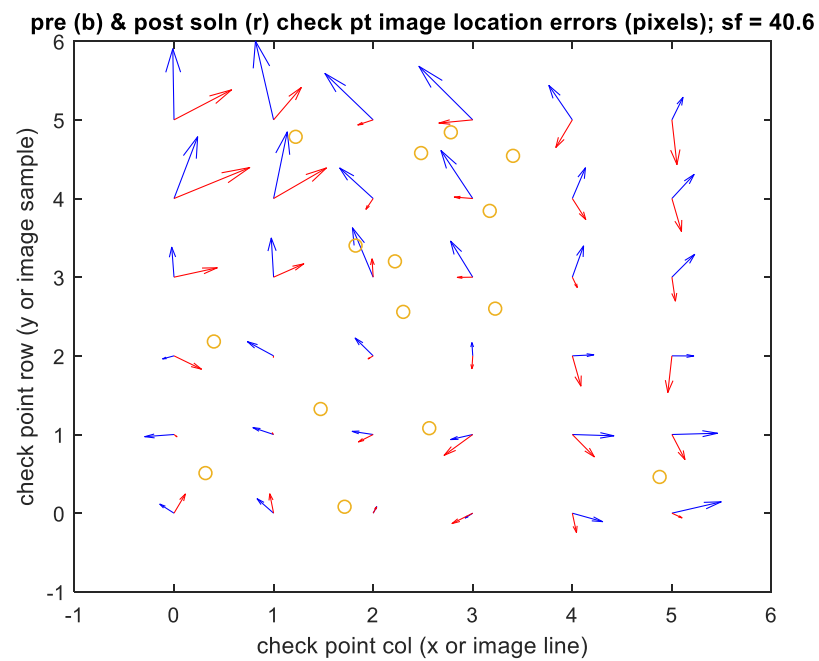


**Figure D.3.1.4-2:** WLS solution “affine” applicable; largest image location radial error equals 40.6 pixels; same realization of errors and measurements as in Figure D.3.1.4-1.

Figures D.3.1.4-3 and D.3.1.4-4 present the same scenario as above but for a different realization. This particular realization was very difficult for the “affine” WLS solution to solve for (correct) as seen in Figure D.3.1.4-4. The actual errors were consistent with “Pred Acc” and were in direct “contradiction” in this particular realization to the WLS solution’s assumed *a priori* affine error model.

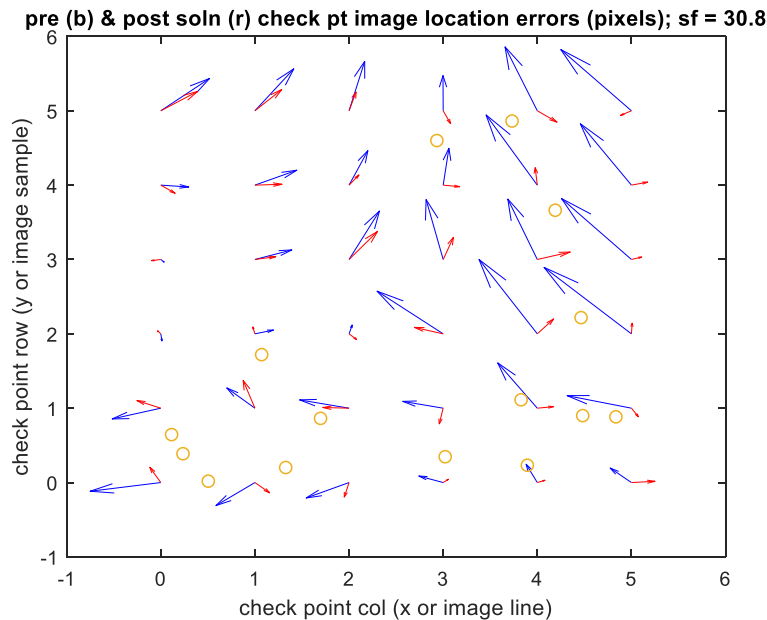


**Figure D.3.1.4-3:** WLS solution “cor grid” applicable; largest image location radial error equals 30.8 pixels

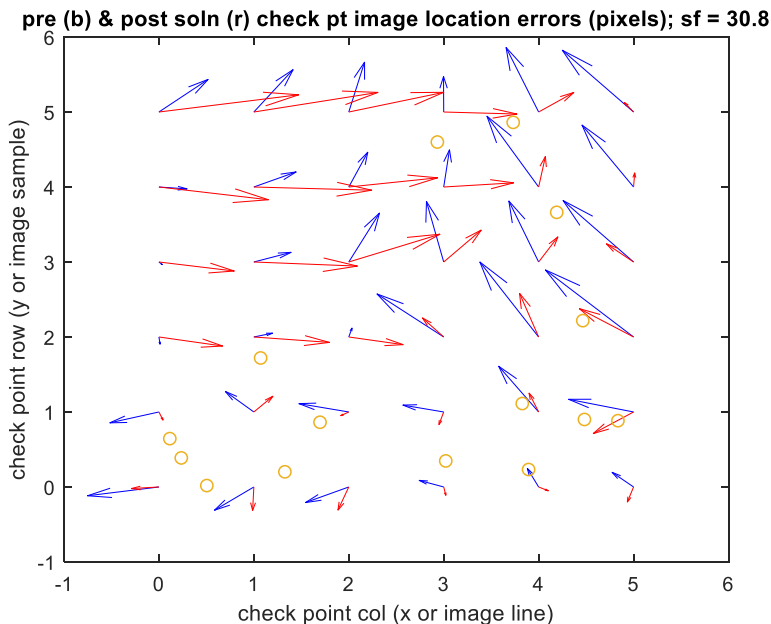


**Figure D.3.1.4-4:** WLS solution “affine” applicable; largest image location radial error equals 30.8 pixels; same realization of errors and measurements as in Figure D.3.1.4-3.

**Actual Error Model: Affine**

In the following, the actual error model used to generate image errors in the realization was “Affine”.

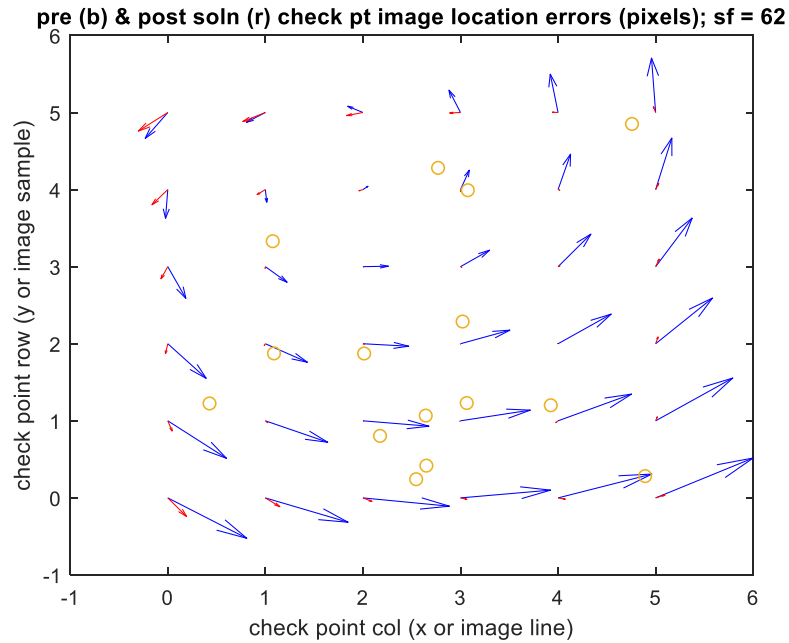


**Figure D.3.1.4-5:** WLS solution “cor grid” applicable; largest image location radial error equals 62.0 pixels

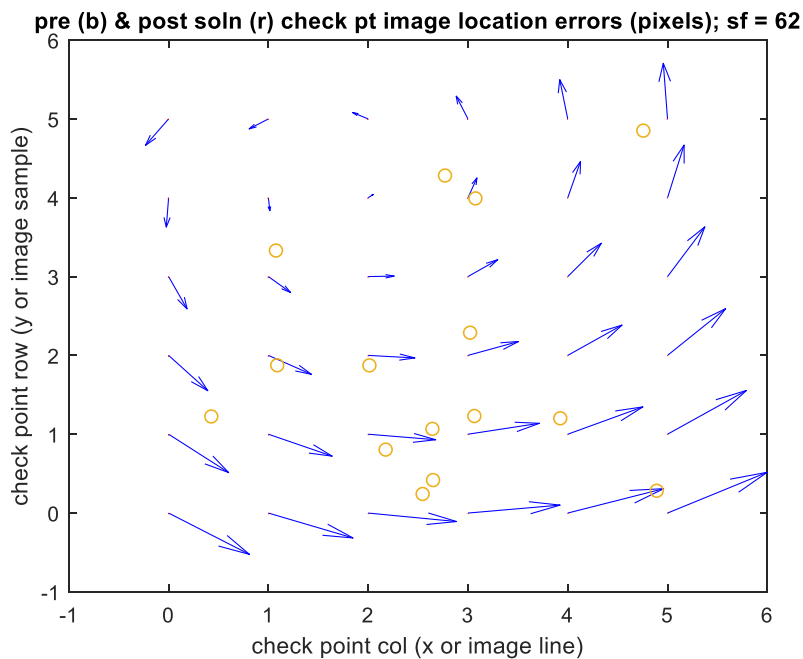


**Figure D.3.1.4-6:** WLS solution “affine” applicable; largest image location radial error equals 62.0 pixels; same realization of errors and measurements as in Figure D.1.2.2-5.

### Affine pros and cons regarding solution observability:

As illustrated in Figure D.3.1.4-6, the “affine” WLS solution performed extremely well when actual errors are affine. This is also applicable to the corresponding Monte-Carlo results present in both Tables D.3.1.3.1-1 and D.3.1.4-1. In particular, relatively few control measurements are needed to get an accurate solution. This is due to “high” solution observability since the actual errors and solution error model correspond to deterministic but unknown parameters (e.g., affine state vector parameters  $s$ ,  $\alpha$ ,  $x_0$ , and  $y_0$ ), as opposed to non-deterministic or “random” corrections corresponding to the correction grid. This is also true for other deterministic correction models that are more general than the affine four parameter model. However, for Commodities data, these deterministic models are not known to be applicable in general, and therefore, the correction grid approach or “cor grid” is more robust.

### D.3.2 Sensitivities of the baseline “cor grid” solution method

The following presents sensitivities of the “cor grid” solution method to various parameters. The actual error model is “Pred Acc” for all cases.

Table D.3.2-1 presents solution performance as a function of *a priori* spatial correlation, with 15 randomly located conjugate measurements assumed and the *a priori* model used in the “cor grid” WLS solution modeled consistent with the actual error model “Pred Acc”.

**Table D.3.2-1:** Monte-Carlo Results regarding image location radial errors and their predicted accuracy (sigma) corresponding to the “cor grid” WLS solution; root-mean-square results in pixels over 200 simulated independent realizations per the actual error Model “Pred Acc” and a 6x6 check point grid; the value of *a priori* spatial correlation ( $D$ ) is parameterized, and applicable to both “Pred Acc” and the WLS solution “cor grid”.

Actual Error Model	Spdcf distance constant $D$ (grid units)	correlation at 1 grid unit	correlation at 7 grid units	Pre-soln errors (pixels)	Post- soln errors: cor grid (pixels)	Post-soln pred sigma: cor grid (pixels)
"Pred Acc"	D=5	0.82	0.25	28.2	12.8	13
	D=10	0.9	0.5	28.7	9.9	9.9
	D=20	0.95	0.7	28.0	6.7	6.8
	D=40	0.975	0.84	29.0	5.1	5
	D=100	0.99	0.93	29.4	3.2	3.2
	D=10000	0.9999	0.9998	29.0	0.6	0.6

As seen in Table D.3.2-1, the higher the spatial correlation of errors, the better the solution results. The corresponding degree of spatial correlation is specified by the value of the distance constant  $D$ . This value is assumed to be made available by the Predicted Accuracy Model: Image-space based on sample statistics of error from previous accuracy assessments of the same type of class of image.

Typical values of  $D$  correspond to  $D = 10$  through  $D = 20$ . These values are also “tunable” via the size of the correction grid specified as part of the “cor grid” solution process, i.e., the above value of  $D$  is

expressed in terms of grid units. That is, the  $D$  in the predicted accuracy model may be specified in terms of pixel distance and then converted to grid units by the solution process, where the size of the correction grid is specified in order to ensure a reasonable amount of spatial correlation between adjacent grid points. However, it should be noted that high solution performance is also predicated on a reasonable number of conjugate measurements – the lower the spatial correlation across the grid, the more measurements desired.

Table D.3.2-2 presents analytic results that illustrate the effects of spatial correlation on the degree to which pre-solution errors are systematic. This is done via the computation of corresponding pre-solution relative (radial) error between two arbitrary locations in the image separated by a specified distance, where relative error is defined as  $rel\_error = \sqrt{(\epsilon x_1 - \epsilon x_2)^2 + (\epsilon y_1 - \epsilon y_2)^2}$ . The table actually tabulates the analytic computation of the square root of the expected value of  $rel\_error$  or “rel sigma”, also termed “relative uncertainty”.

As seen in the table, even with high *a priori* spatial correlation, there is still appreciable variation in errors at different locations in the image. Correlation has to increase to greater than 0.99 at a distance of 1 grid unit apart before relative errors in the image become negligible, consistent with errors across the image that are literally a bias, albeit a different bias for each realization or image. This is consistent with the flexibility and practicality of the correction grid and with the representation of underlying errors as a random field. Note that a distance of 7 grid units in the table is approximately the diagonal distance across the assumed square image.

**Table D.3.2-2:** Analytic results showing sensitivity of relative uncertainty to the spdcf distance constant  $D$

Actual Error Model	Spdcf distance constant $D$ in grid units	correlation at 1 grid unit	correlation at 7 grid units	analytic abs sigma (pixels)	analytic rel sigma (pixels) at 1 grid unit	analytic rel sigma (pixels) at 7 grid units
"Pred Acc"	$D \rightarrow 0$	$\rightarrow 0$	$\rightarrow 0$	28.3	$\rightarrow 40.0$	$\rightarrow 40.0$
	$D=5$	0.82	0.25	28.3	17.0	34.6
	$D=10$	0.9	0.5	28.3	12.7	28.2
	$D=20$	0.95	0.7	28.3	8.9	21.9
	$D=40$	0.975	0.84	28.3	6.3	16.0
	$D=100$	0.99	0.93	28.3	4.0	10.6
	$D=10000$	0.9999	0.9998	28.3	0.4	0.5
	$D \rightarrow \text{infinity}$	$\rightarrow 1$	$\rightarrow 1$	28.3	$\rightarrow 0$	$\rightarrow 0$

Finally, Table D.3.2-3 presents Monte Carlo results of the sensitivity of the performance of the “cor grid” solution method to the validity of its assumed *a priori* predictive statistics. 15 randomly located conjugate measurements were assumed in each of 200 independent realizations per case (assumed vs actual error model pair).

**Table D.3.2-3:** Monte Carlo results (rms) regarding the sensitivity of solution results to correct *a priori* modeling of errors in the “cor grid” WLS solution process

Actual sigma (pixels)	Actual D (grid units)	WLS: cor grid assumed sigma (pixels)	WLS: cor grid assumed D (grid units)	Pre-soln errors (pixels)	Post- soln errors: cor grid (pixels)	Post-soln pred sigma: cor grid (pixels)
20	10	20	10	28.6	9.6	9.6
20	10	20	5	29.0	9.8	13.2
20	10	20	20	28.4	9.6	6.8
20	10	10	10	28.1	9.5	4.8
20	10	40	10	28.9	9.7	18.9

As illustrated in the table, post-solution errors are virtually invariant for the range of *a priori* mismodeling considered, but the solution’s *a posteriori* or predicted accuracy is not, as expected.

In addition, regardless the assumed values of sigma and *D*, image location errors are still assumed to correspond to a homogeneous random field, i.e., (*a priori*) predictive statistics, whatever their correct values, are assumed invariant across the image. In addition, the results in Table D.3.2-3 are also predicated on the assumption that the spatial correlation of errors is reasonably consistent with a CSM four parameter spdcf with the value of the major parameter, distance constant *D*, possibly incorrect.

### D.3.3 Summary and conclusions

The correction grid or “cor grid” solution method worked well and was robust in all circumstances with one exception: solution predicted accuracy (sigma) was not reliable if the *a priori* predictive statistics were significantly different than their actual counterparts, as is to be expected. Also, the higher the *a priori* spatial correlation between adjacent points in the correction grid and the greater the number of conjugate measurements or the better located the measurements (not random), the better the actual solution accuracy or errors.

The “affine” solution was less robust, but performed very well if actual errors were “Affine” and consistent with the solution’s *a priori* predictive statistics. If the actual errors were not consistent with the solution’s *a priori* predictive statistics, the solution predicted accuracy was extremely unreliable and optimistic in particular. Perhaps future applied research of a “hybrid” solution approach that combines “cor grid” with “affine” is warranted in appropriate circumstances. In the interim, the “cor grid” approach is recommended for Commodities data with little or no reliable accuracy pedigree.

As a final comment, only absolute errors corresponding to the adjusted image were addressed. Detailed quantification of relative error awaits further applied research. However, based on the figures presented throughout appendix D and an informal comparison of the degree of similarity for 2d post-adjustment errors (red vectors or quivers) in the same image as a measure of relative accuracy, relative error appears reasonably small for the baseline adjustment method, even when the true error model is affine. Note

that relative error between two locations in an image is the difference between their red quivers in the corresponding figure.

### **Simulation: MATLAB Pseudo-Code**

The following presents non-optimized MATLAB code ("pseudo-code") that was used to generate the simulation results presented earlier in this appendix:

```
%"TGD2f_grid_vs_affine"

%23 November 2018

%This program compares the performance of a correction grid vs an affine
%transformation-based correction for an image using simulated errors and
%measurements

%Actual errors correspond to either "grid" or "affine", i.e., the actual
%error model is selectable

%Implemented correction approach corresponds to either "grid" or "affine", and
%both are implemented below as separate solutions/corrections, but share
%the same measurement errors and image (systematic) errors for valid
%performance comparisons

%grid corrections use "optimal" extended parameters approach

%check points correspond to grid points, regardless the selected
%correction approach.

%check point errors and predicted accuracies are to be plotted, including
%quiver plots of before/after adjustment; Monte Carlo statistics are also
%computed over multiple realizations of the simulation/solutions

%only 1 product (image) is applicable and ground control points are applicable,
%the latter's "pred stats" are input

%The pred stats for measurement errors are input

%number of measurements specified and underlying locations (nominally)
%randomly generated

%grid assumed square and number of points specified per grid row for
%simplicity

%size of square AOI specified in grid units (width)

%All distance units are in number of "grid units". All error units are in
%pixels for simplicity.

%Note: in an actual application, there would be a deterministic
%relationship between pixels and grid units, e.g. a 25k x 25k pixel image
```

```
%with a 6x6 correction grid has 5k pixels per grid unit, which is the
%distance in pixels between adjacent grid points; if an affine
%transformation, there are no grid points per se but they are applicable
%below as check points

% DEFINITIONS OF INPUT PARAMETERS:

%AOI_width: width of square AOI in grid units

%n_grid_pts_row: number of grid points in one direction (rows) of a square
%correction grid

%n_meas: the number of conjugate (product-control point)measurements

%error_flag: 1 (grid) or 2 (affine) for actual error model

%(both soln approaches always performed for comparison)

%pred_sigmas: for corrections and/or actual errors, as applicable, 2x1
%vector for x (line) and y (sample) errors

%spdcf: for corrections and/or actual errors, as applicable, scalar
%function for both image line (x) and sample (y) coordinates errors, a
%function of horizontal distance (isotropic spdcf); if a CSM four parameters
%model,2 parameters defining the spdcf (A and D), otherwise linear decay with
%specified zero crossing distance

%pred_sigma_cntrl: as above but for control points with independent errors
%between control points for simplicity

%affine_sigma: sigmas for 4 affine parameter errors
%(s, alpha,x0,y0, rotations and scale relative to AOI center

%meas_sigma: common sigma for all components of all measurement (mensuration)
%errors

%print_flag: detailed print flag (value of 1 specifies print is enabled)

%specify inputs:

%Monte_Carlo Option:
MC_flag=1
MC_real=200    %specified number of independent realizations

error_flag=1 %1 specifies grid (MGRF) type error model, 2 an affine-type error
model
plot_cntrl_flag=1    %1 specifies plot location of cntrl pts too (in grid units)

print_flag=0
```

```

AOI_width=5      %grid units
n_grid_pts_row=6
n_meas=15
meas_sigma=1     %pixels

if(print_flag==1)    %reduce size of outputs for better intuition/"debug"
AOI_width=2
n_grid_pts_row=3
n_meas=2
end

if(MC_flag==1)
print_flag=0;
end

pred_sigma=zeros(2,1);    %Correction grid model sigmas (pixels) (note:
%Correction grid model consists of predictive stats that corresponds to a
%homogeneous 2D random field in image-space
pred_sigma(1,1)=20;
pred_sigma(2,1)=20;

spdcf=zeros(2,1);    %Correction grid model spdcf (assumed CSM four parameter
model
%with alpha and beta equal to zero)
spdcf(1,1)=1;    %(A unitless)
spdcf(2,1)=10;    %(D in grid units)
spdcf

pred_sigma_cntrl=zeros(2,1);    %control point error sigma (standard deviation)
pred_sigma_cntrl(1,1)=0.25;    %pixels
pred_sigma_cntrl(2,1)=0.25;

affine_sigma=zeros(4,1);    %sigmas for affine systematic errors

affine_sigma(1,1)=4;    %pixels/grid unit    (scale factor)
affine_sigma(2,1)=6;    %pixels/grid unit    (rotation)
affine_sigma(3,1)=12;    %pixels    (x or image line offset)
affine_sigma(4,1)=12;    %pixels    (y or image sample offset)

affine_sigma

%DERIVED PARAMETERS, PREDICTIVE (A PRIORI) STATS, ERRORS, ETC.:

n_cntrl_pts=n_meas
n_grid_pts=n_grid_pts_row^2    %also number of check points
n_grid_extended_pts=n_grid_pts+n_cntrl_pts

pred_cov=zeros(2,2);
pred_cov(1,1)=pred_sigma(1,1)^2;
pred_cov(2,2)=pred_sigma(2,1)^2;
pred_cov

```

```

pred_cov_cntrl=zeros(2,2);
pred_cov_cntrl(1,1)=pred_sigma_cntrl(1,1)^2;
pred_cov_cntrl(2,2)=pred_sigma_cntrl(2,1)^2;
pred_cov_cntrl

rms_radial_pre_soln_errors=0; %initialize ensemble statistics for Monte Carlo
rms_radial_errors_grid=0;
rms_radial_errors_affine=0;
rms_radial_sigmas_grid=0;
rms_radial_sigmas_affine=0;

%LOOP OVER REALIZATIONS

if(MC_flag~=1)
    MC_real=1;
end

for mm=1:MC_real    %loop over realizations

%generate image locations for grid (check) points:

Loc_X_grid=zeros(2,n_grid_pts);
temp=1;
kk=AOI_width/(n_grid_pts_row-1);

for i=1:n_grid_pts_row    %y coordinate
    for j=1:n_grid_pts_row    %x coordinate
        Loc_X_grid(1,temp)=kk*(j-1);
        Loc_X_grid(2,temp)=kk*(i-1);
        temp=temp+1;
    end
end

%generated image locations for (conjugate) cntrl points:
%(NOTE: don't "select" cntrl point locations that are identical to grid pt
%locations otherwise a priori covariance matrix containing all points is not
%positive definite (invertible), i.e., has eigenvalues equal to zero; not an
issue if a random selection as done below)

Loc_X_cntrl=zeros(2,n_cntrl_pts);

for i=1:n_cntrl_pts
    Loc_X_cntrl(1,i)=AOI_width*rand(1,1);
    Loc_X_cntrl(2,i)=AOI_width*rand(1,1);
end

if(print_flag==1)
    Loc_X_grid
    Loc_X_cntrl

```

```

end

%generate a priori cov (Cov_1) for actual errors for corection grid (check pts)
%plus extended (cntrl pts), i.e. n_grid_extended; assumes errors are consistent
%with "grid"or MGRF model

%remember check pts are grid pts; a priori cov applicable for use in the soln
%too as described later, i.e., actual errors are generated consistent with
%the a priori predictive statistics

n=n_grid_extended_pts;

Cov_1=zeros(2*n,2*n);
Loc_X=zeros(2*n,1);    %put all locations of interest in one vector;
                        %grid followed by (conjugate) cntrl

temp=1;
for i=1:n_grid_pts
    Loc_X(temp,1)=Loc_X_grid(1,i);
    Loc_X(temp+1,1)=Loc_X_grid(2,i);
    temp=temp+2;
end

for i=n_grid_pts+1:n
    j=i-n_grid_pts;
    Loc_X(temp,1)=Loc_X_cntrl(1,j);
    Loc_X(temp+1,1)=Loc_X_cntrl(2,j);
    temp=temp+2;
end

if(print_flag==1)
    Loc_X
end

for i=1:n
    for j=1:n
        tempi=2*(i-1)+1;
        tempj=2*(j-1)+1;
        dist=sqrt( (Loc_X(tempi,1)-Loc_X(tempj,1))^2 +...
            (Loc_X(tempi+1,1)-Loc_X(tempj+1,1))^2 );
        for k=1:2
            for l=1:2
                Cov_1(k+tempi-1,l+tempj-1)=pred_cov(k,l)*spdcf(1,1)*...
                    exp(-dist/spdcf(2,1));
            end
        end
    end
end

%generate a priori cov (Cov 2) for actual affine errors; use first part of
%cov for solution process per se if applicable (project to image locations
%of interest later):

Cov_2=zeros(4,4);

```

```

for i=1:4
    Cov_2(i,i)=affine_sigma(i,1)^2;
end

if(print_flag==1)
    Cov_1
    Cov_2
    eig_Cov_1=eig(Cov_1)
    eig_Cov_2=eig(Cov_2)
end

%generated actual errors (Gaussian distributed) based on Cov_1:

Errors_via_Cov_1=sqrtm(Cov_1)*randn(2*n,1);

%generate actual errors (Gaussian distributed) based on Cov_2:

Errors_via_Cov_2=sqrtm(Cov_2)*randn(4,1);

%as a hard coded "option" to the above, can set above errors to deterministic
%values instead

if(print_flag==1)
    Errors_via_Cov_1
    Errors_via_Cov_2
end

%for affine errors, generate corresponding errors at all locations of interest,
%i.e., check pt (grid) locations followed by cntrl pts

n_loc_affine=n_grid_extended_pts;

Loc_X_affine=Loc_X;

Errors_proj_via_Cov_2=zeros(2,n_loc_affine); %second index is location (pt) id

temp_error_matrix=Errors_via_Cov_2(1,1)*eye(2);
temp_error_matrix(1,2)=Errors_via_Cov_2(2,1);
temp_error_matrix(2,1)=-temp_error_matrix(1,2);

temp_vec=zeros(2,1);

temp_vec(1,1)=Errors_via_Cov_2(3,1);
temp_vec(2,1)=Errors_via_Cov_2(4,1);

temp_vec_1=zeros(2,1);

B_partials_temp=zeros(2,4);

B_partials=zeros(2,4,n_loc_affine); %second index is location (pt) id

%center of grid:

```

```

center=zeros(2,1);
center(1,1)=AOI_width/2;
center(2,1)=center(1,1);

for i=1:n_loc_affine

    tempi=2*(i-1)+1;
    temp_vec_1(1,1)=Loc_X_affine(tempi,1);
    temp_vec_1(2,1)=Loc_X_affine(tempi+1,1);
    temp_vec_1=temp_vec_1-center;
    temp_vec_2=temp_error_matrix*temp_vec_1;
    Errors_proj_via_Cov_2(1,i)=temp_vec_2(1,1)+temp_vec(1,1);
    Errors_proj_via_Cov_2(2,i)=temp_vec_2(2,1)+temp_vec(2,1);

    %go ahead and compute partial derivatives of measurements wrt affine
    %parameters used in solution for affine corrections later

    B_partials_temp(1,1)=temp_vec_1(1,1);
    B_partials_temp(1,2)=temp_vec_1(2,1);
    B_partials_temp(1,3)=1;
    B_partials_temp(1,4)=0;
    B_partials_temp(2,1)=temp_vec_1(2,1);
    B_partials_temp(2,2)=-temp_vec_1(1,1);
    B_partials_temp(2,3)=0;
    B_partials_temp(2,4)=1;

    for j=1:2
        for k=1:4
            B_partials(j,k,i)=B_partials_temp(j,k); %third index is location
(pt) id
        end
    end

end

if(print_flag==1)
    Errors_proj_via_Cov_2
    B_partials
end

%generate covariance for (sum of) mensuration errors for cntrl point
%and their conjugate locations in the image:

Cov_meas=meas_sigma^2*eye(2*n_cntrl_pts);

%generate covariance for cntrl points systematic errors:

Cov_cntrl=zeros(2*n_cntrl_pts,2*n_cntrl_pts);

for i=1:n_cntrl_pts
    for j=1:2
        for k=1:2
            Cov_cntrl((i-1)*2+j,(i-1)*2+k)=pred_cov_cntrl(j,k);
        end
    end
end

```

```

    end
end

%generated covariance for (total) measurement errors:

Cov_meas_total=Cov_meas+Cov_cntrl;

%generate measurement errors:

Meas_errors=sqrtm(Cov_meas_total)*randn(2*n_cntrl_pts,1);

if(print_flag==1)
    Cov_meas_total
    Meas_errors
end

%generate measurements (differences) for inputs into WLS, a function of
%measurement errors, and image errors based on either grid or affine,
%as applicable;

%get image errors (only) too at check pts for use later

Errors_cntrl=zeros(2*n_cntrl_pts,1);
temp=n_grid_pts;
Errors_check=zeros(2*temp,1);

if(error_flag==1)    %assume grid error model

%recall that Cov_1 relects grid pts followed by cntrl pts

for i=1:n_cntrl_pts
Errors_cntrl(2*(i-1)+1,1)=Errors_via_Cov_1(2*temp+2*(i-1)+1,1);
Errors_cntrl(2*(i-1)+2,1)=Errors_via_Cov_1(2*temp+2*(i-1)+2,1);
end

for i=1:temp
Errors_check(2*(i-1)+1,1)=Errors_via_Cov_1(2*(i-1)+1,1);
Errors_check(2*(i-1)+2,1)=Errors_via_Cov_1(2*(i-1)+2,1);
end

end

if(error_flag==2)    %assume affine errors

%recall that projected errors based on Cov 2 are explictly indexed by
%location (pt) id unlike those based on Cov_1 above

for i=1:n_cntrl_pts
Errors_cntrl(2*(i-1)+1,1)=Errors_proj_via_Cov_2(1,i+temp);
Errors_cntrl(2*(i-1)+2,1)=Errors_proj_via_Cov_2(2,i+temp);
end

for i=1:temp

```

```

Errors_check(2*(i-1)+1,1)=Errors_proj_via_Cov_2(1,i);
Errors_check(2*(i-1)+2,1)=Errors_proj_via_Cov_2(2,i);
end

end

%remember, a priori pred errors are equal to zero

delta_M=Errors_cntrl+Meas_errors;

if(print_flag==1)
    Cov_meas_total
    Meas_errors
    Errors_cntrl
    delta_M
end

%PERFORM (both) WLS SOLUTIONS:

W=Cov_meas_total^-1;

%correction grid solution

A_priori_cov=Cov_1;

B=zeros(2*n_cntrl_pts,2*n_grid_extended_pts);

temp=2*n_grid_pts;
for i=1:2*n_cntrl_pts
    B(i,temp+i)=1;
end

Cov_X_cor=(A_priori_cov^-1+B'*W*B)^-1;
delta_X_cor=Cov_X_cor*B'*W*delta_M;

Sigma_X_cor=zeros(2*n_grid_extended_pts,1);
for i=1:2*n_grid_extended_pts
    Sigma_X_cor(i,1)=sqrt(Cov_X_cor(i,i));
end

if(print_flag==1)
    B
end

%affine correction

A_priori_cov=Cov_2;

B=zeros(2*n_cntrl_pts,4);

temp=n_grid_pts;

for i=1:n_cntrl_pts

```

```

    temp1=(i-1)*2;
    for j=1:2
        for k=1:4
            B(temp1+j,k)=B_partials(j,k,temp+i);
        end
    end
end

Cov_X_aff=(A_priori_cov^-1+B'*W*B)^-1;
delta_X_aff=Cov_X_aff*B'*W*delta_M;

Sigma_X_aff=zeros(4,1);
for i=1:4
    Sigma_X_aff(i,1)=sqrt(Cov_X_aff(i,i));
end

if(print_flag==1)
    B
end

if(mm==1) %first realization - some detailed print
    delta_X_cor
    Sigma_X_cor
    %Cov_X_cor
    delta_X_aff
    Sigma_X_aff
    %Cov_X_aff
end

%COMPUTE PRE-SOLUTION ERRORS AT CHECK POINTS

%remember applicable errors are check (grid) pts are a function of error_flag,
%i.e., errors are either consistent with grid errors or affine errors

Pre_soln_errors=Errors_check;

if(mm==1)
    Pre_soln_errors
end

%APPLICABLE CORRECTED ERRORS (POST SOLUTION) AND A POSTERIORI COV AT CHECK
POINTS:

% do for each solution

%grid (extended) solution, stored in single vector

Post_soln_errors_grid=zeros(2*n_grid_pts,1);

for i=1:2*n_grid_pts
    Post_soln_errors_grid(i,1)=Pre_soln_errors(i,1)-delta_X_cor(i,1);
end

Sigma_soln_errors_grid=zeros(2*n_grid_pts,1);

```

```

for i=1:2*n_grid_pts
    Sigma_soln_errors_grid(i,1)=Sigma_X_cor(i,1);
end

if(mm==1)
    Post_soln_errors_grid
    Sigma_soln_errors_grid
end

%affine solution (more complicated, have to computed projected errors and
%sigma); store in single vector:

Post_soln_errors_affine=zeros(2*n_grid_pts,1);

delta_X_affine_proj=zeros(2*n_grid_pts,1);

B_temp=zeros(2,4);

for i=1:n_grid_pts
    temp1=(i-1)*2;
    for j=1:2
        for k=1:4
            B_temp(j,k)=B_partials(j,k,i);
        end
    end
    temp_proj=B_temp*delta_X_aff;
    delta_X_affine_proj(temp1+1,1)=temp_proj(1,1);
    delta_X_affine_proj(temp1+2,1)=temp_proj(2,1);
end

if(print_flag==1)
    delta_X_affine_proj
end

for i=1:2*n_grid_pts
    Post_soln_errors_affine(i,1)=Pre_soln_errors(i,1)-delta_X_affine_proj(i,1);
end

if(mm==1)
    Post_soln_errors_affine
end

%computed corresponding a perteriori covariance (sigmas) as well

Sigma_soln_errors_affine=zeros(2*n_grid_pts,1);

B_temp=zeros(2,4);

for i=1:n_grid_pts
    temp1=(i-1)*2;
    for j=1:2
        for k=1:4
            B_temp(j,k)=B_partials(j,k,i);
        end
    end
end

```

```

end
cov=B_temp*Cov_X_aff*B_temp';
Sigma_soln_errors_affine(temp1+1,1)=sqrt(cov(1,1));
Sigma_soln_errors_affine(temp1+2,1)=sqrt(cov(2,2));
end

%PERFORM PLOTS:

%plot pre and post solution errors at grid (check) points for both solution
%methods (same actual error model); do quiver plots

if(mm==1)
plot_grid_image(Pre_soln_errors,Post_soln_errors_grid,...
    n_grid_pts_row,1,Loc_X_cntrl,n_cntrl_pts,plot_cntrl_flag)

plot_grid_image(Pre_soln_errors,Post_soln_errors_affine,...
    n_grid_pts_row,2,Loc_X_cntrl,n_cntrl_pts,plot_cntrl_flag)
end

for k=1:n_grid_pts    %sum ensemble statistics

    rms_radial_pre_soln_errors=rms_radial_pre_soln_errors+...
        Errors_check(2*(k-1)+1,1)^2+Errors_check(2*(k-1)+2,1)^2;

    rms_radial_errors_grid=rms_radial_errors_grid+...
        Post_soln_errors_grid(2*(k-1)+1,1)^2+Post_soln_errors_grid(2*(k-
1)+2,1)^2;

    rms_radial_errors_affine=rms_radial_errors_affine+...
        Post_soln_errors_affine(2*(k-1)+1,1)^2+Post_soln_errors_affine(2*(k-
1)+2,1)^2;

    rms_radial_sigmas_grid=rms_radial_sigmas_grid+...
        Sigma_soln_errors_grid(2*(k-1)+1,1)^2+Sigma_soln_errors_grid(2*(k-
1)+2,1)^2;

    rms_radial_sigmas_affine=rms_radial_sigmas_affine+...
        Sigma_soln_errors_affine(2*(k-
1)+1,1)^2+Sigma_soln_errors_affine(2*(k-1)+2,1)^2;

end

end    %end realization loop

total=MC_real*n_grid_pts;    %compute/output final ensemble sample stats
rms_radial_pre_soln_errors=sqrt(rms_radial_pre_soln_errors/total)
rms_radial_errors_grid=sqrt(rms_radial_errors_grid/total)
rms_radial_error_affine=sqrt(rms_radial_errors_affine/total)
rms_radial_sigmas_grid=sqrt(rms_radial_sigmas_grid/total)
rms_radial_sigmas_affine=sqrt(rms_radial_sigmas_affine/total)

```

```

function[] = plot_grid_image(errors_grid_pre,errors_grid_post, ...
n_grid_pts_row,fcn_number,cntrl_loc,n_c,plot_cntrl_flag)

x=zeros(n_grid_pts_row,n_grid_pts_row);
y=zeros(n_grid_pts_row,n_grid_pts_row);
u=zeros(n_grid_pts_row,n_grid_pts_row);
v=zeros(n_grid_pts_row,n_grid_pts_row);
temp=0;
max_uv=0;



```

%pre-solution errors

    for i=1:n_grid_pts_row
        for j=1:n_grid_pts_row
            x(i,j)=j-1;
            y(i,j)=i-1;
            u(i,j)=errors_grid_pre(temp+1,1);
            v(i,j)=errors_grid_pre(temp+2,1);
            maxu=abs(u(i,j));
            maxv=abs(v(i,j));
            if (maxu>max_uv)
                max_uv=maxu;
            end
            if (maxv>max_uv)
                max_uv=maxv;
            end
            temp=temp+2;
        end
    end

    for i=1:n_grid_pts_row
        for j=1:n_grid_pts_row
            u(i,j)=u(i,j)/max_uv;
            v(i,j)=v(i,j)/max_uv;
        end
    end

    %actual errors are max_uv larger
    r_max_uv=round(max_uv,1);
    figure(fcn_number)
    clf
    scale=0;

    quiver(x,y,u,v,scale,'b');

    xlabel('check point col (x or image line)');
    ylabel('check point row (y or image sample)');
    title(['pre (b) & post soln (r) check pt image location errors (pixels); sf = ',...
        num2str(r_max_uv)]);

    %post-solution errors:
    hold on
    temp=0;

```


```

```

for i=1:n_grid_pts_row
    for j=1:n_grid_pts_row
        x(i,j)=j-1;
        y(i,j)=i-1;
        u(i,j)=errors_grid_post(temp+1,1)/max_uv;
        v(i,j)=errors_grid_post(temp+2,1)/max_uv;
        temp=temp+2;
    end
end

quiver(x,y,u,v,scale,'r');

if(plot_cntrl_flag==1)
x=zeros(n_c,1);
y=zeros(n_c,1);
for i=1:n_c
    x(i,1)=cntrl_loc(1,i);
    y(i,1)=cntrl_loc(2,i);
end
scatter(x,y);
end

hold off

end

```

## Appendix E: MGRF representation and adjustment of Geolocation Products

This appendix details a Mixed Gaussian Random Field (MGRF) associated with a Geolocation Product Predicted Accuracy Model, typically for the representation of the predicted accuracy of a 3d geolocation  $X$  and the predicted relative accuracy between two geolocations  $X_1$  and  $X_2$  contained in the product. This appendix also details product adjustment for improved accuracy based on a correction grid and an MGRF representation of predicted accuracy.

The application and detailed definitions of the MGRF in support of a geolocation product were developed as applied research and were part of the overall development of this document.

This appendix was referenced in Section 5.3.3.3 (“Mixed Gaussian Random Field”) of the main body of this document, where an overview of an MGRF was presented and two important caveats were also made regarding an MGRF and this appendix:

- An MGRF is the recommended core component of a predicted accuracy model for geolocation products, but its implementation is optional. If not implemented, the “standard” predicted accuracy model for a geolocation product is implemented which models errors as a single homogeneous random field as detailed in Appendix B.

- The “standard” predicted accuracy model is also equivalent to an MGRF with only one partition, as defined later in this appendix.
- This appendix (Appendix E) concentrates on the overall concept of an MGRF, its corresponding predictive statistics and their mathematical derivations, and the recommended metadata or its equivalent that contains the predictive statistics. It also discusses the use of these predictive statistics by the “down-stream” user/application, including support for the adjustment of the geolocation product for improved accuracy. However, although this appendix outlines methods for the population of an MGRF based on a populated accuracy assessment, i.e., how to compute the actual values of its predictive statistics, it does not detail these methods.
  - See Appendix B for methods and their details for the population a “standard” predicted accuracy model. They are based on the use of a corresponding populated accuracy assessment model generated using sample statistics of geolocation error. Section B.5.2 also discusses extension of these methods to an MGRF.

Now that the charter of Appendix E has been introduced, its sections are outlined as follows:

- E.1 Preliminaries: Statistics corresponding to Random Variables and Random Vectors
- E.2 Mixed Gaussian Random Fields (MGRF): Descriptive Contents and *a priori* Statistics
  - E.2.1 Geolocation errors represented as a Random Field
  - E.2.2 Geolocation errors corresponding to Partitions in the MGRF
  - E.2.3 Geolocation errors corresponding to arbitrary geolocations in the MGRF
  - E.2.4 Optional Generalizations
  - E.2.5 Computation of scalar accuracy metrics
  - E.2.6 Summary of relevant MGRF statistical terminology/symbology
- E.3 Adjustability of the MGRF (product)
- E.4 Concept of Operations using MGRF with examples
- E.5 Recommended MGRF metadata content-format associated with a geolocation product
- E.6 Summary

Sections E.1 and E.2 include mathematical derivations, analytic examples, and graphics related to MGRF *a priori* or predictive statistics of the geolocation error  $\epsilon X$ .

Section E.3 discusses the optional adjustment or correction of an MGRF (product), possibly when fusing its information with other products. The latter not only provides for improved product accuracy, but consistent geolocations across the products as well.

Section E.4 presents a recommended Concept of Operations for the representation of the predicted accuracy of a geolocation product based on MGRF, i.e., for the population of a Geolocation Product Predicted Accuracy Model and its receipt/use by a “down-stream” user/application. It includes examples for insight; in particular, simulation-based realizations or product “instances” of geolocation errors associated with product geolocations.

Section E.4 also briefly discusses the relationship of an MGRF-based representation of predicted accuracy with corresponding and previous accuracy assessments that consist of sample statistics of geolocation

error that are used to initially populate and subsequently tune the predicted accuracy model. The similarities between the MGRF-based representation of predicted accuracy with the Generic Point Cloud Model (GPM) is also discussed, the latter preferred but typically unavailable for External Data used in the NSG; hence, the recommended use of MGRF.

Section E.5 presents an overview of recommended MGRF metadata content or its equivalent applicable to predicted accuracy, i.e., essentially the contents of a populated Geolocation Product Predicted Accuracy Model.

Section E.6 provides a summary of features regarding the use of MGRF for the representation or modeling of predicted accuracy for a geolocation product. It also includes recommended future applied research.

Readers are encouraged to first read Section 5.3.3.3 in the main body of this document for an overview of an MGRF and its representation of predicted accuracy prior to reading this appendix. Following this, those readers not interested in mathematical details and the definitions of the various predictive statistics may also skip Sections E.1-E.3 of this appendix, if so desired.

Although the mathematical details and definitions regarding the various predictive statistics associated with the representation of product accuracy via MGRF are somewhat detailed/complex as presented in Sections E.1-E.3, Appendix F presents MATLAB code that calculates virtually all of them.

To close out this introduction, Figures E-1 and E-2 present an example of a realization of a random field of 3d geolocation errors over a portion of a 3d geolocation product, where an MGRF of interest consists of one or more such random fields and their combinations in various partitions of the product as detailed later. Figure E-1 represents vertical errors as a heat plot over a horizontal tangent plane (grid) in the product's "footprint".

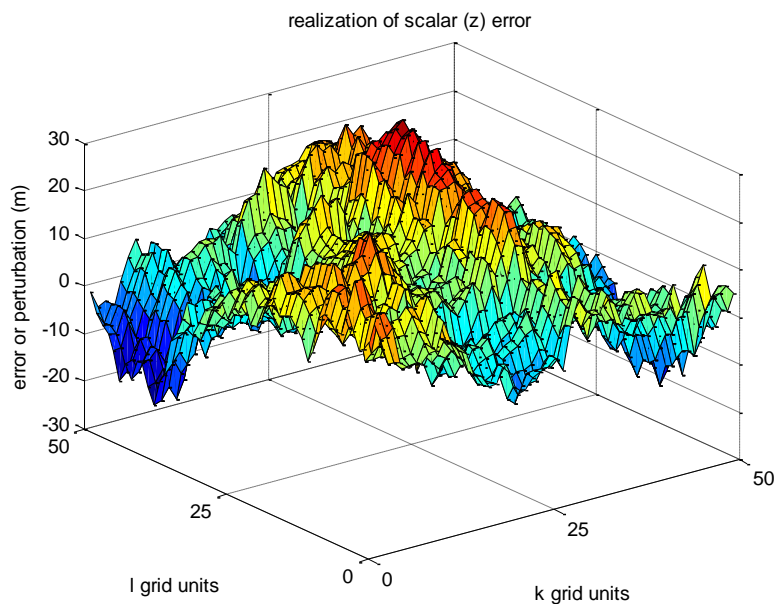


**Figure E-1:** Simulated vertical errors corresponding to a portion of a 3d geolocation product

Figure E-2 represents horizontal errors as an automatically scaled quiver plot (red vectors are interpolated values). Note the spatial correlation (similarity) of nearby errors in each plot, the degree of which is specifiable by *a priori* statistics on a per error component basis in the product's metadata. See TGD 2e (Monte Carlo Simulation) regarding details of the simulation technique used to generate the realization.

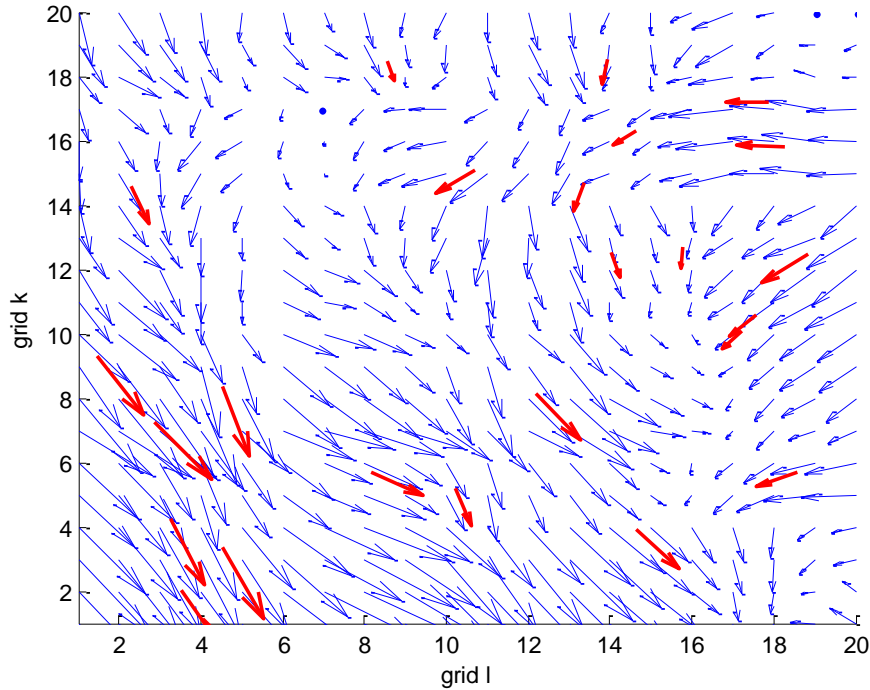


**Figure E-2:** Simulated horizontal errors corresponding to a portion of a 3d geolocation product

Geospatial errors are correlated between geolocation in the same or specific realization of a geolocation product. They are modelled as uncorrelated between different realizations, as is reasonable. A key feature of the MGRF representation of predicted accuracy is its appropriate representation of the spatial correlation of errors – necessary for optimal use of the product and for reliable predicted accuracies.

## E.1 Preliminaries: Statistics corresponding to random variables and random vectors

This section of the appendix provides an overview of random variables and random vectors as background information prior to the description of an MGRF. In general, an MGRF is a collection of random vectors.

Furthermore, this section is recommended to all, even to those familiar with statistics and probability in order to introduce relevant terminology/symbology used throughout this appendix:

Assume that the  $k \times 1$  error  $\epsilon X$  corresponds to the  $k \times 1$  geolocation  $X$  ( $1 \leq k \leq 3$ ) with coordinates aligned with a Local Tangent Plane (LTP) coordinate system, such as East North Up (ENU). Define the corresponding *a priori* statistics for the Gaussian distributed random vector  $\epsilon X$ :

mean-value of error  $\bar{X} \equiv E\{\epsilon X\}$ , where  $E\{\}$  corresponds to expected value; (E.1-1)

covariance matrix about the mean  $C_X \equiv E\{(\epsilon X - \bar{X})(\epsilon X - \bar{X})^T\}$ ; (E.1-2)

multivariate Gaussian distribution with probability density function  $pdf$ , (E.1-3)

$pdf(\epsilon X) \equiv ((2\pi)^k |C_X|)^{-1/2} e^{-1/2(\epsilon X - \bar{X})^T C_X^{-1} (\epsilon X - \bar{X})}$ , and where  $|C_X|$  is the determinant of  $C_X$ ;

corresponding cumulative distribution function  $cdf$ ,

$cdf(\epsilon X^*) \equiv \iiint_{-\infty}^{\epsilon X^*} pdf(\epsilon X) d\epsilon X$ , where the limits of integration apply to all (up to 3) (E.1-4)

integrals, and where  $cdf(\epsilon X^*) = prob(\epsilon X \leq \epsilon X^*)$

Note that in general, regardless the specific type of probability distribution:

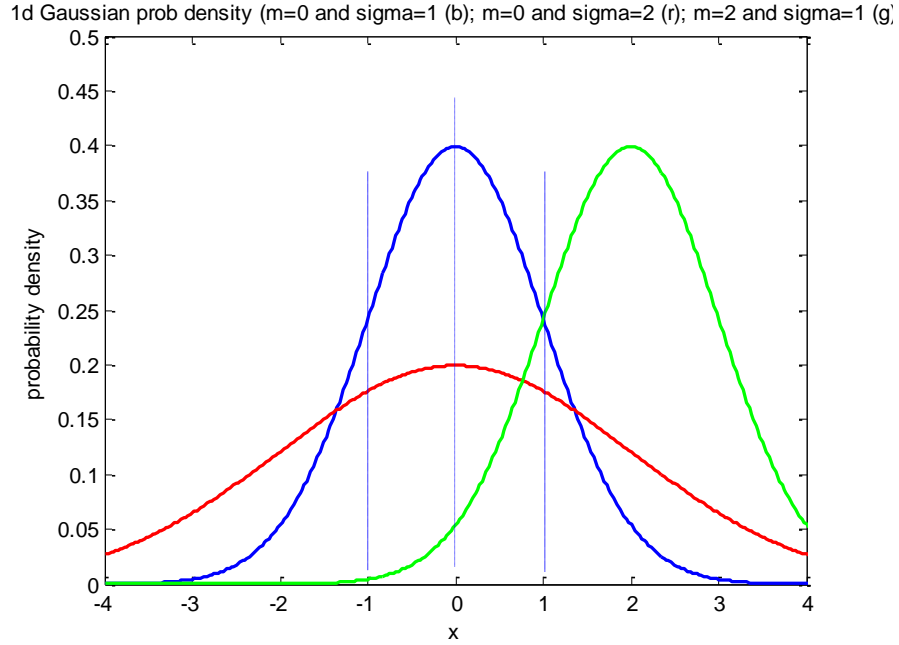
$\bar{X} = E\{\epsilon X\} = \iiint_{-\infty}^{\infty} \epsilon X pdf(\epsilon X) d\epsilon X$ , a  $k \times 1$  vector, and (E.1-5)

$C_X = E\{(\epsilon X - \bar{X})(\epsilon X - \bar{X})^T\} = \iiint_{-\infty}^{\infty} (\epsilon X - \bar{X})(\epsilon X - \bar{X})^T pdf(\epsilon X) d\epsilon X$ , a  $k \times k$  matrix. (E.1-6)

Some of the above notation drops the “error symbol”  $\epsilon$  corresponding to  $\epsilon X$  for convenience, e.g.,  $C_X$  actually corresponds to  $C_{\epsilon X}$ . Also, even though  $pdf$  and  $cdf$  are functions of a random vector, their resultant values are scalars. And since we assume that  $\epsilon X$  is Gaussian distributed, both  $pdf$  and  $cdf$  are completely characterized by the random vector’s mean-value and covariance matrix.

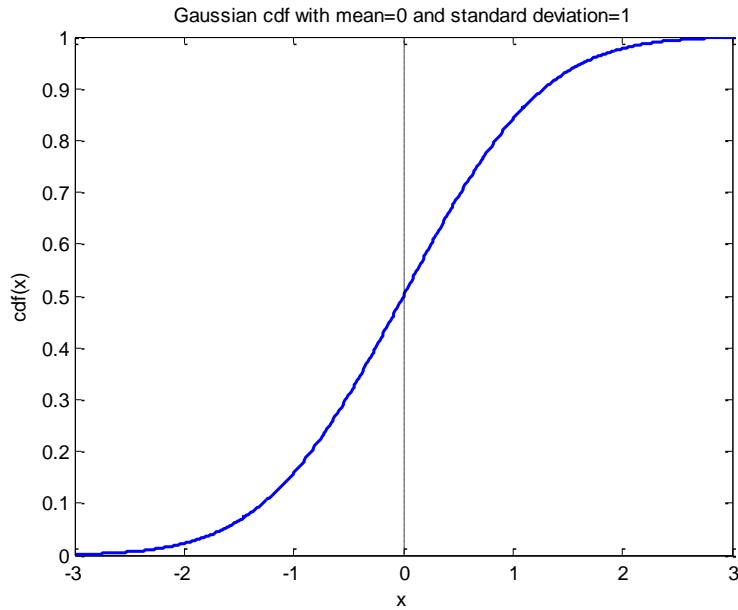
The  $k \times 1$  random vector  $\epsilon X$  is a vector of  $k$  random variables. For example, if  $k = 3$ ,  $\epsilon X = \begin{bmatrix} \epsilon x \\ \epsilon y \\ \epsilon z \end{bmatrix}$ . Thus, if  $k = 1$ , the random vector  $\epsilon X$  is also a random variable, either  $\epsilon x$ ,  $\epsilon y$ , or  $\epsilon z$ , as specified.

Figure E.1-1 presents three different probability density functions ( $pdfs$ ) for a Gaussian (normally) distributed random variable  $\epsilon X = \epsilon x$ , each with a specified mean-value  $\bar{X} = m$  and covariance matrix  $C_X = [\sigma^2]$ . For convenience in the figure’s axis labels and titles,  $\epsilon x$  corresponds to  $x$ , and  $\sigma$  (standard deviation) to sigma.



**Figure E.1-1:** Probability density functions (*pdfs*) for the random variable  $\epsilon x$ ; blue {m=0, sigma=1}, red {m=0, sigma=2}, green {m=2, sigma=1};  $pdf(\epsilon x)$  corresponds to probability density (unit-less/meters) versus  $\epsilon x$  (meters), where  $\epsilon x \equiv x$  in the figure

Figure E.1-2 presents the cumulative distribution function *cdf* corresponding to the first *pdf* (blue) in Figure E.1-1.



**Figure E.1-2:** Cumulative distribution function for a random variable  $\epsilon x$ ;  $cdf(\epsilon x)$  corresponds to the probability (unit-less) that  $\epsilon x \leq \epsilon x^*$  (meters), where  $\epsilon x^* \equiv x$  in the figure

Figure E.1-3 presents the probability density function (*pdf*) for a Gaussian (normally) distributed random vector  $\epsilon X = \begin{bmatrix} \epsilon x \\ \epsilon y \end{bmatrix}$ , with a specified mean-value  $\bar{X} = \begin{bmatrix} 0 \\ 0 \end{bmatrix}$  and covariance matrix  $C_X = \begin{bmatrix} \sigma_1^2 & \rho\sigma_1\sigma_2 \\ \rho\sigma_1\sigma_2 & \sigma_2^2 \end{bmatrix} = \begin{bmatrix} 1 & 0 \\ 0 & 1 \end{bmatrix}$ . Again, the convention in this appendix is that  $\epsilon x$  and  $\epsilon y$  correspond to  $x$  and  $y$  in the figure.

2d Gaussian prob density (means = 0, sigmas = 1, correlation between x and y = 0)

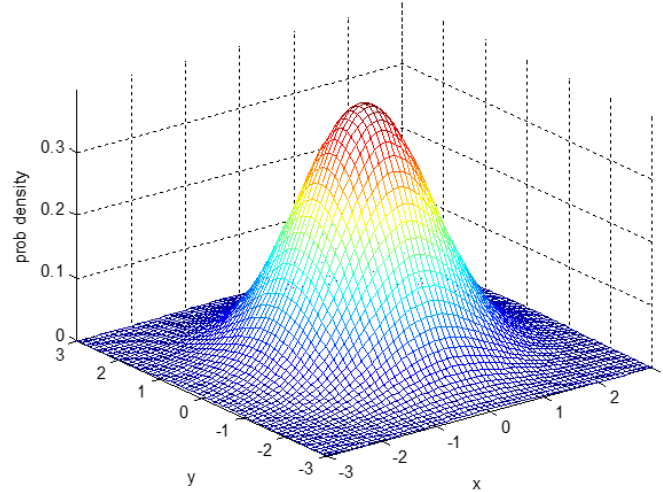


**Figure E.1-3:** Probability density function for a 2d multivariate random vector

Figure E.1-4 presents the probability density function for the same case except that there is high positive correlation between the error components  $\epsilon x$  and  $\epsilon y$ , i.e., the correlation coefficient  $\rho = 0.98$ .

2d Gaussian prob density (means = 0, sigmas = 1, correlation between x and y = 0.98)

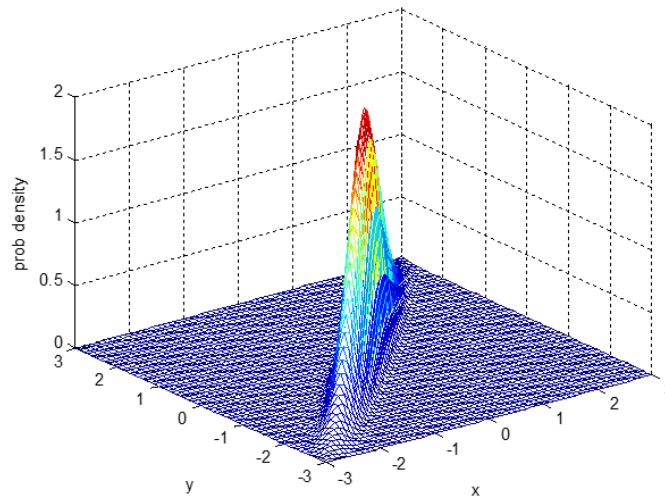


**Figure E.1-4:** Probability density function for a 2d multivariate random vector with high correlation between its two components.

Note that the type of correlation illustrated above is generally termed “intra-state vector” correlation in these Technical Guidance Documents (TGDs), and differs from “inter-state vector” correlation, discussed later in this appendix corresponding to spatial correlation. See TGD 1 (Overview and Methodologies) for more details regarding types of correlation. See TGD 2a (Predictive Statistics) and TGD 2b (Sample Statistics) for further details regarding multivariate statistics.

In addition, the above multivariate Gaussian probability density function  $pdfs$  and cumulative distribution function  $cdfs$ , are available in the MATLAB Statistics and Machine Learning toolbox via “mvnpdf” and “mvncdf”, respectively. A multivariate Gaussian mixture probability density function  $gmpdf$  and cumulative distribution  $gmcdf$ , discussed later, are also available in the same toolbox via “pdf(gm,X)” and “cdf(gm,X)”, respectively.

No toolbox is needed in MATLAB for a scalar random variable, i.e., for  $k \times 1 \in X$ , where  $k = 1$  and corresponding to either  $\epsilon x$ ,  $\epsilon y$ , or  $\epsilon z$  in our application. The corresponding  $pdf$  and  $cdf$  are available via “pdf” and “cdf”, respectively.  $gmpdf$  and  $gmcdf$  are not directly available. Although, not as convenient, multivariate counterparts to all of the above can also be generated without a toolbox in MATLAB by the creation of functions and the numerical integration of functions.

## E.2 Mixed Gaussian Random Field (MGRF): Descriptive content and *a priori* statistics

We now consider a Mixed Gaussian Random Field (MGRF) corresponding to errors  $\epsilon X$  of geolocations  $X$  contained within a 3d geolocation product (aka “product”).

A Mixed Gaussian Random Field is defined by two key entities: (1) a specified collection of random fields and (2) a specified collection of partitions.

An individual random field is a collection of random vectors  $\epsilon X$  indexed by their corresponding geolocation  $X$ . These random vectors are spatially correlated. That is, two geolocations in the same realization (product instance) contain similar errors – the closer together the two geolocations are, the more similar the errors. An individual error  $\epsilon X$  is also assumed Gaussian distributed. See TGD 1 (Overview and Methodologies) for an introduction to random fields.

A collection of random fields corresponds to from 1 to  $n$  independent (uncorrelated) random fields, each random field defined over the entire product. Each random field represents geolocation errors via a set of predictive statistics.

A collection of partitions corresponds to from 1 to  $q$  partitions. Each geolocation in the product is associated with one and only one partition. Each partition also has an *a priori* probability of occurrence that specifies the approximate probability that an arbitrary geolocation in the product corresponds to that particular partition.

In addition, each partition corresponds to a subset of the random fields within the collection of random fields, as specified by a Random Field-to-Partition Mapping: partition  $m$  corresponds to random fields  $m_k$ ,

$k = 1, \dots, q_m$ , where  $q_m \leq n$ . The geolocations associated with partition  $m$  contain errors corresponding to a sum of  $q_m$  independent (uncorrelated) errors, one from each of the specified random fields  $m_k$ .

The recommended (baseline) Random Field-to-Partition Mapping for the representation of predicted accuracy for a geolocation product is detailed as follows and graphically summarized in Figure E.2-1:

- Geolocation errors corresponding to geolocations associated with the first partition,  $Part_1$ , solely correspond to the first random field,  $RF_1$ ;
- Geolocation errors corresponding to geolocations associated with the second partition,  $Part_2$ , correspond to random fields  $RF_1$  and  $RF_2$ ;
- ...
- Geolocation errors corresponding to geolocations in  $Part_n$  correspond to  $RF_1$  and  $RF_n$ .
- Note that the number of partitions  $q$  is equal to the number of random fields  $n$ , i.e.,  $q = n$ , in the baseline approach.

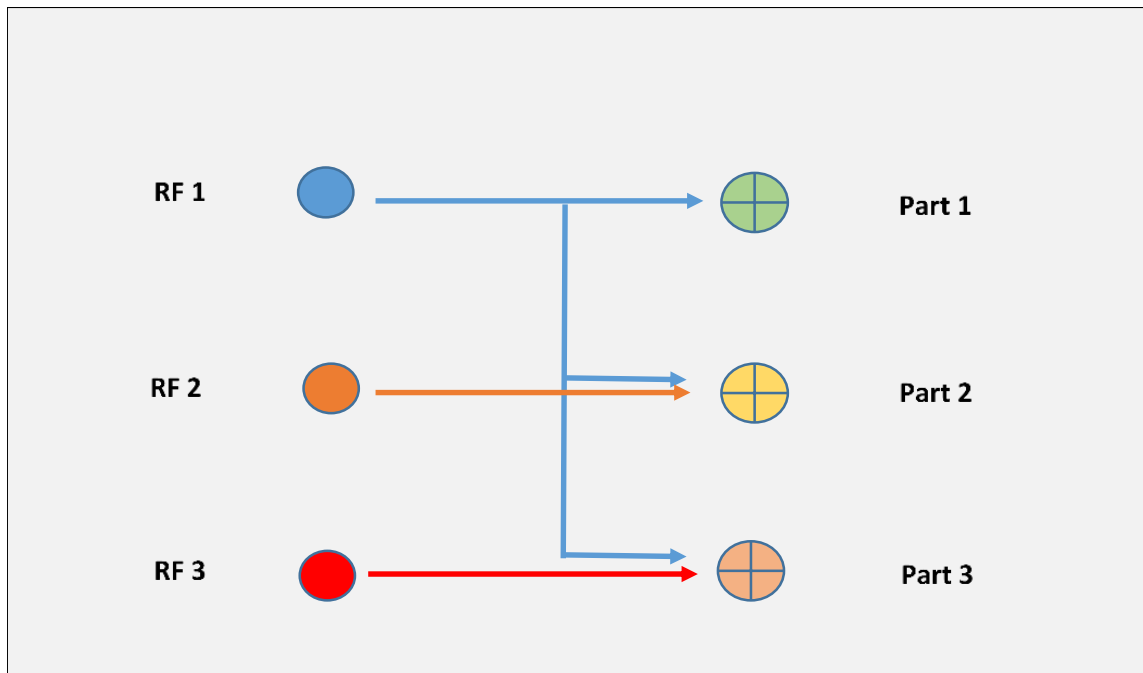


Figure E.2-1: The Baseline Random Field-to-Partition Mapping assuming three partitions

In particular, all geolocations in the MGRF contain errors characterized by  $RF_1$ . Geolocations associated with  $Part_1$  contain errors that are solely characterized by  $RF_1$ . Geolocations associated with partition  $Part_m$ ,  $1 < m \leq n$ , contain the sum of two uncorrelated geolocation errors, one characterized by  $RF_1$  and the other characterized by  $RF_m$ . Random Field  $RF_1$  corresponds to “product-wide” systematic errors. The other random fields contain “additive errors”, usually associated with problem areas in the product’s generation.

Partition  $Part_1$  is defined to consist of all geolocations not associated with any of the other partitions and is termed the “nominal partition”. Typically, most geolocations in the product are associated with the nominal partition.

The MGRF predictive statistics include the approximate *a priori* probabilities that an arbitrary geolocation in the product realization is contained in each of the  $n$  partitions, i.e., there are  $n$  probabilities that sum to 1. However, the corresponding partition for a specific geolocation in a product realization is typically discernable (known) by the “down-stream” user of the product based on the partition’s description and visualization of the product by the user or possibly by an automated/automatic process.

The relationship of the random fields and the partitions and their various predictive statistics are documented in the remainder of this section and its corresponding subsections.

One possible variation to the baseline Random Field-to-Partition Mapping is termed “baseline mapping variation 1” and includes a new random field that is associated with partition 1 only, i.e., partition 1 contains its usual random field plus one more random field. The new random field corresponds to the geolocation product equivalent to sensor-mensuration (aka “unmodeled”) error. It corresponds to product-wide errors that are “high frequency” and not as systematic (spatially correlated) as the errors in random field 1.

The baseline approach assumes that sensor-mensuration error is either: (1) not applicable, (2) not separable/identifiable in the corresponding sample-statistics used to generate or “tune” the predictive statistics, or (3) its predictive statistics were already combined with the predictive statistics for random field 1. See Section C.3 for a general methodology for the latter as applied to image errors and its subsequent effects on predicted accuracy. The baseline Random Field-to-Partition Mapping is assumed applicable for the remainder of this appendix.

In summary, a specific geolocation  $X$  in the product is associated with a unique partition  $m$  and its corresponding random fields. This is clarified in the following sections, and in particular, by the example contained in Section E.4.

An interim top-level example that excludes details of relevant predictive statistics is as follows: A product instance contains a total of  $4 \times 10^6$  geolocations associated with 2 partitions, Partition 1 with  $3.5 \times 10^6$  corresponding geolocations and Partition 2 with the other  $0.5 \times 10^6$  geolocations. The product not only consists of all  $4 \times 10^6$  3d geolocations, but also metadata or its equivalent that includes the *a priori* statistics that define the Mixed Gaussian Random Field that represents the corresponding 3d geolocation errors (predicted accuracy) of all geolocations in an efficient and compact manner. Of course, the actual errors in the product are unknown; otherwise, the 3d geolocations would be pre-corrected.

In the example presented in Section E.4, Partition 2 is associated with geolocations with poor accuracy corresponding to “melted” roof-top edges in an EO-derived 3d Point Cloud, while Partition 1 is associated with all other geolocations in the 3d Point Cloud with corresponding good accuracy.

The use of partitions in the MGRF allows for flexibility, and prohibits any “mask-over” or obfuscation of the effects of large errors associated with low-probability partitions on an arbitrary geolocation in the product (specific partition unknown), as described in the Section E.2.3. However, as detailed in Section E.2.2, if a geolocation is known to be associated with partition  $m$ , corresponding statistics provide for a higher-fidelity representation of the geolocation’s predicted accuracy. In addition, and as detailed later in this appendix, a partition does not necessarily correspond to a connected region of geolocations. An example is “melted roof-top” edges that correspond to features (buildings) geographically dispersed across the product.

Finally, although the various definitions and derivations presented in following (sub)sections of Section E.2 may appear numerous and somewhat complicated, respectively, the subsequent MGRF predictive statistics that are included in the product’s metadata or its equivalent are not, and their use by the “down-stream” user straight-forward. The inclusion of pre-computed scalar accuracy metrics (CEXX and LEXX) for both horizontal and vertical predicted accuracies and for predicted relative accuracies at various probability levels (XX) also facilitates “down-stream” use.

### E.2.1 Geolocation errors represented by random fields

The predictive statistics defined in this section define wide-sense homogeneous random fields. More specifically, the predictive statistics characterize a multivariate, Gaussian distributed, geolocation error  $\epsilon X$  that is represented by or “contained in” a Random Field  $RF_i$ ,  $i = 1, \dots, n$ , and which also corresponds to geolocation  $X$ .

The predictive statistics also characterize the relative error  $rel\_ \epsilon X = \epsilon X_1 - \epsilon X_2$ , where  $\epsilon X_1$  is contained in  $RF_i$  and corresponds to geolocation  $X_1$ , and  $\epsilon X_2$  is contained in  $RF_j$  and corresponds to geolocation  $X_2$ . This characterization is further categorized by whether the two random fields are one in the same ( $i = j$ ) or not ( $i \neq j$ ).

The above random fields are termed “wide-sense homogeneous” and are similar to a “stationary stochastic process”, since the error statistics are independent of the actual geolocation  $X$ , and are only a function of  $\Delta X$  between two geolocations for the relative error statistics.

Errors contained in different random fields are independent (uncorrelated) by definition.

#### Random Field $RF_i$ – defining statistics

The following predictive statistics completely define the random field  $RF_i$ :

$$\bar{X}_{RF\ i} \equiv E\{\epsilon X\} : \text{the mean-value of error; a } k \times 1 \text{ vector;} \quad (\text{E.2.1-1})$$

$$C_{X_{RF\ i}} \equiv E\{(\epsilon X - \bar{X}_{RF\ i})(\epsilon X - \bar{X}_{RF\ i})^T\} : \text{the covariance matrix about the mean-value,} \quad (\text{E.2.1-2})$$

a  $k \times k$  matrix, assumed a valid (symmetric and positive definite) covariance matrix;

$$spdcf_{RF\ i}(\Delta X) : \text{a strictly positive definite correlation function,} \quad (\text{E.2.1-3})$$

a  $k \times 1$  vector-valued function, a function of the difference  $\Delta X$  between two geolocations. The particular spdcf is arbitrary, but typically a member of the “CSM four parameter” family.

The evaluation of  $spdcf_{RF\ i}(\Delta X)$  corresponds to the value of the spatial correlation coefficient for each component of error – defined in more detail later in this section.

### **Random Field $RF_i$ – derived statistics**

The above mean-value and covariance matrix completely characterize the multi-variate probability density function and multi-variate cumulative probability distribution function of the geolocation error  $\epsilon X$  contained in  $RF_i$  since the errors are assumed Gaussian distributed:

$$pdf_{RF\ i}(\epsilon X) \text{ and } cdf_{RF\ i}(\epsilon X). \quad (E.2.1-4)$$

Both of the above functions are scalar-valued and correspond to the value of probability density and of probability, respectively.

### **Random Fields $RF_i$ and $RF_j$ – derived statistics**

**Cross-covariance matrix:**

$cross\_C_{X_{RF\ ij}} \equiv E\{(\epsilon X_1 - \bar{X}_{RF\ i})(\epsilon X_2 - \bar{X}_{RF\ j})^T\}$ : the cross-covariance matrix of geolocation errors  $\epsilon X_1$  and  $\epsilon X_2$  contained in Random Fields  $RF_i$  and  $RF_j$ , respectively, about their mean-values of error; a  $k \times k$  matrix computed as follows:

$$cross\_C_{X_{RF\ ij}} = C_{X_{RF\ i}}^{1/2} (S_{ij}(\Delta X)) C_{X_{RF\ j}}^{1/2}, \quad (E.2.1-6)$$

where the superscript  $1/2$  corresponds to principal matrix square-root, and the spdcf  $k \times k$  diagonal matrix  $S_{ij}$  is defined as follows:

$$S_{ij}(\Delta X) = 0_{k \times k} \text{ if } i \neq j, \text{ and} \quad (E.2.1-7)$$

$$S_{ij}(\Delta X) = \begin{bmatrix} spdcf_{RF\ i\ 1}(\Delta X) & 0 & \dots \\ \vdots & \ddots & \ddots \\ 0 & \dots & spdcf_{RF\ i\ k}(\Delta X) \end{bmatrix}, \text{ if } i = j,$$

where  $spdcf_{RF\ i\ m}(\Delta X_{12})$ ,  $m = 1, \dots, k$ , corresponds to component  $m$  of the vector-valued function  $spdcf_{RF\ i}(\Delta X)$ , and  $\Delta X = X_1 - X_2$ .

If either  $C_{X_{RF\ i}}$  is a diagonal matrix or if the  $k$  components of  $spdcf_{RF\ i}(\Delta X)$  are identically defined,  $cross\_C_{X_{RF\ ii}} = S_{ii}(\Delta X) C_{X_{RF\ i}}$ .

Equation (E.2.1-6) is very general and is derived in reference [3].

Note that when the two random fields are different ( $i \neq j$ ) the cross covariance between the two errors  $\epsilon X_1$  and  $\epsilon X_2$  that are contained in the random fields is equal to zero ( $0_{k \times k}$ ), i.e., they are uncorrelated.

#### Relative error:

The relative error  $rel\_eX$  is defined as  $rel\_eX \equiv (\epsilon X_1 - \epsilon X_2)$ , with the two errors  $\epsilon X_1$  and  $\epsilon X_2$  corresponding to  $RF_i$  and  $RF_j$ , respectively, and also to geolocations  $X_1$  and  $X_2$ , respectively.

The following define and compute the predictive statistics corresponding to relative error:

$$rel\_X_{RF\ ij} \equiv E\{rel\_eX\}: \text{the mean-value of relative error; a } k \times 1 \text{ vector} \quad (E.2.1-8)$$

and computed as follows:

$$rel\_X_{RF\ ij} = E\{\epsilon X_1 - \epsilon X_2\} = E\{\epsilon X_1\} - E\{\epsilon X_2\} = \bar{X}_{RF\ i} - \bar{X}_{RF\ j}. \quad (E.2.1-9)$$

$$rel\_C_{X_{RF\ ij}} \equiv E\{(rel\_eX - rel\_X_{RF\ ij})(rel\_eX - rel\_X_{RF\ ij})^T\}: \text{the relative error error covariance matrix; a } k \times k \text{ matrix computed as follows:} \quad (E.2.1-10)$$

$$rel\_C_{X_{RF\ ij}} = E\left\{\left((\epsilon X_1 - \bar{X}_{RF\ i}) - (\epsilon X_2 - \bar{X}_{RF\ j})\right)\left((\epsilon X_1 - \bar{X}_{RF\ i}) - (\epsilon X_2 - \bar{X}_{RF\ j})\right)^T\right\} = C_{X_{RF\ i}} + C_{X_{RF\ j}} - cross\_C_{X_{RF\ ij}} - cross\_C_{X_{RF\ ji}}, \text{ and therefore:} \quad (E.2.1-11)$$

$$rel\_C_{X_{RF\ ij}} = C_{X_{RF\ i}} + C_{X_{RF\ j}}, \text{ if } i \neq j, \text{ and} \quad (E.2.1-12)$$

$$rel\_C_{X_{RF\ ij}} = 2(C_{X_{RF\ i}} - cross\_C_{X_{RF\ ii}}), \text{ if } i = j.$$

#### For convenience of notation when the two random fields are the same ( $i = j$ ):

The following definitions correspond to simplifications in notation applicable when  $i = j$ , i.e., when the two errors are contained in the same random field  $RF_i$ :

$$cross\_C_{X_{RF\ i}} \equiv cross\_C_{X_{RF\ ii}} \quad (\text{see Equation (E.2.1-6)}) \quad (E.2.1-13)$$

$$rel\_X_{RF\ i} \equiv rel\_X_{RF\ ii} = 0_{k \times 1}, \quad (\text{see Equation (E.2.1-9)}) \quad (E.2.1-14)$$

$$rel\_C_{X_{RF\ i}} \equiv rel\_C_{X_{RF\ ii}} = 2(C_{X_{RF\ i}} - cross\_C_{X_{RF\ i}}), \quad (\text{see Equation E.2.1-12}). \quad (E.2.1-15)$$

In addition, the above mean-value  $rel\_X_{RF\ i}$  and covariance matrix  $rel\_C_{X_{RF\ i}}$  completely characterize the multivariate Gaussian *pdf* and *cdf* for the relative error  $rel\_eX$  corresponding to two errors in the same Random Field  $RF_i$  since relative error is the sum (difference) between two Gaussian distributed errors:

$$rel\_pdf_{RF\ i}(rel\_eX) \text{ and } rel\_cdf_{RF\ i}(rel\_eX). \quad (E.2.1-16)$$

Further note that, although  $rel\_X_{RFi}$ ,  $rel\_pdf_{RFi}(rel\_eX)$ , and  $rel\_cdf_{RFi}(rel\_eX)$  are indexed by the corresponding random field  $RF_i$  which contains the two geolocation errors that make-up the relative error, they are also functions of the errors' corresponding geolocations  $X_1$  and  $X_2$ , or more specifically, their difference  $\Delta X$ .

### Multiple geolocation errors:

In addition, the same principles used above can be used to compute a multi-geolocation mean-value " $multi\_X_{RFi}$ " and a full covariance matrix about the mean-value " $multi\_C_{X_{RFi}}$ " for  $l$  geolocation errors associated with Random Field  $RF_i$  instead of a single geolocation error as is applicable for  $\bar{X}_{RFi}$  and  $C_{X_{RFi}}$  defined in Equations (E.2.1-1) and (E.2.1-2), respectively.

$multi\_X_{RFi}$  is a  $lk \times 1$  vector and  $multi\_C_{X_{RFi}}$  is a  $lk \times lk$  matrix. The latter's computation relies on  $spdcf_{RFi}(\Delta X)$  in order to specify the spatial correlation between the geolocation errors corresponding to each pair of the  $l$  geolocations and is used to compute their corresponding cross-covariance matrix. For example, assuming that there are three geolocations ( $l = 3$ ) of interest:

$$multi\_X_{RFi} = [\bar{X}_{RFi}^T \quad \bar{X}_{RFi}^T \quad \bar{X}_{RFi}^T]^T; \quad (E.2.1-17)$$

$$multi\_C_{X_{RFi}} = \begin{bmatrix} C_{X_{RFi}} & cross\_C_{X_{RFi}}(\Delta X_{12}) & cross\_C_{X_{RFi}}(\Delta X_{13}) \\ \cdot & C_{X_{RFi}} & cross\_C_{X_{RFi}}(\Delta X_{23}) \\ \cdot & \cdot & C_{X_{RFi}} \end{bmatrix}, \quad (E.2.1-18)$$

and where, for example,  $\Delta X_{13} = X_1 - X_3$  is the difference between the geolocations 1 and 3.

The above equations are also easily generalized to  $l$  geolocation errors associated with arbitrary random fields: If an error  $eX_m$  is associated with  $RF_{m*}$ , where  $1 \leq m \leq l$  and where  $1 \leq m* \leq n$ , the corresponding mean-value entry in Equation (E.2.1-17) is equal to  $\bar{X}_{RFm*}^T$  and the corresponding diagonal entry in Equation (E.2.1-18) is equal to  $C_{X_{RFm*}}$ . A corresponding cross-covariance entry in Equation (E.2.1-18) is equal to zero if the other geolocation error is not in  $RF_{m*}$ , otherwise it is equal to  $cross\_C_{X_{RFm*}}(\Delta X)$ , where  $(\Delta X)$  is the appropriate difference between geolocation  $m$  and the other geolocation.

### Random Fields - miscellaneous

#### The spdcf:

The spdcf, or degree of spatial correlation, has a large impact on predicted relative accuracy for two geolocation errors corresponding to the same random field. The higher the (positive) correlation, the smaller the relative error covariance matrix  $rel\_C_{X_{RFi}}$  due to the statistical cancellation of similar errors. The spdcf has similar effects on the multi-geolocations error covariance matrix  $multi\_C_{X_{RFi}}$ .

Figure E.2.1-1 presents two examples of an spdcf corresponding to the vertical component (z) of error versus horizontal "distance", or more specifically, dx in the x-direction and dy in the y-direction between

two corresponding geolocations. More specifically, and consistent with the definitions and notation presented in this section, the strictly positive definite correlation function is designated as  $spdcf_{RF\ i\ 3}(\Delta X_{12})$ , which corresponds to the third (vertical) component of error in a random field  $RF_i$  and to two geolocations  $X_1$  and  $X_2$ , with  $\Delta X_{12}$  equal to their difference. See TGD 1 (Overview and Methodologies) and TGD 2a (Predictive statistics) for further details regarding spdcf, as there are various spdcf families for flexibility. Proper use of an spdcf, as detailed in this document, ensures the construction of valid covariance matrices.

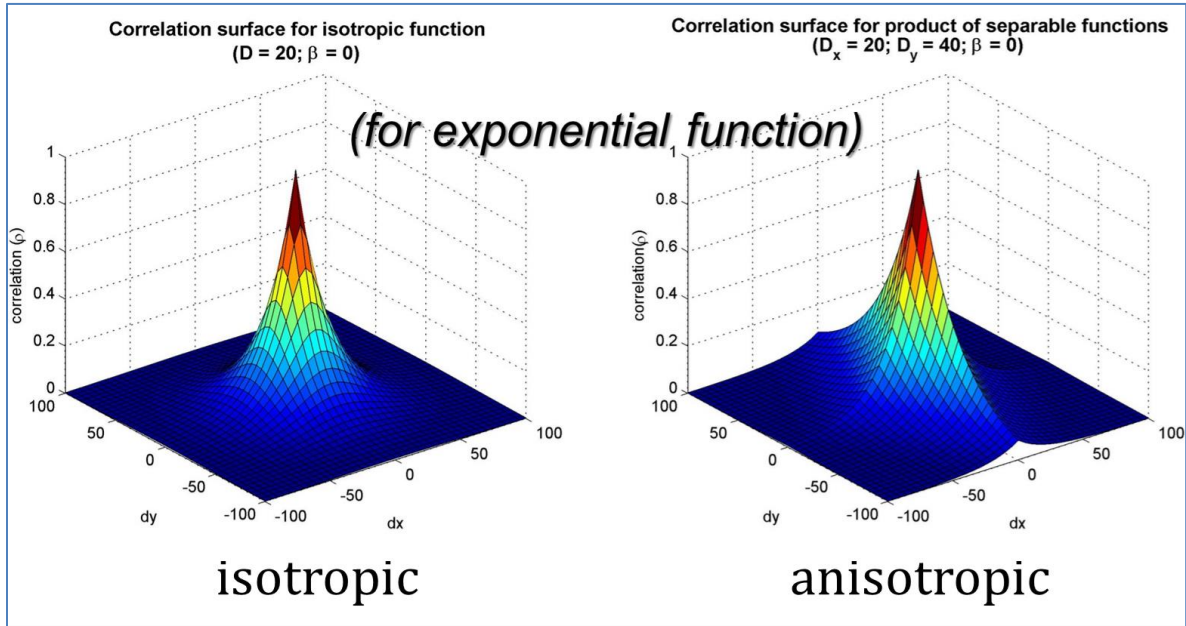


**Figure E.2.1-1:** Correlation (unit-less) verses 2d horizontal distance (meters) – two spdcf examples: exponential decay (isotropic) and separable exponential decay (anisotropic) as a function of horizontal distance between 3d geolocations

#### Consequences of a possible direct Random Field-to-Partition Assignment:

An MGRF contains both partitions and random fields. In particular, each partition is made-up of, or is assigned to, one or more random fields as discussed earlier in Section E.2 and in the next Section E.2.2. More specifically, each geolocation in the product is associated with a unique partition, and the geolocation's error is the sum of independent errors, each error from a different random field assigned to the partition. If only one random field is assigned to a partition, the geolocation error consists solely of an error from that random field, i.e., is statistically characterized completely by the random field.

A direct "Random Field-to-Partition Mapping" assigns Random Field  $i$  exclusively to Partition  $i$ , assuming that there are the same number of random fields as there are partitions in the MGRF. If a direct assignment were applicable, all defining and derived statistics presented in this section for random fields would be directly applicable (one-in-the-same) for partitions. However, as described in the next section and discussed earlier in Section E.2, the baseline assignment for an MGRF is not direct. That is, a direct

Random-Field-to-Partition Mapping is not the recommended (baseline) Random-Field-to-Partition Mapping for an MGRF-based representation of predicted accuracy for a geolocation product.

#### Scalar accuracy metrics:

Scalar accuracy metrics, such as CEXX, LEXX, rel\_CEXX, and rel\_LEXX, for various probability levels XX are also derived statistics of interest and their definitions and computations are presented in Section E.2.5, but correspond to partitions instead of random fields per se. However, if Partition  $i$  is made-up of geolocations with corresponding errors exclusively from Random Field  $j$ , the scalar accuracy metrics computed for Partition  $i$  per Section E.2.5 would be directly applicable to Random Field  $j$  as well.

### E.2.2 Statistics corresponding to geolocations and their errors contained in partitions

As discussed earlier, an MGRF used to characterize the predicted accuracy of a geolocation product is defined as containing from 1 to  $n$  partitions:  $Part_m$ ,  $m = 1, \dots, n$ . Each geolocation in the product corresponds to one and only one partition.

In addition, as discussed earlier and further detailed below, each partition corresponds to a specified set of one or more random fields in order to statistically represent geolocation errors. Each partition also corresponds to a specified description of the geolocations in the product to which it applies, e.g. geolocations corresponding to “melted roof-top edges”.

For this recommended application of MGRF, the baseline Random Field-to-Partition Mapping is assumed applicable. As such, Partition 1 contains Random Field 1 only and is applicable to all geolocations in the product that are not associated with any other partitions. The other partitions contain Random Field 1 and one other unique random field. The latter is considered to contain “additive” errors relative to the former. More detailed examples of partitions, the random fields that they contain as well as the geolocations that they are applicable to, are presented later in this appendix. In particular, Section E.5 describes/tabulates all parameters that define the relevant partitions in corresponding product metadata or its equivalent.

The remainder of this section describes the predictive statistics that correspond to one or more partitions. These predictive statistics are directly related to the predictive statistics of their corresponding random fields. The predictive statistics for partitions that are presented below do not include a partition’s definition in terms of relevant geolocations, but does include the partition’s *a priori* probability of occurrence, i.e., the probability that an arbitrary geolocation in the product is associated with the partition.

#### Partition $Part_m$ – predictive statistics

The error  $\epsilon X$  in a geolocation  $X$  corresponding to Partition  $Part_1$  is contained in the Random Field  $RF_1$ . The error  $\epsilon X$  in a geolocation  $X$  corresponding to  $Part_m$ ,  $1 < m \leq n$ , is the sum of two independent (uncorrelated) errors, one contained in the Random Field  $RF_1$  and the other contained in the Random Field  $RF_m$ . Let us term these two independent errors  $\epsilon X_{RF_1}$  and  $\epsilon X_{RF_m}$ , respectively, in the derivations below:

The *a priori* or predictive statistics of geolocation error  $\epsilon X = (\epsilon X_{RF\ 1} + \epsilon X_{RF\ m})$  corresponding to a geolocation in  $Part_m$  are as follows and based on the above definitions and the definitions for a random field presented in Section E.2.1:

$$\bar{X}_{Part\ m} \equiv E\{\epsilon X\} = E\{\epsilon X_{RF\ 1} + \epsilon X_{RF\ m}\} \equiv \bar{X}_{RF\ 1} + \bar{X}_{RF\ m}, \text{ the } k \times 1 \text{ mean-value of error;} \quad (E.2.2-1)$$

$$C_{X_{Part\ m}} \equiv E\{(\epsilon X - \bar{X}_{Part\ m})(\epsilon X - \bar{X}_{Part\ m})^T\} = \quad (E.2.2-2)$$

$$E\left\{\left((\epsilon X_{RF\ 1} - \bar{X}_{RF\ 1}) + (\epsilon X_{RF\ m} - \bar{X}_{RF\ m})\right)\left((\epsilon X_{RF\ 1} - \bar{X}_{RF\ 1}) + (\epsilon X_{RF\ m} - \bar{X}_{RF\ m})\right)^T\right\} =$$

$$C_{X_{RF\ 1}} + 0 + 0 + C_{X_{RF\ m}} = C_{X_{RF\ 1}} + C_{X_{RF\ m}},$$

a  $k \times k$  covariance matrix.

The above equations and similar equations in the remainder of this section are also applicable to errors in geolocations corresponding to  $Part_1$  – simply remove references to Random Field  $RF_m$  in the corresponding equations. For example, remove  $\bar{X}_{RF\ m}$  from Equation (E.2.2-1), i.e.,  $\bar{X}_{Part\ 1} = \bar{X}_{RF\ 1}$ .

In addition, the mean-value and covariance matrix defined in Equations (E.2.2-1) and (E.2.2-2), respectively, completely characterize the multi-variate probability density function and multi-variate cumulative probability distribution function of the geolocation error  $\epsilon X$  since it is Gaussian distributed due to the fact that it is the sum of two Gaussian distributed errors:

$$pdf_{Part\ m}(\epsilon X) \text{ and } cdf_{Part\ m}(\epsilon X). \quad (E.2.2-3)$$

#### Relative error:

Similarly, the statistics for the relative error  $rel\ \epsilon X$  between two geolocations  $X_1$  and  $X_2$  in  $Part_m$  are derived below based on the following definitions:

$$rel\_ \epsilon X = \epsilon X_1 - \epsilon X_2, \text{ where} \quad (E.2.2-4)$$

$$\epsilon X_1 = \epsilon X_{1\ RF\ 1} + \epsilon X_{1\ RF\ m} \text{ and } \epsilon X_2 = \epsilon X_{2\ RF\ 1} + \epsilon X_{2\ RF\ m}. \quad (E.2.2-5)$$

$\epsilon X_{1\ RF\ 1}$  and  $\epsilon X_{2\ RF\ 1}$  are correlated since they belong to the same Random Field 1, and  $\epsilon X_{1\ RF\ m}$  and  $\epsilon X_{2\ RF\ m}$  are also correlated because they belong to the same Random Field  $m$ . Therefore:

$$rel\_ \bar{X}_{Part\ m} \equiv E\{rel\_ \epsilon X\} = E\{(\epsilon X_1 - \epsilon X_2)\} = \bar{X}_{Part\ m} - \bar{X}_{Part\ m} = 0; \quad (E.2.2-6)$$

$$rel\_ C_{X_{Part\ m}} \equiv E\{(rel\_ \epsilon X - rel\_ \bar{X}_{Part\ m})(rel\_ \epsilon X - rel\_ \bar{X}_{Part\ m})^T\} = \quad (E.2.2-7)$$

$$rel\_ C_{X_{RF\ 1}} + rel\_ C_{X_{RF\ m}}.$$

Equation (E.2.2-7) is based on:

$$\begin{aligned}
 rel\_eX &= eX_1 - eX_2 = (eX_{1\ RF\ 1} + eX_{1\ RF\ m}) - (eX_{2\ RF\ 1} + eX_{2\ RF\ m}) = \\
 &= (eX_{1\ RF\ 1} - eX_{2\ RF\ 1}) + (eX_{1\ RF\ m} - eX_{2\ RF\ m}), \text{ and correspondingly,} \\
 rel\_C_{X_{Part\ m}} &= E\{(rel\_eX)(rel\_eX)^T\} = \\
 rel\_C_{X_{RF\ 1}} &- E\{(eX_{1\ RF\ 1} - eX_{2\ RF\ 1})(eX_{1\ RF\ m} - eX_{2\ RF\ m})^T \\
 &- E\{(eX_{1\ RF\ m} - eX_{2\ RF\ m})(eX_{1\ RF\ 1} - eX_{2\ RF\ 1})^T + rel\_C_{X_{RF\ m}} = \\
 rel\_C_{X_{RF\ 1}} &- 0 - 0 + rel\_C_{X_{RF\ m}} = rel\_C_{X_{RF\ 1}} + rel\_C_{X_{RF\ m}}.
 \end{aligned} \tag{E.2.2-8}$$

The above mean-value and error covariance matrix completely define or characterize the probability distribution function (*pdf*) for relative error since relative error is Gaussian distributed - the sum (or difference) of two Gaussian distributed random variables:  $eX_1$  and  $eX_2$ ; or equivalently, four Gaussian distributed random variables:  $eX_{1\ RF\ 1}$ ,  $eX_{2\ RF\ 1}$ ,  $eX_{1\ RF\ m}$ , and  $eX_{2\ RF\ m}$ . The integral of the *pdf* is the *cdf*. The *pdf* and the *cdf* for relative error are designated as follows:

$$rel\_pdf_{Part\ m}(rel\_eX) \text{ and } rel\_cdf_{Part\ m}(rel\_eX) \tag{E.2.2-9}$$

If we are interested in the relative error statistics for geolocations associated with  $Part_1$ , they are simply equal to:  $rel\_X_{Part\ 1} = 0$ ,  $rel\_C_{X_{Part\ 1}} = rel\_C_{X_{RF\ 1}}$ , and  $rel\_pdf_{Part\ 1}(rel\_eX)$  defined accordingly from the two preceding statistics.

### Multiple geolocation errors:

In addition, based on a derivation similar to the above as well as the definitions and derivations of Section E.2.1 for random fields, the multi-geolocation mean-value of error and the covariance matrix about the mean-value for  $q$  geolocations in  $Part_m$  are as follows:

$$multi\_X_{Part\ m} = [\bar{X}_{Part\ m}^T \quad \bar{X}_{Part\ m}^T \quad \bar{X}_{Part\ m}^T]^T; \tag{E.2.2-10}$$

$$multi\_C_{X_{Part\ m}} = multi\_C_{X_{RF\ 1}} + multi\_C_{X_{RF\ m}}, \tag{E.2.2-11}$$

where  $\bar{X}_{Part\ m}$  is defined in Equation (E.2.2-1) and  $multi\_C_{X_{RF\ 1}}$  and  $multi\_C_{X_{RF\ m}}$  are defined in Equation (E.2.1-18).  $multi\_X_{Part\ m}$  is a  $qk \times 1$  vector and  $multi\_C_{X_{Part\ m}}$  a  $qk \times qk$  matrix.

If we are interested in the statistics for geolocations associated with  $Part_1$ , they are simply equal to:  $multi\_X_{Part\ 1} = multi\_X_{RF\ 1}$  and  $multi\_C_{X_{Part\ 1}} = multi\_C_{X_{RF\ 1}}$ .

### Partitions $Part_m$ and $Part_q$ — predictive statistics

Define  $eX_1$  as the error in a geolocation associated with  $Part_m$ , and similarly,  $eX_2$  as the error in a geolocation associated with  $Part_q$ . Furthermore, decompose these errors as the sum of independent errors associated with corresponding random fields:  $eX_1 \equiv X_{1\ RF\ 1} + eX_{1\ RF\ m}$  and  $eX_2 \equiv eX_{2\ RF\ 1} + eX_{2\ RF\ q}$ , assuming that  $m \neq 1$  and  $q \neq 1$ .

**Cross-covariance matrix:**

$$cross\_C_{X_{Part\ mq}} \equiv E\{(\epsilon X_1 - \bar{X}_{Part\ m})(\epsilon X_2 - \bar{X}_{Part\ q})^T\} = \quad (E.2.2-12)$$

$$E\{((\epsilon X_{1\ RF\ 1} - \bar{X}_{RF\ 1}) + (\epsilon X_{1\ RF\ m} - \bar{X}_{RF\ m}))((\epsilon X_{2\ RF\ 1} - \bar{X}_{RF\ 1}) + (\epsilon X_{2\ RF\ q} - \bar{X}_{RF\ q}))^T\} =$$

$$cross\_C_{X_{RF\ 1}} + cross\_C_{X_{RF\ mq}}, \text{ for all } m \neq 1 \text{ and } q \neq 1;$$

$$\text{otherwise, } cross\_C_{X_{Part\ 11}} \equiv cross\_C_{X_{Part\ 1}} = cross\_C_{X_{RF\ 1}}.$$

**Relative error:**

$$rel\_eX \equiv \epsilon X_1 - \epsilon X_2 = (\epsilon X_{1\ RF\ 1} + \epsilon X_{1\ RF\ m}) - (\epsilon X_{2\ RF\ 1} + \epsilon X_{2\ RF\ q}).$$

$$rel\_X_{Part\ mq} = E\{\epsilon X_1 - \epsilon X_2\} = \bar{X}_{RF\ m} - \bar{X}_{RF\ q}; \quad (E.2.2-13)$$

$$rel\_C_{X_{Part\ mq}} = E\{(rel\_eX - rel\_X_{Part\ mq})(rel\_eX - rel\_X_{Part\ mq})^T\} = \quad (E.2.2-14)$$

$$E\{((\epsilon X_{1\ RF\ 1} - \epsilon X_{2\ RF\ 1}) + (\epsilon X_{1\ RF\ m} - \bar{X}_{RF\ m}) - (\epsilon X_{2\ RF\ q} - \bar{X}_{RF\ q}))((\epsilon X_{1\ RF\ 1} - \epsilon X_{2\ RF\ 1}) + (\epsilon X_{1\ RF\ m} - \bar{X}_{RF\ m}) - (\epsilon X_{2\ RF\ q} - \bar{X}_{RF\ q}))^T\} =$$

$$rel\_C_{X_{RF\ 11}} + C_{X_{RF\ m}} + C_{X_{RF\ q}} \equiv rel\_C_{X_{RF\ 1}} + C_{X_{RF\ m}} + C_{X_{RF\ q}}.$$

If  $m = 1$ , remove  $rel\_C_{X_{RF\ m}}$  from the above equation; similarly, if  $q = 1$ , remove  $C_{X_{RF\ q}}$  from the above equation. For example, if  $m = 1$  and  $q > 1$ ,  $rel\_X_{Part\ 1q} = rel\_C_{X_{RF\ 1}} + C_{X_{RF\ q}}$ .

The above mean-value and error covariance matrix completely define the probability distribution function for the relative error since relative error is the sum (or difference) of two Gaussian distributed random variables:  $\epsilon X_1$  and  $\epsilon X_2$ ; or equivalently, four Gaussian distributed random variables:  $\epsilon X_{1\ RF\ 1}$ ,  $\epsilon X_{2\ RF\ 1}$ ,  $\epsilon X_{1\ RF\ m}$ , and  $\epsilon X_{2\ RF\ q}$ . The *pdf* is designated as follows:

$$rel\_pdf_{Part\ mq}(rel\_eX). \quad (E.2.2-15)$$

The corresponding *cdf* is defined as the integral of the above and designated as:

$$rel\_cdf_{Part\ ij} \quad (E.2.2-16)$$

### E.2.3 Statistics corresponding to arbitrary geolocations and their errors in the MGRF

We now extend the above to an arbitrary geolocation  $X$  in the MGRF or product, i.e., the particular partition in which it resides is unknown. We also extend the above to an arbitrary pair of geolocations  $X_1$  and  $X_2$  in the MGRF, i.e., the particular partitions in which they reside are unknown and may be different.

Correspondingly, the following also extends the concept of a multivariate Gaussian distribution to a multivariate Gaussian mixture distribution by taking into account that the geolocation(s) may be in any of the  $n$  partitions consistent with the partitions' specified *a priori* probabilities of occurrence.

#### An arbitrary geolocation $X$ in the product

$$gmpdf(\epsilon X) \equiv \sum_{i=1}^n p_i pdf_{Part\ i}(\epsilon X), \quad (E.2.3-1)$$

the Gaussian mixture probability density function for the random vector  $\epsilon X$ , where  $p_i$  and  $pdf_{Part\ i}$  are the probability of partition  $i$ 's occurrence and the probability density function of the corresponding geolocation error, respectively, associated with MGRF partition  $i$ .

Note:  $p_i$  utilizes the subscript  $i$  for convenience instead of  $Part_i$  since there is no counterpart to  $p_i$  for random fields.

Simplifying notation,  $gmpdf(\epsilon X)$  can also be represented as  $gmpdf = \sum_{i=1}^n p_i pdf_{Part\ i}$ . The various  $pdf_{Part\ i}$  in Equation (E.2.3-1) are the Gaussian probability density functions for partitions  $i$  ( $Part_i$ ),  $i = 1, \dots, n$ , and defined in Equation (E.2.2-3).

Corresponding mean-value of  $\epsilon X$ :

$$\bar{X} \equiv E\{\epsilon X\} = \iiint_{-\infty}^{\infty} \epsilon X gmpdf(\epsilon X) d\epsilon X = \quad (E.2.3-2)$$

$$\iiint_{-\infty}^{\infty} \epsilon X gmpdf(\epsilon X) d\epsilon X = \iiint_{-\infty}^{\infty} \epsilon X (\sum_{i=1}^n p_i pdf_{Part\ i}(\epsilon X)) d\epsilon X =$$

$$\sum_{i=1}^n p_i (\iiint_{-\infty}^{\infty} \epsilon X pdf_{Part\ i}(\epsilon X) d\epsilon X) = \sum_{i=1}^n p_i \bar{X}_{Part\ i}$$

The above equation can also be expressed in terms of the predictive statistics of the  $n$  random fields:

$$\bar{X} = \sum_{i=1}^n p_i \bar{X}_{Part\ i} = \bar{X}_{RF\ 1} + \sum_{i=2}^n p_i \bar{X}_{RF\ i}. \quad (E.2.3-3)$$

Corresponding error covariance matrix of  $\epsilon X$ :

$$C_X \equiv E\{(\epsilon X - \bar{X})(\epsilon X - \bar{X})^T\} = \iiint_{-\infty}^{\infty} (\epsilon X - \bar{X})(\epsilon X - \bar{X})^T gmpdf(\epsilon X) d\epsilon X = \quad (E.2.3-4)$$

$$\iiint_{-\infty}^{\infty} (\epsilon X - \bar{X})(\epsilon X - \bar{X})^T \sum_{i=1}^n p_i pdf_{Part\ i}(\epsilon X) d\epsilon X =$$

$$\sum_{i=1}^n p_i (\iiint_{-\infty}^{\infty} (\epsilon X - \bar{X})(\epsilon X - \bar{X})^T pdf_{Part\ i}(\epsilon X) d\epsilon X) =$$

$$\sum_{i=1}^n p_i (\iiint_{-\infty}^{\infty} (\epsilon X \epsilon X^T + \bar{X} \bar{X}^T - \epsilon X \bar{X}^T - \bar{X} \epsilon X^T) pdf_{Part\ i}(\epsilon X) d\epsilon X) =$$

$$\sum_{i=1}^n p_i ((\iiint_{-\infty}^{\infty} (\epsilon X \epsilon X^T) pdf_{Part\ i}(\epsilon X) d\epsilon X) + (\bar{X} \bar{X}^T - \bar{X}_{Part\ i} \bar{X}^T - \bar{X} \bar{X}_{Part\ i}^T)) =$$

$$\sum_{i=1}^n p_i ((C_{X_{Part\ i}} - \bar{X}_{Part\ i} \bar{X}_{Part\ i}^T) + (\bar{X} \bar{X}^T - \bar{X}_{Part\ i} \bar{X}^T - \bar{X} \bar{X}_{Part\ i}^T)) =$$

$$\sum_{i=1}^n p_i ((\bar{X}_{Part\ i} - \bar{X})(\bar{X}_{Part\ i} - \bar{X})^T + C_{X_{Part\ i}}).$$

The above equation can also be expressed solely in terms of the predictive statistics of the  $n$  random fields, where  $\bar{X}$  is computed per Equation (E.2.3-3):

$$C_X = \sum_{i=1}^n p_i ((\bar{X}_{Part\ i} - \bar{X})(\bar{X}_{Part\ i} - \bar{X})^T + C_{X_i}) = \quad (E.2.3-5)$$

$$p_1 (\bar{X}_{RF\ 1} - \bar{X})(\bar{X}_{RF\ 1} - \bar{X})^T + p_1 C_{X_1} +$$

$$\sum_{i=2}^n p_i ((\bar{X}_{RF\ 1} + \bar{X}_{RF\ i} - \bar{X})(\bar{X}_{RF\ 1} + \bar{X}_{RF\ i} - \bar{X})^T + C_{X_{RF\ i}}).$$

The above random vector  $\epsilon X$  is not Gaussian distributed (unless the number of partitions  $n = 1$ ). That is, the Gaussian mixture probability density function *gmpdf* for the random vector  $\epsilon X$  is the weighted sum of Gaussian *pdfs*, but  $\epsilon X$  itself is not the weighted sum of Gaussian distributed random vectors; hence, is not Gaussian distributed.

*gmcdf* is the corresponding Gaussian mixture cumulative distribution function, (E.2.3-6)  
i.e., the appropriate integral of *gmpdf* that was defined in Equation (E.2.3-1).

Note that “Gaussian mixture” is also termed “mixed Gaussian” or “mixture of Gaussians”.

### Example 1 of *gmpdf* and corresponding *gmcdf*:

Figure E.2.3-1 presents an example of the Gaussian mixture *gmpdf* (black curve) for a 1d  $\epsilon X \equiv \epsilon z$ . It was generated corresponding to an MGRF consisting of 3 partitions, with corresponding statistics  $\{p_i, \bar{X}_{Part\ i}, \text{ and } C_{X_{Part\ i}}\}$ :  $\{.5, 0, 1\}$ ,  $\{.1, -3, 4\}$ , and  $\{.4, 1, 16\}$  for partition  $i = 1, 2, 3$ , respectively. The blue curve, green curve, and red curve in the figure correspond to the individual *pdfs* for partition  $i = 1, 2, 3$ , respectively.

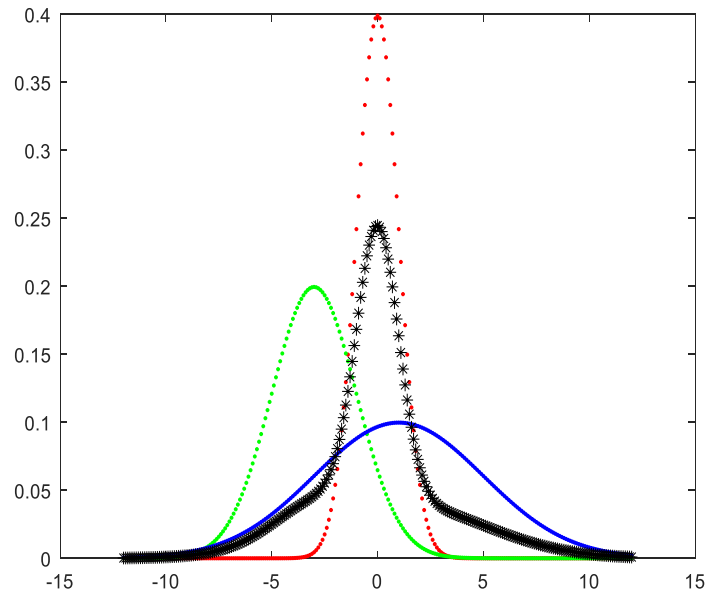


**Figure E.2.3-1:** The Gaussian mixture probability density function *gmpdf* (black) corresponding to a 1d error  $\epsilon z$  corresponding to an arbitrary 3d geolocation  $X = [x \ y \ z]^T$  in the MGRF (product), and its underlying Gaussian probability density functions *pdf* for each partition; the plot is probability density (unit-less/meters) versus value of the error  $\epsilon z$  (meters)

The Gaussian mixture *gmpdf* (black curve) is the applicable probability density function for  $\epsilon X$  corresponding to an arbitrary geolocation  $X$  in the product. If the geolocation was known to correspond to a particular partition, the corresponding *pdf* for that partition would be applicable instead; for example, the green curve in the above figure if the geolocation was known to correspond to partition 2.

Figure E.2.3-2 presents the Gaussian mixture *gmcdf* (black curve) that corresponds to *gmpdf* of Figure E.2.3-1, and includes the corresponding individual *cdfs* for the partitions (blue, green, and red curves).

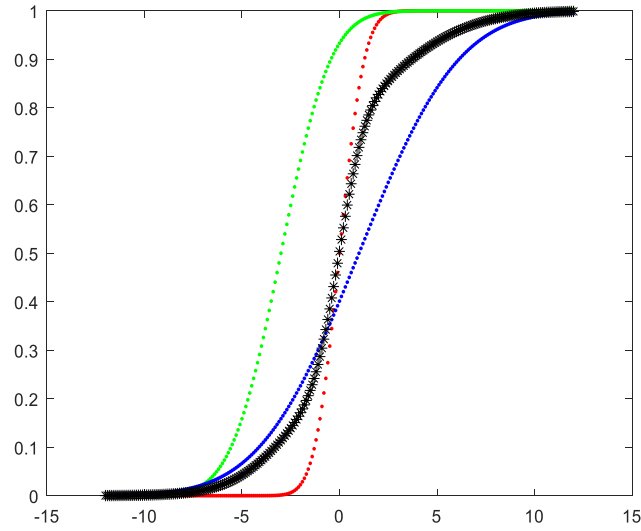


**Figure E.2.3-2:** The corresponding cumulative distribution functions: *gmcdf* (black) and underlying *cdf* of the partitions (blue, red, green); the plot is cumulative probability (unit-less) versus value of  $\epsilon z$  (meters)

**Example 2 of *gmpdf* and corresponding *gmcdf*:**

As a further example, Figure (E.2.3-3) presents an example of the Gaussian mixture *gmpdf* for a 2d  $\epsilon X \equiv \begin{bmatrix} \epsilon x \\ \epsilon y \end{bmatrix}$  corresponding to an MGRF consisting of 2 partitions with corresponding *a priori* statistics  $\{p_i, \bar{X}_{Part\ i}, C_{X_{Part\ i}}\}$ :

$$\text{Partition 1: } p_1 = 0.6, \bar{X}_{Part\ 1} = \begin{bmatrix} 0 \\ 0 \end{bmatrix}, \text{ and } C_{X_{Part\ 1}} = \begin{bmatrix} 1 & 0 \\ 0 & 1 \end{bmatrix}, \text{ and} \quad (\text{E.2.3-7})$$

$$\text{Partition 2: } p_2 = 0.4, \bar{X}_{Part\ 2} = \begin{bmatrix} 2 \\ -6 \end{bmatrix}, \text{ and } C_{X_{Part\ 2}} = \begin{bmatrix} 3 & 0 \\ 0 & 2 \end{bmatrix}.$$

In the figure's axis labels and title,  $\epsilon x$  and  $\epsilon y$  are designated x and y, respectively, for convenience.

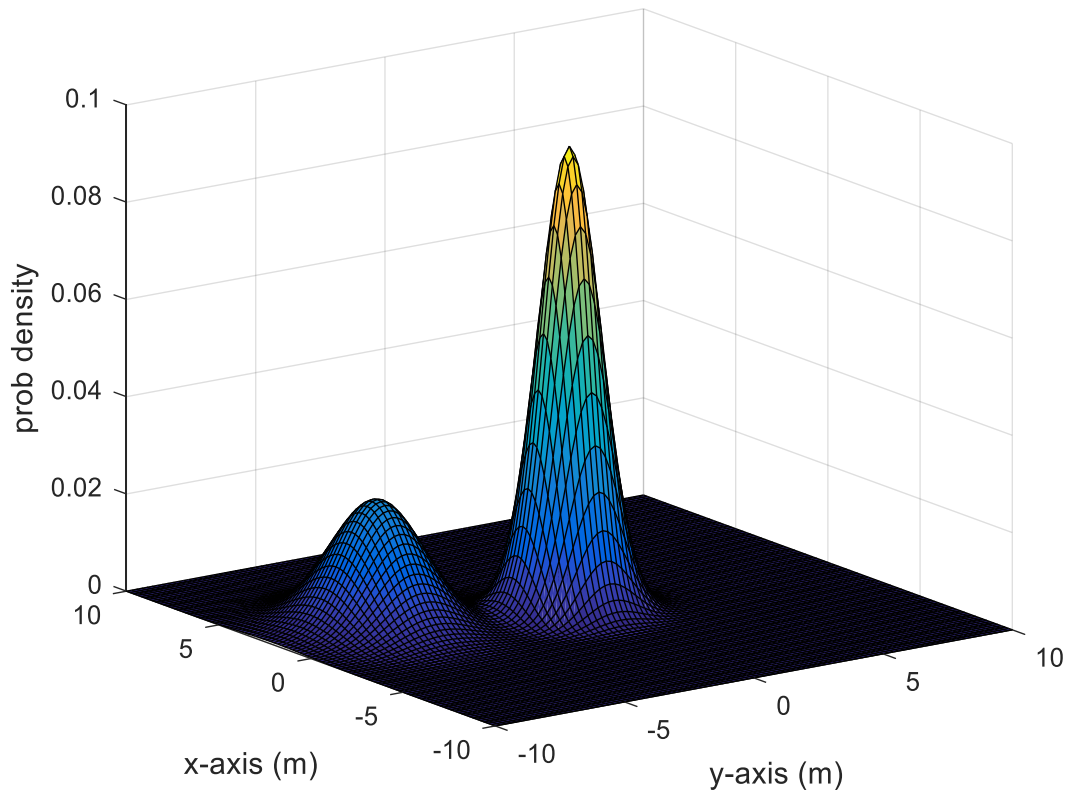


**Figure E.2.3-3:** The Gaussian mixture probability density function  $gmpdf$  for a 2d error  $\epsilon X = [\epsilon x \ \epsilon y]^T$  corresponding to an arbitrary 3d geolocation  $X = [x \ y \ z]^T$  in the MGRF (product); the plot is probability (unit-less/meters-squared) versus value  $\epsilon X$  (meters), with error components  $\epsilon x$  and  $\epsilon y$  represented as x and y, respectively, in the figure

Figure (E.2.3-4) presents the corresponding Gaussian mixture  $gmcdf$ :

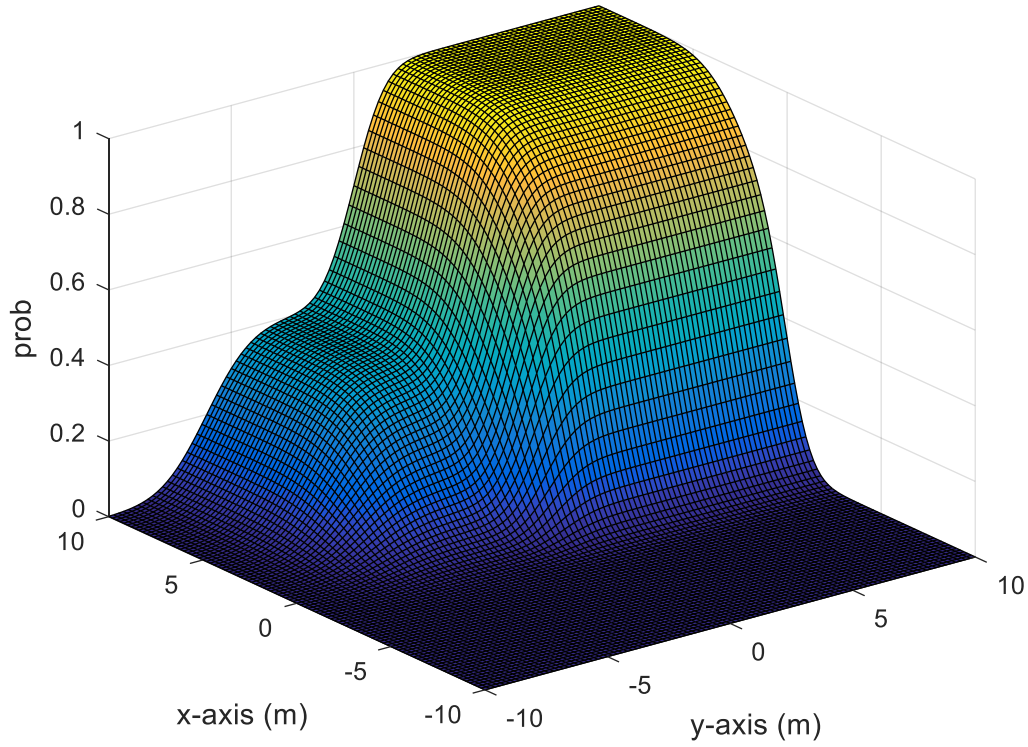


**Figure E.2.3-4:** The corresponding Gaussian mixture cumulative distribution function  $gmcdf$ ; the plot is cumulative probability (unit-less) versus the value  $\epsilon X$  (meters) with error components represented as  $x$  and  $y$  in the figure

As further information, the predictive statistics for the partitions of Equation (E.2.3-7) were based on the predictive statistics for the two underlying random fields that follow:

$$\text{Random Field 1: } \bar{X}_{RF_1} = \begin{bmatrix} 0 \\ 0 \end{bmatrix}, \text{ and } C_{X_{RF_1}} = \begin{bmatrix} 1 & 0 \\ 0 & 1 \end{bmatrix}, \text{ and} \quad (\text{E.2.3-8})$$

$$\text{Random Field 2 : } \bar{X}_{RF_2} = \begin{bmatrix} 2 \\ -6 \end{bmatrix}, \text{ and } C_{X_{RF_2}} = \begin{bmatrix} 2 & 0 \\ 0 & 1 \end{bmatrix}.$$

Recall that per the baseline random Field-to-Partition Mapping function, the errors in the geolocations associated with Partition 1 are from Random Field 1, and those associated with Partition 2 are the sum of two errors, one from Random Field 1 and one from Random Field 2.

#### **Arbitrary geolocations $X_1$ and $X_2$ in the product and their relative error**

Using the equations of Section E.2.2 and taking into account that  $p_i$  is the *a priori* probability that geolocation  $X_1$  is in partition  $i$  and  $p_j$  is the *a priori* probability that geolocation  $X_2$  is in partition  $j$ , for  $i = 1, \dots, n$  and  $j = 1, \dots, n$ , we have the following formula for the probability density function corresponding to the error in an arbitrary geolocation in the product:

$$rel\_gmpdf(\epsilon X) \equiv \sum_{i=1}^n \sum_{j=1}^n p_i p_j rel\_pdf_{Part\ ij}(\Delta X), \quad (E.2.3-9)$$

where  $rel\_pdf_{Part\ ij}$  was defined in Equation (E.2.2-15); this is also equivalent to:

$$rel\_gmpdf(\epsilon X) = \sum_{i=1}^n p_i^2 rel\_pdf_{Part\ i}(\Delta X) + 2 \sum_{i=1}^n \sum_{j=i+1}^n p_i p_j rel\_pdf_{Part\ ij}(\Delta X); \quad (E.2.3-10)$$

Integrating  $rel\_gmpdf$ , we obtain the cumulative distribution function, where  $rel\_cdf_{Part\ ij}$  was defined in Equation (E.2.2-16)

$$rel\_gmcdf(\epsilon X) \equiv \sum_{i=1}^n \sum_{j=1}^n p_i p_j rel\_cdf_{Part\ ij}(\Delta X). \quad (E.2.3-11)$$

Based on  $rel\_gmpdf$ , the corresponding mean-value of the random vector  $rel\_eX$  corresponding to two arbitrary geolocations in the product is computed as follows:

$$\begin{aligned} rel\_X &= E\{rel\_X\} = \iiint_{-\infty}^{\infty} rel\_eX rel\_gmpdf(\epsilon X) d\epsilon X = \\ &\iiint_{-\infty}^{\infty} rel\_eX \left[ \sum_{i=1}^n \sum_{j=1}^n p_i p_j rel\_pdf_{Part\ ij}(\Delta X) \right] d\epsilon X = \\ &\iiint_{-\infty}^{\infty} \left[ \sum_{i=1}^n \sum_{j=1}^n p_i p_j (\epsilon X_1 - \epsilon X_2) rel\_pdf_{Part\ ij}(\Delta X) \right] d\epsilon X = \\ &\sum_{i=1}^n \sum_{j=1}^n p_i p_j \iiint_{-\infty}^{\infty} (\epsilon X_1 - \epsilon X_2) rel\_pdf_{Part\ ij}(\Delta X) d\epsilon X = \sum_{i=1}^n \sum_{j=1}^n p_i p_j (\bar{X}_{Part\ i} - \bar{X}_{Part\ j}) = 0, \end{aligned} \quad (E.2.3-12)$$

where the last equality is also based on the fact that the *a priori* probabilities are required to sum to 1.

Applying the same techniques used for the above mean-value derivation, we have

$$\begin{aligned} rel\_C_X &\equiv E\{(rel\_X - 0)(rel\_X - 0)^T\} = \\ &\sum_{i=1}^n \sum_{j=1}^n p_i p_j \left( (X_i - X_j) - 0 \right) \left( (X_i - X_j) - 0 \right)^T rel\_pdf_{Part\ ij}(\Delta X) = \\ &\sum_{i=1}^n \sum_{j=1}^n p_i p_j \left( (X_i - X_j) \right) \left( (X_i - X_j) \right)^T rel\_pdf_{Part\ ij}(\Delta X) = \\ &\sum_{i=1}^n \sum_{j=1}^n p_i p_j (rel\_C_{X_{Part\ ij}} - (\bar{X}_i - \bar{X}_j)) = \sum_{i=1}^n \sum_{j=1}^n p_i p_j (rel\_C_{X_{Part\ ij}}). \end{aligned} \quad (E.2.3-13)$$

The above can also be expressed solely in terms of the underlying random fields as follows:

$$rel\_C_X = rel\_C_{X_{RF\ 1}} + \sum_{i=2}^n \sum_{j=2}^n p_i p_j (C_{X_{RF\ i}} + C_{X_{RF\ j}}) + 2p_1 \sum_{i=1}^n p_i C_{X_{RF\ i}}. \quad (E.2.3-14)$$

Note that the above mean-value and covariance matrix are for “interest only”. That is, since  $rel\_eX$  is not Gaussian distributed, these statistics do not completely characterize the corresponding probability density function and cumulative distribution function – these functions need to be computed directly using Equations (E.2.3-9) and (E.2.3-11), respectively, if of interest.

### **Multiple geolocations in the product - partitions known**

In addition, the same principles used above and those used to compute the covariance matrix  $rel\_C_{Part\ ij}$  (Equation E.2.2-14) of the relative error between two geolocations in partitions  $i$  and  $j$  can be used to compute a mean-value “ $multi\_X$ ” and a full multi-geolocation covariance matrix “ $multi\_C_X$ ” about the

mean-value for  $m$  errors with corresponding geolocations in  $m$  arbitrary but known partitions. For example, assuming that there are three geolocations 1, 2, and 3 of interest in corresponding partitions  $i1$ ,  $i2$ , and  $i3$ , respectively, the following is applicable and expressed in terms of the underlying random fields:

$$\epsilon X \equiv \begin{bmatrix} \epsilon X_1 \\ \epsilon X_2 \\ \epsilon X_3 \end{bmatrix}; \quad (\text{E.2.3-15})$$

$$multi\_X = E\{\epsilon X\} = \begin{bmatrix} \bar{X}_{Part\ i1} \\ \bar{X}_{Part\ i2} \\ \bar{X}_{Part\ i3} \end{bmatrix} = \begin{bmatrix} \bar{X}_{RF\ 1} \\ \bar{X}_{RF\ 1} \\ \bar{X}_{RF\ 1} \end{bmatrix} + \begin{bmatrix} \bar{X}_{RF\ i1} \\ \bar{X}_{RF\ i2} \\ \bar{X}_{RF\ i3} \end{bmatrix}, \quad (\text{E.2.3-16})$$

and where  $\bar{X}_{RF\ il} = 0$ ,  $l = 1, \dots, 3$ , if Random Field  $il = 1$ ;

$$multi\_C_X = E\{(\epsilon X - \bar{X})(\epsilon X - \bar{X})^T\} = \quad (\text{E.2.3-17})$$

$$\begin{bmatrix} C_{X_{RF\ 1}} & cross\_C_{X_{RF\ 1}} & cross\_C_{X_{RF\ 1}} \\ \cdot & C_{X_{RF\ 1}} & cross\_C_{X_{RF\ 1}} \\ \cdot & \cdot & C_{X_{RF\ 1}} \end{bmatrix} + \begin{bmatrix} C_{X_{RF\ i1}} & cross\_C_{X_{RF\ i1\ i2}} & cross\_C_{X_{RF\ i1\ i3}} \\ \cdot & C_{X_{RF\ i2}} & cross\_C_{X_{RF\ i2\ i3}} \\ \cdot & \cdot & C_{X_{RF\ i3}} \end{bmatrix},$$

and where  $C_{X_{RF\ il}} = 0$  if Random Field  $il = 1$ , and  $cross\_C_{X_{RF\ il\ lm}} = 0$  if either Random Field  $il = 1$  or Random Field  $lm = 1$ , for all  $l$  and  $m$  equal to 1, 2, or 3.

Note: the above predictive statistics for random field 1 are equivalent to the predictive statistics for a geolocation product that are described in Appendix B, i.e., correspond to a populated predicted accuracy model for the geolocation product. The appendix also details methods for population.

The multi-geolocation covariance matrix allows for the proper weighting of the corresponding  $m$  geolocations as “control” information in other geolocation products or related objects. It properly accounts for their correlation.

### **Scalar Accuracy metrics**

Scalar accuracy metrics, including CE90 and LE90, should also be computed for the predicted accuracy and predicted relative accuracy for geolocations in each specific partition and for geolocations in the product in general (partition(s) unknown) as detailed in Section E.2.5.

Probability levels XX for the scalar accuracy metrics corresponding to the product in general should include XX=90, XX=99, and possibly XX=999 (99.9 %). The latter two probability levels “capture” any long Gaussian mixture “probability” tails possible with multiple partitions when some of the partitions have a low-probability of occurrence but statistically large errors relative to the other partitions.

### **E.2.4 Optional generalizations**

An MGRF as presented in the previous sections is very general, both in practice and theoretically. In fact, regarding the latter, an MGRF with only one partition corresponds to a wide-sense homogeneous

("stationary") random field since the predictive statistics do not change with geolocation  $X$  in the MGRF or product. On the other hand, if the MGRF contains multiple partitions, the predictive statistics change with geolocation  $X$ ; hence, the MGRF corresponds to a non-homogeneous ("non-stationary") random field - see TGD 1, TGD 2a, and TGD 2e for more details regarding random fields.

In addition, there are additional and practical generalizations that are optional, as described below:

### **Random Field-to-Partition Mapping**

The equations of Section E.2.2 are based on the baseline "Random Field-to-Partition Mapping", i.e., Partition 1 consists of error corresponding to Random Field 1, and all other Partitions  $i > 1$  (if present) consist of the sum of two independent errors, one from Random Field 1 and one from Random Field  $i$ . Random Field 1 represents MGRF or product-wide systematic errors and the other random fields represent additive errors generally associated with "problem" product generation corresponding to different areas or types of features in the product.

These equations can be generalized to an arbitrary "Random Field-to-Partition Mapping" if so desired, i.e., an arbitrary subset of the random fields is mapped to each partition, and where the number of partitions  $m$  is not necessarily equal to the number of random fields  $n$ . However, only equations based on the baseline mapping were previously presented, partially in order to keep the corresponding notation from getting too complicated. If a more general mapping is desired, the equations in Section E.2.1 corresponding to random fields remain the same, however the equations of Sections E.2.2 and E.2.3 corresponding to partitions require straight-forward modifications, primarily to account for the correlation of errors between any pair of the  $m$  partitions that contain from 0 to  $n$  of the same random fields.

As a final comment regarding possible generalizations, one such generalization is termed "direct mapping" and can be implemented using the equations as currently documented. This particular generalization corresponds to each Partition  $i$ ,  $i = 1, \dots, m = n$ , solely consisting of errors from Random Field  $i$ . That is, errors between partitions are not correlated, but of course, are still correlated for any two geolocations associated with the same partition. This generalization can be performed as follows using the baseline mapping and corresponding documented equations: define  $n + 1$  partitions and  $n + 1$  random fields, where the probability of occurrence of Partition 1 is set to a negligible value (essentially zero). Set the predictive statistics for partitions and random fields  $i = 2, \dots, n + 1$  to their desired counterparts  $i - 1$  described earlier in this paragraph.

### **Conditional partitions**

The various equations in Section E.2.3 can also be generalized in a straight-forward manner consistent with the assumption that relevant geolocations correspond to arbitrary partitions contained in a subset of the entire set of partitions. All that needs to be done is to renormalize the applicable partition probabilities so that they sum to 1. Thus, for example, if there are a total of 4 partitions specified for the MGRF, we can compute relevant *gmpdf*, *gmcdf*, *rel\_gmpdf*, and *rel\_gmcdf* for geolocation(s) known not to reside in partitions 2 and 3.

### “Random Regions”

Regarding MGRF content (Section E.2) in general: there can be multiple partitions, but no specific descriptions of the partitions other than for partition 1 which is applicable to all geolocations not in the other partitions by definition, i.e., descriptions for the partitions are “random region”, in which case we simply want more realistic (higher fidelity) probability density functions than those that are explicitly Gaussian.

### **E.2.5 Computation of scalar accuracy metrics and their importance**

Scalar accuracy metrics, such as circular error CE90, CE99, relCE90, and relCE99 associated with random vectors (errors)  $\epsilon X$  corresponding to an MGRF are important for practical applications, and a summary of how they may be computed based on the *a priori* statistics of the MGRF (product) is presented below.

If errors are associated with geolocation(s) in a specific partition of the MGRF or with an MGRF with only one partition, errors are multivariate Gaussian distributed and techniques for their computation (simulation) are presented in TGD 2a (Predictive Statistics) and TGD 2e (Monte Carlo Simulation). If errors are associated with arbitrary geolocations in an MGRF with multiple partitions, they are not multivariate Gaussian distributed – they are multivariate mixed Gaussian distributed. However, they can still be computed (simulated) using a simple modification of the Monte-Carlo simulation technique that was detailed in TGD 2a (Section 5.4.2.2), TGD 2e (Example 2 of Section 5.2.2), and [4].

The technique is illustrated below for use in the computation of the predictive statistics CEXX, with straight-forward modifications for the computation of both LEXX and SEXX, where XX corresponds to the probability level, e.g., CE90 is the radius of a circle such that there is a 90% probability that horizontal geolocation error resides within, or equivalently, if the circle is centered at the geolocation instead of at zero, that the true geolocation resides within. The technique is applicable to relative errors as well, by simply using their associated *a priori* statistics. Also, regardless whether for predicted accuracy or predicted relative accuracy, if an MGRF has only one partition, this same technique can also be used for convenience. See Appendix F for corresponding pseudo-code that includes the generation of scalar predicted accuracy metrics CEXX for horizontal errors, LEXX for vertical errors, and corresponding plots.

A note regarding the symbology used in this section: scalar accuracy metrics with no subscript correspond to arbitrary geolocations in the MGRF or product, whereas scalar accuracy metrics with subscript  $i$  correspond to geolocations associated with or “in” partition  $i$ ,  $i = 1, \dots, n$ . Similarly, underlying predictive statistics corresponding to partition  $i$  are subscripted with  $i$  instead of *Part i* for convenience, such as  $C_{X_i}$  instead of  $C_{X_{Part\ i}}$ .

### **Algorithm for the generation of Circular Error corresponding to predicted accuracy**

- (1) Convert XX probability in percent to a strict probability:  $XX \rightarrow XX/100$ ; (E.2.5-1)
- (2) Compute  $p_i \times 10^7$  Gaussian distributed horizontal (2d) error samples corresponding to each partition  $i$  and consistent with the partition’s specified mean-value  $\bar{X}_i$  and covariance matrix  $C_{X_i}$

corresponding to horizontal errors; e.g., the desired  $C_{X_i}$  is the upper left  $2 \times 2$  of the provided  $3 \times 3$   $C_{X_i}$ ;  $3 \times 3$   $rel\_C_{X_i}$  if for relative accuracy.

- (3) Combine the samples into one concatenated  $2 \times N$  vector with  $N = 1 \times 10^7$  2d elements. Convert to radial errors (error magnitude) and order the 1d entries by ascending magnitude. Set CEXX corresponding to the MGRF (Gaussian mixture distribution) to the  $(XX) \times 10^7$  ordered entry;  $rel\_CEXX$  for relative accuracy.

The total number of  $N$  2d entries equal to  $1 \times 10^7$  used in the above is a recommended value. It can be lowered to  $1 \times 10^6$  if there is only one partition with adequate statistical significance. If there is more than one partition it can also be lowered to  $1 \times 10^6$ , but with lessor statistical significance of results possibly corresponding to higher values of  $XX$ , such as  $XX \geq 99$ , particularly if some of the partitions have a relatively small probability of occurrence along with *a priori* statistics that include either a significant non-zero mean-value or a relatively large covariance of error. The use of  $1 \times 10^7$  samples on a notebook computer requires approximately less than 1 second of wall-clock time using non-optimized MATLAB pseudo-code, and less than 0.1 seconds if  $1 \times 10^6$  samples are used.

The following presents an example of the computation of CE90 for an arbitrary geolocation corresponding to an MGRF with three partitions; corresponding *a priori* statistics are as follows for the horizontal (x and y) geolocation errors:

<u>partition</u>	<u>probability</u>	<u>mean-value</u>	<u>covariance matrix</u>	(E.2.5-2)
1	.6	$\begin{bmatrix} 0 \\ 0 \end{bmatrix}$	$\begin{bmatrix} 2 & 0 \\ 0 & 2 \end{bmatrix}$	
2	.2	$\begin{bmatrix} -2 \\ -2 \end{bmatrix}$	$\begin{bmatrix} 11 & 8 \\ 8 & 11 \end{bmatrix}$	
3	.2	$\begin{bmatrix} 2 \\ 2 \end{bmatrix}$	$\begin{bmatrix} 18 & 0 \\ 0 & 18 \end{bmatrix}$	

Note that the off-diagonal entries in the covariance matrix for partition 2 correspond to non-zero intra-state vector correlation between the x and y geolocation error components.

The actual statistics for the MGRF are usually relative to 3d errors, not 2d horizontal errors alone. Thus, the mean-value and covariance matrix in Equation (E.2.5-2) are typically the first two elements in a 3x1 mean-value and the upper left 2x2 in a 3x3 covariance matrix.

Figure E.2.5-1 presents the first 2,000 independent samples of the combined (by probability of partition) horizontal error samples using the *a priori* statistics of Equation (E.2.5-2). The dots represent the individual samples: red dots, cyan dots, and green dots, corresponding to samples from partitions 1, 2, and 3, respectively, in correct proportions based on their *a priori* probability of occurrence. (Magenta dots (.m), when present, correspond to any remaining partitions, i.e., the summed effects of all partitions greater than 3.)

Figure E.2.5-1 also includes  $CE_{90}$ ,  $CE_{99}$ , and  $CE_{999}$  (99.9%) corresponding to an arbitrary geolocation in the MGRF, computed using all  $1 \times 10^7$  samples, and correspond to the radius of the blue, blue dashed-dot, and blue dashed circles, respectively. The underlying probability distribution is a Gaussian mixture distribution.

$CE_{90_1}$  is also included in Figure E.2.5-1 and corresponds to a geolocation known to be in partition 1 and was computed for comparison. It corresponds to the red circle in the figure. It was calculated based on samples from partition 1 only, i.e., corresponds to a Gaussian distribution.

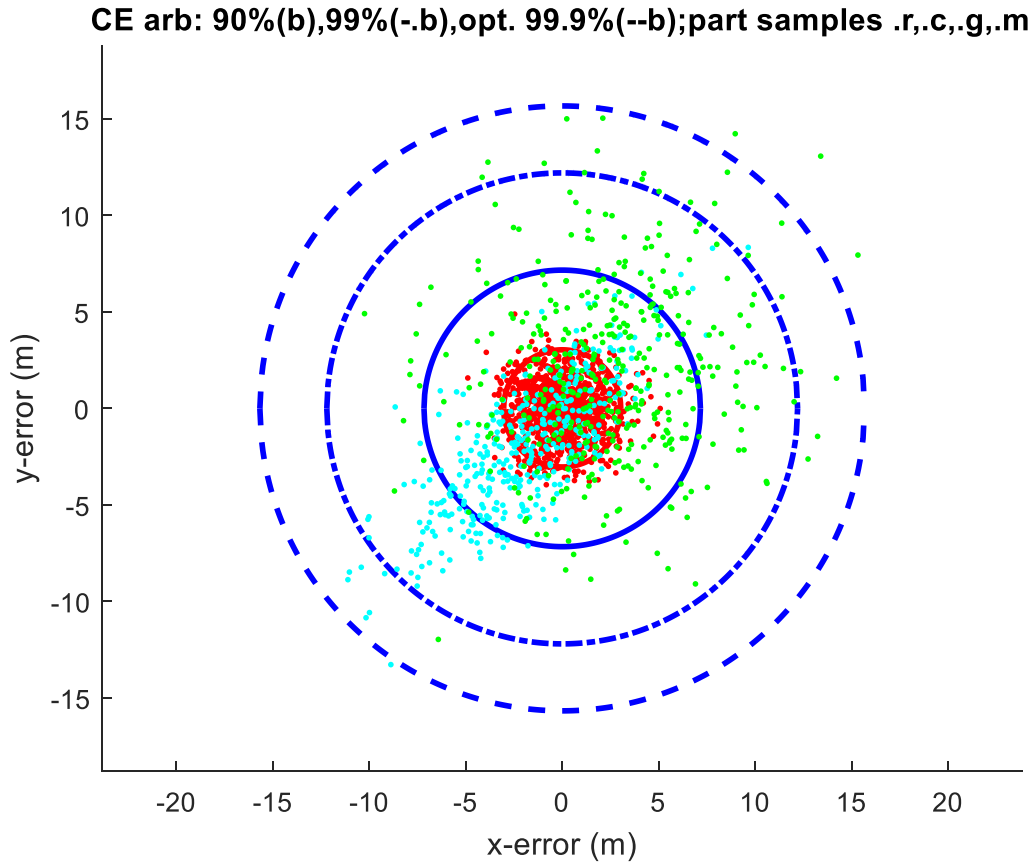


**Figure E.2.5-1:** Example 1: Graphical representation of the computed *a priori*  $CE_{90}$  (blue circle),  $CE_{99}$  (dashed-dot blue circle), and  $CE_{999}$  (dashed blue circle) for the MGRF corresponding to an arbitrary geolocation; red, cyan, and green dots correspond to representative error samples from partition 1, partition 2, and partition 3, respectively; computed *a priori*  $CE_{90_1}$  (red circle) corresponding to a geolocation known to be in partition 1 included for comparison.

For an MGRF containing a partition with a low probability of occurrence and with either a large non-zero mean-value of error or a large covariance matrix relative to the other partitions, it is recommended that the 99.9% probability  $CE_{999}$  be computed as well, as illustrated above.

The following table summarizes the above results.

**Table E.2.5-1:** Example 1: CE in meters for different probability levels for an arbitrary geolocation (first row) and for a geolocation assumed in partition 1 (second row) of the MGRF or product:

location:	CE90 m	CE99 m	CE999
arbitrary	7.2	12.2	15.7
partition 1	3.0	4.3	5.3

As discussed above, CE99 and possibly CE999 are recommended in addition to CE90 for MGRF applications. This is further illustrated in the more extreme and two-partition Example 2 below. The *a priori* statistics for the MGRF are presented first, followed by Table E.2.5-2 of scalar predicted accuracy CE results (no plots):

<u>partition</u>	<u>probability</u>	<u>mean-value</u>	<u>covariance matrix</u>	(E.2.5-3)
1	.95	$\begin{bmatrix} 0 \\ 0 \end{bmatrix}$	$\begin{bmatrix} 1 & 0 \\ 0 & 1 \end{bmatrix}$	
2	.05	$\begin{bmatrix} 0 \\ 0 \end{bmatrix}$	$\begin{bmatrix} 20^2 & 0 \\ 0 & 20^2 \end{bmatrix}$	

**Table E.2.5-2:** Example 2: CE in meters for different probability levels for an arbitrary geolocation (first row) and for a geolocation assumed in partition 1 (second row) of the MGRF or product:

location:	CE90 m	CE99 m	CE999
arbitrary	2.4	35.9	56
partition 1	2.1	3	3.7

Without the inclusion of CE99 and possibly CE999 for an arbitrary geolocation, the effect of the non-nominal partition 2, with only a 0.05 probability of occurrence but with a very large covariance matrix relative to the nominal partition 1, cannot be readily seen. It is these larger probability values for CE (e.g. CE99) that let the user conveniently understand the potential effects on an arbitrary geolocation of a low-probability partition “with” a very high *a priori* statistical error. Furthermore, note the much larger  $CE99/CE90$  and  $CE999/CE90$  ratios corresponding to an arbitrary geolocation versus those corresponding to a geolocation in partition 1. For example,  $CE99/CE90 = 35.9/2.4 \cong 15$  versus  $CE99_1/CE90_1 = 3/2.1 \cong 1.5$ .

Of course, if a geolocation of interest is known to reside in partition  $i$ ,  $CE90_i$  is of interest, and possibly  $CE99_i$  and  $CE999_i$  as well. Therefore, it is recommended that all relevant scalar accuracy metrics be computed and be made available to the “down-stream” user via metadata or its equivalent:  $\{CE90, CE99, CE999\}$  as well as  $\{CE90_i, CE99_i\}$ , for partitions  $i = 1, \dots, n$ , as detailed in Section E.5. Note that, since errors in partition  $i$  are assumed Gaussian distributed,  $CE99_i$  (and  $CE999_i$ ) can be computed from  $CE90_i$  as a scalar multiple. However,  $CE99_i$  is recommended for inclusion in the metadata for convenience of the “down-stream” user.

Finally, as discussed above, scalar accuracy metrics corresponding to an MGRF are convenient, practical, and important statistics. However, as a reminder, the corresponding probability distribution function (*gmpdf*) and cumulative distribution function (*gmcdf*) contain more information than do the scalar accuracy metrics and can be computed using the partitions' *a priori* statistics as detailed earlier. In particular, *gmpdf* may be useful for more advanced, typically non-linear, applications. Recall that *gmpdf* corresponds to a Gaussian mixture distribution of errors corresponding to an arbitrary geolocation in the MGRF or product. It reduces to a Gaussian distribution if there is only one partition in the MGRF.

Figure E.2.5-2 presents a *gmpdf* that corresponds to a somewhat extreme case in order to better illustrate the information that it can contain. The *gmpdf* was computed based on the following predictive statistics for the partitions:

<u>partition</u>	<u>probability</u>	<u>mean-value</u>	<u>covariance matrix</u>	(E.2.5-4)
1	.2	$\begin{bmatrix} 0 \\ 0 \end{bmatrix}$	$\begin{bmatrix} 1 & 0 \\ 0 & 1 \end{bmatrix}$	
2	.4	$\begin{bmatrix} -6 \\ -6 \end{bmatrix}$	$\begin{bmatrix} 3 & 1.9 \\ 1.9 & 3 \end{bmatrix}$	
3	.4	$\begin{bmatrix} 3 \\ 3 \end{bmatrix}$	$\begin{bmatrix} 2 & 0 \\ 0 & 8 \end{bmatrix}$	

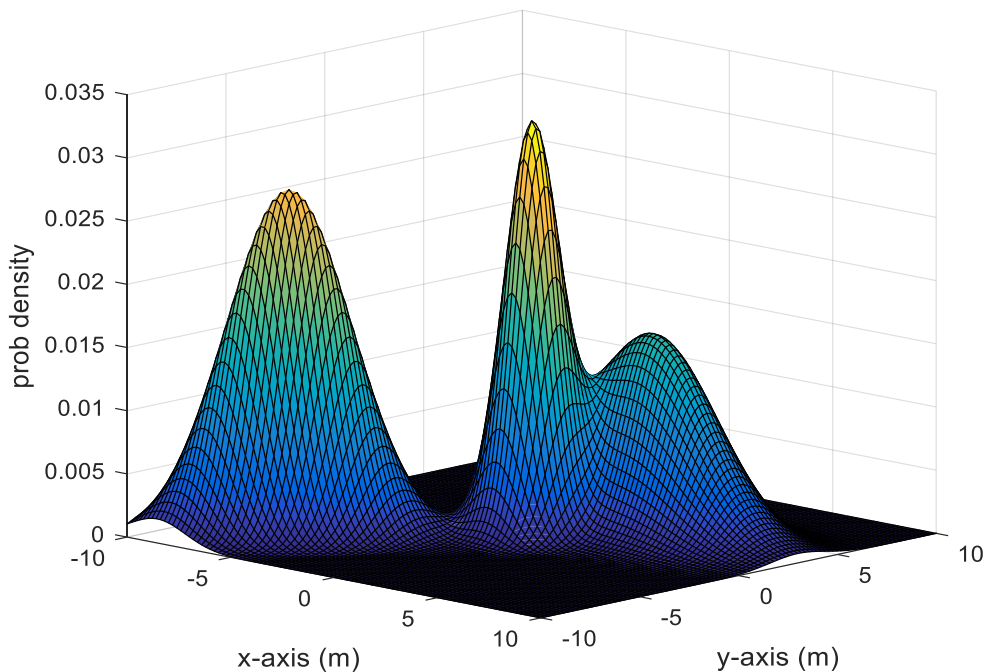


**Figure E.2.5-2:** *gmpdf* corresponding to the statistics of Equation (E.2.5-4)

## E.2.6 Summary of relevant MGRF statistical terminology/symbology

The following is a summary of the terminology/symbology of the major predictive statistics corresponding to geolocation errors represented by an MGRF for the predicted accuracy of a geolocation product. Included are the relevant equation numbers corresponding to their original definition/derivations for further reference.

### **(1) Random Field $RF_i, i = 1, \dots, n$**

Statistics for  $\epsilon X$  corresponding to Random Field  $RF_i$ , the error in a geolocation  $X$ :

number of random fields: $n$	a defining input	
mean-value: $\bar{X}_{RF_i}$	a defining input	(original) Equation (E.2.1-1)
covariance matrix: $C_{X_{RF_i}}$	a defining input	Equation (E.2.1-2)
spdcf: $spdcf_{RF_i}(\Delta X)$	a defining input	Equation (E.2.1-3)
probability density function: $pdf_{RF_i}(\epsilon X)$		Equation (E.2.1-4)
cumulative distribution function: $cdf_{RF_i}(\epsilon X)$		Equation (E.2.1-4)

Statistics associated with the errors  $\epsilon X_1$  and  $\epsilon X_2$  – both errors correspond to Random Field  $RF_i$  (cross-covariance = 0 if errors correspond to different random fields):

cross-covariance matrix: $cross\_C_{X_{RF_i}}$	Equation (E.2.1-13)
--	---------------------

Statistics for the relative error  $rel\_ \epsilon X = (\epsilon X_1 - \epsilon X_2)$ , where both errors correspond to Random Field  $RF_i$ :

mean-value: $rel\_ \bar{X}_{RF_i} = 0$	Equation (E.2.1-14)
covariance matrix: $rel\_ C_{X_{RF_i}}$	Equation (E.2.1-15)

### **(2) Partition $Part_i, i = 1, \dots, n$**

It is assumed that an error in a geolocation associated with  $Part_1$  corresponds to  $RF_1$  and an error in a geolocation associated with  $Part_i, 1 < i \leq n$ , is the sum of two independent errors, one corresponding to  $RF_1$  and one corresponding to  $RF_i$ . Correspondingly, the number of partitions  $n$  is equal to the number of random fields  $n$ .

number of partitions: $n$	a defining input	Equation n/a
partition description: $\{description\}_{Part_i}$	a defining input	Equation n/a
partition probability of occurrence: $p_i$	a defining input	Equation n/a

### **Geolocations known to correspond to Partition $Part_i$**

Statistics for  $\epsilon X$  corresponding to arbitrary geolocation  $X$  in  $Part_i$ :

mean-value:	$\bar{X}_{Part_i}$	(original) Equation (E.2.2-1)
covariance matrix:	$C_{X_{Part_i}}$	Equation (E.2.2-2)
probability density function:	$pdf_{Part_i}$	Equation (E.2.2-3)
cumulative distribution function:	$cdf_{Part_i}$	Equation (E.2.2-3)
scalar accuracy metrics	$LEXX_i, CEXX_i; XX = 90 \text{ and } 99$	Equation (E.2.4-1)

Statistics for relative error  $rel_{\epsilon X} = (\epsilon X_1 - \epsilon X_2)$  corresponding to arbitrary geolocations  $X_1$  and  $X_2$  in  $Part_i$ :

mean-value:	$rel_{\bar{X}_{Part_i}}$	Equation (E.2.2-6)
covariance matrix:	$rel_{C_{X_{Part_i}}}$	Equation (E.2.2 -7)
probability density function:	$rel_{pdf_{Part_i}}$	Equation (E.2.1-8)
cumulative distribution function:	$rel_{cdf_{Part_i}}$	Equation (E.2.1-8)
scalar rel accuracy metrics:	$rel_{LEXX_i}, rel_{CEXX_i}; XX = 90 \text{ and } 99$	Equation (E.2.5-1)

#### **Arbitrary geolocation(s) in the MGRF – specific partition(s) unknown**

Statistics for  $\epsilon X$  corresponding to arbitrary geolocation  $X$ :

mean-value:	$\bar{X}$	Equation (E.2.3-2)
covariance matrix:	$C_X$	Equation (E.2.3-4)
probability density function:	$gmpdf$	Equation (E.2.3-1)
cumulative distribution function:	$gmcdf$	Equation (E.2.3-6)
scalar accuracy metrics:	$LEXX, CEXX; XX = 90, 99, \text{ and } 999$	Equation (E.2.5-1)

Statistics for relative error  $rel_{\epsilon X} = (\epsilon X_1 - \epsilon X_2)$  corresponding to arbitrary geolocation  $X_1$  and  $X_2$ :

mean-value:	$rel_{\bar{X}}$	Equation (E.2.3-12)
covariance matrix:	$rel_{C_X}$	Equation (E.2.3-13)
probability density function:	$rel_{gmpdf}$	Equation (E.2.3-9)
cumulative distribution function:	$rel_{gmcdf}$	Equation (E.2.3-11)
scalar rel accuracy metrics:	$LEXX, CEXX; XX = 90, 99, \text{ and } 999$	Equation (E.2.5-1)

#### **Multiple geolocation(s) in the MGRF - partitions known**

mean-value:	$multi_{\bar{X}}$	Equation (E.2.3-16)
covariance matrix:	$multi_{C_X}$ : covariance matrix	Equation (E.2.3-17)

All the above statistics can be derived per the equations of Section E.2 from the small subset of predictive statistics that correspond to “a defining input” in the above section.

Typically, the “down-stream” user of the product is only interested in a subset of the statistics that correspond to partitions and it is recommended that they be pre-computed and included in the product’s metadata or its equivalent for the convenience of the user. However, for completeness, a subset of the statistics corresponding to random fields is also recommended for inclusion, and is required for optional near-optimal adjustment of the product (Section E.3). Section E.5 details recommended metadata.

### **E.3 Adjustability of the MGRF (product)**

For some applications of a product, it may be desirable to adjust or correct the product prior to its subsequent use, or more generally, to fuse it with other products. This is described below assuming an MGRF representation of the (pre-corrected) product’s predicted accuracy. Section E.3.1 describes adjustment of a product of interest and Section E.3.2 generalizes this to the fusion or simultaneous adjustment of multiple products of interest. Fusion of multiple products is preferred in general; however, its description in Section E.3.2 does rely on the description of product adjustment in Section E.3.1.

Adjustment/fusion of the product(s) is not applicable to the typical “down-stream” user of the product(s). However, when implemented, a user should “call” an available application or code module via a standardized API (Application Program Interface) that essentially implements the following descriptions/designs.

For those readers not interested in details regarding either product adjustment (Section E.3.1) or the fusion of multiple products (Section E.3.2), it is recommended that they still review Section E.3.2.5 which presents an example of fusion in order to better understand its overall purpose and its effectivity in conjunction with the use of MGRF for the representation of predicted accuracy.

#### **E.3.1 Adjustment of a product**

This section describes the adjustment of a product of interest based on other overlapping products and/or surveyed ground control. Only the product of interest is adjusted.

The adjustment technique for a geolocation product relies on a populated Geolocation Product Predicted Accuracy Model, or more specifically, a populated MGRF. It is very similar to the adjustment technique for data/products that correspond to an image and that relies on a populated Geolocation Data Predicted Accuracy Model: Measurement-space. Both adjustment techniques rely on the concept of a correction grid. Differences in the two adjustment techniques, including some symbology, are primarily due to:

- The use of 3d (geolocation) versus 2d (image location) in the data/product
- The explicit use of multiple random fields (and partitions) for representation of predicted accuracy for the geolocation product

The adjustment technique for a geolocation product is based on the correction grid (Adjustment Model) that was described in general in Section 5.3.3.1 of the main body of this document. Section 5.3.3.1 also includes an example of the adjustment technique as applied to an image and which is further detailed in Appendix D including various performance results.

The performance results presented in Appendix D are also generally applicable to the use of the correction grid for a 3d geospatial product. In Addition, Appendix D also contrasts the use of a correction grid with a correction model that is based on the solution for deterministic but unknown parameters, such as a sparse set of parameters corresponding to an affine transformation – applicable to either an image or, with the use of a few more parameters, to a 3d geolocation product. As discussed in Appendix D, if errors are known *a priori* to correspond to the affine transformation, a corresponding correction model performs better than a correction grid. However, a correction grid is more robust and therefore recommended for Commodities data with little or no reliable accuracy pedigree, i.e., an affine transformation is not known to be applicable in general.

### ***E.3.1.1 Solution/algorithm overview***

Figure E.3.1.1-1 presents an example of a correction grid for a geolocation product and related definitions. The correction grid is rectangular and contains an arbitrary number of grid points in both the grid's rows and columns, but is a square ( $3 \times 3$ ) grid in this example for simplicity and clarity. This particular correction grid is also assumed applicable in some of the definitions and equations that follow in terms of indexing. However, indexing is easily generalized in an intuitive manner to correspond to a correction grid of arbitrary size.

In addition, geolocations are assumed 3d and their corresponding errors to be corrected are assumed 3d as well. The correction grid spans a corresponding horizontal plane, i.e., is indexed by the geolocation's horizontal coordinates ( $x, y$ ) More specifically, the representation of geolocations and their errors are assumed relative to a local tangent plane typically centered at the approximate center of the product's AOI or "footprint".

The underlying geolocations or grid points in the product that correspond to the elements of the correction vector  $\delta X$  and are represented by the gray circles in the figure. The blue circle and the blue square represent measurements (geolocations) in the product and are explained later.

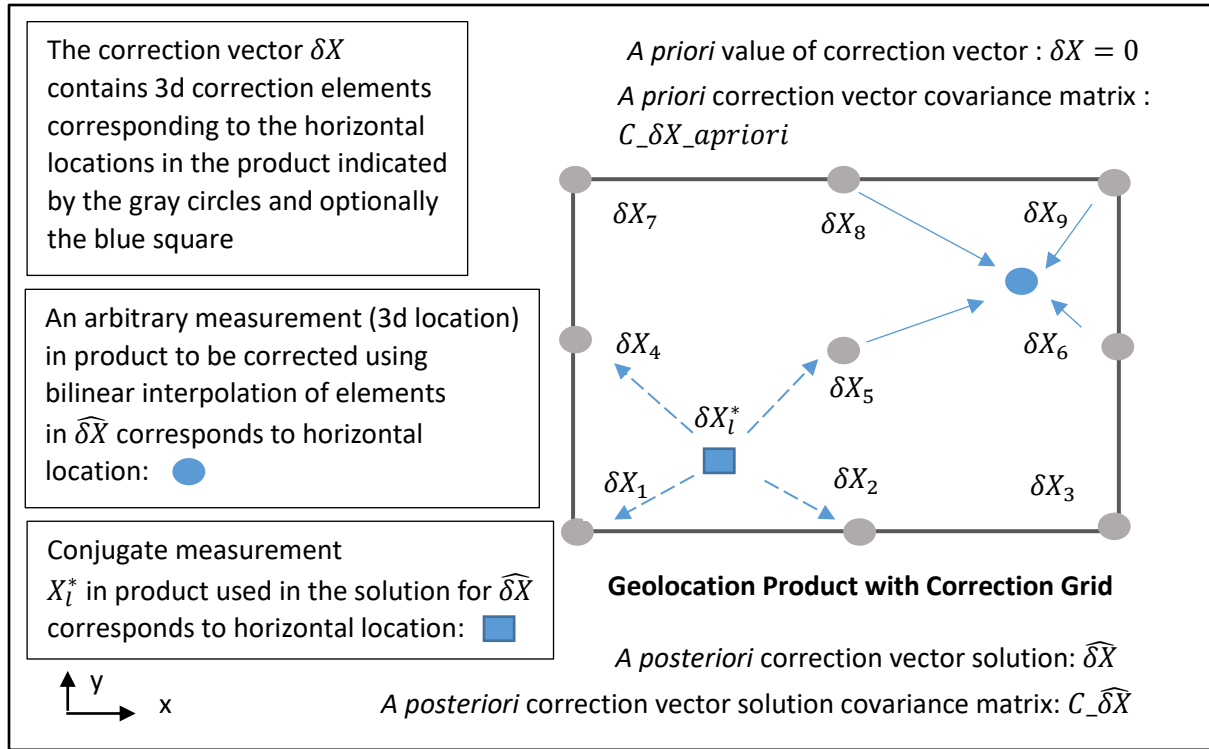


**Figure E.3.1.1-1:** Correction grid ( $3 \times 3$ ) and related definitions for a geolocation product

The correction grid is used to correct for product-wide systematic errors, i.e., errors in Random Field 1 which are present in all partitions of the MGRF (product).

### Preliminary definitions

$\delta X = [\delta X_1^T \ \dots \ \delta X_n^T]^T$  is defined as the correction vector for solution, and consists of individual  $3 \times 1$  geolocation corrections  $\delta X_j$ , for  $j = 1, \dots, n$ , each with an underlying geolocation  $X_j$  in the product. The dimension of  $\delta X$  is  $3n \times 1$ .

The various  $\delta X_j, j = 1, \dots, n$ , are the elements of the correction grid, where  $n = 9$  in this example.

### A priori values

The *a priori* mean-value and error covariance matrix for  $\delta X$  are equal to  $multi\_X$  and  $multi\_C_X$ , respectively, defined earlier in Equations E.2.3-16 and E.2.3-17, respectively. These derived predictive statistics are applicable to the errors in  $X_j, j = 1, \dots, n$ , and assume that their corresponding partitions in the MGRF (product) are known.  $multi\_X$  is typically equal to zero and assumed as such for the remainder of this section. If it is not equal to zero for a specific product, simply subtract its components from corresponding conjugate measurements and then add it back to the resultant solution for  $\delta X$  ( $\widehat{\delta X}$ ) which is derived later in this section.

In summary, the *a priori* predictive statistics applicable to the correction vector for solution are:

$$E\{\delta X\} = 0 \quad (3n \times 1) \text{ and } E\{\delta X \delta X^T\} = multi\_C_X \quad (3n \times 3n).$$

As such, the actual value for  $\delta X$  whenever used in the remainder of this section is zero, i.e.,  $\delta X = 0$ .

For the best solution results, it is recommended that adjacent corrections (locations) in the correction grid have an *a priori* spatial correlation of at least 0.9 for each (x,y,z) component, and preferably 0.95 or higher. This can be achieved by specifying a larger sized correction grid if necessary, in coordination with the spdcf used to compute  $multi\_C_X$ .

### **Conjugate measurements**

Assume that there are  $l = 1, \dots, m$  geolocations available from external or control data (surveyed control points, other products, etc.) that overlap the product for adjustment. More specifically, assume that there are  $m$  pairs of conjugate 3d geolocations or measurements:

$M\_cntrl_l$ ,  $l = 1, \dots, m$ , geolocation identified/measured in the external or control data ( $3 \times 1$ ).

$M\_prod_l \equiv X_l^*$ ,  $l = 1, \dots, m$ , geolocation identified/measured in the product for adjustment ( $3 \times 1$ ), see the blue square in Figure E.3.1.1-1. The  $M\_prod_l$  are the predicted value for the  $M\_cntrl_l$  based on the (unadjusted) product.

Define the corresponding control measurement vector and product measurement vector as follows:

$$M\_cntrl = [M\_cntrl_1^T \quad \dots \quad M\_cntrl_m^T]^T \quad (3m \times 1),$$

$$M\_prod = [M\_prod_1^T \quad \dots \quad M\_prod_m^T]^T \quad (3m \times 1),$$

Define the actual measurement vector in the WLS solution as their difference:

$$\Delta M = M\_cntrl - M\_prod \quad (3m \times 1), \text{ where}$$

$$\Delta M = [\Delta M_1^T \quad \dots \quad \Delta M_m^T]^T.$$

### **Measurement errors**

We first examine the various quantities that make up the conjugate measurements  $M\_cntrl_l$ ,  $M\_prodl_l$ , and their difference  $\Delta M_l$ ,  $l = 1, \dots, m$ :

$$M\_cntrl_l = X_l^*_{true} + \epsilon\_cntrl\_sys_l + \epsilon\_cntrl\_mens_l,$$

$$M\_prod_l = X_l^*_{true} - \delta X_l^* + \epsilon\_prod\_mens_l, \text{ and therefore}$$

$$\Delta M_l = -\delta X_l^* + \epsilon\_cntrl\_sys_l + \epsilon\_prod\_mens_l, \text{ where}$$

$$\epsilon\_prod\_mens_l \equiv \epsilon\_cntrl\_mens_l + \epsilon\_prod\_mens_l.$$

The systematic error in the product associated with the underlying geolocation  $X_l^*$  is defined as equal to minus its correction  $\delta X_l^*$  which is to be estimated. This correction is not explicitly in the correction grid, but is related to the various components that are in the correction grid and contained in  $\delta X = [\delta X_1^T \dots \delta X_n^T]^T$  as shown later.

The identification/measurement errors ( $\epsilon_{\Delta M\_mens}$ ) associated with  $\Delta M$  are termed mensuration errors, and represent the summed effects of the identification/measurement errors associated with both the External Data ( $M\_cntrl$ ) and the identification/measurement of its conjugate geolocations contained in the unadjusted product ( $M\_prod$ ).

The above mensuration errors are assumed to have a mean-value of zero and an *a priori* covariance matrix defined as  $Cov\_mens$  ( $3m \times 3m$ ), a block diagonal matrix since errors between two different  $3 \times 1$  components  $\epsilon_{\Delta M\_mens_l}$  are assumed uncorrelated.  $Cov\_mens$  is also typically a strictly diagonal matrix since errors between the three components (x,y,z) of  $3 \times 1$   $\epsilon_{\Delta M\_mens_l}$  are typically assumed uncorrelated as well.

The measurement vector  $M\_cntrl$  also has additional errors ( $\epsilon_{cntrl\_sys}$ ) associated with the external or control data source itself. These errors are typically systematic or spatially correlated as well. Their corresponding mean value is assumed equal to zero and their *a priori* error covariance matrix assembled and designated as  $Cov\_cntrl$ , a full  $3m \times 3m$  with non-zero cross-covariance blocks associated with spatial correlation. For example, if the control data corresponded to another geolocation product with MGRF-based predicted accuracy,  $Cov\_cntrl$  would be identical in form (not content) as the *a priori* error covariance matrix ( $multi\_C_X$ ) of the product for adjustment.

The *a priori* covariance for the sum of all of the above errors associated with the measurement vector  $\Delta M$  is defined and computed as follows:

$$Cov\_meas = Cov\_mens + Cov\_cntrl \quad (3m \times 3m).$$

### Partial derivative matrix

$$B \equiv \partial(\Delta M)/\partial(\delta X) = \begin{bmatrix} B_1 \\ \vdots \\ B_l \\ \vdots \\ B_m \end{bmatrix}, \text{ where } B_l \text{ is a } 3 \times 3n \text{ matrix associated with measurement } \Delta M_l \text{ and is}$$

defined as follows based on the measurement  $M\_prod_l = X_l^*$  corresponding to the blue square in Figure E.3.1.1-1 and its corresponding correction for solution  $\delta X_l^*$ . However, in this solution approach,  $\delta X_l^*$  is not in the adjustment vector and is approximated by the four adjustment elements  $\{\delta X_1, \delta X_2, \delta X_4, \text{ and } \delta X_5\}$  in the correction grid cell that are:

Let  $a_1 - a_4$  represent the adjustment elements' corresponding scalar bilinear interpolation coefficients, respectively, computed based on the 2d distances between  $X_l^*$  and  $X_1, X_2, X_4$ , and  $X_5$ , respectively.

Define  $A_k = a_k I_{2 \times 2}$ , for  $k = 1, \dots, 4$ . (Note: the  $a_k$  are non-negative and sum to 1.)

Therefore:

$\delta X_l^* \cong A_1 \delta X_1 + A_2 \delta X_2 + A_3 \delta X_4 + A_4 \delta X_5$ , and the

corresponding entry in the  $B$  matrix is equal to:

$$B_l = [A_1 \quad A_2 \quad 0_{3 \times 3} \quad A_4 \quad A_5 \quad 0_{3 \times 3} \quad 0_{3 \times 3} \quad 0_{3 \times 3} \quad 0_{3 \times 3}].$$

That is, the measurement  $M_{prod_l} = X_l^*$  is assumed to be related to the components explicitly contained in the adjustment vector.

### **WLS solution**

The WLS solution for the correction vector is as follows:

$$\widehat{\delta X} = (C_{\widehat{\delta X}})^T B^T W \Delta M, \text{ a } 3n \times 1 \text{ vector,}$$

where  $W = (Cov_{meas})^{-1}$ ,

and the *a posteriori* solution error covariance matrix is equal to:

$$C_{\widehat{\delta X}} = (multi_{C_X}^{-1} + B^T W B)^{-1}, \text{ a } 3n \times 3n \text{ matrix.}$$

It is recommended that the number of elements in the correction grid is such that the *a priori* spatial correlation of errors corresponding to adjacent corrections  $\delta X_j$  in the correction grid is approximately 0.9 or higher. The higher the correlation, the more effective the solution. In the extreme, as the *a priori* spatial correlation approaches 1.0 between virtually all corrections in the grid, this is essentially equivalent to solving for a product-wide bias error; and if applicable, yields the highest solution accuracy and corresponding predicted accuracy possible.

In addition, it is recommended that the WLS solution includes processing for quality control, such as measurement editing and examination of the *a posteriori* (post-solution) measurement residuals normalized by their predicted accuracy. If these residuals are outside their expected range, modify (scale up or down) the solution vectors *a priori* error covariance matrix  $C_{\delta X\_apriori}$  and/or modify (scale up or down) the *a priori* error covariance for the measurements  $Cov_{meas}$  accordingly and re-perform the WLS solution as needed. In addition, the *a priori* spdcf may need similar modifications for best solution results. See Section B.2.2 regarding the solution for an image correction grid for further details, and more generally, TGD 2d (Estimators and their Quality Control).

Although not repeated again, the above quality control and “tuning” of the *a priori* predictive statistics for a reliable WLS solution are applicable to all of the WLS solutions described in the remaining (sub)sections of Section E.3.

#### ***E.3.1.2 Alternate solution approach: optimal and recommended***

The above solution process is near optimal, but not theoretically optimal, due to the use of interpolation associated with the conjugate measurements. An optimal solution process (assuming correct *a priori* modeling) is recommended as a simple extension of the above solution process that does not require the interpolation, and that is defined as follows:

Augment the state (correction) vector for solution with  $3 \times 1$  corrections explicitly associated with the conjugate measurements (3d locations) in the product for correction, i.e.,  $\delta X_l^*$  associated with  $X_l^*$ ,  $l = 1, \dots, m$  (see Figure E.3.3.1-1):

$$\delta X \equiv [\delta X_1^T \quad \dots \quad \delta X_n^T \quad \delta X_1^{*T} \quad \dots \quad \delta X_m^{*T}]^T, \text{ a } (3n + 3m) \times 1 \text{ vector.}$$

Augment the *a priori* covariance matrix as well:  $C_{\delta X\_apriori}$ , an  $(3n + 3m) \times (3n + 3m)$  matrix.

The same method used to compute the *a priori* covariance matrix (*multi\_C<sub>x</sub>*) in the first place is used to augment it in order to reflect the augmented correction vector for solution. The method was defined earlier in Equations E.2.3-17 and E.2.3-18. Augmentation of the matrix takes into account the *a priori* spatial correlation between all errors, computed based on the difference between all geolocation pairs that underline all correction elements, both  $\delta X_i$ ,  $i = 1, \dots, n$  and  $\delta X_l^*$ ,  $l = 1, \dots, m$ , combined.

Redefine the partial derivative matrix  $B$  as follows:

$$B = [0_{3m \times 3n} \quad I_{3m \times 3m}].$$

The remaining steps in the solution are identical to those for the first solution, yielding an  $(3n + 3m) \times 1$  *a posteriori* solution  $\widehat{\delta X}$  and a  $(3n + 3m) \times (3n + 3m)$  *a posteriori* solution error covariance matrix  $C_{\widehat{\delta X}}$ .

This optimal solution method updates the new elements in the augmented correction vector directly via the measurements, whereas the original elements are now updated via their spatial correlation with the new elements as specified in the corresponding cross-covariance block in the augmented  $C_{\delta X\_apriori}$ .

The augmented elements can then be removed from  $\widehat{\delta X}$  and their corresponding covariance block and cross-block from  $C_{\widehat{\delta X}}$  if so desired, making the subsequent processing for the correction of an arbitrary geolocation in the corrected product identical for both solution methods, and defined as follows:

### ***E.3.1.3 Correction of the product***

For an arbitrary geolocation in the product (see blue circle in Figure E.3.1.1-1), compute its correction as the bilinear interpolation of the four elements in  $\widehat{\delta X}$  that correspond to the correction cell in which it resides, i.e.,  $\widehat{\delta X}_5$ ,  $\widehat{\delta X}_6$ ,  $\widehat{\delta X}_8$ , and  $\widehat{\delta X}_9$  in this example. The correction is added to the geolocation (the corrected geolocation is not shown in the figure.) Its corresponding  $3 \times 3$  error covariance matrix is defined as the bilinear interpolation of the four surrounding  $3 \times 3$  diagonal blocks in  $C_{\widehat{\delta X}}$ .

Such a correction and its predicted accuracy are approximate due to the interpolation, but are reasonable. Furthermore, they are virtually optimal if *the a priori* spatial correlation between adjacent corrections in the correction grid is high, a minimum of 0.9.

A theoretically optimal correction would require an additional augmented correction  $\delta X_l^{**}$ , for each geolocation in the product of interest, similar to the augmented corrections  $\delta X_l^*$  associated with the optimal solution for the correction vector that were defined earlier. Optimality is defined as the smallest solution errors possible (minimization of the WLS cost function), given the set of available external or control measurements (geolocations), and that also includes reliable predicted accuracy.

### E.3.2 Generalization to the fusion of products

The above solution/algorithm was for the adjustment of a geolocation product of interest based on geolocations from other overlapping products and/or external control. Only the product of interest was adjusted or corrected. This can be generalized to the simultaneous fusion of all relevant overlapping products, i.e., all products are simultaneously adjusted or corrected. The corrections are automatically “allocated” to the various products based on measured discrepancies between their geolocations as well as the products’ *a priori* uncertainties or predicted accuracies. For example, if there are two products for fusion, the first with *a priori* uncertainty (predicted accuracy) larger than the second, it will be automatically allocated larger corrections.

The fusion of overlapping products improves the accuracy of each product and enables consistent geolocations across each product-pair.

The approach presented in this section is similar to the earlier algorithms of Section E.3.1 with relevant changes outlined below assuming the simultaneous fusion of two overlapping products for simplicity of example, i.e., the fusion of two products of interest. It also assumes that there is no explicit external control information available for simplicity of example as well.

Fusion is either based on a near-optimal solution (Section E.3.2.1) or an optimal solution (Section E.3.2.2), where the former relies on bilinear interpolation and the latter relies on an augmented state vector for solution.

#### E.3.2.1 Relevant modifications: bilinear interpolation assumed

The following outlines the appropriate modifications relative to Section E.3.1.1 which corrected the product only. The subscripts 1 and 2 indicate the two products of interest. Product 1 is assumed to have a correction grid containing  $n_1$  corrections and product 2 a correction grid containing  $n_2$  corrections.

- Expand the adjustment vector for solution as follows:

$\delta X \equiv \begin{bmatrix} \delta X^1 \\ \delta X^2 \end{bmatrix}$ , where  $\delta X^i$  is defined as containing the elements of the correction grid for product  $i$  and has dimension  $3n_i \times 1$ ,  $i = 1, 2$ . The dimension of  $\delta X$  is  $3n \times 1$ , where  $n \equiv (n_1 + n_2)$ .

Note that  $\delta X^i$  has been redefined to correspond to the  $\delta X$  of Section E.3.1.1, but is assumed applicable to product  $i$ , for  $i = 1, 2$ . In particular,  $\delta X_j^i$  corresponds to the  $j$ -th  $3 \times 1$  element of the correction grid corresponding to product  $i$ .

Similarly, expand the corresponding *a priori* error covariance matrix for  $\delta X$  as follows:

$$multi\_C_X = \begin{bmatrix} multi\_C_X^1 & 0 \\ 0 & multi\_C_X^2 \end{bmatrix}. \text{ The dimension of } multi\_C_X \text{ is } 3n \times 3n.$$

As a reminder, and consistent with the above note regarding notation,  $multi\_C_X^1$  actually corresponds to  $multi\_C_X$  of Section E.3.1.1, but assumed applicable to product 1. The *a priori* values of  $\delta X^1$  and  $\delta X^2$  reasonably assumed uncorrelated.

- Redefine the measurement vector as input to the WLS solution as follows:

$\Delta M \equiv M_{prod}^2 - M_{prod}^1$ , where the dimension of all three vectors is  $3m \times 1$ , assuming a total of  $m$  pairs of conjugate 3d measurements.

$M_{prod}^i$  is the vector of conjugate geolocations identified/measured in product  $i$ ,  $i = 1, 2$ . That is, they are assumed to be conjugate across the two products.

- Redefine the partial derivative matrix  $B$  as follows:

$B = [B^1 \quad -B^2]$ , where  $B^i$  corresponds to product  $i$ ,  $i = 1, \dots, 2$ , has dimension  $3m \times 3n_i$ , and is analogous to  $B_l$  of Section E.3.1.1 but applicable to product  $i$ .

The dimension of the redefined  $B$  is  $3m \times 3n$ .

As an example, assuming the same product size and the same grid size and layout for both products and consistent with Figure E.3.1.1-1, the matrix entry  $B_l$  is equal to:

$$B_l = [B_l^1 \quad -B_l^2], \text{ where}$$

$$B_l^i = [A_1 \quad A_2 \quad 0_{3 \times 3} \quad A_4 \quad A_5 \quad 0_{3 \times 3} \quad 0_{3 \times 3} \quad 0_{3 \times 3} \quad 0_{3 \times 3}], i = 1, 2,$$

and the  $A_k$ ,  $k = 1, \dots, 4$ , are equal to  $A_k = a_k I_{3 \times 3}$  where the  $a_k$  are the scalar bilinear interpolation coefficients.

- Redefine the *a priori* measurement error covariance matrix as follows:

$Cov_{meas} = Cov_{mens}$ , a  $3m \times 3m$  *a priori* error covariance matrix corresponding to the summed effects of conjugate geolocation identification/measurement or mensuration error in products 1 and 2.

Note that  $Cov_{meas}$  no longer contains a contribution due to systematic error as the latter is being solved for both products 1 and 2. There is also no contribution for sensor-mensuration error as this also contributes to  $multi\_C_X$  if applicable.

- Implement the same top-level solution (Equation (E.3.1.3-1)) and subsequent processing steps (Equation (E.3.1.3-2)) of Section E.3.1.3, but with appropriate changes to the corresponding vectors and matrices as described above.

The subsequent  $3n \times 1$  solution and its  $3n \times 3n$  *a posteriori* error covariance matrix are as follows:

$$\widehat{\delta X} \equiv \begin{bmatrix} \widehat{\delta X^1} \\ \widehat{\delta X^2} \end{bmatrix} \text{ and } C_{\widehat{\delta X}} = \begin{bmatrix} C_{\widehat{\delta X^1}} & C_{\widehat{\delta X^1}^2} \\ C_{\widehat{\delta X^2}^1} & C_{\widehat{\delta X^2}} \end{bmatrix}.$$

### E.3.2.2 Relevant modifications: expanded adjustment vector assumed

- Expand the adjustment vector for solution as follows:

$\delta X \equiv \begin{bmatrix} \delta X^1 \\ \delta X^2 \end{bmatrix}$ , where  $\delta X^i$  has been redefined to contains the grid corrections of product  $i$  followed by its ancillary corrections and has dimension  $3(n_i + m) \times 1$ ,  $i = 1, 2$ , relative to the notation in Section E.3.1.2, including the definitions of the ancillary corrections. The resultant dimension of  $\delta X$  is  $3n \times 1$ , where  $n \equiv (n_1 + n_2 + 2m)$ .

Similarly, expand the corresponding *a priori* error covariance matrix as follows:

$$multi\_C_X \equiv \begin{bmatrix} multi\_C_X^1 & 0 \\ 0 & multi\_C_X^2 \end{bmatrix}. \text{ The dimension of } multi\_C_X \text{ is } n \times n.$$

- Redefine the partial derivative matrix  $B$  as follows:

The dimension of  $B$  is  $3m \times 3n$  and can be partitioned as follows:

$$B = [B^1 \quad -B^2],$$

where  $B^i = [0_{3m \times 3n_i} \quad I_{3m \times 3m}]$ , for products  $i = 1, 2$ .

- Implement the same top-level solution (Equation (E.3.1.3-1)) and subsequent processing steps (Equation (E.3.1.3-2)) of Section E.3.1.3, but with appropriate changes to the corresponding vectors and matrices as described above.

The subsequent  $n \times 1$  solution and its  $n \times n$  *a posteriori* error covariance matrix are:

$$\widehat{\delta X} \equiv \begin{bmatrix} \widehat{\delta X}_{-1} \\ \widehat{\delta X}_{-2} \end{bmatrix} \text{ and } C_{\widehat{\delta X}} = \begin{bmatrix} C_{\widehat{\delta X}_{-1}} & C_{\widehat{\delta X}_{-12}} \\ C_{\widehat{\delta X}_{-21}} & C_{\widehat{\delta X}_{-2}} \end{bmatrix}.$$

### ***E.3.2.3 Relevant modifications for the correction of products***

The corrected geolocations and their predicted accuracies in product  $i$ ,  $i = 1, 2$ , are based on bilinear interpolation of their corresponding grid corrections and their predicted accuracies contained in  $\widehat{\delta X}^i$  and  $C_{\widehat{\delta X}^i}$ , respectively.

### **Generalization of the entire fusion process to more than two products**

The entire fusion process described in Sections E.3.2.1 through E.3.2.3 can be generalized in a straightforward manner for the simultaneous fusion of  $n > 2$  products, but requires more complex notation to document. In particular, the various components of the measurement vector  $\Delta M$  still correspond to conjugate geolocations from two different products regardless the total number of products  $n$ . However, the various components of  $\Delta M$  are further categorized by the conjugate measurements in  $n$ -choose-2 different product-pair combinations.

It is further recommended that the specific geolocations from a particular product are different for each product-pair that it is involved with in order to help ensure independent measurement errors.

### ***E.3.2.4 Ancillary and detailed comments/recommendations***

The following presents an ancillary comment followed by more detailed comments/recommendations, the latter applicable to those implementing the fusion design based on MGRF described in Sections E.3.2.1 through E.3.2.3:

- Ancillary Comment: The modeling of errors based on random fields is also utilized in the geospatial analysis community, a subset of Geographic Information Science (GIScience). The correction grid approach recommended in this document is also similar in concept to a form of optimal interpolation termed “Kriging” by the geospatial analysis community [9].
- A correction grid can have variable spacing, i.e., densified in those parts of the product that need it to ensure reasonably high spatial correlation between adjacent corrections in the correction grid.
- If partitions associated with all relevant geolocations are unknown, proceed as usual but use corresponding *a priori* predicted accuracy for “arbitrary” geolocations.

- Conjugate geolocations between the other product(s) and the product of interest are identified/measured by either visual inspection of the products (possibly color-coded renderings) or by automatic correlation of their local multi-dimensional spatial or geometric shapes.
- As mentioned earlier, the solution for the product realization of interest corresponds to corrections to systematic errors across the product realization – essentially to errors associated with Random Field  $RF_1$  which are applicable to all partitions. As such, and as a conservative approach, the predicted accuracy of an interpolated correction of an arbitrary geolocation in the product should also include the addition of the *a priori* error covariance matrix  $C_{RF_i}$  for Random Field  $RF_i$  if the corresponding geolocation is associated with a Partition  $Part_i, i > 1$ . This addition should consist of a full *a priori* error covariance,  $multi\_C_{X_{RF_i}}$  (Equation E.2.1-18), if the predicted relative accuracy between multiple interpolated corrections is also of interest.
- It is preferred that a conjugate measurement for the solution corresponds to a geolocation in the product that is associated with Partition 1. If not possible and associated with Partition  $i > 1$  instead, its corresponding components in the measurement error covariance matrix ( $Cov\_meas$ ) should be increased by the addition of the covariance matrix for an error corresponding to Random Field  $i > 1$ .

If conjugate measurements are selected automatically, the following may be a reasonable approach assuming that the non-nominal partitions have large covariance matrices and low probability of occurrence relative to the nominal partition, as typical: (1) automatically select a large number of conjugate geolocations, (2) assume that they correspond to the nominal partition, and (3) edit measurements based on their *a posteriori* (post-solution) measurement residuals, which should remove those measurements associated with non-nominal partitions, and then perform (iterate) the solution again.

- Random Field  $RF_1$  may also contain “random” or spatial uncorrelated additive errors, such as sensor-mensuration error, in addition to systematic errors. The presence of the former are reflected by the difference from a value of 1 in the corresponding spdcf’s value at a geolocation difference arbitrarily close to zero.

Essentially, the above solution process ( $\widehat{\Delta X}$  and  $C_{\widehat{\Delta X}}$ ) still includes this random error and its associated “power” after the solution is performed, as appropriate.

- All conjugate geolocations affect the solution. The contribution of a specific (conjugate) geolocation in the product realization of interest to the overall solution is based on its applicable spdcf evaluated at a geolocation difference greater than zero – equal to the difference (distance) of the geolocation with those geolocations in the product realization directly corresponding to

the correction grid. The lower the spdcf's computed correlation, the less impact the measurement has on the solution for the various components in the correction grid.

### ***E.3.2.5 Fusion example***

The following presents an example of fusion based on the above design and the use of simulated data: Ten overlapping products were fused together using five geolocation conjugate pairs (measurements) for each product-pair. No external control was used. The *a priori* (pre-fusion) predicted accuracy of all products is represented via MGRF.

#### **Measurements**

The geolocation corresponding to a conjugate pair was generated randomly for each conjugate pair corresponding to each product-pair. A conjugate pair's  $3 \times 1$  measurement  $\Delta M_i$  (*a priori* measurement residual) consists of the difference between the two geolocations and includes a random  $3 \times 1$  measurement error consistent with a diagonal covariance matrix equal to  $I_{3 \times 3}$  (standard deviation of errors or "sigma" equal to 1 meter) and uncorrelated with all other such measurements.

There are 10-choose-2 or 45 product-pairs, each with 5 conjugate pairs of measurements, for a total of 225 conjugate measurements, i.e., the measurement vector  $\Delta M$  is a  $3(225) \times 1$  vector and its *a priori* error covariance  $Meas\_cov$  is a  $3(225) \times 3(225)$  diagonal matrix. Use of the same number of conjugate pairs of measurements for each product-pair combination was assumed for simplicity of example and related pseudo-code. The pseudo-code is not included in this document in order to keep its size somewhat reasonable.

#### **A priori (pre-solution) predicted accuracy**

Geolocation errors associated with product  $i$ ,  $i = 1, \dots, 10$ , were assumed to correspond to the nominal partition for that product; hence, were represented using only one random field  $RF_i$  for simplicity of example and with a corresponding *a priori*  $3 \times 3$  error covariance matrix  $C_{X_{RF_i}} = \begin{bmatrix} 4 & 0 & 0 \\ 0 & 4 & 0 \\ 0 & 0 & 9 \end{bmatrix}$  for products

$i = 1, 2, 4, 5, 6, 7, 8, 9, 10$  and  $C_{X_{RF_3}} = \begin{bmatrix} 16 & 0 & 0 \\ 0 & 36 & 0 \\ 0 & 0 & 81 \end{bmatrix}$  for product 3. These specific error covariance matrices and their diagonal elements (variances) were selected for clarity of example and for the illustration of underlying principles, and are not necessarily typical.

As a reminder, when the MGRF representation of predicted accuracy for a product contains only one random field, as detailed above, there is also only one partition applicable for all geolocations in the product; hence, partitions are essentially not applicable in this example.

The *a priori* spatial correlation of errors contained in each random field  $RF_i$  were represented using the same correlation function for all error components as well as for all products for simplicity of example:  $spdcf_{RF}(\Delta X) = Ae^{-\sqrt{dx^2+dy^2}/D}$ , where  $A = 0.98$  and the distance constant  $D$  is equal to 2.5 times the width of the common AOI for all products. Thus, for example, the x-components of error corresponding

to two geolocations in the same product and separated by a horizontal distance equal to the width of the AOI are correlated by the amount  $spdcf_{RF}(\Delta X) = 0.98(0.67) = 0.66$ . Those geolocations that are closer together are, of course, more highly correlated. For example, two geolocations in the same product separated by the distance between two adjacent grid points in the same grid row or column are correlated by an amount  $spdcf_{RF}(\Delta X) = 0.98(0.95) = 0.93$ . The highest correlation possible for two non-identical geolocations is equal to 0.98 when their distance approaches zero.

As reminders: (1)  $spdcf_{RF}(\Delta X) \equiv 1$ , for the correlation of a geolocation with itself in the same product ( $\Delta X = 0$ ), and (2) two geolocations in two different products are reasonably assumed uncorrelated prior to fusion, i.e.,  $spdcf_{RF}(\Delta X) \equiv 0$  regardless the value of  $\Delta X$ .

The *a priori* error covariance  $multi\_C_X$  for the solution vector  $\delta X$  was computed using the above predictive statistics for the various random fields. All errors in the (pre-corrected) products were simulated consistent with  $multi\_C_X$ , including their spatial correlations. All measurement errors were simulated consistent with  $Meas\_cov$ .

More specifically, a  $9 \times 9$  grid of 3d corrections was defined for each product and solved for simultaneously for all products as a subset of the elements in the WLS solution vector  $\delta X$  using the alternate and theoretically optimal solution approach described earlier. Since there were 10 products, each with correction grids containing 81 3d corrections and each associated with a total of 45 measurements that are also associated with the other 9 products,  $\delta X$  is a  $3(10)(81 + 45) \times 1$  vector or a  $3(1260) \times 1$  vector. Recall that with the alternate solution approach,  $\delta X$  contains 3d corrections associated with both the grids and the conjugate measurements.

### **Check points for the evaluation of performance**

There was also a  $8 \times 8$  grid of check points defined for each product that represented arbitrary locations in the product to be corrected for errors by subsequent interpolation of the surrounding grid corrections following the WLS solution.

The check points also had known locations (“ground-truth”) which were also common across all products and not used (solved for) in the WLS solution. Each check point was located at one-fourth the interior x coordinate and one-fourth the interior y coordinate of the corresponding grid correction cell. Of course, since results were based on simulation, the true locations of all geolocations were also known, including those corresponding to the correction grids themselves allowing for the computation of both pre-solution and post-solution errors for performance assessment. All *a priori* or pre-solution errors for each product were simulated consistent with the *a priori* predicted accuracy represented in the product’s MGRF, including those corresponding to the check points.

See reference [2] for further details regarding fusion and this example, including timing (throughput) results and well as ensemble performance results taken over 100 independent realizations of the product. This reference also includes an overview of the MGRF concept.

### **Results**

Figures E.3.2.5-1 through E.3.2.5-4 present a subset of solution results corresponding to this example (one realization). Figure E.3.2.5-1 presents the pre-solution 3d correction grid errors for products 2 through 4 and their *a priori* sigma envelopes or predicted accuracy. Figure E.3.2.5-2 presents the corresponding post-solution results – note the reduction in the range of the y-axis consistent with the improvement in predicted accuracy and the smaller errors relative to the pre-solution results. This improvement is as expected for each of the products due to the fusion or influx of independent information from the other nine products. This is particularly true for the improvements in product 3 due to its larger initial uncertainty relative to the other nine products.

In addition, *a posteriori* solution accuracy and corrected product accuracy are consistent with *a posteriori* errors, as desired. Also, as a reminder, only information from multiple products was used to correct the products; no External Data was used, such as ground control points.

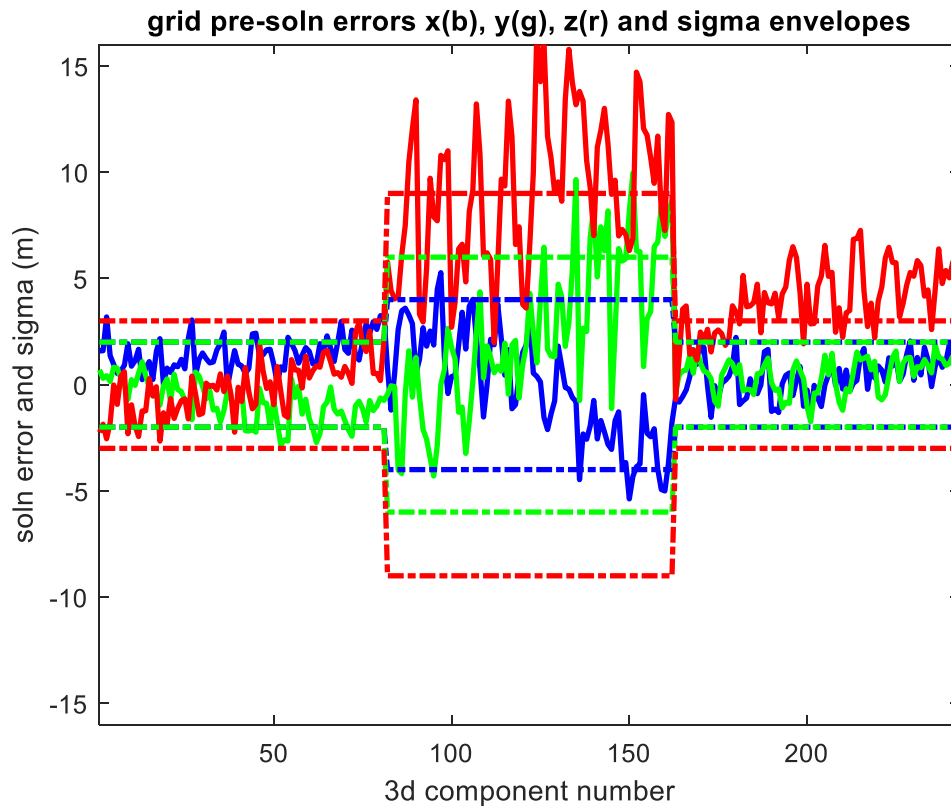


**Figure E.3.2.5-1:** Pre-solution grid correction errors (solid line) and sigma envelopes (dashed lines) for products 2 through 4.

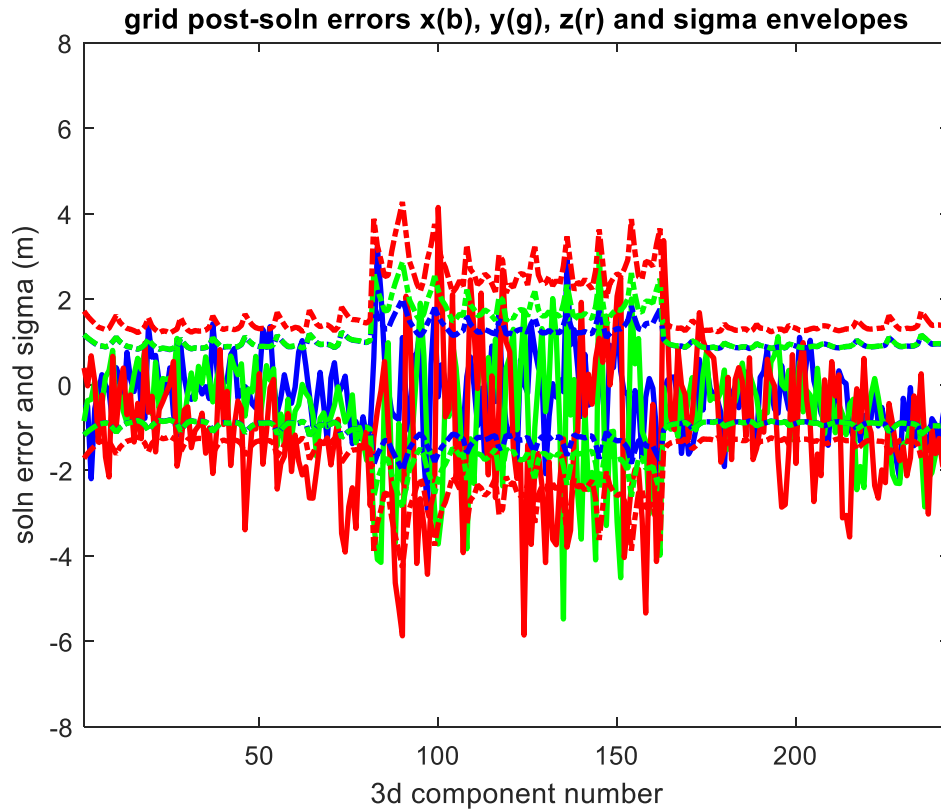


**Figure E.3.2.5-2:** Post-solution grid correction errors (solid line) and sigma envelopes (dashed lines) for products 2 through 4; note y-axis scale change relative to Figure E.3.2.5-2

In both Figures E.3.2.5-1 and E.3.2.5-2, results were presented for products 2 through 4 only in order to keep the plots of reasonable size. In particular, the 3d components on the plot's x-axis correspond to the 81 3d grid corrections for product 2 in the solution vector, followed by the 81 3d grid corrections for product 3 in the same solution vector, and followed by the 81 3d grid corrections for product 4 in the same solution vector. The grid corrections for each product are contained in the solution vector in row-major order.

Note: the more “deterministic oscillations” in the solution results between adjacent grid points in the same product occur when a new row in the correction grid is applicable with a corresponding sudden change in the *a priori* correlation between adjacent grid points. This is particular apparent for the z error (red) of product 3 in Figure E.3.2.5-1, i.e., for components numbered 82 through 162.

Figure E.3.2.5-3 presents both the pre-solution and the post-solution horizontal (x and y) errors for the grid of check points in product 3. Post-solution errors are significantly smaller than pre-solution errors as expected. The largest horizontal error vector was blue with a magnitude of 8.8 meters corresponding to “sf=8.8” in the title of the automatically scaled 2d quiver plot.

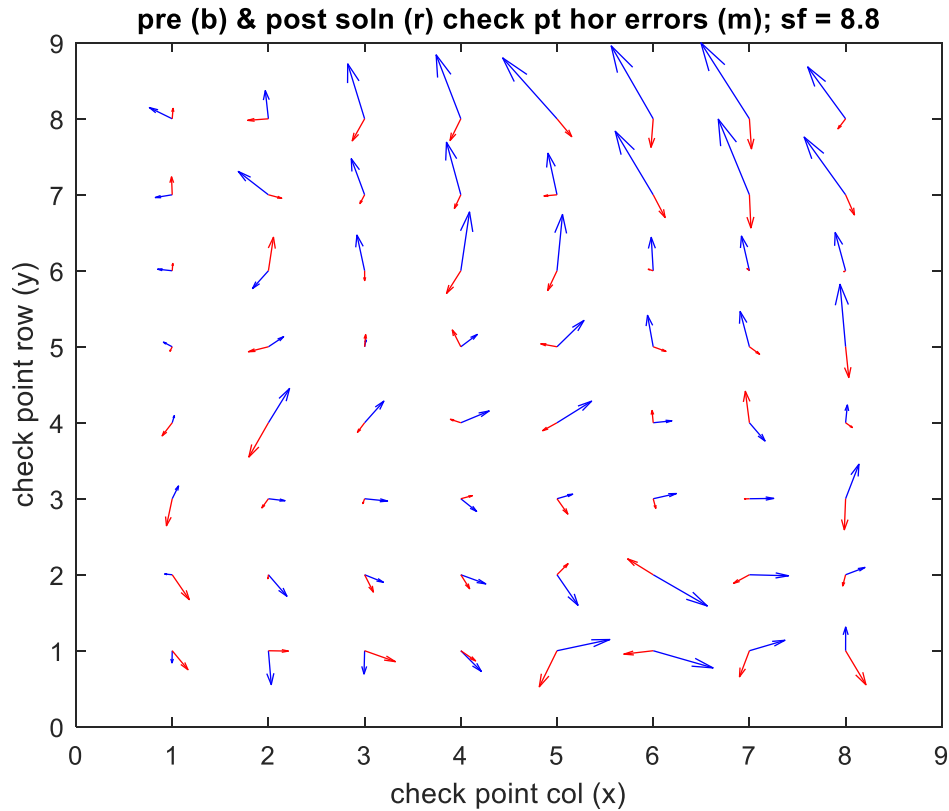


**Figure E.3.2.5-3:** Pre-solution (blue) and post-solution (red) check point horizontal (x and y) errors for product 3; check-points located in horizontal grid across the product’s AOI or “footprint” with corresponding grid row/column specified in plot.

The similarity or spatial correlation of *a priori* (pre-solution) errors across the AOI is readily seen via the blue arrows in the above plot – the closer the check points the greater the similarity of error. If the *a priori* correlation (spdcf) were specified with very high correlation (e.g.,  $D$  very large) instead of the reasonable values that were specified, the blue arrows would approach a common 2d bias, i.e., same direction and magnitude; if specified with very low correlation (e.g.,  $D$  very small), the blue arrows would appear random (uncorrelated) and would point in random directions with random magnitudes constrained by their *a priori* sigmas. Of course, the degree of *a priori* correlation is also relative to the size (spacing) of the correction grid which also dictates the size of the check point grid in this example.

Figure E.3.2.5-4 presents both the pre-solution and the post-solution horizontal relative errors between common check points in products 2 and 4. The fusion process ensures consistent geolocations across products as illustrated by the reduction of the post-solution relative errors as compared to the pre-solution relative errors.

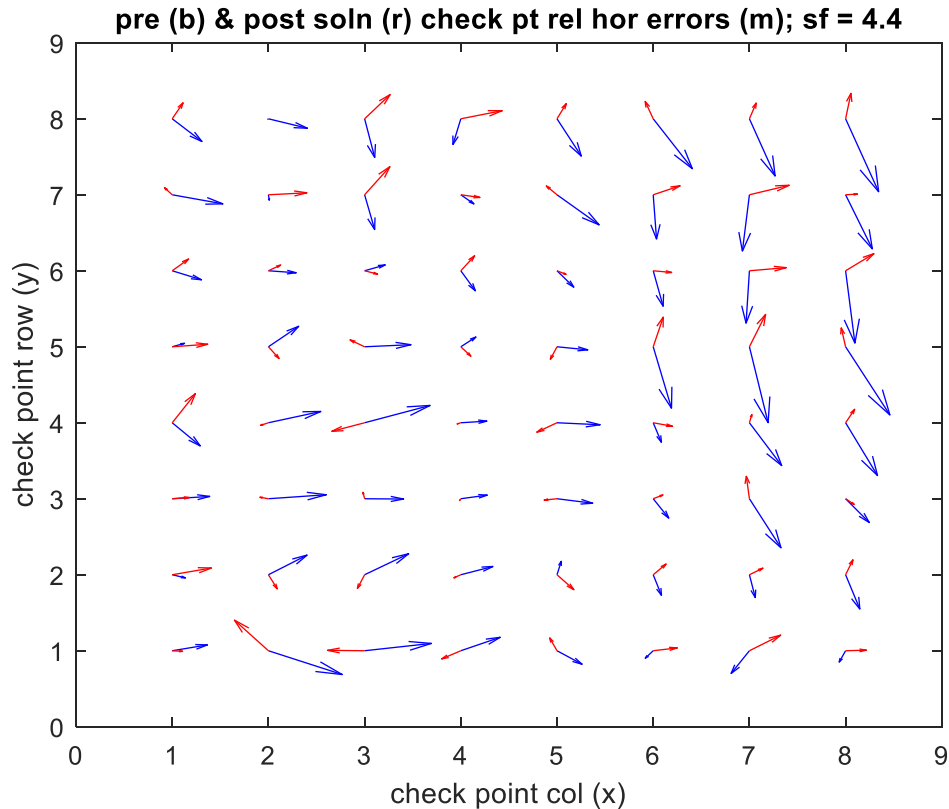


**Figure E.3.2.5-4:** Pre-solution (blue) and post-solution (red) check point relative horizontal errors between products 2 and 4; check-points located in horizontal grid across the products' common AOI.

Note that only horizontal errors are presented in both Figures E.3.2.5-3 and E.3.2.5-4 consistent with the use of 2d quiver plots in order that pre-solution spatial correlation can be readily seen via the similarity of near-by 2d error vectors or quivers.

In summary, this example demonstrated improved product accuracy (smaller errors) with consistent predicted accuracy (sigmas) due to fusion, although the predicted accuracy was not included in all of the plots and did not include error ellipsoids in order to keep results somewhat brief. In addition, as demonstrated with similar examples, an increase in the number of conjugate measurements and/or a decrease in their measurement error sigma and/or an increase in the *a priori* spatial correlation associated with a random field(s) will yield even smaller resultant errors and corresponding improved predicted accuracies. Also, a more uniform spread for the locations of the conjugate measurements across the AOI instead of the random locations used in the simulation improves the results as well. The random locations were used primarily for the compilation of ensemble results as detailed in [2].

## E.4 Concept of Operations using MGRF with examples

This section of the appendix presents a recommended Concept of Operations for the representation of the predicted accuracy of a geolocation product based on MGRF. It includes examples for insight; in

particular, simulation-based realizations or product “instances” of geolocation errors associated with each geolocation contained in a product. Section E.4.1 presents the examples and Section E.4.2 presents the Concept of Operations.

#### **E.4.1 Examples of MGRF-based realizations of errors associated with instances of the product**

First, we give an example of specific instances or realizations of a product as they relate to geolocation errors and the MGRF. By a product, we mean an arbitrary product from a specific type or class of products, for example, EO-based 3d Point Clouds generated based on specific sensor(s), generation process, date-range, and/or a general AOI. By a specific instance of the product or simply a specific product, we mean an actual instance of the product, i.e., a specific set of 3d geolocations with accompanying or associated metadata. This metadata includes MGRF-based *a priori* statistics for the product prepared ahead of time, and typically tuned using sample statistics (accuracy assessment) from previous instances of the product that had associated ground truth available.

Figures E.4.1-1 and E.4.1-2 present two different views of a realization of geolocation errors simulated consistent with an MGRF-based *a priori* model of errors. The corresponding product AOI corresponds to a semi-rural landscape. There were three partitions: the nominal partition, a partition corresponding to crop anomalies (the “circular” regions), and a partition corresponding to “melted roof-tops” (rectangular regions) – see Appendix G for further details. The simulation implemented Fast Sequential Simulation (FSS) for the generation of errors consistent with specified *a priori* statistics per TGD 2e (Monte Carlo Simulation).

3d errors were generated, but only z errors are illustrated for clarity of the plots. The errors (meters) are illustrated across a horizontal grid in the product’s AOI with 2 meter spacing between geolocations (thinned by a factor of 2), which represents a contiguous subset of the particular instance of the product. The actual geolocations are not presented, just their errors. More specifically, the plots present z errors (meters) versus grid point, with 2 meters of horizontal spacing between grid points.

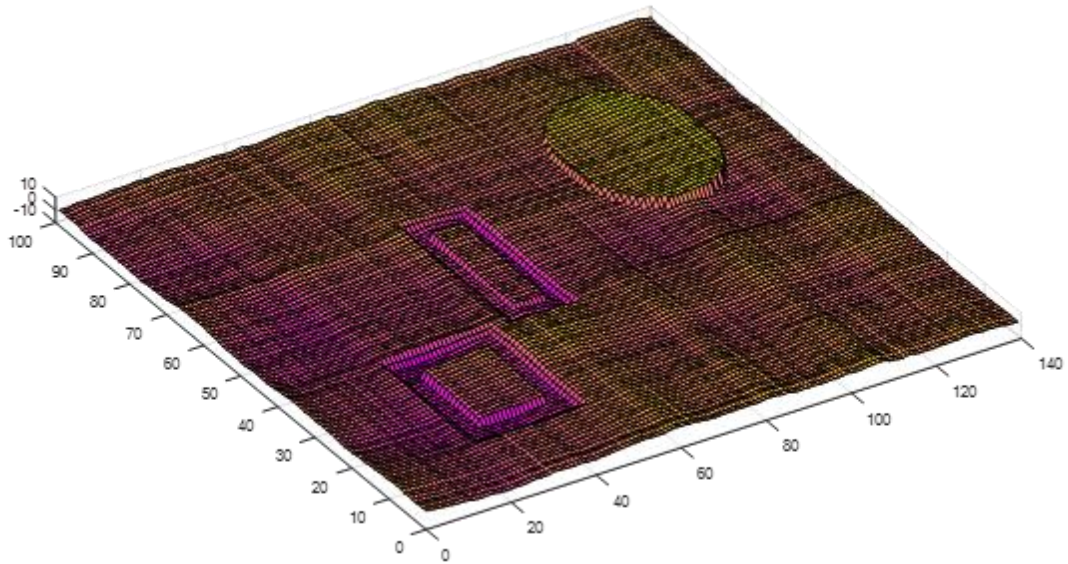


**Figure E.4.1-1:** Realization #1 of vertical errors as presented across a horizontal grid within the product's AOI

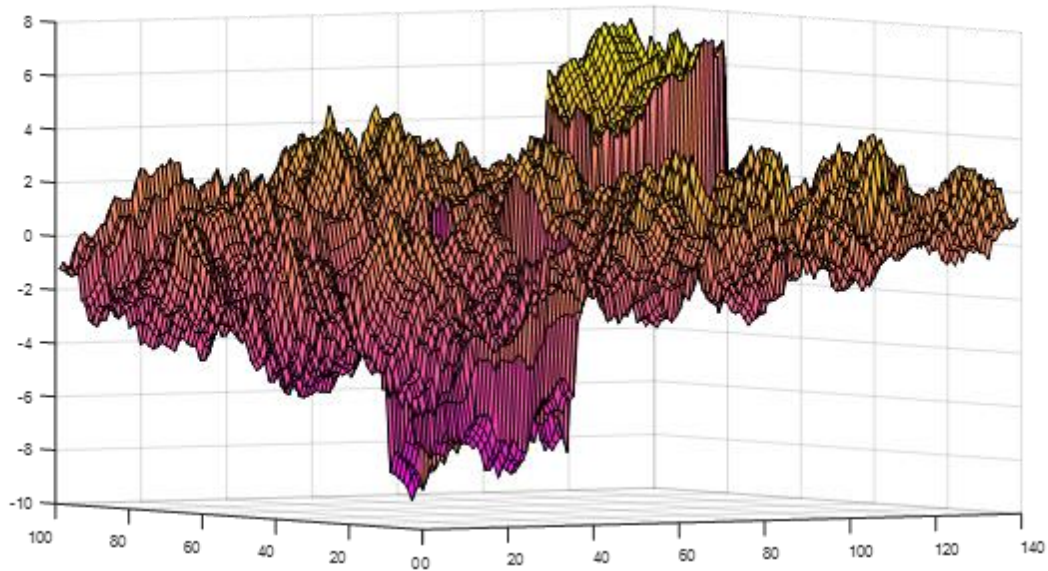


**Figure E.4.1-2:** Realization #1 of vertical errors as presented across a horizontal grid within the product's AOI – an alternate view illustrating vertical errors and their spatial correlation (similarity) more clearly

Figures E.4.1-3 and E.4.1-3 present results for a different realization and over a different part of the product but using the same *a priori* statistics. Note that geolocations associated with the non-nominal partitions are in different areas of the product AOI.

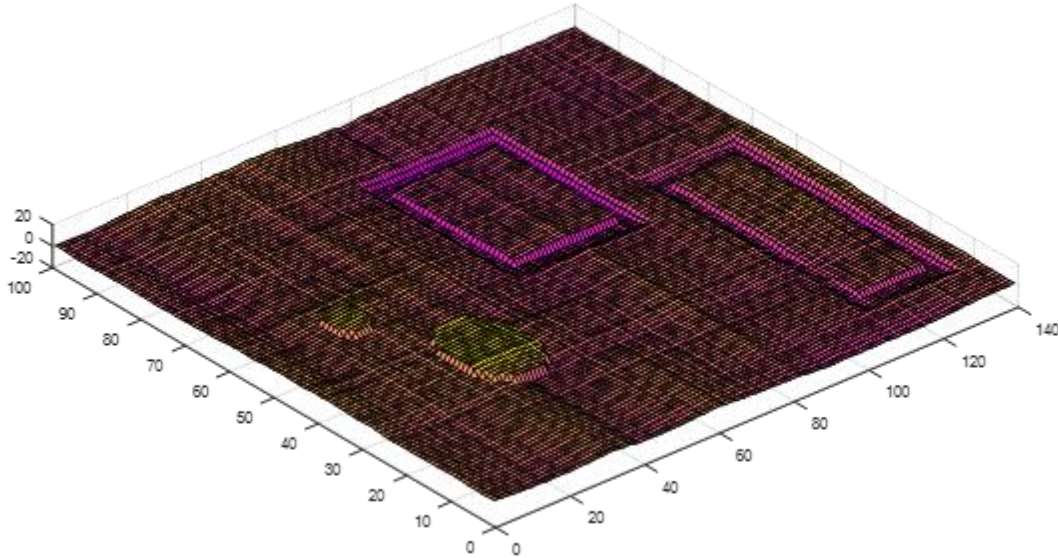


**Figure E.4.1-3:** Realization #2 of vertical errors as presented across a horizontal grid within the product's AOI

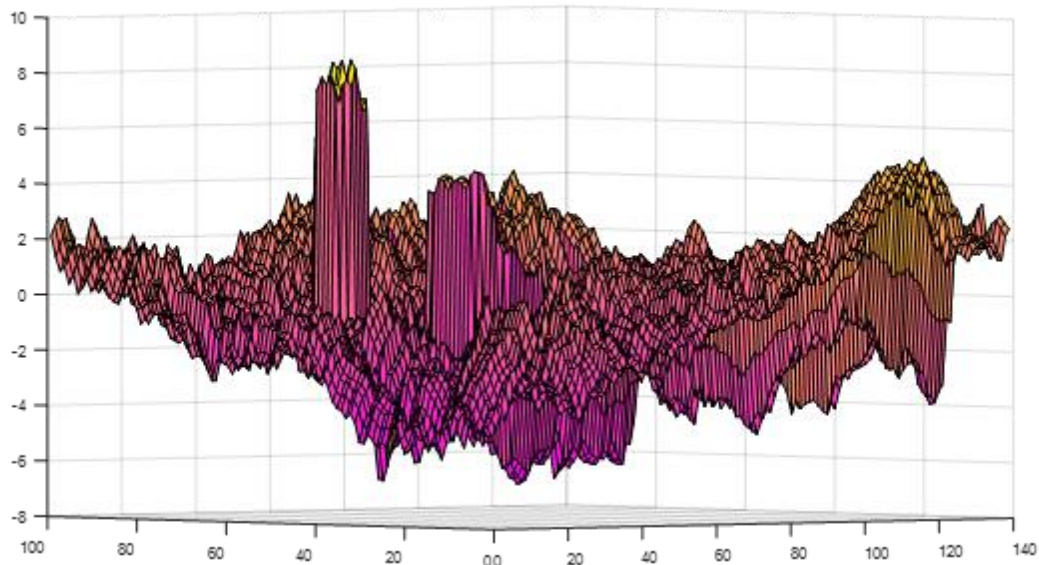


**Figure E.4.1-4:** Realization #2 of vertical errors as presented across a horizontal grid within the product's AOI - an alternate view illustrating vertical errors and their spatial correlation (similarity) more clearly

In general, errors associated with geolocations in non-nominal partitions are larger than those corresponding to the nominal partition. Use of an MGRF and its predictive statistics allows the user/application to either compute a corresponding and applicable predicted accuracy for geolocations identified as corresponding to a particular partition, or if a particular partition is not identified, compute an applicable predicted accuracy that accounts for the *a priori* probability of all partitions and their different predicted accuracies.

Figures E.4.1-5 and E.4.1-6 correspond to two different realizations of the product and applicable to the nominal partition only. The *a priori* statistics common to these realizations is different than those common to the previous plots in order to better illustrate that concept of “bias”:

The *a priori* mean-value of error is zero but each realization appears “bias-like”, i.e., has a significant non-zero sample mean-value. This is as expected due to the spatial correlation of errors within each product realization. However, this “bias” varies between the two realizations in both sign and magnitude. This is as expected and consistent with an *a priori* mean-value equal to zero and applicable to an arbitrary realization of the product, past or future.

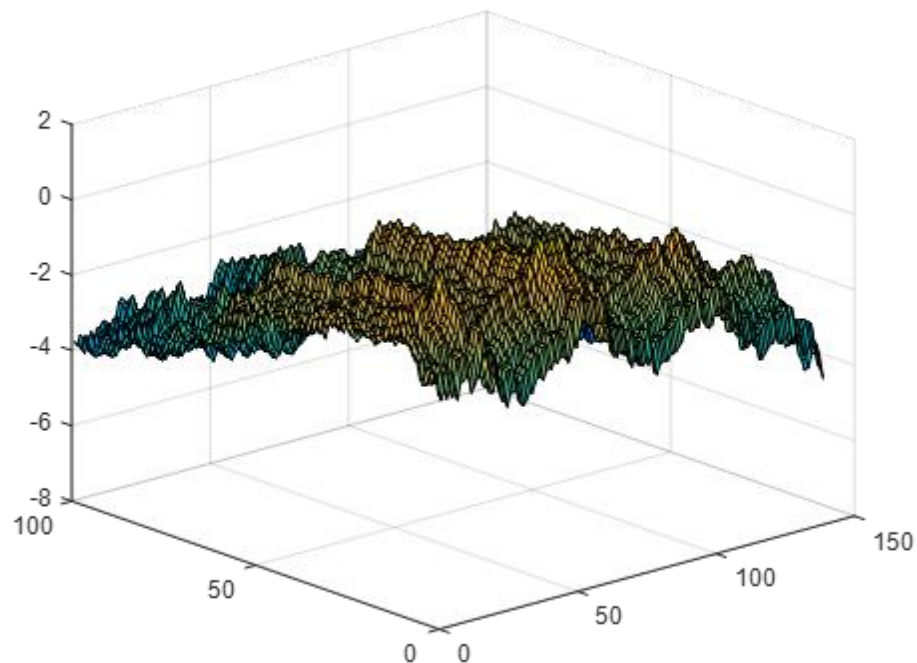


**Figure E.4.1-5:** Realization #3: z-errors corresponding to the nominal partition assumed applicable across the entire grid, with a mean-value of 0 meters, a standard deviation of 10 meters, and high spatial correlation

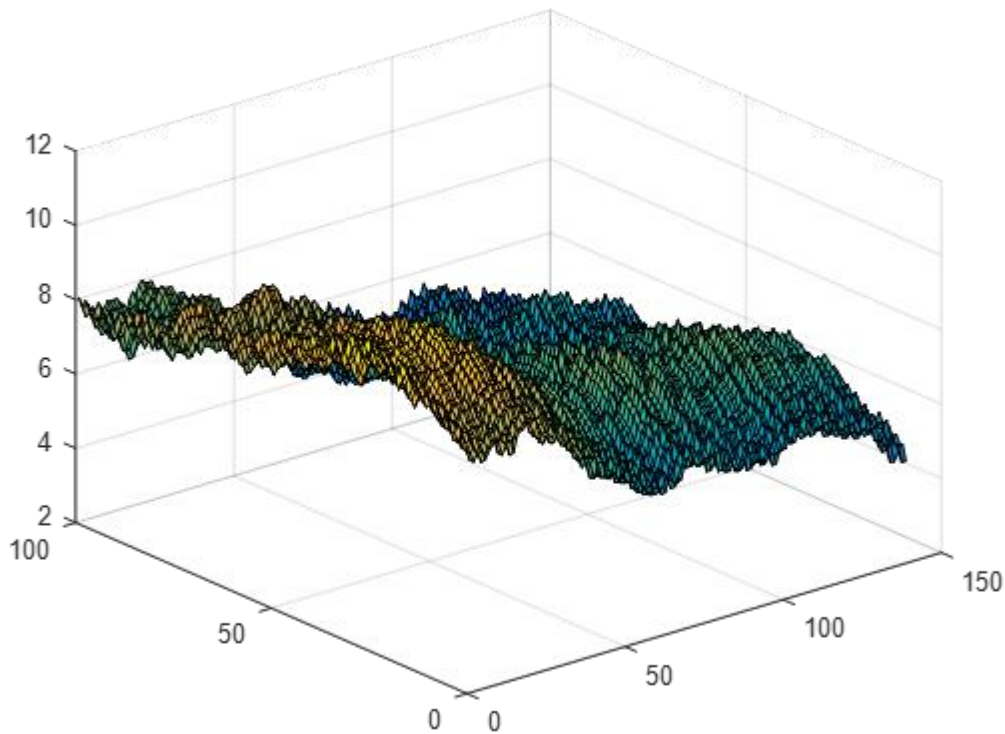


**Figure E.4.1-6:** Realization #4: z-errors corresponding to the nominal partition assumed applicable to the entire grid, with a mean-value of 0 meters, a standard deviation of 10 meters, and high spatial correlation

See Figures B.4.1-1 and B.4.1.2 in Appendix B that illustrate similar concepts regarding “bias” as above but applicable to 2d image location errors in different realizations of an image instead of 1d vertical errors in different realizations of a geolocation product. Partitions are not applicable in the “standard” (non-MGRF) predicted accuracy model for an image, but a nominal partition can be considered applicable to all image-locations, if so desired.

Note: Most partitions in most products have an *a priori* mean-value of error equal to zero, i.e., equal the  $3 \times 1$  zero vector. However, if a geolocation(s) of interest identified by the user/application corresponds to a specific partition  $i$  with an *a priori* mean-value of error that is significantly different than zero and an *a priori* error covariance matrix about this mean-value, it is recommended that the mean-value be subtracted from the geolocations prior to their use. If not subtracted, and if the user’s application also requires a covariance matrix relative to an assumed mean-value of error equal to zero (typical), it is recommended that the effects of the mean-value be “root-summed-squared” with the covariance matrix, i.e., the  $3 \times 3$  matrix  $\bar{X}\bar{X}^T$  is added to the supplied covariance matrix prior to its use along with a mean-value now assumed to equal zero.

## E.4.2 Overview of Concept of Operations

The following presents an overview of the recommended Concept of Operations associated with the use of MGRF for the representation of the predicted accuracy of a geolocation product. It assumes that the MGRF is part of a populated predicted accuracy model generated by the Quality Assessment Management/Analysis functions per the main body of this document and made available to an NSG user in the form of a corresponding file/report or equivalent metadata. The following are applicable steps in the Concept of Operations:

- Generate MGRF *a priori* statistics for the representation of the predicted accuracy for a type or class of a geolocation product of interest
  - Performed by the Quality Assessment Management/Analysis functions
  - Based on analysis and tuned using populated accuracy assessment model(s) corresponding to various instances of the product (realizations) corresponding to the same type or class of product
  - Place the MGRF in a populated predicted accuracy model and make available to the NSG
- Generate a specific instance of the product
  - Performed by an External Data provider (or possibly a specific NSG program)
- Down-stream user obtains the product (instance) directly or indirectly from the provider (e.g. a specific 3d Point Cloud)
- User associates/obtains the corresponding MGRF contained in the populated predicted accuracy model or its equivalent metadata made available by the Quality Assessment Management function
- As an option, the user then reviews the product and adjusts the *a priori* probability of occurrence of the various partitions accordingly
- For the geolocation(s) in the product of interest to the user, appropriate MGRF *a priori* statistics are applied/computed per Section E.2 for corresponding predicted accuracies:
  - Either as arbitrary geolocation(s) in the product or geolocation(s) identified by the user/application as part of a specific partition in the product instance. The latter allows for more specific (tailored) predicted accuracy for the geolocations of interest, i.e., conditional predicted accuracies based on a known partition.

Figure E.4.2-1 presents a flow-chart of processing associated with the above Concept of Operations:

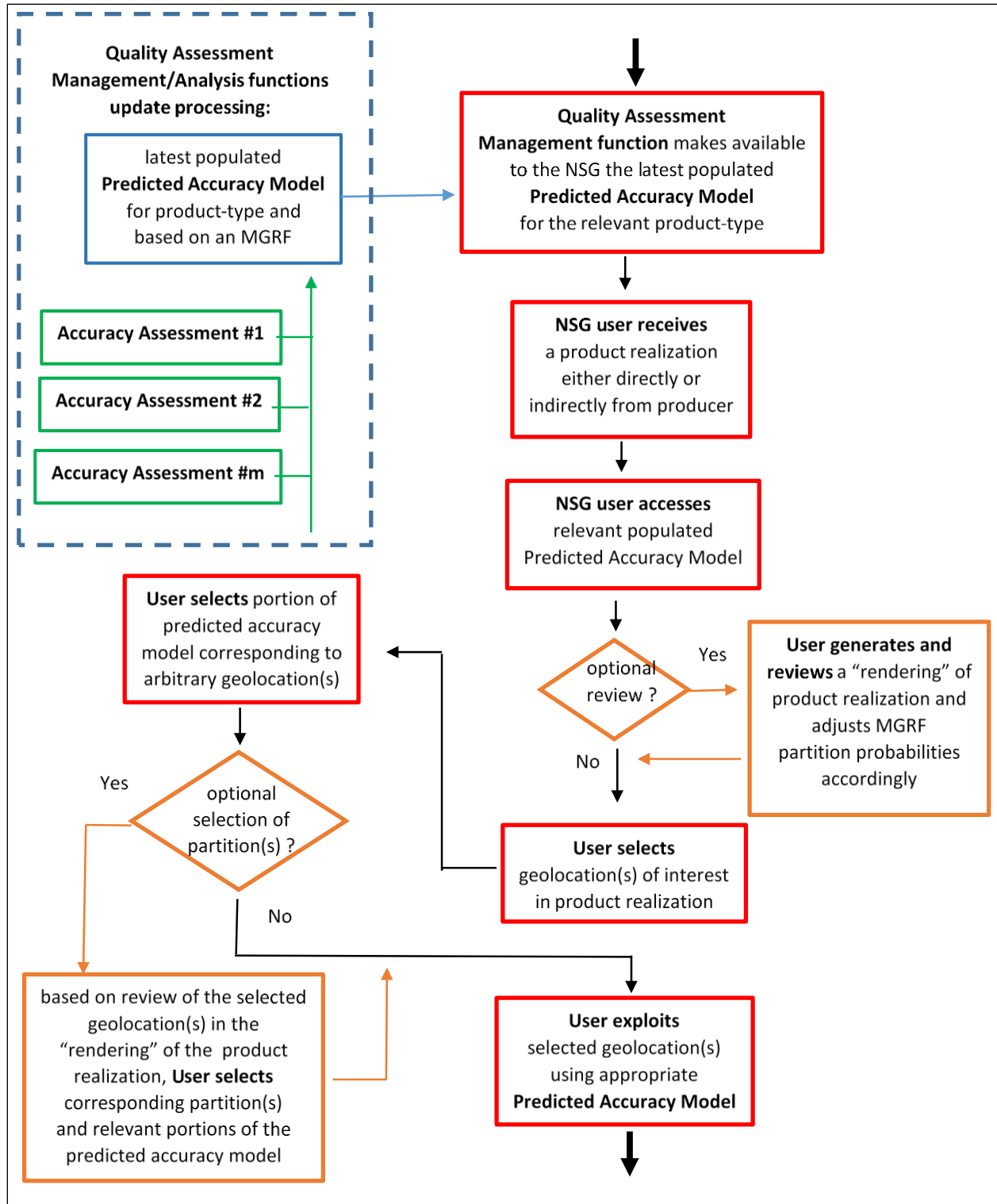


**Figure E.4.2-1:** Processing associated with the Concept of Operations involving the predicted accuracy of a 3d geolocation product; optional adjustment of the product not included

#### ***E.4.2.1 Alternate Concepts of Operations***

It is possible that an MGRF may also eventually be generated and placed in the corresponding metadata directly by a provider, thus, precluding the need for the Quality Assessment Management/Analysis functions to do so for some types of products. If done this way, the provider may also adjust the *a priori* probability of occurrence for the various partitions based on the specific instance of the product.

In addition, some providers that already generate a (non-MGRF) predicted accuracy model and include the corresponding metadata with the product, may want to consider expanding their model to include aspects of an MGRF. One such model was discussed in Section 5.2.3.1 – the Generic Point Cloud Model (GPM). As such, the use of MGRF partitions can conveniently represent the geolocation uncertainty (errors) of:

- geolocations “not included” in the product, such as the tops of towers “cut-off” in an EO-derived 3d Point Cloud; currently not practical using GPM if geolocations are included in the product but with truncated values for  $z$ , and not possible using GPM if geolocations (all 3 coordinates) are not explicitly included in the product
- geolocations included in the product, such as building roof-top edges, that are too prevalent to realistically express their larger uncertainty with “extra” error specified on a per geolocation basis as required using GPM.

#### ***E.4.2.2 Relationships of the MGRF with accuracy assessments and GPM***

##### Relationship with accuracy assessments

As mentioned earlier, the contents of an MGRF are based on/tuned using accuracy assessments corresponding to multiple realizations of products from the same type or class of products. The sample statistics contained in the accuracy assessments are categorized by applicable partition, which can range in number from 1 (nominal partition only) to  $n$ , depending on the type of class of product and its error characteristics.

However, as described in Section E.2.2, the baseline MGRF approach defines Partition 1 as containing errors from Random Field 1 only, whereas all other Partitions  $i > 1$  contain errors from Random Field 1 and additive errors from Random Field  $i$ . Therefore, sample statistics corresponding to all partitions should be used together in order to estimate the predictive statics for each random field, which are then used via the equations of Section E.2.2 to estimate the predictive statistics for the partitions in the MGRF, which are of direct interest to the down-stream user.

However, if the sample statistics corresponding to Partition  $i > 1$  clearly dominate (represent relatively significantly larger errors) those corresponding to Partition 1, as typical for many types or classes of products, the sample statistics for Partition  $i$  alone reasonably represent the sample statistics for the corresponding Random Field  $i$ , for  $i = 1, \dots, n$ ; hence, the predictive statistics of all partitions then follow per the equations of Section E.2.2.

In addition, reasonable approximations are typically applicable, which may also remove geometric dependencies associated with the sample statistics that are not applicable to the predictive statistics for arbitrary realizations of a product from the same general type or class of product. For example, a sample error covariance matrix applicable to Partition  $i$  might reasonably be mapped to a corresponding predictive error covariance matrix for Random Field  $i$  as follows:

$$\text{sample } C_i = \begin{bmatrix} 4 & 1.4 & -1 \\ 1.4 & 6 & -1.3 \\ -1 & -1.3 & 7.9 \end{bmatrix} \rightarrow C_{X_{RF_i}} = \begin{bmatrix} 5 & 0 & 0 \\ 0 & 5 & 0 \\ 0 & 0 & 8 \end{bmatrix}, \quad (\text{E.4.2.2-1})$$

where the average of the sample x and y error variances (one-half the matrix trace or average eigenvalue) was used as the corresponding variances in the diagonal predictive covariance matrix, and where the sample z error variance was rounded-up for simplicity and in recognition that a finite number of samples were used to generate the sample error covariance matrix.

#### Relationship with GPM

As discussed in Section 5.2.3 of the main body of the document, GPM is preferred over the explicit use of an MGRF for the representation of predicted accuracy as well as adjustability of the product. However, GPM requires simultaneous generation with the generation of explicit product (realization). See reference [16] for a detailed description of GPM.

Currently, GPM is almost always unavailable for products considered as External (Commodities) Data in the NSG and the use of MGRF is a realistic alternative. However, there are explicit correspondences between the two approaches:

- The adjustable parameters of MGRF described in Section E.3 are the recommended counterparts to the adjustable parameters in GPM
- The errors in Random Field 1 of MGRF contain the systematic errors in the product that are adjustable, as well as “random” errors similar to sensor-mensuration errors (aka “unmodeled”) errors in GPM. Partition 1 contains Random Field 1 only and is the nominal partition, i.e., is applicable to the majority of geolocations.
- The errors in Random Field  $i > 1$  are included in Partition  $i$  and represent additive “problem” errors that are similar to specifiable additive errors in GPM; however the latter are required to be non-spatially correlated and are specified on a per geolocation basis in GPM.
- Both “unmodeled” errors and uncorrelated additive errors are required to be explicitly specified by a specified region and on a specified per geolocation basis, respectively, in GPM. This is not required in MGRF.

There are actually two variations of GPM: GPM (sensor-space) and GPM (ground-space). The former represents uncertainty in sensor-space (sensor pose, etc.) and the latter in ground-space using a grid of “anchor points” similar to a correction grid for product adjustability with MGRF. However, the anchor point covariance matrix is full with non-identical (in general) 3x3 anchor point covariance matrices down its diagonal. This covariance matrix corresponds to errors consistent with a non-homogeneous random

field and is computed during the product generation using information not available outside of this process; hence, the use of MGRF and a correction grid for our applications of interest. In addition, MGRF includes the concept of partitions, not currently available with GPM.

## E.5 Recommended MGRF content-format associated with a geolocation product

The following is recommended for inclusion in the product's metadata or the corresponding Predicted Accuracy file/report. It is used by the "down-stream" user/application to represent the predicted accuracy of geolocations in the product.

### Required Content

#### Top-level parameters:

$k$ : the dimension of modeled geolocation error,  $1 \leq k \leq 3$ ; their corresponding identities: x-error, y-error, and/or z-error; identification of the Local Tangent Plane coordinate system which they reference

$n$ : the number of MGRF partitions and random Fields, where  $1 \leq n \leq 10$  (tbr)

#### A description/probability of occurrence for Partition $i$ , for $i = 1.., n$ :

Description: textual description of Partition  $i$

$p_i$ : the *a priori* probability of occurrence; the probability that an arbitrary geolocation in the product is associated with partition  $i$ , where  $p_i > 0$  and  $\sum_{i=1}^n p_i = 1$

#### A statistical description of Random Field $i$ , for $i = 1, \dots, n$ :

$\bar{X}_{RF_i}$ : the  $k \times 1$  mean-value of geolocation error

$C_{X_{RF_i}}$ : the  $k \times k$  covariance matrix of geolocation error

$spdcf_{RF_i}$ : the  $k \times 1$  vector-valued strictly positive definite correlation function; specifies the spatial correlation between the error in two geolocations as a function of  $\Delta X$  between the geolocations ;  $spdcf_{RF_i}$  is a member of the CSM 4-parameter family of spdcf and specified by 4 parameters for each component

All of the above allow for the computation of all derived statistics by the "down-stream" user (application) per the equations of Section E.2.2, including probability density functions that completely characterize all relevant errors, including relative errors.

### Highly Recommended Content: Scalar Accuracy Metrics

#### Predicted Accuracy for Partition $i$ , for $i = 1, \dots, n$ :

$CEXX_i$  Circular Error at probability-level  $XX$  for horizontal geolocation error for an arbitrary geolocation associated with partition  $i$ , for both  $XX = 90\%$  and  $99\%$

$LEXX_i$  Linear Error at probability-level  $XX$  for vertical geolocation error for an arbitrary geolocation associated with partition  $i$ , for both  $XX = 90\%$  and  $99\%$

**Predicted Accuracy for Product (Partition Unknown):**

$CEXX$  Circular Error at probability-level  $XX$  for horizontal geolocation error for an arbitrary geolocation associated with partition  $i$ , for both  $XX = 90\%$ ,  $99\%$ , and  $99.9\%$

$LEXX$  Linear Error at probability-level  $XX$  for vertical geolocation error for an arbitrary geolocation associated with partition  $i$ , for both  $XX = 90\%$ ,  $99\%$ , and  $99.9\%$

**Relative Accuracy for Partition  $i$ , for  $i = 1, \dots, n$ :**

$rel\_CEXX_{ij}$  Circular Error at probability-level  $XX$  for horizontal geolocation error for an arbitrary geolocation associated with partition  $i$ , for both  $XX = 90\%$  and  $99\%$ . Further categorized by distance bin  $j$  also defined in metadata (not included in this description).

$rel\_LEXX_{ij}$  Linear Error at probability-level  $XX$  for vertical geolocation error for an arbitrary geolocation associated with partition  $i$ , for both  $XX = 90\%$  and  $99\%$ . Further categorized by distance bin  $j$  also defined in metadata.

**Relative Accuracy for Product (Partition Unknown):**

$rel\_CEXX$  Circular Error at probability-level  $XX$  for horizontal geolocation error for an arbitrary geolocation associated with partition  $i$ , for both  $XX = 90\%$ ,  $99\%$ , and  $99.9\%$ . Further categorized by distance bin  $j$  also defined in metadata.

$rel\_LEXX$  Linear Error at probability-level  $XX$  for vertical geolocation error for an arbitrary geolocation associated with partition  $i$ , for both  $XX = 90\%$ ,  $99\%$ , and  $99.9\%$ . Further categorized by distance bin  $j$  also defined in metadata.

**Recommended Content: Mean-Values and Covariance Matrices for Partition  $i$ , for  $i = 1, \dots, n$**

$\bar{X}_{Part_i}$  the  $k \times 1$  mean-value of geolocation error for Partition  $i$

$C_{X_{Part_i}}$  the  $k \times k$  covariance matrix of geolocation error for Partition  $i$

**Recommended Content: Mean-Values and Covariance Matrices for Product (partition unknown)**

$\bar{X}$  the  $k \times 1$  mean-value of geolocation error

$C_X$  the  $k \times k$  covariance matrix of geolocation error

Optional: specification of a Random Field-to-Partition Mapping (Section E.2) if the default (baseline) mapping is not applicable; in which case, the number of partitions and number of random fields no longer need to be identical. This optional specification is recommended for a more general/flexible design for MGRF metadata content.

Optional: Explicit CE/LE figures in accompanying files similar to Figure E.2.5-1 for more information regarding the distribution of errors corresponding to geolocations in different partitions – provides for additional insight to the down-stream user.

Optional: A flag indicating that an accompanying file presents an optional vector or raster map of the 3d Product with corresponding geolocations associated with Partition  $i$ ,  $i = 1, \dots, n$ , explicitly identified, and where one and only one partition corresponds to each geolocation. Identification is typically via rendered geolocation boundaries.

Metadata containing all of the recommended contents presented above is of relatively small size (bytes). A simple example of Metadata content is presented in Section E.5.1 that follows:

**E.5.1 Metadata example**

The following is an example of metadata corresponding to an MGRF representation of the predicted accuracy of a 3d geolocation product that specifically illustrates the metadata content listed above for a somewhat non-complicated case. The case could correspond to *a priori* statistics of a somewhat “simple” form due to a limited number of corresponding accuracy assessments used for the derivation of these statistics. On the other hand, the somewhat “simple” form may be due to the nature of the 3d geolocation product itself and generated based on numerous accuracy assessments.

The following lists the metadata content without use of a specific “file” format, the latter not in the scope of this document. Mathematical symbols are included as well that reference previous sections of the appendix, and would not be explicitly included in the actual metadata. Specific numbers are notational and for the purpose of illustration only.

All applicable units are meters (m), unless specifically stated otherwise. The following includes required data and recommended data (+) per Section E.5. Recommended data, if not included, can be computed by the “down-stream” user using the required data and implementation of the equations/algorithms of Section E.2. However, this does place additional requirements on the user. In addition, even when the recommended data is included, the user may want to compute additional data, such as scalar accuracy metrics at additional probability levels and/or relative scalar accuracy metrics at additional distance bins.

Finally, recall that the baseline MGRF approach assumes that errors in geolocations associated with Partition 1 correspond to errors contained in Random field 1, and errors in geolocations associated with Partition  $i > 1$  correspond to a sum of errors, one contained in random Field 1 and one contained in Random Field  $i$ .

**Metadata (required)**

The dimension of geolocation errors:  $k = 3$   
corresponding to  $\epsilon x$ ,  $\epsilon y$ , and  $\epsilon z$

The number of partitions:  $n = 2$

**Partition 1:**

Description: “all geolocations not in partition 2”, aka “nominal partition”

Partition probability of occurrence  $p_1 = 0.85$

**Partition 2:**

Description: “all geolocations corresponding to building roof-top melted edges”

Partition probability of occurrence  $p_2 = 0.15$

**Random field 1:**

Error mean value:  $\bar{X}_1 = \begin{bmatrix} 0 \\ 0 \\ 0 \end{bmatrix} \text{ m}$

Error covariance matrix:  $C_{X_1} = \begin{bmatrix} 1^2 & 0 & 0 \\ 0 & 1^2 & 0 \\ 0 & 0 & 2^2 \end{bmatrix} \text{ m-squared}$

Spdcf parameters:  $\{A = 0.9 \text{ (unit-less)}, \alpha = 0 \text{ (unit-less)}, \beta = 0 \text{ (unit-less)}, D = 5000 \text{ m}\}^*$

**Random field 2:**

Error mean value:  $\bar{X}_2 = \begin{bmatrix} 0 \\ 0 \\ -3 \end{bmatrix} \text{ m}$

Error covariance matrix:  $C_{X_2} = \begin{bmatrix} 3^2 & 0 & 0 \\ 0 & 3^2 & 0 \\ 0 & 0 & 4^2 \end{bmatrix} \text{ m-squared}$

Spdcf parameters:  $\{A = 0.9 \text{ (unit-less)}, \alpha = 0 \text{ (unit-less)}, \beta = 0 \text{ (unit-less)}, D = 500 \text{ m}\}^*$

**Metadata (recommended; derived from the above required metadata)**

**Partition 1:**

Error mean value:  $\bar{X}_1 = \begin{bmatrix} 0 \\ 0 \\ 0 \end{bmatrix} \text{ m}$

Error covariance matrix:  $C_{X_1} = \begin{bmatrix} 1^2 & 0 & 0 \\ 0 & 1^2 & 0 \\ 0 & 0 & 2^2 \end{bmatrix} \text{ m-squared}$

**Partition 2:**

Error mean value:  $\bar{X}_2 = \begin{bmatrix} 0 \\ 0 \\ -3 \end{bmatrix} \text{ m}$

Error covariance matrix:  $C_{X_2} = \begin{bmatrix} 10 & 0 & 0 \\ 0 & 10 & 0 \\ 0 & 0 & 20 \end{bmatrix} \text{ m-squared}$

**Arbitrary geolocation in product (partition unknown):**

Error mean value:  $\bar{X} = \begin{bmatrix} 0 \\ 0 \\ -0.45 \end{bmatrix} \text{ m}$

Error covariance matrix:  $C_X = \begin{bmatrix} 2.35 & 0 & 0 \\ 0 & 2.35 & 0 \\ 0 & 0 & 7.5475 \end{bmatrix} \text{ m-squared}$

**Partition 1 (scalar accuracy metrics provided in the following tables):**

Scalar Accuracy Metrics (m) for partiton 1			
CE90 =	CE99 =	LE90 =	LE99 =
2.1	3	3.3	5.1

	Scalar Relative Accuracy Metrics (m) for partiton 1			
distance (m) <=	relCE90 <=	relCE99 <=	relLE90 <=	relLE99 <=
50	1	1.4	1.5	2.4
500	1.3	1.8	2	3.1

**Partition 2:**

Scalar Accuracy Metrics (m) for partiton 2			
CE90 =	CE99 =	LE90 =	LE99 =
6.8	9.6	8.8	13.4

	Scalar Relative Accuracy Metrics (m) for partiton 2			
distance (m) <=	relCE90 <=	relCE99 <=	relLE90 <=	relLE99 <=
50	4.1	5.7	4.2	6.7
500	7.6	10.7	7.9	12.3

Arbitrary geolocations in product (note extra columns corresponding to probability level 99.9%):

Scalar Accuracy Metrics (m) for arbitrary geolocation					
CE90 =	CE99 =	CE999 =	LE90 =	LE99 =	LE999 =
3.1	7.4	10	4.2	9.8	14.1

	Scalar Relative Accuracy Metrics (m) for arbitrary geolooction					
distance (m) <=	relCE90 <=	relCE99 <=	relCE999 <=	relLE90 <=	relLE99 <=	relLE999 <=
50	4.2	7.7	10.1	3.6	8.4	11.9
500	4.4	8	10.5	3.9	8.9	12.4

#### Comment 1

\*\*Since there is only one entry {...} under spdcf parameters for each random field, the corresponding spdcf is assumed applicable (common) to all three error components for this example. In addition, the spdcf is assumed to correspond to the “CSM four parameter” family of spdcf; as such, based on the specified parameters above, the specific spdcf equals:

$Ae^{-d/D}$ , where  $d$  is horizontal distance, the parameter  $A$  satisfies  $0 < A \leq 1$ , the parameter  $D$  (horizontal distance constant, meters)) satisfies  $0 < D$ , and the other two parameters  $\alpha$  and  $\beta$  are set to zero in this example, and thus, have no effect.

Note that the specified value of  $A$  is the corresponding maximum value for the correlation coefficient between two errors in the same random field; hence, directly affects the corresponding minimum value for relative predicted accuracy between the geolocations, i.e.,  $A < 1$  prevents the relative error covariance matrix from approaching zero when the horizontal distance  $d$  approaches zero, as desired in all practical applications. Of course, by definition, the correlation coefficient equals 1 and the relative error covariance matrix equals zero when the distance  $d$  is identically equal to zero, i.e., the two geolocations (errors) are one in the same.

Based on the above and general flexibility, the “CSM four parameter” family of spdcf is recommended for use. Specified non-zero values of the parameters  $\alpha$  and  $\beta$  also allow for the specification of a correlation minimum value other than zero for large values of the distance  $d$  and the modification of the correlation function’s shape to some degree, respectively.

In addition, recall the Partition 1 contains errors from Random Field 1 only; hence the spdcf for Random Field 1 is also directly applicable to errors in geolocations associated with Partition 1. And because Partition 2 contains errors from both Random Field 1 and Random Field 2, their spdcfs are jointly but separately applicable to errors in geolocations associated with Partition 2. However, since Random Field 2 errors are significantly larger than those from Random Field 1, the former's spdcf influences the relative errors in Partition 2 the most.

### **Comment 2**

\* Relative accuracy distance bins refer to a range of horizontal distance between two 3d geolocations in the same partition. For example, distance bin 1 may be specified in the metadata as corresponding to two geolocations separated less than 50 meters, and distance bin 2 between 50 and 500 meters.

### **Comment 3**

See Appendix F for further examples of metadata; more specifically, the various derived statistics corresponding to a specified set of required statistics for underlying partitions. It includes corresponding plots for scalar predicted accuracy metrics (both CEXX and LEXX) corresponding to an arbitrary geolocation in the product. The above example was generated by MATLAB pseudo-code, which is also included in Appendix F.

## **E.6 Summary**

This appendix has described both the theoretical aspects of an MGRF and its ability to represent the predicted accuracy corresponding to a 3d geolocation product in a rigorous yet practical manner. The MGRF takes into account that geospatial accuracy can vary over different “parts” or partitions of the product.

The user/application of the product may or may not be able to associate geolocations of interest with a particular partition when multiple partitions are applicable. If not, the predicted accuracy can be computed in a rigorous manner corresponding to an arbitrary geolocation, i.e., a geolocation with its associated partition unknown. When a geolocation of interest can be associated with a particular partition, as is typical, a more detailed “high-fidelity” predicted accuracy can be computed instead.

The above allows the “down-stream” user/application of the product to make informed decisions as well as optimal use of the product due to available predicted accuracies.

Finally, a significant number of mathematical derivations were included in this appendix for background, but their understanding is not required for applications of an MGRF. In particular, examples were also presented, including the contents of MGRF metadata or its equivalent. Appendix F presents pseudo-code for their generation, including various CE and LE scalar accuracy plots.

## Appendix F: Pseudo-code for the generation of MGRF derived statistics

This appendix presents non-optimized MATLAB code (“pseudo-code”) for the generation of MGRF derived statistics corresponding to a specified set of MGRF required statistics. This pseudo-code was referenced in Section 5.3.3.3 of the main body of this document and also in Appendix E.

The derived statistics include those recommended for inclusion in corresponding 3d geolocation product metadata, as well as other derived statistics. The pseudo-code is simple and non-optimized. For example, specified statistics are “hard coded” but are easily changed. They consist of the number of partitions in the MGRF and their probability of occurrence, and for each of the underlying random fields, its 1x3 mean-value of 3d error, 3x3 covariance matrix of 3d error, and various parameters that specify its strictly positive definite correlation functions – one for the spatial correlation of horizontal errors and one for the spatial correlation of vertical errors.

Derived statistics include the scalar predicted accuracy metrics CE and LE at various probability levels XX corresponding to an arbitrary geolocation in each specific MGRF partition as well as corresponding to an arbitrary geolocation in the overall MGRF (product) when the geolocation’s partition is unknown. Both sets also include CE/LE corresponding to absolute and relative predicted accuracies, the latter also applicable to different specifiable distances between geolocations.

Pseudo-code output not only includes the above, but CE/LE plots as well for arbitrary geolocations in the overall MGRF or product. The CE plots include CE90, CE99, and optionally CE999 (probability equals 99.9%) circles, as well as a subset of 2000 random horizontal error samples in correct proportion from each partition used by the Monte Carlo generation method to compute CEXX for an arbitrary geolocation in the product as described in Section E.2.5 of Appendix E. The plots also optionally include the CE90 circle corresponding to geolocations exclusively from partition 1 for comparison. Output also includes similar LE plots corresponding to vertical errors. Figures F-1 presents an example of a CE plot and Figure F-2 an example of an LE plot, both corresponding to the same specified set of required statistics for the MGRF included as part of the pseudo-code output.

Plot examples:

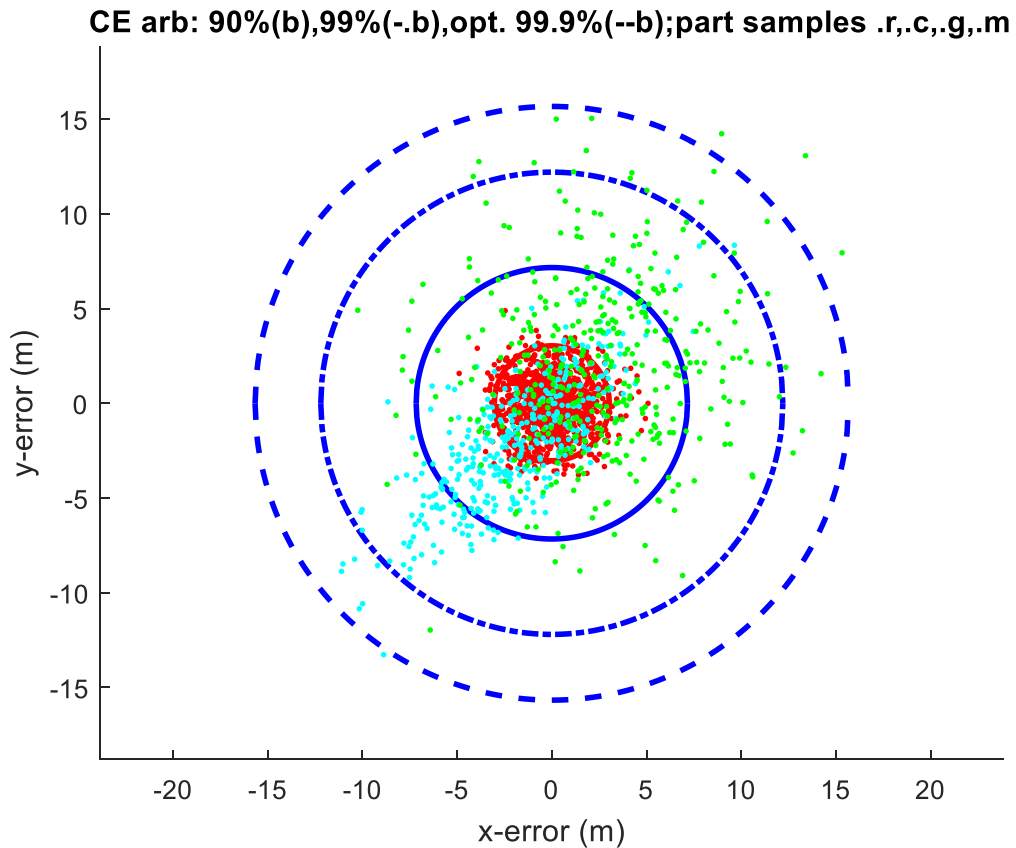


**Figure F-1:** CEs corresponding to an arbitrary geolocation in the MGRF or product (circle radii in meters), including a total of 2000 random samples of horizontal error corresponding to each partition in correct proportion as colored dots, e.g., green dots correspond to partition 3; also includes CE90 for partition 1 (red) for comparison

Note the increase in CE90 for an arbitrary geolocation in the product (blue circle) relative to an arbitrary geolocation in partition 1 (red circle) which is due to the combined effects of all 3 partitions and the fact that error statistics for partitions 2 and 3 were specified greater than for partition 1 (see printout example below for details).

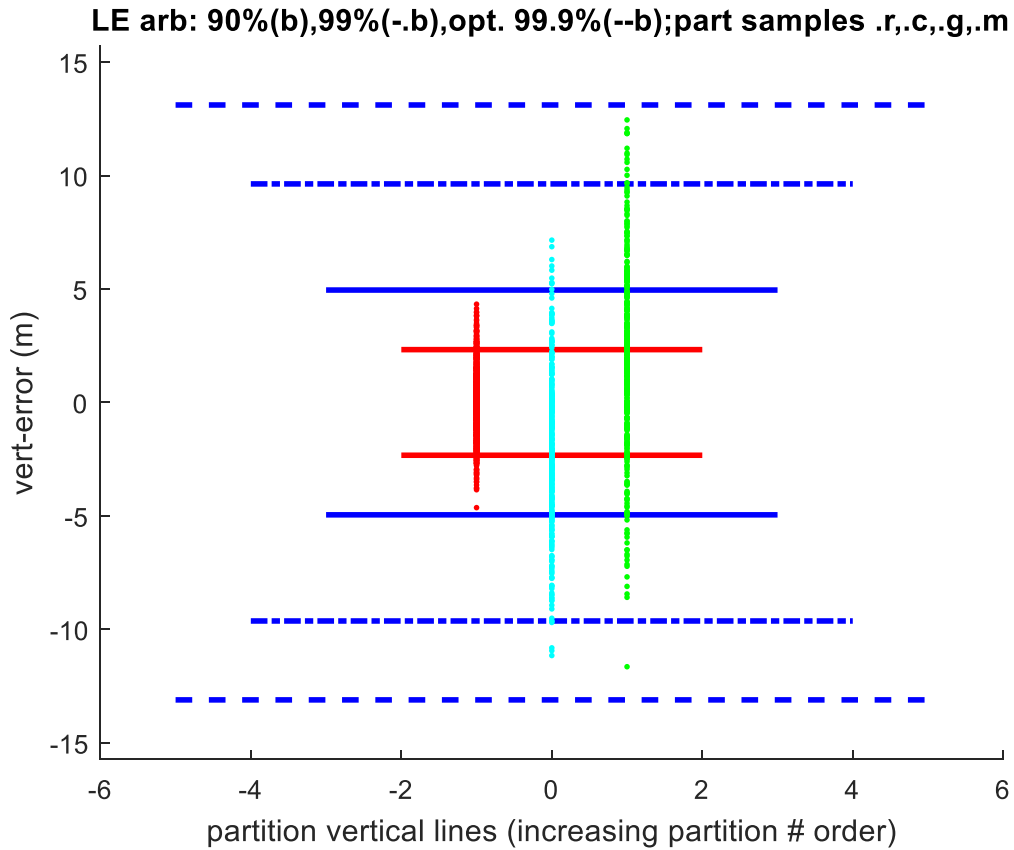


**Figure F-2:** LEs corresponding to arbitrary geolocation (horizontal lines in meters), including 2000 random samples of vertical error in each underlying partition as colored dots along vertical lines; also included is LE90 for partition 1 (red horizontal line)

In addition and corresponding to the same specified set of required statistics, Figure F-3 presents a plot of the spdcf for vertical errors for random field 1 for insight into the form of a spatial correlation function. A different spdcf corresponding to either horizontal errors and/or a different partition can be plot instead by a simple modification of the pseudo-code.

**spdcf for hor errors (ex amd ey) as a function of hor distance; selected part**

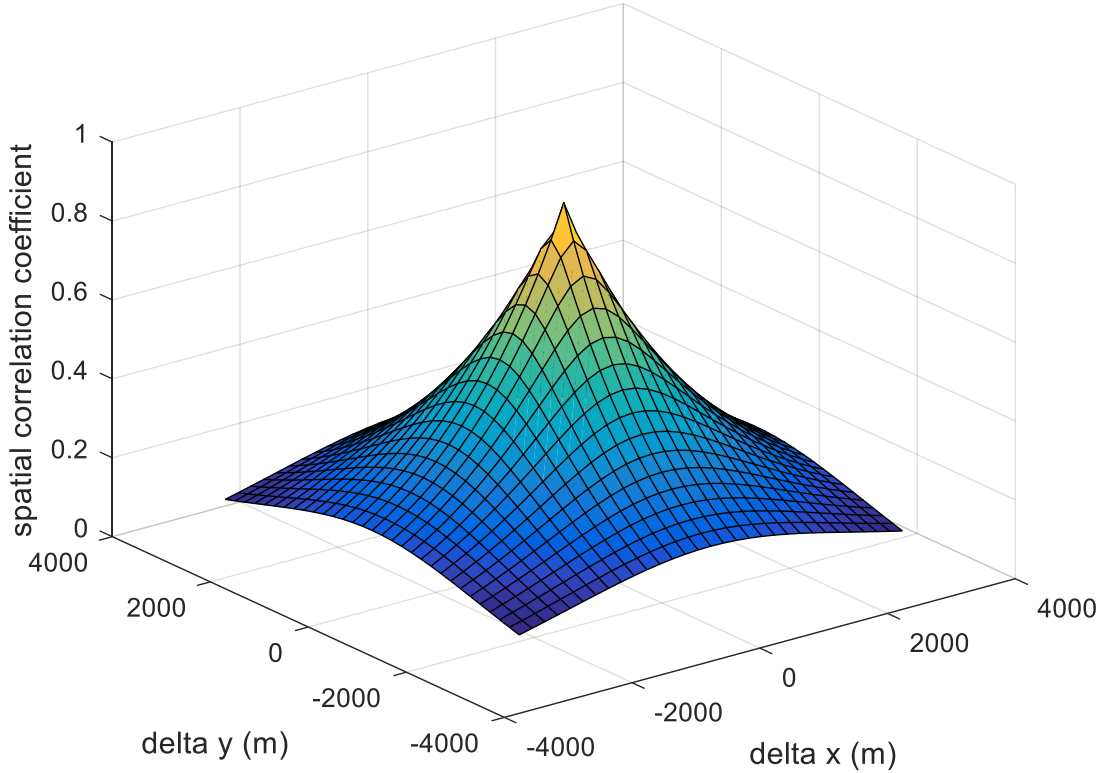


**Figure F-3:** Spdcf for vertical errors in partition 1; its value  $\rho$  at  $(\Delta x, \Delta y) = (0,0)$  is equal to 1.0 by definition, but is less than or equal to 0.9 at all other values of  $(\Delta x, \Delta y)$  for this particular spdcf

The spdcf corresponding to Figure 3 is an isotropic “CSM four parameter” spdcf defined by four parameters:  $\{A = 0.9$  (unit-less),  $\alpha = 0$  (unit-less),  $\beta = 0$  (unit-less),  $D = 2000$  m  $\}$ , where correlation  $\rho = A(\alpha + \frac{(1-\alpha)(1+\beta)}{\beta + e^{d/D}})$  and  $d = \sqrt{\Delta x^2 + \Delta y^2}$ .

In general, the allowed ranges for the four parameters are:  $0 < A \leq 1$ ,  $0 \leq \alpha < 1$ ,  $0 \leq \beta \leq 10$ , and  $0 < D$  per Section of 5.8.3.1 of TGD 2a. Note that the value of  $A$  specifies the maximum value of the spdcf at a non-zero distance, the value  $\alpha A$  specifies the minimum value or “floor”, the distance constant  $D$  dictates the general rate at which correlation decreases with distance, and the parameter  $\beta$  modifies the function’s shape somewhat.

Detailed documentation of the computation of all of the derived statistics is included as comment statements in the pseudo-code.

## F.1 Printed output example

Specific derived statistics corresponding to the above case also include the following explicit printed outputs of the pseudo code. The following includes some addition descriptors (%) for this appendix only – see the pseudo code for detailed definitions of the output.

```
>> TGD_2f_compute_derived_a_priori_stats_August_24_2018
```

```
plot_flag = 1  1  1  1  %plotting options
```

```
p_levels = 0.9000  0.9900  0.9990  %probability levels for scalar accuracy metrics (CEXX, etc.)
```

```
n_dist = 3  %number of distances for computed relative accuracies
```

```
dist = 0  50  500  %corresponding distances in meters
```

```
case_flag = 1  0  0  0  0  0  0  %case flag – specified case presented below
```

```
%required MGRF a priori predictive statistics (hard coded inputs via case flag):
```

```
n = 3  % number of specified partitions in MGRF
```

```
part_p = 0.6000  0.2000  0.2000  %partition probabilities of occurrence
```

```
mean_rf =  %random field (rf) mean values: first row the 1x3 mean value (x,y,z) for rf 1, etc.
```

```
0  0  0
```

```
-2 -2 -2
```

```
2  2  2
```

```
cov_rf =  %random field 3x3 covariance matrices: first 3 rows the covariance matrix for rf 1, etc.
```

```
2  0  0
```

```
0  2  0
```

```
0  0  2
```

```
9  8  0
```

```
8  9  0
```

```
0  0  9
```

```
16  0  0
```

```
0  16  0
```

```
0  0  16
```

```
spdcf_hor_rf = % random field spdcf spatial correlation function for horizontal error (both x and y) - 4
                defining parameters: first row corresponds to the spdcf for rf 1, etc.
```

```
1.0e+03 *
```

```
0.0009  0  0  2.0000
```

# NGA.SIG.0026.08\_1.0\_ACCESQC

```
0.0009    0    0  1.0000
0.0009    0    0  0.2000
```

spdcf\_vert\_rf = % as above but for vertical errors

```
1.0e+03 *
0.0009    0    0  2.0000
0.0009    0    0  1.0000
0.0009    0    0  0.2000
```

%Computed for info only:

cor\_h = %corresponding computed correlation coefficient for horizontal errors for info only: row 1 corresponds to the first distance and the three random fields, etc.

```
0.9000  0.9000  0.9000
0.8778  0.8561  0.7009
0.7009  0.5459  0.0739
```

cor\_v = %as above but for vertical errors

```
0.9000  0.9000  0.9000
0.8778  0.8561  0.7009
0.7009  0.5459  0.0739
```

%Derived outputs (derived statistics recommended for metadata):

mean = partition (part) mean values: first row the 1x3 mean value for part 1, etc.

```
0  0  0
-2 -2 -2
2  2  2
```

cov = %partition (part) 3x3 covariance matrices: first 3 rows the covariance matrix for part 1, etc.

```
2  0  0
0  2  0
0  0  2
11 8  0
8  11 0
0  0  11
18 0  0
0  18 0
```

# NGA.SIG.0026.08\_1.0\_ACCESQC

0 0 18

mean\_arb=0 0 0 %1x3 mean value of error for arbitrary geolocation in product  
(partition unknown)

cov\_arb = % 3x3 covariance matrix for error in arbitrary geolocation

8.6000 3.2000 1.6000  
3.2000 8.6000 1.6000  
1.6000 1.6000 8.6000

CE\_partitions = % CE for each probability level corresponding to a geolocation in the  
specified partition; row 1 is CE90, CE99, CE999 for partition 1, etc.

3.0340 4.2849 5.2650  
8.7144 13.1264 16.3989  
10.0399 14.0608 17.1041

LE\_partitions = % as above except for LE

2.3273 3.6513 4.6672  
6.3669 9.7365 12.2479  
7.7169 11.9749 15.1729

CE\_arbitrary=7.1621 12.1980 15.6668 % CE for each probability level for an arbitrary geolocation in  
product (partition unknown)

LE\_arbitrary = 4.9524 9.6303 13.107 % as above except for LE

distance =0 % distance for following relative predicted accuracy scalar accuracy metrics, i.e.,  
for two geolocations the specified distance apart

relCE\_partitions = % rel CE for three probability levels for each partition; first row is CE90, CE99,  
CE999 for partition 1, etc.

1.3562 1.9163 2.3485  
3.3141 5.0977 6.4688  
4.0724 5.7508 7.0333

relLE\_partitions = % as above except for LE

1.0405 1.6271 2.0898  
2.4430 3.8207 4.8879  
3.1247 4.8903 6.2581

distance =50

relCE\_partitions =

1.5016	2.1252	2.6070
3.9246	6.0535	7.7306
6.8064	9.6225	11.8026

relLE\_partitions =

1.1505	1.8008	2.3039
2.8893	4.5252	5.7670
5.2195	8.1644	10.4464

distance =500

relCE\_partitions =

2.3474	3.3150	4.0754
6.8802	10.6244	13.4603
11.9085	16.8412	20.6149

relLE\_partitions =

1.7985	2.8198	3.6059
5.0312	7.8962	10.0238
9.1240	14.2668	18.2558

distance = 0                      %distance for following relative predicted scalar accuracy metrics, i.e. for two geolocations the specified distance apart

relCE\_arb = 7.1685   11.7935   15.7075   %rel\_CE for each probability level for arbitrary geolocations in product (partition unknown)

relLE\_arb = 5.0623   9.4545   13.1426   %same as above for rel\_LE

distance =50

relCE\_arb = 7.2662   11.8491   15.7239

relLE\_arb = 5.1663   9.4974   13.1755

distance = 500

relCE\_arb =7.8078   12.6826   16.7958

relLE\_arb=5.5705 10.2175 14.2452

>>

## F.2 Pseudo-code

```
%"TGD_2f_compute_derived_a_priori_stats_August_24_2018"
```

```
%24 August 2018
```

```
%This program computes derived statistics from a priori statistics that are
%input; the a priori statistics specify an MGRF for the representation of
%Predicted Accuracy for a 3d Geolocation Product and are required in its
%metadata or an equivalent file.
```

```
%Ancillary plots of scalar accuracy metrics are also generated, if so specified.
%A plot of a strictly positive definite %correlation function (spdcf) can also
%be specified for general insight.
```

```
%In general, there are n partitions and n underlining random fields making up
%the MGRF. Each geolocation in the product (realization) is associated with
%one and only one partition.
```

```
%Partition 1 is associated with geolocations that have errors represented by
%random field 1; this is characterized as
%"partition 1 'contains' random field %1".
%Partition i>1 contains both random field 1 and random field i, i.e., is
%the sum of two independent (uncorrelated) errors, one from random field 1 and
%one from random field i. Random field 1 contains product-wide systematic
%errors, and random fields i>1 contains additive errors, typically much less
%spatially correlated (systematic) than those in random field 1.
```

```
%The following is "non-optimized" pseudo-code for convenience, where for
%example, inputs are "hard coded" and their values not checked for validity.
%Simply change the "hard coded" values for the desired case of interest.
```

```
%DEFINE and "read in" inputs:
```

```
%plot option flag vector:
plot_flag=zeros(1,4);
```

```
%perform plots of CEXX and LEXX (XX nominally =90, 99) for arbitrary
%geolocation in product (partition unknown):
plot_flag(1,1)=1;
```

```
%include CE999 and LE999 (99.9%)in above plots:
plot_flag(1,2)=1;
```

```
%include partition 1's CE90 and LE90 in above plots for comparison:
plot_flag(1,3)=1;
```

```
%include independent plot of random field 1's vertical error spdcf associated
%with predicted relative accuracy for general info regarding spdcf functions;
```

```
%because the errors associated with geolocations in random field 1 are the
%errors in partition 1, this plot corresponds to the spdcf of partition 1
%as well:
plot_flag(1,4)=1;

plot_flag    %print value of plot flag

%probability levels XX for scalar accuracy metrics CEXX and LEXX (0<values<1):
p_levels=[0.9 0.99 0.999]
%some later comment statements in the code assume that these particular
%nominal values are applicable for convenience

%nominal number of distances and their nominal values (meters) for relative
%accuracy computations:
n_dist=3
dist=[0 50 500]    %where square bracket [ ] corresponds to "define" in MATLAB

%The following defines the MGRF with a priori statistics. These consist of
%(1)the number of random fields (n) which is the same as the number of
%partitions in the MGRF (product), (2) the probability of occurrence for
%each partition, and (3) the defining predictive statistics for each random
%field:

%More specifically, there are 7 different cases or experiments defined below
%via %"hard coding" for convenience, many of them corresponding to experiments
%documented in Appendix D of TGD 2f (External Data and its Quality Assessment)".

%Set the corresponding case_flag appropriately for the case of interest or
%redefine a particular case as desired:

case_flag=[1 0 0 0 0 0 0]

if(case_flag(1)==1) %case #1:

%number of partitions in MGRF:

n=3

%define and read in a 1xn vector of partition probabilities (must sum to 1)

part_p=[.6, 0.2, 0.2]

%read in n rows of random field 1x3 mean-values; first row corresponds to 1x3
%mean-value for random field 1, etc.:

mean_rf=[0 0 0; -2 -2 -2; 2 2 2]

%read in 3*n rows of random field 3x3 covariance matrices; first 3 rows
%correspond to 3x3 covariance matrix for random field 1, etc.:

cov_rf=[2 0 0; 0 2 0; 0 0 2; 9 8 0; 8 9 0; 0 0 9; 16 0 0; 0 16 0; 0 0 16]

%above entry must be such that all random field covariance matrices are
```

```

%valid (symmetric and positive definite (eigenvalues > 0)).

%read in n rows of random field spdcf parameters for hor (x,y) errors; row 1
%corresponds to 1x4 vector of random field 1's spdcf parameters, etc.:

spdcf_hor_rf=[0.9 0 0 2000; 0.9 0 0 1000; 0.9 0 0 200]

%same for vertical (z) errors:

spdcf_vert_rf=[0.9 0 0 2000; 0.9 0 0 1000; 0.9 0 0 200]

end %end case 1 test

if(case_flag(2)==1) %extreme experiment - partition 2 low prob. but large
    %errors
    n=2
    part_p=[.95, 0.05]
    mean_rf=[0 0 0; 0 0 0]
    cov_rf=[1 0 0; 0 1 0; 0 0 1; 20^2 0 0; 0 20^2 0; 0 0 20^2]
    spdcf_hor_rf=[0.9 0 0 2000; 0.9 0 0 1000]
    spdcf_vert_rf=[0.9 0 0 2000; 0.9 0 0 1000]
end

if(case_flag(3)==1)
    n=2
    part_p=[.85, 0.15]
    mean_rf=[0 0 0; 0 0 -3]
    cov_rf=[1 0 0; 0 1 0; 0 0 2^2; 3^2 0 0; 0 3^2 0; 0 0 4^2]
    spdcf_hor_rf=[0.9 0 0 5000; 0.9 0 0 500]
    spdcf_vert_rf=[0.9 0 0 5000; 0.9 0 0 500]
end

if(case_flag(4)==1)
    n=3
    part_p=[.6, 0.2, 0.2]
    mean_rf=[0 0 0; 0 0 0; 0 0 0]
    cov_rf=[1 0 0; 0 1 0; 0 0 1; 3^2 0 0; 0 3^2 0; 0 0 3^2; 5^2 0 0; 0 5^2 0; 0 0 5^2]
    spdcf_hor_rf=[0.9 0 0 2000; 0.9 0 0 200; 1 0 0 200]
    spdcf_vert_rf=[0.9 0 0 2000; 0.9 0 0 200; 0.5 0 0 200]
end

if(case_flag(5)==1)
    n=1
    part_p=[1]
    mean_rf=[-2 2 2]
    cov_rf=[2^2 0 0; 0 3^2 0; 0 0 4^2]
    spdcf_hor_rf=[0.9 0 0 2000]
    spdcf_vert_rf=[0.9 0 0 100]
end

if(case_flag(6)==1)
    n=5
    part_p=[.51111, 0.1, 0.1, 0.1, 0.18889]
    mean_rf=[2 0 2; 0 0 0; 0 0 0; -2 -2 -2; 0 0 0]
    cov_rf=[1 0 0; 0 1 0; 0 0 1; 3^2 0 0; 0 3^2 0; 0 0 3^2; 5^2 0 0; 0 5^2 0; 0 0 5^2; ...
        1 0 0; 0 1 0; 0 0 1; 3^2 0 0; 0 3^2 0; 0 0 4^2]

```

## NGA.SIG.0026.08\_1.0\_ACCESQC

```
spdcf_hor_rf=[0.9 0 0 2000; 0.9 0 0 200; 0.9 0 0 200; 0.9 0 0 200; 0.9 0 0 200]
spdcf_vert_rf=[0.9 0 0 2000; 0.9 0 0 200; 0.9 0 0 200; 0.9 0 0 200;...
0.9 0 0 200]
end

if(case_flag(7)==1)
n=3
part_p=[.5, 0.25 0.25]
mean_rf=[0 0 0; 5 5 0; -2 -3 0]
cov_rf=[1 0 0;0 1 0;0 0 1; 0.5 0 0;0 0.5 0;0 0 0.5; 9 0 0;0 1 0;0 0 1]
spdcf_hor_rf=[1.0 0 0 2000; 0.9 0 0 200; 0.9 0 0 200]
spdcf_vert_rf=[0.9 0 0 2000; 0.9 0 0 200; 0.9 0 0 200]
end

%DEFINE later outputs corresponding to errors in geolocations corresponding
%to specific partitions and to the general product (partition unknown) -
%outputs are "print only" in this pseudo-code:

%mean_arb: 1x3 vector of geolocations errors for arbitrary geolocation

%cov_arb: 3x3 covariance matrix of geolocation errors for arbitrary
%geolocation

%CE_partitions: n rows of 1x3 CEs at the three different probability levels
%for each of the n partitions

%LE_partitions: n rows of 1x3 LEs at the three different probability
%levels for each of the n partitions

%CE_arbitrary: a 1x3 vector of CEs at the three different probability levels
%applicable to an arbitrary geolocation in the product

%LE_arbitrary: 1 1x3 vector of LEs at the three different probability levels
%applicable to an arbitrary geolocation in the product

%relCE_partitions: n rows of 1x3 relative CEs at the three different
%probability levels for each of the n partitions; computed for each of the
%n_dist distances

%relLE_partitions: n rows of 1x3 relative LEs at the three different
%probability levels for each of the n partitions; computed for each distance

%relCE_arb: a 1x3 vector of relative CEs at the three different probability
%levels applicable to an arbitrary geolocation in the product; computed for
%each distance

%relLE_arb: a 1x3 vector of relative LEs at the three different probability
%levels applicable to an arbitrary geolocation in the product; computed for
%each distance

%PROCESSING:

%Define and compute partition predictive stats from random field predictive
%stats:
```

```

mean=mean_rf;
cov=cov_rf;

for i=2:n
mean(i,:)=mean(i,:)+mean_rf(1,:);
cov(3*(i-1)+1:3*i,:)=cov(3*(i-1)+1:3*i,:)+cov_rf(1:3,:);
end

mean
cov

%compute horizontal error spatial correlation coefficient at specified
%distances for each random field for use later to compute relative CEXxs and
%LEXxs for partitions

cor_h=zeros(n_dist,n); % defined as an (n_dist x n) matrix
cor_v=zeros(n_dist,n);

for i=1:n

A=spdcf_hor_rf(i,1);%partition i's first spdcf parameter for horizontal
errors.

%It is assumed that (0<A<1), instead of (0<A<=1), as well as the following
%check since we're never really interested in cor at d=0 explicitly but later
%use d=0 for convenience instead of the desired d = positive epsilon.
%Note: if A=1 and d=0, cor=1 and rel error covariance matrix equals zero
%(undesirable - matrix not positive definite)
if(A==1)
    A=0.999;
end

alpha=spdcf_hor_rf(i,2);    %(0<=alpha<1)
beta=spdcf_hor_rf(i,3);    %0<=beta<10
D=spdcf_hor_rf(i,4);       %0<D in meters

for j=1:n_dist
d=dist(j); % distance j
cor_h(j,i)=A*(alpha+(1-alpha)*(1+beta)/(beta+exp(d/D))); %correlation
%coefficient for distance j for partition i
end

A=spdcf_vert_rf(i,1); %partition i's first spdcf parameter for vertical errors;
if(A==1)
    A=0.999;
end
alpha=spdcf_vert_rf(i,2);
beta=spdcf_vert_rf(i,3);
D=spdcf_vert_rf(i,4);

for j=1:n_dist
d=dist(j); % distance j
cor_v(j,i)=A*(alpha+(1-alpha)*(1+beta)/(beta+exp(d/D)));
end

```

```

end

%Note that an arbitrary spdcf is defined as to equal 1 when evaluated at a
%distance d=0, and is equal to A at a distance d=epsilon, where epsilon is an
%arbitrary small positive number

cor_h    %print output for info; values used later in this program (script);
          %remember, rows are different distances and columns diff partitions
cor_v

%compute mean and covariance for arbitrary geolocation for information only.
%i.e., not used in this program after its computation; also corresponds to
%a non_gaussian distribution if number of partitions n>1:

mean_arb=zeros(1,3);    % a 1x3 row vector containing mean-value of
                        %arbitrary geolocation's x, y, z errors
cov_arb=zeros(3,3);    % a 3x3 covariance matrix for arbitrary geolocation's
                        %x, y, z errors about its mean-value

for i=1:n
temp=mean(i,:);    %temp is 1x3 vector of partition i's mean-value
mean_arb=mean_arb+part_p(1,i)*temp;
end

for i=1:n
temp=mean(i,:) - mean_arb; %temp is a 1x3 vector of partiton i's mean - mean_arb
temp_cov_1=temp'*temp;    % a 3x3 matrix
temp_cov_2=cov(3*(i-1)+1:3*i,:); % partition i's 3x3 covariance matrix
cov_arb=cov_arb+part_p(1,i)*(temp_cov_1+temp_cov_2);
end

mean_arb %print output partions' mean-value and covariance matrix as
          %which correspond to recommended metadata
cov_arb

%Compute CEs and LEs for each partition (no plotting specified)

plot_flag_temp=zeros(1,4);

CE_partitions=zeros(n,3);
LE_partitions=zeros(n,3);

for i=1:n

n_specific=i;
[CE,LE]=M_Carlo_CE_LE(p_levels,n,part_p,mean,cov,n_specific, ...
plot_flag_temp,0,0);

CE_partitions(i,:)=CE;
LE_partitions(i,:)=LE;

end

```

```

CE_partitions    %print output of highly recommended metadata;
LE_partitions

%Save CE90 and LE90 results for possible plotting of partition 1 later
part_1_CE90=CE_partitions(1,1);
part_1_LE90=LE_partitions(1,1);

%Compute CEs and LEs for arbitrary geolocation regardless the value of n;
%also specify possible plotting of results (via plot flag), and if so
%specified, including possible plotting of CE90 and LE90 for partition 1 for
%comparison

n_specific=0;

[CE_arbitrary,LE_arbitrary]=M_Carlo_CE_LE(p_levels,n,part_p,mean,cov,...
    n_specific,plot_flag,part_1_CE90,part_1_LE90);

CE_arbitrary    %print output of highly recommended metadata; remember,
                %columns correspond to different probability levels

LE_arbitrary

%Now for relative accuracies:

%In general, compute relCEs and relLEs at three different
%probability levels at three different (n_dist) distance values, the latter
%can be used to define the min and max for each of two different distance
%bins; relative errors have a mean-value of zero.  No plotting performed.

%First, for two geolocations associated with the same partition:

%Since partitions correspond to one or the sum of two random fields, this
%approach first solves for the relative accuracy for two errors in the
%same random field i, i=1,...,n, and then combines these results to compute
%the relative accuracy for partition i, i=1,...,n. Recall that partition 1
%contains random field 1, and that partition i>1 contains random field 1
%and random field i.

for ii=1:n_dist
    m_rel=zeros(n,3);    %the second dimension with a value of 3 corresponds to
                        %3d geolocations
    cov_rel=zeros(3*n,3);
    relCE_partitions=zeros(n,3); %the second dimension with a value of 3
    %corresponds to number of different distances between geolocations
    relLE_partitions=zeros(n,3);

    for jj=1:n
        cov_temp=cov_rf((jj-1)*3+1:jj*3,:);    %3x3 cov for rf jj
        S=zeros(3,3);
        S(1,1)=cor_h(ii,jj);
        S(2,2)=cor_h(ii,jj);
        S(3,3)=cor_v(ii,jj);
    end
end

```

```

rel_cov_temp=2*(cov_temp-sqrtm(cov_temp)*S*sqrtm(cov_temp)); %3x3
                                %rel_cov for rf jj

cov_rel((jj-1)*3+1:jj*3,:)=rel_cov_temp(:,:); %load into appropriate
%location of rel cov for the partitions

if (jj>1)    %add rel cov for partition 1 (rf 1) to rel cov for partitions %> 1
cov_rel((jj-1)*3+1:jj*3,:)=cov_rel((jj-1)*3+1:jj*3,:)+...
                                cov_rel(1:3,:);
end

n_specific=jj;
[relCE,relLE]=M_Carlo_CE_LE(p_levels,n,part_p,m_rel,cov_rel,...
    n_specific,plot_flag_temp,0,0);

relCE_partitions(jj,:)=relCE;
relLE_partitions(jj,:)=relLE;

end

distance=dist(1,ii) %print output for recommended metadata
relCE_partitions
relLE_partitions

end

%Next, do as above but for two errors associated with two arbitrary
%geolocations in the product. No plotting specified.

%Compute the relative error covariance matrix associated with each possible
%corresponding partition-pair (one geolocation in partition i and the other
%in j), also compute the corresponding probability of occurrence for this
%partition pair.

%Associate each such pair with corresponding probability of occurrence to a
%"pseudo partition" and then call M_Carlo_CE_LE to compute relCEs and relLEs
%for two arbitrary geolocations.

%The following code takes into consideration that geolocations in different
%partitions have correlated errors due to the fact that all partitions i
%include errors from random field 1, which complicates things somewhat.

for ii=1:n_dist

n_pseudo=n*(n+1)/2; %number of partition pairs in n partitions
pseudo_p=zeros(1,n_pseudo);
rel_m=zeros(n_pseudo,3); %mean-value of relative error associated with
                        %partition pairs
rel_c=zeros(3*n_pseudo,3); %covariance matrix of relative error associated with
                        %partition pairs

count=1;
n_specific=0;

%precompute the cross-covariance for two errors in random field 1:

```

```

cov_temp_rf1=cov_rf(1:3,:);
S=zeros(3,3);
    S(1,1)=cor_h(ii,1);
    S(2,2)=cor_h(ii,1);
    S(3,3)=cor_v(ii,1);
    cross_cov_rf1=sqrtm(cov_temp_rf1)*S*sqrtm(cov_temp_rf1);

for i=1:n    %loop over partitions
for j=i:n

cov_temp_1=cov((i-1)*3+1:i*3,:);    %partition i covariance
cov_temp_2=cov((j-1)*3+1:j*3,:);    %partition j covariance

cov_temp_sum=cov_temp_1+cov_temp_2;
pseudo_p(1,count)=part_p(1,i)*part_p(1,j);
if(j>i)
    pseudo_p(1,count)=2*pseudo_p(1,count);%2 accounts for i-j % j-i combos
end

%if partitions i=j and not equal to 1, subtract off 2*cross-covariance for
%rf 1 and for rf i.  If this is not the case, subtract off 2*cross-covariance
%for rf 1.

cov_temp_sum=cov_temp_sum-2*cross_cov_rf1;

if(i~=1&&j~=1&i==j)

cov_temp_1=cov_rf((i-1)*3+1:i*3,:);

S=zeros(3,3);
    S(1,1)=cor_h(ii,j);
    S(2,2)=cor_h(ii,j);
    S(3,3)=cor_v(ii,j);
    cross_cov_temp=sqrtm(cov_temp_1)*S*sqrtm(cov_temp_1);

cov_temp_sum=cov_temp_sum-2*cross_cov_temp;

end

rel_c(3*(count-1)+1:3*count,:)=cov_temp_sum;
count=count+1;

end
end

[relCE_arb,relLE_arb]=M_Carlo_CE_LE(p_levels,n_pseudo,pseudo_p,rel_m,...
rel_c,n_specific,plot_flag_temp,0,0);

distance=dist(1,ii) %print output for recommended metadata
relCE_arb
relLE_arb

```

```

end      %end ii distance loop

%plot a (hard coded) selected partition's spdcf_vert for general info,
%if plot_flag(1,4) is on (equals 1); only spdcf_vert and for one random field
%is plotted for convenience; note that this is not related to the CE/LE
%plots; the default

if(plot_flag(1,1)==1 && plot_flag(1,4)==1)
sel_part=1;      %select first random field (also applicable to partition 1) as
%default
numSamples=30;  %keep number of samples for plot low or plot too dense (dark)
Z=zeros(numSamples+1,1);
X=zeros(numSamples+1,1);
Y=zeros(numSamples+1,1);
A=spdcf_vert_rf(sel_part,1);%doesn't matter if 0<A<1 instead of 0<A<=1 for
plots
alpha=spdcf_vert_rf(sel_part,2);
beta=spdcf_vert_rf(sel_part,3);
D=spdcf_vert_rf(sel_part,4);
max_dist=1.5*D;
for ii=1:numSamples+1
    X(ii,1)=-max_dist+2*max_dist*(ii-1)/numSamples;
for jj=1:numSamples+1
    Y(jj,1)=-max_dist+2*max_dist*(jj-1)/numSamples;
    d=sqrt(X(ii,1)^2+Y(jj,1)^2);
    Z(ii,jj)=A*(alpha+(1-alpha)*(1+beta)/(beta+exp(d/D)));
    if(d==0)
        Z(ii,jj)=A;
    end
end
end
end

figure(3)
clf
surf(X,Y,Z);
xlabel('delta x (m)');
ylabel('delta y (m)');
zlabel('spatial correlation coefficient');
title('spdcf for hor errors (ex amd ey) as a function of hor distance; selected
part');
end

function[CE,LE]=M_Carlo_CE_LE(p_levels,n,pp,M,C,n_specific,plot_flag,...
    part_1_CE90,part_1_LE90)

%compute CEXX and LEXX for each XX value for each partition as well as for an
%arbitrary geolocation in the MGRF (product); also call plotting functions
%as appropriate

%INPUTS:

%p_levels is a 1x3 vector containing specified probability levels for both CE
%and LE;

```

```

%n is the total number of partitions in the MGRF (product).  Alternatively,
%the total number of "pseudo partitions" if this function was called to
%compute scalar accuracy metrics for relative accuracy;

%pp is a 1xn vector of partition probabilities;

%plot_flag: a 1x4 vector of plot flags for CE and LE for arbitrary geolocation;
%if plot_flag(1,1)=1 plotting is specfied;
%it is assumed that there is no plotting (plot_flag(1,1)=0) if this function
%was called to compute scalar accuracy metrics for predicted relative
%accuracy

%M: n rows of partition 1x3 mean-values,i.e., M is nx3;

%C: 3n rows of 1x3 columns of partition covariance matrices, i,e, C is 3nx3,
%where the first 3 rows correspond to partition 1's covariance matrix

%n_specific is the particular partition of interest for which CE and LE are to
%be computed; if equal to 0, CE and LE corresponding to an arbitrary
%geolocation in the product are to be computed instead

%EXPLICIT OUTPUTS:

%CE is a 1x3 containing the applicable CE at the 3 probability levels
%LE is a 1x3 containing the applicable LE at the 3 probability levels

%IMPLICIT OUTPUTS as inputs to plotting function called by this function:

%h_samp_plot is a 2 x m_tot_plot array of corresponding horizontal error
%samples for plotting;

%v_samp_plot is a 1 x m_tot_plot array of corresponding vertical error
%samples for plotting

% PROCESSING:

%m_tot_part is the total number of random samples to be used in the Monte
%Carlo method for the computation of CE and LE for a specific partition:
m_tot_partitions=1000000;

%m_tot is the total number of random samples to be used in the Monte Carlo
%method for the computation of CE and LE for an arbitrary geolocation:
m_tot=10000000;

%m_tot_plot is the total number of random samples to be saved for possible
%plotting in the calling program (MATLAB script) for either a specific
%partition or for an arbitrary geolocation:
m_tot_plot=2000;
%m_tot_plot=5000; % for "higher-resolution" plots - takes more bytes to place
%into a document

CE=zeros(1,3);

```

```

LE=zeros(1,3);

%compute CE and LE for arbitrary geolocation (otherwise
%for a specific partition)

arb_flag=1;
n_appl=n;
if(n_specific~=0)
    arb_flag=0;
    n_appl=1;
end

sum1=0;
sum2=0;
ns=zeros(1,n_appl);
ns_plot=zeros(1,n_appl);

%Do CE first and then LE in order to reduce internal memory requirements

for i=1:n_appl

    %assume arb_flag=1
    m=M(i,:);
    c=C((i-1)*3+1:i*3,:);
    m_total=m_tot;

    if(arb_flag==0)
        m=M(n_specific,:);
        c=C((n_specific-1)*3+1:n_specific*3,:);
        m_total=m_tot_partitions; %total number of samples if for a specific
                                   %partition
    end

    m_hor=m(1,1:2);
    c_hor=c(1:2,1:2);
    c_hor_sqrt=sqrtm(c_hor);

    %assume arb_flag=1
    ns(1,i)=floor(m_total*pp(1,i));
    sum1=sum1+ns(1,i);
    ns_plot(1,i)=floor(m_tot_plot*pp(1,i));
    sum2=sum2+ns_plot(1,i);

    if(arb_flag==0)
        ns(1,i)=m_total;
        sum1=ns(1,i);
        ns_plot(1,i)=m_tot_plot;
        sum2=ns_plot(1,i);
    end

    if(i==1)
        Y_hor=m_hor'*ones(1,ns(1,i))+c_hor_sqrt*randn(2,ns(1,i));
        h_samp_plot=Y_hor(:,1:ns_plot(1,i));
    end
end

```

```

end

if(i>=2)    %only occurs if arb_flag=1
Y_hor_temp=m_hor'*ones(1,ns(1,i))+c_hor_sqrt*randn(2,ns(1,i));
Y_hor= cat(2,Y_hor,Y_hor_temp);
h_samp_plot=cat(2,h_samp_plot,Y_hor_temp(:,1:ns_plot(1,i)));
clear Y_hor_temp
end

end

m_total_floored=sum1;
m_tot_plot_floored=sum2;

mag_samples=zeros(m_total_floored,1);
for j=1:m_total_floored
    mag_samples(j,1)=sqrt(Y_hor(1,j)^2+Y_hor(2,j)^2);
end

sorted_mag_samples=sort(mag_samples);

for k=1:3
kk=floor(p_levels(1,k)*m_total_floored);
CE(1,k)=(sorted_mag_samples(kk,1));
if((kk+1)<=m_total_floored)
CE(1,k)=(sorted_mag_samples(kk,1)+sorted_mag_samples(kk+1,1))/2;
end
end

clear Y_hor
clear mag_samples
clear sorted_mag_samples

%if plot flag on, plot hor error samples and CEs at the different prob
%levels for an arbitrary geolocation

if(plot_flag(1,1)==1&&arb_flag==1)
    CE_plot(CE,n,h_samp_plot,m_tot_plot_floored,pp,plot_flag,part_1_CE90)
end

%Now do LE

for i=1:n_appl

    %assume arb_flag==1)
    m=M(i,:);
    c=C((i-1)*3+1:i*3,:);

    if(arb_flag==0)
    m=M(n_specific,:);
    c=C((n_specific-1)*3+1:n_specific*3,:);
    end

```

```

m_vert=m(1,3);
c_vert=c(3,3);
c_vert_sqrt=sqrtm(c_vert);

if(i==1)
Y_vert=m_vert'*ones(1,ns(1,i))+c_vert_sqrt*randn(1,ns(1,i));
v_samp_plot=Y_vert(:,1:ns_plot(1,i));
end

if(i>=2) %only occurs if arb_flag=1
Y_vert_temp=m_vert'*ones(1,ns(1,i))+c_vert_sqrt*randn(1,ns(1,i));
Y_vert=cat(2,Y_vert,Y_vert_temp);
v_samp_plot=cat(2,v_samp_plot,Y_vert_temp(:,1:ns_plot(1,i)));
clear Y_vert_temp
end

end

mag_samples=zeros(m_total_floored,1);
for j=1:m_total_floored
mag_samples(j,1)=sqrt(Y_vert(1,j)^2);
end

sorted_mag_samples=sort(mag_samples);

for k=1:3
kk=floor(p_levels(1,k)*m_total_floored);
LE(1,k)=(sorted_mag_samples(kk,1));
if((kk+1)<=m_total_floored)
LE(1,k)=(sorted_mag_samples(kk,1)+sorted_mag_samples(kk+1,1))/2;
end
end

clear Y_vert
clear mag_samples
clear sorted_mag_samples

%if plot flag on, plot vert error samples and LEs

if(plot_flag(1,1)==1&&arb_flag==1)
LE_plot(LE,n,v_samp_plot,m_tot_plot_floored,pp,plot_flag,part_1_LE90)
end

end

function CE_plot(CE_levels,n,hor_samples,m_total_plot,p_partitions,...
plot_flag,part_1_CE90)

%(1) plot circles corresponding to CE probability levels, nominally CE90
%and CE99, for an arbitrary geolocation;
%include CE999 if plot_flag(1,2)=1;

```

```

%include CE90 for partition 1 if plot_flag(1,3)=1 and number of partitions
%n>1;all plots described here and below are in the same figure

%(2) also plot horizontal error samples corresponding to the n partitions
%(in proportion): unique colors for up to the first 3 partitions, and a
%common color for all partitions greater than 3, when applicable

%(3) note that if above is desired exclusively for geolocations in a specific
%partition (not an arbitrary geolocation), run the script but temporarily
%change script's inputs such that only that partition is "active".
%One such method to do so is to set the entry of part_p for the desired
%partition to 1 and the others to 0.

figure(1)
clf
%plot CE circles
r=CE_levels(1,1);
xlimit=r;
x1=zeros(401,1);
y1=zeros(401,1);
y2=zeros(401,1);
dx=xlimit/200;
for i=1:401
    x1(i,1)=-xlimit+(i-1)*dx;
    y1(i,1)=sqrt(r^2-x1(i,1)^2);
    y2(i,1)=-y1(i,1);
end
hold on
ax=1.2*CE_levels(1,3);
if(plot_flag(1,2)~=1)
    ax=1.2*CE_levels(1,2);
end
plot(x1,y1,'b',x1,y2,'b','Linewidth',2); %CE90 for arbitrary geolocation
    %ignore any "imaginary parts ignored" warning due to finite
    %precision
axis([-ax ax -ax ax]);
axis equal
xlabel('x-error (m)');
ylabel('y-error (m)');
title('CE arb: 90%(b),99%(-.b),opt. 99.9%(--b);part samples .r,.c,.g,.m');
r=CE_levels(1,2);
xlimit=r;
x1=zeros(401,1);
y1=zeros(401,1);
y2=zeros(401,1);
dx=xlimit/200;
for i=1:401
    x1(i,1)=-xlimit+(i-1)*dx;
    y1(i,1)=sqrt(r^2-x1(i,1)^2);
    y2(i,1)=-y1(i,1);
end
plot(x1,y1,'-.b',x1,y2,'-.b','Linewidth',2); %CE99 for arbitrary geolocation

if(plot_flag(1,2)==1) %% include CE999 (99.9%) for arbitrary geolocation
r=CE_levels(1,3);

```

```

xlimit=r;
x1=zeros(401,1);
y1=zeros(401,1);
y2=zeros(401,1);
dx=xlimit/200;
for i=1:401
    x1(i,1)=-xlimit+(i-1)*dx;
    y1(i,1)=sqrt(r^2-x1(i,1)^2);
    y2(i,1)=-y1(i,1);
end
plot(x1,y1,'--b',x1,y2,'--b','Linewidth',2); %CE999 for arbitrary geolocation
end

if(plot_flag(1,3)==1&&n>1) %add CE90 for part 1
r=part_1_CE90;
xlimit=r;
x1=zeros(401,1);
y1=zeros(401,1);
y2=zeros(401,1);
dx=xlimit/200;
for i=1:401
    x1(i,1)=-xlimit+(i-1)*dx;
    y1(i,1)=sqrt(r^2-x1(i,1)^2);
    y2(i,1)=-y1(i,1);
end
plot(x1,y1,'r',x1,y2,'r','Linewidth',2);
end

%plot correct portion of partition 1 samples
k_1=floor(p_partitions(1,1)*m_total_plot);
x1=zeros(k_1,1);
y1=zeros(k_1,1);
for i=1:k_1
    x1(i,1)=hor_samples(1,i);
    y1(i,1)=hor_samples(2,i);
end
plot(x1,y1,'.r');

if(n>1)
%plot correct portion of partition 2 samples
k_2=floor(p_partitions(1,2)*m_total_plot);
x1=zeros(k_2,1);
y1=zeros(k_2,1);
for i=1:k_2
    x1(i,1)=hor_samples(1,i+k_1);
    y1(i,1)=hor_samples(2,i+k_1);
end
plot(x1,y1,'.c');
end

if(n>2)
%plot correct portion of partition 3 samples
k_3=floor(p_partitions(1,3)*m_total_plot);
x1=zeros(k_3,1);
y1=zeros(k_3,1);
for i=1:k_3

```

```

        x1(i,1)=hor_samples(1,i+k_1+k_2);
        y1(i,1)=hor_samples(2,i+k_1+k_2);
    end
    plot(x1,y1,'.g');
end

if(n>3)
    %plot correct portion of partitions' 4 to n samples together
    sum1=k_1+k_2+k_3; %total number of samples for plotting in partitions 1-3
    sum2=0; %initialize total number of samples for plotting in partitions
                %4 and up
    sum3=sum1;
    sum4=0;
    for ii=4:n
        sum2=sum2+floor(p_partitions(1,ii)*m_total_plot);
    end
    hortot=zeros(2,sum2);
    for ii=4:n
        n_plot_current=floor(p_partitions(1,ii)*m_total_plot); %total number of
        %samples for plotting for this partition
        for jj=1:n_plot_current
            hortot(1,sum4+jj)=hor_samples(1,sum3+jj);
            hortot(2,sum4+jj)=hor_samples(2,sum3+jj);
        end
        sum4=sum4+n_plot_current;
        sum3=sum3+n_plot_current;
    end

    x1=zeros(sum2,1);
    y1=zeros(sum2,1);
    for i=1:sum2
        x1(i,1)=hortot(1,i);
        y1(i,1)=hortot(2,i);
    end
    plot(x1,y1,'.m');
end %end if n>3

hold off

end %end function

function LE_plot(LE_levels,n,vert_samples,m_total_plot,p_partitions,...
    plot_flag,part_1_LE90)

%(1) plot vertical lines corresponding to LE, nominally LE90 and LE99,
%for an arbitrary geolocation;
%include LE999 if plot_flag(1,2)==1;
%include LE90 for partition 1 if plot_flag(1,3)=1 and number of partitions
%n>1; all plots described here and below are in the same figure

%(2) also plot vertical error samples corresponding to the n partitions
%(in proportion): unique colors for up to the first 3 partitions, and a
%common color for all partitions greater than 3, when applicable

```

%(3) note that if above is desired exclusively for geolocations in a specific  
 %partition (not an arbitrary geolocation), run the script but temporarily  
 %change script's inputs such that only that partition is "active".  
 %One such method to do so is to set the entry of part\_p for the desired  
 %partition to 1 and the others to 0.

```
figure(2)
clf
%plot LE horizontal lines:

r=LE_levels(1,1);
x1=zeros(401,1);
y1=zeros(401,1);
y2=zeros(401,1);
for i=1:401
x1(i,1)=-3+6*(i-1)/400;
y1(i,1)=-r;
y2(i,1)=r;
end

hold on
ax=6;
ay=1.2*LE_levels(1,3);
if(plot_flag(1,2)~=1)
    ay=1.2*LE_levels(1,2);
end
plot(x1,y1,'b',x1,y2,'b','Linewidth',2);
axis([-ax ax -ay ay]);
xlabel('partition vertical lines (increasing partition # order)');
ylabel('vert-error (m)');
title('LE arb: 90%(b),99%(-.b),opt. 99.9%(--b);part samples .r,.c,.g,.m');

r=LE_levels(1,2);
for i=1:401
x1(i,1)=-4+8*(i-1)/400;
y1(i,1)=-r;
y2(i,1)=r;
end
plot(x1,y1,'-.b',x1,y2,'-.b','Linewidth',2);

if(plot_flag(1,2)==1)
r=LE_levels(1,3);
for i=1:401
x1(i,1)=-5+10*(i-1)/400;
y1(i,1)=-r;
y2(i,1)=r;
end
plot(x1,y1,'--b',x1,y2,'--b','Linewidth',2);
end

if(plot_flag(1,3)==1&&N>1)
r=part_1_LE90;
for i=1:401
x1(i,1)=-2+4*(i-1)/400;
y1(i,1)=-r;
```

```

y2(i,1)=r;
end
plot(x1,y1,'r',x1,y2,'r','Linewidth',2);
end

%plot correct portion of partition 1 samples along a vertical line:

k_1=floor(p_partitions(1,1)*m_total_plot);
x1=zeros(k_1,1);
y1=zeros(k_1,1);
for i=1:k_1
    x1(i,1)=-1;
    y1(i,1)=vert_samples(1,i);
end
plot(x1,y1,'.r');

if(n>1)
%plot correct portion of partition 2 samples
k_2=floor(p_partitions(1,2)*m_total_plot);
x1=zeros(k_2,1);
y1=zeros(k_2,1);
for i=1:k_2
    x1(i,1)=0;
    y1(i,1)=vert_samples(1,i+k_1);
end
plot(x1,y1,'.c');
end

if(n>2)
%plot correct portion of partition 3 samples
k_3=floor(p_partitions(1,3)*m_total_plot);
x1=zeros(k_3,1);
y1=zeros(k_3,1);
for i=1:k_3
    x1(i,1)=1;
    y1(i,1)=vert_samples(1,i+k_1+k_2);
end
plot(x1,y1,'.g');
end

if(n>3)
%plot correct portion of partitions' 4 to n samples together
sum1=k_1+k_2+k_3; %total number of samples for plotting in partitions 1-3
sum2=0; %initialized total number of samples for plotting in partitions
           %4 and up

for ii=4:n
sum2=sum2+floor(p_partitions(1,ii)*m_total_plot);
end
verttot=zeros(2,sum2);
sum3=sum1;
sum4=0;
for ii=4:n
n_plot_current=floor(p_partitions(1,ii)*m_total_plot); %total number of

```

```

                                %samples for plotting for this partition
for jj=1:n_plot_current
    vertot(1,sum4+jj)=vert_samples(1,sum3+jj);
end
sum4=sum4+n_plot_current;
sum3=sum3+n_plot_current;
end
x1=zeros(sum2,1);
y1=zeros(sum2,1);
for i=1:sum2
    x1(i,1)=2;
    y1(i,1)=vertot(1,i);
end
plot(x1,y1,'.m');
end    %end if n>3

hold off

end    %end function

```

## Appendix G: Melted Roof-top Edges, Crop/forest Anomalies, and General Production anomalies

This appendix describes possible MGRF partitions other than the nominal partition – see Section 5.3.3.3 in the main body of this document and Appendix E for further background regarding partitions.

### G.1 Melted Roof-Top Edges

A “melted roof-top edge” and its corresponding geospatial errors are conceptually illustrated in Figure G-1. It can occur in an EO-derived 3d geolocation products (Point Clouds) due to a combination of effects associated with imaging geometry, correlation image patch size associated with conjugate image measurements between multiple images, general interpolation, and the abrupt change in the building delineation from the base of a building’s side to its roof-top. Corresponding *a priori* error statistics are associated with an MGRF partition that is identified as corresponding to melted roof-top edges.

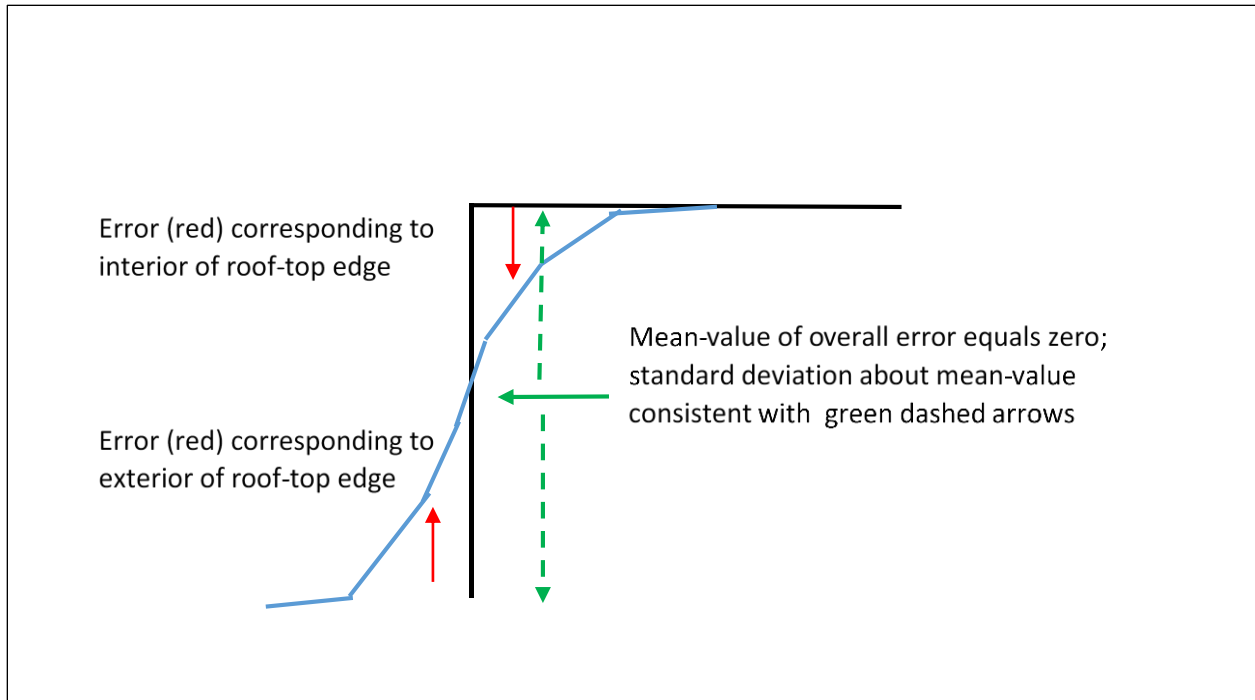


**Figure G-1:** 3d geolocation product's delineation of building edge/root-top (blue) versus true delineation (black) and corresponding geolocation errors and statistics

A reasonable set of these statistics includes a mean-value of zero and a standard deviation about this mean-value which are based on the assumption that a geolocation of interest is equally likely to correspond to the interior of the roof-top edge as to correspond to the exterior of the roof-top edge. A higher fidelity model could correspond to two separate partitions: (1) interior melted roof-top edges with a negative mean-value, and (2) exterior melted roof-top edges with a positive mean-value. However, the added complexity is not considered warranted for most applications of interest, although it is supported by the general MGRF approach if so desired.

Further approximations associated with the baseline mean-value of zero approach include an spdcf that specifies positive spatial correlation between two geolocations of interest within the partition. This assumes that the two geolocations are either both within an interior edge or both within an exterior edge which allow for the positive correlation and corresponding statistical reduction of their relative error. This is a reasonable assumption for most applications. In addition, the spdcf is also usually specified such that the positive correlation reduces quickly as a function of distance between the two geolocations. Another approximation associated with the baseline mean-value of zero approach is based on the assumption that the standard deviation about the mean-value of error is reasonably invariant to building height. If higher fidelity error modeling is preferred for melted roof-top edges, further research is warranted.

## G.2 Crop/Forest Anomalies

A "crop/forest anomaly" can sometimes occur in EO-derived 3d geolocation products (Point Clouds) and may be associated with a "crop/forest anomaly" partition in the MGRF. It is usually associated with

geolocation errors that are statistically significantly larger than those corresponding to the nominal partition for the product; however, not as large as errors associated with a “general anomaly” partition, if present, which corresponds to actual generation problems. Errors associated with crop/forest anomalies correspond to the effects of crop or forest “rows” (or other similar patterns) on the measurement of conjugate image measurements between the images used to make the product. For example, an automatic correlator might select non-conjugate rows in the two images due to similarity of adjacent rows, a complicated function of the row pattern, height of the crop, image ground-sample distance, image geometry, etc., that is hard to predict analytically.

### **G.3 General Production Anomalies**

A general production anomaly corresponds to a collection of 3d geolocations in a 3d geolocation product that had a generation problem and correspondingly very large geolocation errors and are essentially unsuitable for use. For example: (1) a tower with a missing or truncated top or spire, or (2) a severe spike/well in an agricultural or forested region. This does not include geolocations that are actually missing in the 3d geolocation product, such as voids. However, the latter do affect the product reliability metric introduced in Section 5.2.1 of the main body of this document.

## **Appendix H: Alternate methods for the generation of ground truth**

As discussed in Section 5.3.5.1, ground truth is necessary for the generation of sample statistics of error but is not always available. Alternate methods for its generation are presented in this appendix in support of the populated of accuracy assessment models and the subsequent population of predicted accuracy models. Three alternate methods for the generation of ground truth are summarized in Table H-1, with brief descriptions following the table. They are not “high-fidelity” methods (usually poor statistical significance) but may be better than no ground-truth at all, as long as their use is caveated as appropriate. Additional applied research is recommended.

**Table H-1:** Alternate Methods for the Generation of Ground Truth

<p><b>(1) Generation using solution residuals: same sensor:</b></p> <p>Perform WLS solution of geolocation using measurements from multiple overlapping realizations of data/product from same sensor and type or class of data/product of interest</p> <p>Solution becomes an estimate of ground truth</p> <p>Sample-statistics of solution measurement residuals becomes estimate of <i>a priori</i> predicted error covariance of measurement (data/product) errors</p>
<p><b>(2) Generation using multiple solutions: same data/product type:</b></p> <p>Perform multiple WLS solutions for the same geolocation using overlapping data/products from the same type or class of data/product of interest</p> <p>WLS Solutions typically corresponding to one specific data/product realization (e.g., MIG monoscopic solution)</p> <p>Compute average of solutions for estimate of ground truth</p> <p>Compute corresponding solution residuals from average</p> <p>Map geolocation residuals to measurement-space if necessary and corresponding sample statistics become estimate <i>a priori</i> predicted error covariance</p>
<p><b>(3) Generation using multiple solutions: different data/product types:</b></p> <p>Compute/extract common geolocations from different types or classes of overlapping data/products of interest (e.g., Crowd-sourcing)</p> <p>Define "measurements" as difference in solutions from each pair of different data/products</p> <p>Perform WLS solution for predicted accuracy (error covariance matrix elements) for each type or class of data/product</p> <p>Simultaneously perform WLS estimate of each element of each error covariance matrix corresponding to each type of class of data/product</p>

**(1) Alternative to explicit ground truth: Self-generation using solution residuals**

An alternate approach to obtaining ground truth suitable for data/products consisting of

data/metadata from the same sensor, such as images from the same sensor and their metadata, which includes RPCs (ground-to-image rational polynomials) or estimates of sensor pose, is described as follows: Assuming images and their metadata for ease of description, this approach performs MIG – a weighted Least Squares (WLS) solution for the same geolocation’s 3d coordinates using many images that contain the geolocation in their footprint, if available. The solution becomes “ground truth” and the *a posteriori* image residuals become samples of the error in this data/product expressed in image-space that can be used to populate a corresponding accuracy assessment model and then a Geolocation Data Predicted Accuracy Model: Measurement-space. This technique is similar to “scaling by the reference variance”, presented in TGD 2d (Estimators and their Quality Control), and requires a large number of images, at least approximately 20 and preferably many more for reasonable results. It also cannot detect a common bias in errors across the images/metadata if present.

### **(2) Alternative to explicit ground truth: Self-generation using multiple solutions**

An alternate approach to obtaining ground truth suitable for the same type of data/products corresponding to similar sensors, such as images from sensors in the same Small-Sat constellation and their metadata that includes either RPC or estimates of sensor pose, etc., is described as follows: Assuming images and their metadata for ease of description, this approach performs a monoscopic MIG for the 3d coordinates of a common geolocation within each image’s ground footprint. An external elevation source (e.g., DEM) supplies the necessary elevation information to the MIG. Sample statistics consist of the difference of each solution from their average, which are then projected to image-space and used to populate a corresponding accuracy assessment model and then a Geolocation Data Predicted Accuracy Model: Measurement-space. Again, the greater the number of images, the better the results. It also cannot detect a common bias in errors across the images/metadata if present.

### **(3) Alternative to ground truth: Common geolocations from “competing” products**

geolocation products corresponding to Commodities data from different providers or corresponding to Crowd-sourcing data from different providers are compared, such as digital maps, in this alternate approach. More explicitly regarding Crowd-sourcing, 3d coordinates of the same geolocation(s) contained or accessible in multiple digital maps with intersecting AOIs are compared, where the digital maps must correspond to at least three different providers or types of product. Sample statistics of the relative difference of common geolocations are computed and the unique error covariance matrix applicable to each product (digital map) is subsequently estimated in a simultaneous Weighted Least Squares solution. More specifically, measurements into the WLS consist of sample error covariance matrices of the difference between two geolocations from different products, where the latter approximates the 3d sum of their 3d geolocations errors. At least three different products are assumed in order to solve for (estimate) a unique predicted error covariance matrix of geolocation errors for each of the products. Of course, the more products and the more sample error covariance matrices associated with each product the better. A product’s predicted error covariance matrix solved via WLS is assumed representative of an arbitrary geolocation in product.

This alternative is particularly suited to Commodities data and Crowd-sourcing data with accuracy that is not well known, and of course, with no explicit ground truth available. This method is also unique in that it doesn't solve for geolocations explicitly as a "substitute" for ground truth, but estimates applicable error covariance matrices directly. However, a common bias between all providers cannot be detected. Examples of digital map vendors/collectors include OpenStreetMap, Wikimapia, and Google Maps.